Characterising the Regional Immunity of Lung Disease

A thesis submitted to the University of Manchester for the degree of

Doctor of Philosophy

in the Faculty of Biology, Medicine and Health

Year of Submission

2020

Rebecca J Edge

School of Biological Sciences

Division of Infection, Immunity & Respiratory Medicine

Table of Contents

Word Count: 47,625

List of Figures

Chapter One

Chapter Two

Chapter Three

List of Tables

Abbreviations

A.	*Aspergillus*
AAT	Alpha-1-antitrypsin
AATD	Alpha-1-antitrypsin deficiency
ADRB2	Beta-2 adrenergic receptor
AEC	Airway epithelial cells
APA	American Psychological Association
APCs	Antigen presenting cells
ARDS	Acute respiratory distress syndrome
BAL	Bronchoalveolar lavage
BCA	Bicinchoninic acid
BMI	Body mass index
BPIFA1	BPI fold containing family A member 1
BSA	Bovine serum albumin
CAD	Coronary artery disease
C_c	Cell count
CF	Cystic fibrosis
CFTR	CF transmembrane conductance regulator
COP	Cryptogenic organising pneumonia
COPD	Chronic obstructive pulmonary disease
CT	Computed tomography
CTLA-4	Cytotoxic T-lymphocyte-associated protein 4
CyTOF	Cytometry by time of flight
DCs	Dendritic cells
DIP	Desquamative interstitial pneumonia
DLTx	Double lung transplantation
DMSO	Dimethyl sulfoxide
eB_c	eBead count
eB_{conc}	eBead concentration
eB_v	eBead volume
ECM	Extracellular matrix

EF	Established fibrosis
EMT	Epithelial to mesenchymal transition
EPHX1	Epoxide hydrolase 1
FACS	Fluorescence-activated cell sorting
FCS	Fetal calf serum
FDA	Food and Drug Administration
FEV_1	Forced expiratory volume in one second
FF	Fibroblastic foci
^{18}F-FDG	Fluorodeoxyglucose
FITC	Fluorescein isothiocyanate
FMO	Fluorescence minus one
FOV	Field of view
FSC	Forward scatter
FVC	Forced vital capacity
Ga	Gallium
GEE	Generalized estimating equation
GG	Ground-glass
GM-CSF	Granulocyte macrophage colony stimulating factor
GOLD	Global Initiative for Chronic Obstructive Lung Disease
GSTM1	Glutathione S-transferases mu1 (a GST class)
GSTP1	Glutathione S-transferases pi1 (a GST class)
GSTs	Glutathione S-transferases
HBSS	Hank's buffered saline solution
HLA-DR	Human leukocyte antigen-DR isotype
Hx	History
IBS	Inflammatory bowel syndrome
ICM	Immune checkpoint molecules
ICOS	Inducible T cell costimulator
ICOSL	ICOS ligand
IFNγ	Interferon gamma
IHC	Immunohistochemistry
IIPs	Idiopathic interstitial pneumonias
IL	Interleukin

IL-1RA	IL-1 receptor antagonist
ILD	Interstitial lung disease
IPF	Idiopathic pulmonary fibrosis
LCH	Langerhans cell histiocytosis
Ling	Lingula
LL	Left lower
LOD	Limit of detection
LPS	Lipopolysaccharide
LTx	Lung transplant
LU	Left upper
LV	Left ventricular
LVRS	Lung volume reduction surgery
M.	*Mycobacterium*
ManARTS	Manchester Allergy, Respiratory & Thoracic Surgery
MCCIR	Manchester Collaborative Centre for Inflammation Research
MCP-1	Monocyte chemoattractant protein 1
MDT	Multidisciplinary team
MFT	Manchester University NHS Foundation Trust
MI	Mononuclear infiltration
MMPs	Metalloproteinases
MPS	Mononuclear phagocyte system
NHS	National Health Service
NICE	National Institute for Health and Care Excellence
NK	Natural killer
NKT	Natural killer T cell
NSIP	Nonspecific interstitial pneumonia
OP	Organizing pneumonia
P.	*Pseudomonas*
PA	Pulmonary artery
PAMPs	Pathogen-assiosiated molecular patterns
PBMCs	Peripheral blood mononuclear cells
PBS	Phosphate buffered saline
PD-1	Programmed cell death protein 1

PD-L1	Programmed death-ligand 1
PET	Positron emission tomography
PF	Pulmonary fibrosis
PF-ILD	Progressive fibrosisng-ILD
PH	Pulmonary hypertension
RA	Rheumatoid arthritis
RB	Respiratory bronchiolitis
RIPA	Radioimmunoprecipitation
RL	Right lower
RM	Right middle
RPMI	Roswell Park Memorial Institute
RU	Right upper
S.	*Staphylococcus*
SERPINA1	Serpin family A member 1
SLTx	Single lung transplantation
SSc	Systemic sclerosis
SSC	Side scatter
SSTR	Somatostatin receptor
STAT4	Signal transducer and activator of transcription 4
TCR	T cell receptor
TGF-β1	Transforming growth factor-β1
Tfh	T follicular helper
Th	T helper
TL	Thermolysin
TMA	Tissue microarray
TNFα	Tumor necrosis factor alpha
Treg	Regulatory T cell
t-SNE	T-distributed stochastic neighbour embedding
T_w	Tissue weight
Tx	Transplant
UIP	Usual interstitial pneumonia
UK	United Kingdom
US	United States

V_s	Staining volume
V_{ts}	Total sample volume
Zombie UV	Zombie UV™ (Ultraviolet) viability dye

Abstract

Background; Chronic lung diseases are a major cause of morbidity and premature mortality worldwide, and pose a significant public health concern. An aberrant inflammatory response plays a key role in respiratory diseases, however many of these diseases are severely heterogeneous. Although there is a recognised regional variation in underlying inflammatory processes, there is a fundamental lack of research into immunophenotyping of the lung as a whole, and as such, cellular immunity across the lungs is poorly understood. **Hypothesis;** There are fundamental differences in inflammation across the lungs of patients with end stage chronic lung disease that could be characterised by regional sampling of different lobes of the lungs. It was expected that fundamental discovery in the early phases would dictate the direction of later investigations. **Methods;** Wedge biopsy samples were obtained from the upper, middle and lower lobes of explanted lungs from transplant recipients with chronic obstructive pulmonary disease (COPD), interstitial lung disease (ILD) and cystic fibrosis. Leukocyte phenotyping, cytokine expression and immune checkpoint signaling were explored. **Results;** The results demonstrated a high degree of heterogeneity in inflammatory distribution across the lungs, as well as between patients, and led to several important observations. Firstly, female patients with emphysematous COPD have greater heterogeneity in leukocytes, compared to males. The number of leukocytes is significantly elevated in the left lungs of patients with ILD compared to the right lung, and there was an unprecedented increase in the frequency of intermediate monocytes in ILD, which coincided with areas of disease severity. The study is also the first of its kind to characterise immune checkpoint molecules in lung tissue without cancer, in two different chronic lung conditions, identifying significant differences in expression between the two cohorts. **Conclusion;** Is it clear from the evidently heterogenic inflammation described between patients, lungs and lobes, that we should not generalise inflammation in lung disease. Isolated sampling techniques can place exorbitant or insubstantial importance to a finding that may not be relevant to the lung or disease as a whole. The characterisation of regional heterogeneity in chronic lung disease provides an important first step to greater insight into end stage inflammation in lung disease, and could eventually overcome the barriers of lobar heterogeneity to accelerate the effectiveness of lung specific inflammation treatments.

Declaration

No portion of the work referred to in the thesis has been submitted in support of an application for another degree or qualification of this or any other university or other institute of learning. This thesis contains the author's original work and contains no previously published or written material, unless specifically referenced in the text.

All data presented in this thesis are the author's own work, with the following exceptions described below.

- The control group samples in chapter four were collected and processed by Dr Anu Goenka (University of Manchester) for another study (Ref:10/H1010/7). However, the flow cytometry data was acquired using antibodies from the same panel and could therefore be re-gated by the author to explore monocyte subsets. This enabled the provision of a control cohort for the three disease groups.
- All elements of the PD-L1 and B7-H3 immunohistochemistry in chapter six were performed by Senior Biomedical Scientist Catherine McNulty (Manchester University NHS Foundation Trust - MFT). This is with the exception of the analysis, which was performed by the author, with support from Dr Angeles Montero at MFT.

Copyright Statement

The author of this thesis (including any appendices and/or schedules to this thesis) owns certain copyright or related rights in it (the “Copyright”) and s/he has given The University of Manchester certain rights to use such Copyright, including for administrative purposes.

Copies of this thesis, either in full or in extracts and whether in hard or electronic copy, may be made only in accordance with the Copyright, Designs and Patents Act 1988 (as amended) and regulations issued under it or, where appropriate, in accordance Presentation of Theses Policy You are required to submit your thesis electronically Page 11 of 25 with licensing agreements which the University has from time to time. This page must form part of any such copies made.

The ownership of certain Copyright, patents, designs, trademarks and other intellectual property (the “Intellectual Property”) and any reproductions of copyright works in the thesis, for example graphs and tables (“Reproductions”), which may be described in this thesis, may not be owned by the author and may be owned by third parties. Such Intellectual Property and Reproductions cannot and must not be made available for use without the prior written permission of the owner(s) of the relevant Intellectual Property and/or Reproductions.

Further information on the conditions under which disclosure, publication and commercialisation of this thesis, the Copyright and any Intellectual Property and/or Reproductions described in it may take place is available in the University IP Policy (see http://documents.manchester.ac.uk/DocuInfo.aspx?DocID=2442 0), in any relevant Thesis restriction declarations deposited in the University Library, The University Library’s regulations (see http://www.library.manchester.ac.uk/about/regulations/) and in The University’s policy on Presentation of Theses

Acknowledgements

Firstly, I would like to thank my primary supervisor, Dr James Fildes, for giving me the opportunity to carry out research towards a PhD I so desperately wanted. I have learnt an incredible amount over the last four years and will be forever grateful for the chance. This is also echoed in my thanks to my GSK supervisor, Dr Paul Redford, who always came back with sound advice whenever I needed it. I've had the pleasure of working with some brilliant people within the Fildes team, both past and present. To Alex, John, Will, Kav, Triin, Bhuvana and Tim – thank you for welcoming me into the group, and for your continuous support, time and patience. A special thank you must be reiterated to Alex, who was instrumental in supporting me throughout the project. To the Salford students I've worked with over the years, I appreciate each and every one of you for the help, and I hope you all go on to do great things. I'd also like to give thanks to Gareth Howell, for his endless knowledge of flow cytometry but first and foremost his friendship.

This project would not have been possible without the staff and patients at Wythenshawe Hospital. I am deeply indebted to the transplant coordinators; Ruth, Helen, Laura, Jane and Christina, as well as Mr Venkat and his surgical team. Most importantly, I give thanks to the lung transplant patients who consented to be part of this research study. Without the 118 of you who decided to say yes when asked, I wouldn't have a project. I am eternally grateful.

A PhD is a long process, and one not possible without the support of great friends. I'd like to thank my biology nerds, Ashley, Lou & Soph, the El Porto 3C's, Vicki & Adelle, and my Medimmune friends for their support, reassurances and friendship.

Finally, I dedicate this thesis to my family and partner. To my Mum & Dad, Brother, Nan and Aunty; thank you for always supporting me, and guiding me as I grew into the person I am today. And lastly to Tom, my life and my love. Thank you for putting up with the career indecision and neurotic behaviour. I'm finished with being a student now, I promise.

Chapter One: Introduction

Chronic lung diseases are a major cause of morbidity and premature mortality worldwide, and pose a significant public health concern. The respiratory system is complex, with an intrinsic immune compartment continually exposed to the external environment. It is the failure of this immune compartment to effectively regulate its response to pathogenic and non-pathogenic stimuli that results in disease.

1.1 Lung Homeostasis

1.1.1 The Importance of Lung Homeostasis

Immunological homeostasis is a maintained state of equilibrium within a physiological environment, achieved by the timely recognition and differentiation between harmful and innocuous antigens, and the initiation of an appropriate immune response [1]. There are a number of important innate and adaptive components that must effectively work together to achieve this homeostatic state [2]. The immunophenotyping of leukocytes has led to the discovery of organ specific immunity, particularly in organs such as the lungs which are continually exposed to the external environment [3].

Given the airway is not a sterile environment, it is essential that the intrinsic immune compartment within the lung is able to not only appropriately respond to pathogenic antigens, but also retain an unresponsiveness to innocuous antigens in order to prevent chronic inflammation that could culminate in damage [4]. The act of remaining unresponsive to harmless antigens is commonly described as immune tolerance, and is tightly controlled by negative regulatory signals [5]. It is thought that this tolerance to airborne particles, and indeed innate homeostasis, is an adaptable process upon which the threshold for reactivity adjusts to age, stress and environmental influence [6].

The composition of human lungs is complex, consisting of airway, pulmonary vasculature and parenchymal tissue, all of which have a role in immune homeostasis [4]. The respiratory epithelium, which is composed of specialized cells tightly adhered together, lines the airway to form an important defensive barrier between the lungs and the external environment. Antigen presenting cells (APCs) reside within the epithelium, as well as in the pulmonary vasculature and parenchymal

tissue, and are an essential element of the innate immune system, acting as immune sentinels in the recognition of potentially harmful pathogens. The capture, processing and presentation of antigens provide an important link between innate and adaptive immunity and can drive a cellular immune response. Leukocyte recruitment then represents a key stage of this cellular response, whereby neutrophils and lymphocytes are recruited to the site of infection or damage. These innate and adaptive immune responses are essential to maintain lung homeostasis and mitigate the consequences of an organ exposed to constant external stimuli.

1.1.2 The Epithelial and Leukocyte Subsets Essential to Lung Homeostasis.

The epithelium of the lungs provides the interface between the external environment and the respiratory circulation, and is composed of numerous specialised airway epithelial cells (AEC) [7]. The pseudo-stratified respiratory tract epithelium is largely composed of ciliated cells at the apical surface, a limited amount of secretory cells, and basal cells below the epithelial surface, all of which contribute to pulmonary homeostasis [8]. The basal cells and submucosal glands, amongst others, fulfill a vital role in the airway through the replenishment of the ciliated cells lost through injury. Other cells present in the human airway epithelium include serous, club and mucosal cells that all support the ability of the epithelium to maintain homeostasis [9], [10], [11]. The defensive function of the epithelium can be grouped into two types; passive and active protection. The existence of the epithelium and the formation of tight junctions between the cells provide an inert barrier between the non-sterile airway and the circulation, as a passive first line of defense against external pathogens. Active protection is provided via the use of pattern recognition receptors and the secretion of mucins, defensins, lysozyme and nitric oxide, which shield the epithelium and trap foreign bodies to enable their clearance [12] [2]. There are also several key inflammatory mediators secreted by the epithelium, such as cytokines and granulocyte macrophage colony stimulating factor (GM-CSF), which can act as a feedback loop to promote further mucus secretion [2].

The innate and adaptive arms of the immune system possess an array of diverse leukocytes with varying roles and functions. In health, these cell populations, in conjunction with the airway epithelium, interact to maintain homeostasis and keep the lungs free from harm (Figure 1.1).

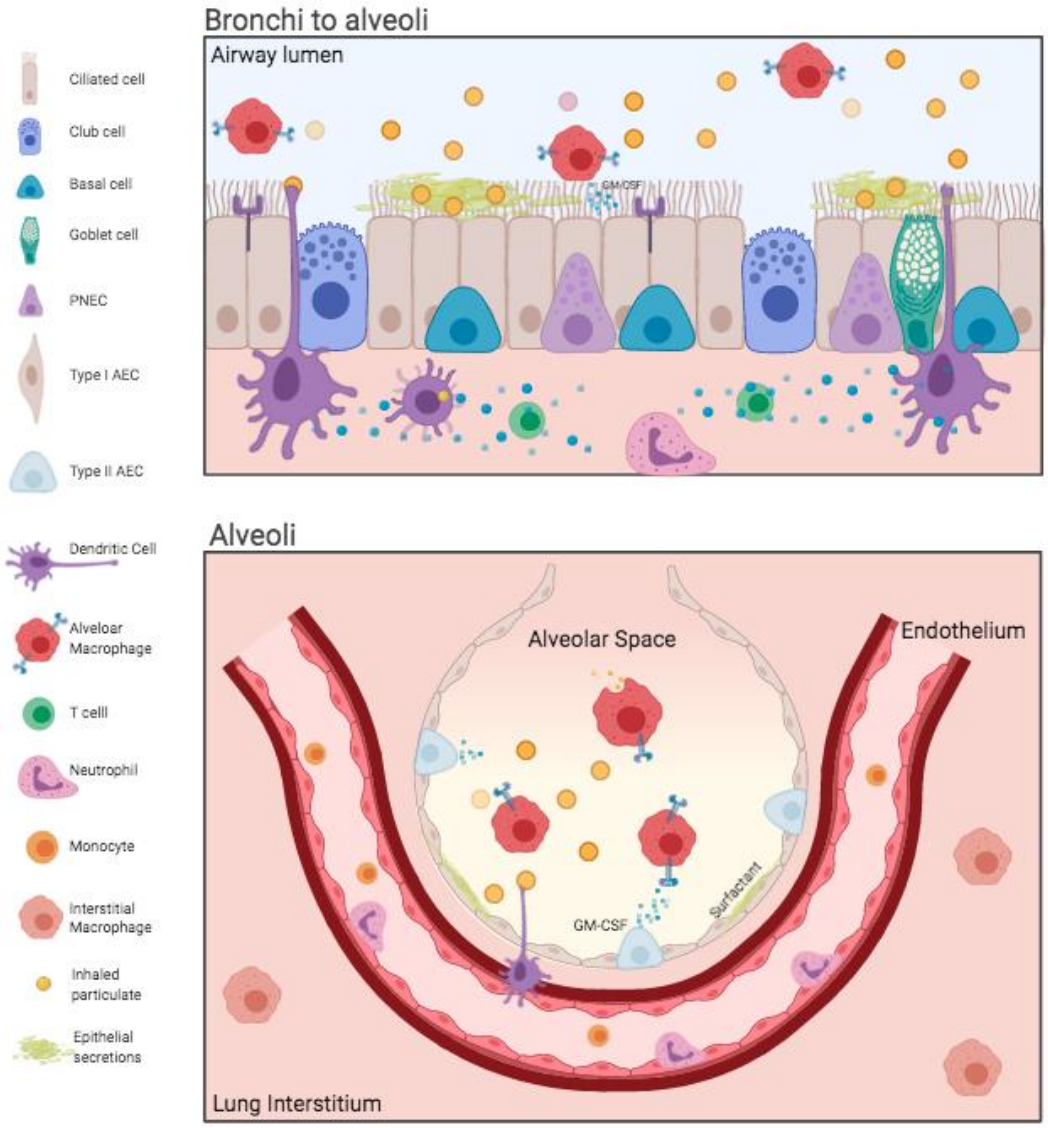

Figure 1.1 The pulmonary airways and the interactions between epithelial and immune cell subsets to maintain lung homeostasis. In the bronchi, epithelial cells form an inert barrier to the external environment, and secrete mucins and defensins to trap and enable clearance of foreign particulates. Cells of the innate immune system, such as macrophages and dendritic cells, perform airway surveillance and phagocytosis of potential pathogens. Crosstalk between the epithelium, innate immune cells and adaptive immune cells, such as T cells, contribute towards homeostasis and appropriate immune responses. Within the alveoli, alveolar macrophages are the predominant immune cell subset, possessing inherently suppressive and regulatory characteristics, that act via feedback from the type I and type II airway epithelial cells (AECs), which secrete mediators such as granulocyte macrophage colony stimulating factor (GM-CSF). Other cell types such as interstitial macrophages can orchestrate a pro-inflammatory response to harmful pathogens. Neutrophils that are sequestered within the pulmonary microvasculature are then readily mobilised to the site of injury. Parts of image adapted from Puttur, Gregory & Lloyd (2019) [13] and "Respiratory epithelium" by BioRender.com (2020) [14].

APCs are a primary component of the innate immune system, which identify and endocytose antigens for processing and presentation to T cells, in order to mount an adaptive immune response. Dendritic cells (DCs) are recognised as professional APCs, exhibiting high antigen capturing and presentation proficiency. The DC network is dispersed throughout the lungs in different densities, however it is most abundant in the upper respiratory tract and larger airways to enhance the sampling of inhaled antigen [15]. They are positioned within the pulmonary interstitium, directly below the airway epithelial cells, but can protrude through the epithelial barrier to perform their integral antigenic sampling role [16]. Macrophages, eosinophils and B cells also possess APC capabilities to varying degrees [17], [18], [19].

Macrophages are a fundamental component of the primary innate immune response, playing a key role in the regulation of both acute and chronic inflammatory responses. Whilst they are present in nearly every tissue type, there are at least two described macrophage populations that reside specifically within the lung; alveolar macrophages (AMs) and interstitial macrophages (IMs), both of which have specific locations, roles and functions [20, 21]. AMs are inherently suppressive and employ regulatory effects in a nonspecific fashion, through the secretion of antimicrobials and a high aptitude for phagocytosis. In contrast, IMs secrete specific cytokines that are capable of orchestrating adaptive immune responses [22, 23]. However macrophages, similar to DCs, possess a high degree of plasticity, and can fine-tune their phenotype in response to the local microenvironment.

Leukocyte recruitment is an important part of the inflammatory process, and the mechanisms by which leukocytes are recruited and sequestered into the lungs are an important consideration to the overall leukocyte content of the lungs. Human lungs have been estimated to have a marginated pool of over 40 x 10^9 leukocytes [24], predominantly residing within the capillary bed [25]. These cells accumulate due to the small diameter of vessels, requiring leukocytes to adjust their size, which takes time.

Neutrophils are the most abundant leukocyte in circulation, and play a major role in the innate immune response by performing functions such as pathogen phagocytosis, and the secretion of

effector proteins such as proteases [26]. The lung boasts an extensive reservoir of neutrophils within the pulmonary microvasculature, and subsequently, neutrophils have a prolonged interaction with the lung endothelium. Given the endothelium is highly responsive to changes in stimuli, the surface expression of key selectins can be readily altered, facilitating neutrophil extravasation into the lung tissue [27].

Lymphocytes are adaptive immune cells, and primarily consist of populations of T cells and B cells, which mount highly specialized antigen specific responses. T cells can be divided into two key elements, CD4+ or CD8+ T cells that are described as helper or cytotoxic T cells, respectively. Naïve CD4+ T cells can be directed to differentiate into specific subsets based on their exposure to key cytokines; T helper (Th)1, Th2, Th9, Th17 and Th22 subsets, T regulatory (Treg) and T follicular helper (Tfh) which can all secrete further specific cytokines to influence downstream anti- or pro-inflammatory effects [28]. Upon encountering and recognizing specific pathogenic antigens, CD8+ cytotoxic cells possess the capability to directly kill infected cells by driving apoptosis [29]. However, it is necessary for this response to be tightly regulated to prevent the destruction of healthy tissue.

B cells are the other key lymphocyte in the adaptive immune response, providing a humoral antibody mediated response to antigen specific targets to resolve pathogen invasion. The effector functions of antibodies enhance the recognition of pathogens by nearby effector cells such as macrophages [30]. Memory B cells are capable of recognisng subsequent exposure to the same antigen and continue to reside with the lung mucosa, long after the resolution of the first insult.

The immune system requires effective regulation of each of the different leukocyte subpopulations within the lung in order to differentiate between harmful pathogenic antigen and non-harmful stimuli [31]. This, in addition to effective crosstalk between the structural cells of the lung, maintains respiratory homeostasis. However, the loss of regulation for any component in this vital balance can culminate in respiratory disease.

1.2 Respiratory Disease

The global prevalence of lung disease extends into the hundreds of millions, and is the cause of four million premature deaths each year [32]. Approximately 12.7 million people are currently diagnosed with a form of lung disease within the United Kingdom (UK), with 500,000 new diagnoses each year, resulting in an increased burden on the National Health Service (NHS), (BLF, 2016) [33]. Diseases that occur as a result of inflammation can be acute, an accelerated response that can occur within hours of injury and usually declines as the cause of injury resolves or is removed, or chronic, in response to a persistent trigger, which over time results in loss of tissue function [34]. Within both acute and chronic disease categories, many occur primarily as a result of a dysregulated inflammatory response and a loss of homeostasis. Acute respiratory distress syndrome (ARDS) is an example of acute injury driven by inflammation through the involvement of cellular infiltration, cytokine secretion and the induction of apoptosis and necrosis [35]. Whilst ARDS is a severe form of respiratory disease, the acute nature of the inflammatory response and damage induced is usually reversible upon treatment of the primary stimuli. In contrast, there are respiratory diseases whereby sustained inflammatory responses result in chronic disease, causing permanent lung damage. This thesis will focus on three forms of chronic lung disease: chronic obstructive pulmonary disease (COPD), interstitial lung disease (ILD) and cystic fibrosis (CF).

1.2.1 Chronic Obstructive Pulmonary Disease

COPD is a chronic lung condition affecting approximately 65 million individuals globally [36]. Within the UK, there has been a 27% increase in diagnosis rates over the last decade, affecting 1.2 million individuals, and resulting in an estimated annual cost to the NHS of £1.9 billion [37]. It is thought to be a preventable and treatable, although not reversible, lung disease, that is usually progressive and associated with inflammatory effects linked to environmental influences, including cigarette smoking [38]. Traditionally, COPD has been considered as a disease of the older male smoker, although prevalence in women continues to rise and the gender gap between those affected is falling [39, 40]. New diagnoses of COPD most commonly occur in people over the age of 40, and mortality rates are highest for people in their 70's [37].

COPD is an umbrella term for a spectrum of different pathological processes, the hallmark of which is progressive airflow obstruction resulting in progressive breathlessness and a chronic, productive cough. Chronic bronchitis and emphysema are phenotypes of COPD (Figure 1.2). Chronic bronchitis is defined clinically as a productive cough, which is present on most days for a minimum of three months over two consecutive years. It is driven by a number of factors including excessive mucus production, airway remodeling or smooth muscle hyperplasia, culminating in reduced forced expiratory volume. Whilst mucociliary clearance plays an important role in the defence against exogenous insult, the hypersecretion of mucus by airway epithelial cells during COPD contributes to a worsening quality of life [41]. Emphysema is defined histologically as the destruction of alveolar walls creating a permanent enlargement of airspaces and a reduction in the surface area for gaseous exchange, without any obvious fibrosis [42]. Bullae, which are air filled cysts within the lung parenchyma, are also commonly associated with the emphysematous process [43]. Lung tissue requires a high degree of elasticity to be able function correctly, with elastin a critical extracellular matrix protein that composes between 3-7% of the lung tissue [44]. This protein is slow to replenish once lost and so destruction of elastin is thought to contribute to the development of emphysema in COPD patients. Airflow limitation occurs through both the physical loss of the alveolar walls, decreasing the vital elastic capabilities, and a reduction of alveolar supporting structures that result in narrowing. Patients with COPD may only exhibit one pathological process, or experience them in combination, although airflow obstruction is the hallmark of a COPD diagnosis.

The pathophysiology of COPD is complex and multifactorial. Systemic and local oxidative stresses as well as inflammation are commonly associated with COPD development and progression [45]. During the development of COPD, the airway epithelium undergoes changes that disrupt its function as a barrier, resulting in increased permeability and excess mucus production that aids airway obstruction and the progression of the disease [46]. The oxidative stress incurred by these epithelial changes contributes significantly to the chronic inflammation that occurs in COPD. Alveolar epithelial cells are a major source of pro-inflammatory cytokines, including interleukin (IL)-6 and tumor necrosis factor alpha (TNFα) as well as the chemokine IL-8. As such, these cells are able to significantly influence leukocyte migration and behaviour [47]. Both neutrophils [48] [49] and

macrophages [50] have been implicated as key leukocytes involved in the onset of COPD. Macrophage numbers correlate with COPD severity [51], whilst neutrophils promote elastin degradation and tissue damage [52]. However, there are also many other components of the immune system that are thought to be complicit in disease progression, including CD8+ T cells [53] [54] [55].

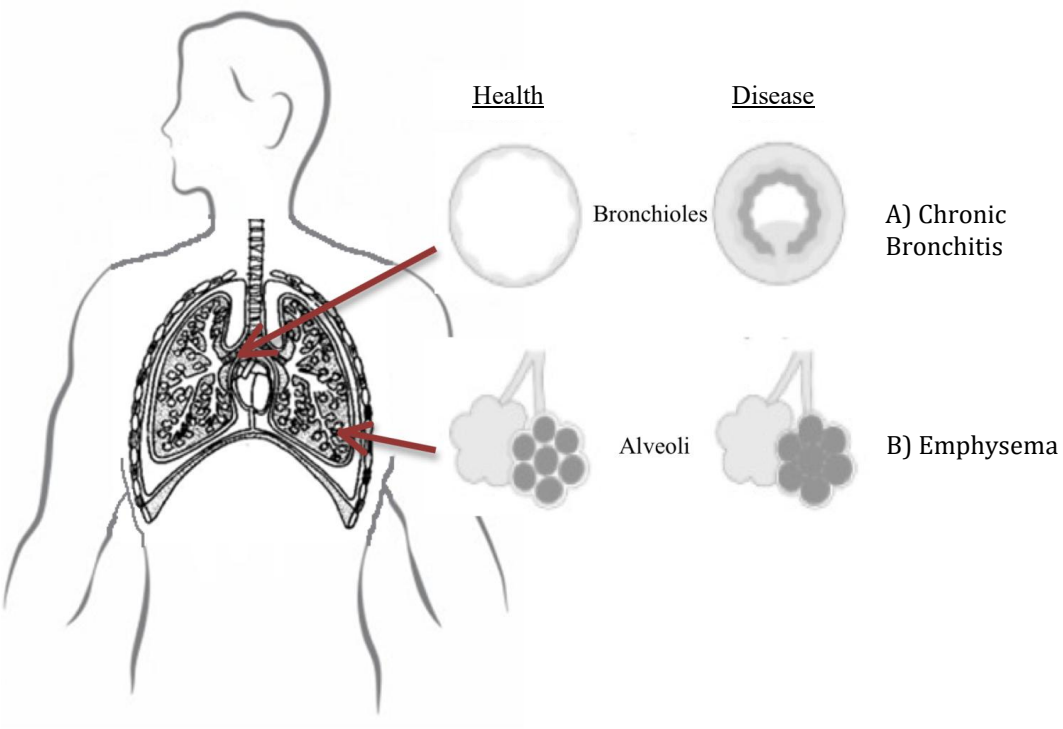

Figure 1.2 The pathological phenotypes of chronic obstructive pulmonary disease (COPD). A) Chronic bronchitis results in the narrowing of lung bronchioles and excessive mucus production that drive clinical symptoms of a chronic cough, whilst B) emphysema is the destruction of alveoli tissue structures. Both phenotypes of COPD result in a reduction of forced expiratory volume in one second (FEV_1). Image adapted from British Lung Foundation (2019) [37].

In addition to smoking, there are a number of environmental and genetic factors that can predispose someone to COPD. This includes workplace dust and vapours, air pollutants, ageing, infections and gene variants or mutations [56]. There are 192 genes that have been linked to a predisposition for COPD, although only seven of these genes have been validated by more than 10 independent studies [57].

Of these seven, the most well established genetic driver of COPD relates to mutations in the serpin family A member 1 (SERPINA1) gene, which results in alpha-1-antitrypsin (AAT) deficiency and a protease-antiprotease misbalance [58]. AAT is an anti-protease inhibitor, which normally inhibits neutrophil elastase, a proteolytic enzyme that destroys alveolar wall connective tissue. Mutation within the SERPINA1 gene, with subsequent AAT deficiency, therefore drives lung matrix destruction and damage to the lung with resultant COPD [59].

Three of the seven genes described relate to the way in which smoke products are detoxified. The Epoxide hydrolase 1 (EPHX1) gene encodes an enzyme expressed by the bronchial epithelium, and has two polymorphisms that enhance or decrease the activity of EPHX1. Try113His drives fast enzymatic activity, detoxifying noxious substances and conveying protection against the development of COPD [60], whilst the His139Arg polymorphism results in reduced and inefficient enzyme activity. Glutathione S-transferases (GSTs) are another family of enzymes responsible for detoxification, metabolism and excretion of smoke products. Two classes within this enzyme family, mu1 (M1; GSTM1) and pi1 (P1; GSTP1), have been associated with COPD driven by different polymorphisms [61]. Polymorphisms of the GSTP1 gene in particular have been associated with apical-dominant emphysematous damage in the lung [62].

Another of the seven genes is the Beta-2 adrenergic receptor (ADRB2) gene, which regulates airway contraction and bronchodilation. A number of mutations in this gene have been linked to COPD, including changes in the Gly16 allele, which has been shown to increase susceptibility to the development of COPD, and the Gln27 allele, which has been correlated with a more severe COPD phenotype [63].

However most relevantly, two of the seven described genes relate to inflammation; the genes encoding tumor necrosis factor (TNF) and transforming growth factor-β1 (TGF-β1). TNFα has a pro-inflammatory effect by enhancing the expression of other inflammatory genes. A polymorphism (TNFα-308*2) in the gene encoding for TNF is over expressed in COPD patients and results in increased TNFα expression, perpetuating an exaggerated inflammatory response [64]. TGF-β1 is a multifunctional cytokine important for lung homeostasis, but is increased in the airway of patients

with COPD [65]. Polymorphisms of the TGF-β1 gene have been implicated in the susceptibility to COPD in independent populations, but only in conjunction with cigarette smoking [66]. It is also thought that polymorphisms in the gene can contribute to airway hyper responsiveness [67].

Inhaled bronchodilators and corticosteroids are the main staples of COPD treatment, aimed at providing symptom relief, preserving lung function and preventing exacerbation occurrences [68]. Long term oxygen therapy and pulmonary rehabilitation are also common therapeutic options for patients with COPD, as are seasonal vaccinations. In addition to symptomatic relief, anti-inflammatory drugs have been a predominant focus to combat the pathophysiological effects of COPD. Drugs of this type have been the goal of many pharmaceutical companies in recent years, with IL-8 and TNFα both targeted [69]. Surgical interventions for COPD include lung volume reduction surgery (LVRS) and transplantation. There are strict guidelines for patients to be referred for transplant evaluation, including a markedly progressive disease course and/or a forced expiratory volume in one (FEV_1) of <25% predicted, along with smoking cessation and a suitable body mass index (BMI) [70]. COPD is the most common transplantable lung condition, with over 1000 lung transplants performed worldwide for end-stage COPD each year.

1.2.2 Interstitial Lung Disease

ILD is an umbrella term for a heterogeneous group of over 300 different diseases, which drive fibrosis of the lungs and result in impaired lung function. Individually they are very rare, and as a collective have an incidence of one in 3-4000 in the UK [71]. It is difficult to precisely determine the incidence rates of ILD globally given the heterogenic nature of the disease, and the complexity of its diagnosis. However, idiopathic pulmonary fibrosis (IPF) is universally recognised as one of the most common forms of ILD, accounting for between 20-40% of all ILD diagnoses [72, 73]. IPF is extremely progressive in nature, with a median survival of two to four years. Given the progressive nature and increased mortality associated with IPF, early identification and accurate diagnosis is critical.

A multidisciplinary team (MDT) approach is therefore considered the gold standard for establishing an ILD diagnosis and consists primarily of respiratory physicians, radiologists and histopathologists [74], although other disciplines may be included where appropriate. Together, the members of the MDT will seek to confirm a diagnosis, quantify severity and determine other complications through the exchange of clinical, histological and radiological evidence. Although histological analysis remains part of diagnostic algorithms, obtaining lung biopsies from ILD patients is not without risk given their disease severity and associated comorbidities [75]. As such, they are often only performed in a small minority of patients, making the MDT process even more vital.

The pathogenesis of ILD is poorly understood, with most sub-groups falling under the category of idiopathic interstitial pneumonias (IIPs). There is a common structural remodelling of the lungs, which reduces the rate of oxygen transfer. This causes a worsening of dyspnoea and acute exacerbations, which culminate in respiratory failure [76]. Lung fibrosis is thought to be a form of aberrant AEC repair [77], occurring from injury to the lung airspace after exposure to external stimuli. This is thought to drive a pro-fibrotic environment via the amassing of fibroblasts and myofibroblasts [78]. These cells are highly activated and drive inappropriate lung remodelling. There is often a causality dilemma regarding inflammation in ILD; it is a consequence in many forms

of ILD but also trigger for others [79]. Conversely, fibrosis and inflammation can both occur independently of the other in ILD and are associated with very different prognosis outcomes.

Table 1.1 identifies the six major subgroups of ILD and highlights the major radiological and histological findings. Usual interstitial pneumonia (UIP) is the most common morphological and pathological pattern of ILD. It is the hallmark feature of IPF, and the distribution of UIP is characteristically basal and peripheral. Nonspecific interstitial pneumonia (NSIP) is the second most common morphological pattern, and its distribution is typically more diffuse throughout the lung. NSIP is commonly associated with secondary ILDs [80] relating to a variety of diseases including connective tissue and drug induced disorders. Organizing pneumonia is another common morphological feature, and characteristically presents in peripheral areas and chiefly in the lower lobes

Whilst 'idiopathic' dictates that the exact causes of disease and subsequent fibrosis are unknown, proposed risk factors for many ILDs include cigarette smoke [81], infectious agents [82] [83], exposure to antidepressants and a genetic predisposition [84]. Connective tissue disorders like systemic sclerosis (SSc) often have strong genetic components. The presence of anti topo-isomerase autoantibodies in SSc strongly correlates with the advancement of disease [85]. Patients with common variable immunodeficiency disorders have a 10-20% chance of ILD occurring [86].

Appropriate treatment options depend on a correct diagnosis, which is aided by the utilisation of an MDT as previously described. The most common forms of treatment for ILDs consist of immunosuppression and anti-inflammatory drugs, along with anti-fibrotic agents. However, in IPF, anti-inflammatory drugs can be ineffective or detrimental, some having correlated with increased disease progression and hospitalisations [87] [88]. Although disease specific therapies vary by ILD aeitiology, common treatments across ILD focus upon symptomatic relief, with pulmonary rehabilitation and oxygen therapy. Lung transplantation is also a consideration for patients with progressive disease, unresponsive to pharmacological treatment. However, the median survival rate post transplantation for patients with ILD is lower than in other lung diseases [89]. This may be

due to a past preference for performing SLTx in ILD, which may have comparable short-term survival rates, but DLTx has since demonstrated better long-term survival [90].

Table 1.1 Descriptive comparison of six major Interstitial Lung Disease (ILD) subgroups. An overview of the radiological and histopathological characteristics of the most common ILD subgroups and their therapeutic considerations. Adapted from Kalchiem-Dekel (2018) [87].

ILD Subgroup	Radiographic Findings	Histologic Patterns	Therapeutic Considerations
Smoking-Related	GG, emphysema with fibrosis, mosaic attenuation	RB, DIP, LCH, emphysema, fibrosis	Smoking cessation, removal from exposure, anti-inflammatory therapy in advanced disease
Hypersensitivity Pneumonitis	GG, mosaic attenuation, upper-lobe fibrosis, centrilobular nodules	Poorly-formed granulomas with multinucleated giant cells	Removal from exposure, remediation of environment, anti-inflammatory and/or immunosuppressive therapy in advanced disease
Connective Tissue Disease-Related	GG, reticular opacities, consolidation, fibrosis, peripheral sparing	Chronic inflammation, UIP, NSIP, or OP	Anti-inflammatory and/or immunosuppressive therapy
Occupation-Related	GG, reticular opacities, fibrosis, nodules, pleural plaques (asbestos)	Chronic inflammation, UIP, NSIP, OP, or granulomatous inflammation	Removal from exposure, use of respiratory protective equipment
Medication-Induced	GG, reticular opacities, consolidation, nodules, fibrosis	Chronic inflammation, UIP, NSIP, OP, or granulomatous inflammation	Medication discontinuation if possible, anti-inflammatory and/or immunosuppressive therapy in advanced disease
Idiopathic Pulmonary Fibrosis	Peripheral and basilar fibrosis with honeycombing	UIP	Consideration of antifibrotic therapies, lung transplantation evaluation in selected patients

Abbreviations: ILD, Interstitial lung disease; GG, ground-glass; RB, respiratory bronchiolitis; DIP, desquamative interstitial pneumonia; LCH, Langerhans cell histiocytosis; UIP, usual interstitial pneumonia; NSIP, nonspecific interstitial pneumonia; OP, organizing pneumonia.

1.2.3 Cystic Fibrosis

CF is a genetically inherited multifaceted disease that disrupts both lung and digestive function, affecting over 10,000 people in the UK, and an estimated 70,000 to 100,000 people worldwide [91]. CF manifests when a mutated gene, encoding the CF transmembrane conductance regulator (CFTR) protein [92], is inherited from both carrier parents. The median age of diagnosis in the UK is now 2 months; largely due to the inclusion of CF in the neonatal screening programme [93]. However, the many different forms of gene mutation has led to some patients not being diagnosed until adulthood. The condition is most common in Caucasian populations, at a rate of one in every 3000-4000 births, whilst incidence rates are much less frequent in other races and ethnicities [94]. The median age of death for CF patients in 2017 was 31, although the median predicted survival was indicated to be 47 years between 2013-17 [95].

The CFTR gene, located at 7q31.2, encodes a transmembrane protein that is expressed on the apical surface of epithelial cells [96]. There has been over 2000 mutations identified in this gene, which can be broken down into six classes: affecting protein production (I), processing (II), regulation (III), conduction (IV) as well as reduced function (V) and normal function (VI) outcomes [97] (Figure 1.3). The most common form is F508del [98], a processing class ii mutation, although any mutation relating to production (I), processing (II) or regulation (III) results in the most severe disease manifestations. The wide variance in CFTR mutations results in high clinical heterogeneity between patients. Common complications with CF include a very low BMI, meconium ileus, vitamin deficiency, male infertility, CF related diabetes and joint pains [93]. However, pulmonary complications present one of the biggest mortality risks.

In the lungs, the dysfunction of the CFTR transmembrane protein causes an increase in the viscosity of mucosal secretions from epithelial cells. This is due to an increase in the uptake of sodium ions and a decrease in the secretion of chloride ions, resulting in a net reduction in the amount of water available for mucosal secretions [101]. The subsequent thickening of mucus contributes to airway obstruction and promotes persistent bacterial infection [102]. Common infections include *Pseudomonas (P.) aerugionasa* and *Staphylococcus (S.)* aureus. The persistence

of bacterial infection causes an inflammatory response, resulting in the production of pro-inflammatory cytokines such as IL-1β, IL-6 and IL-8 [103]. Persistent chronic airway inflammation then drives tissue destruction, ultimately leading to respiratory insufficiency [104]. Bronchiectasis is the most common manifestation of this tissue destruction, and ultimately leads to the requirement of lung transplantation.

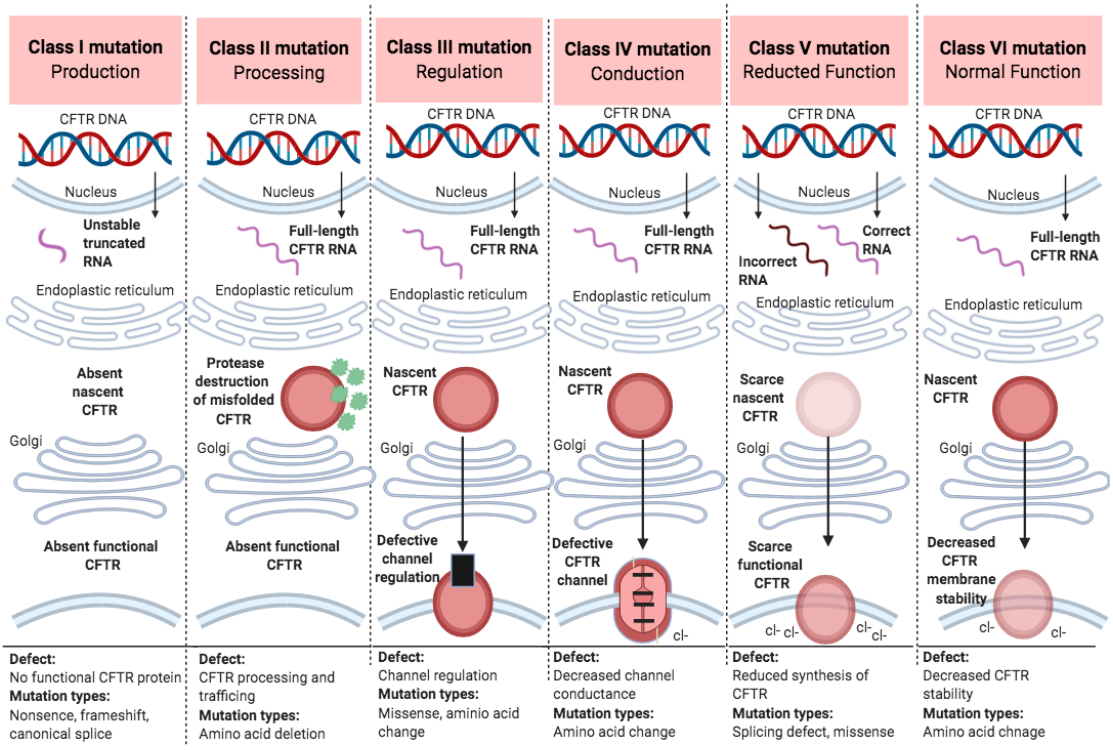

Figure 1.3 Cystic fibrosis transmembrane conductance regulator protein mutation classes. Mutations of the CFTR gene, encoding the CF transmembrane conductance regulator (CFTR) protein, can be organised into six distinct classes of mutation. Class I mutations affect protein production, class II mutations affect how the protein is processed and class III mutations result in the production of a protein that has defective regulation preventing chloride ion secretion. Class IV mutations affect conduction, severely limited chloride ion transport, whilst class V mutations reduce the function of the CFTR protein. Finally, class VI mutations do not affect the function of the CFTR protein, thus permitting normal function, but they do decrease the stability of the protein in the membrane. Image adapted from [99] and created using BioRender [100].

Therapeutic targets for CF focus on several key factors; CFTR correction, inflammation management, mucus clearance and nutrition [97]. There are a number of CFTR modulators that target the underlying mutations in CF, including Ivacaftor that has United States (US) Food and Drug Administration (FDA) approval. Initially approved for a rare G551D class III mutation in

children older than 6, Ivacaftor approval has since expanded to include other mutations whilst reducing the age requirement. Other drugs are in varying stages of clinical trial, with many focusing on the treatment of mutation F508del [105], [106]. The targeting of inflammation is a vital step to delay bronchiectasis, with two key concepts focusing on broad-spectrum anti-inflammatory drugs or a more targeted approach against specific inflammatory mediators [104]. Ibuprofen has demonstrated long-term efficacy in the treatment of CF patients, with minimal side effects [107], whilst corticosteroids, such as prednisone, have also been trialed [108]. Modulating intracellular signalling [109], inhibiting neutrophil influx and secretions [110, 111], and anti-proteases [112] are all avenues that are being explored for more targeted treatment options.

1.3 Disease Heterogeneity and Regional Variation

Within each of the chronic lung conditions considered within this thesis, there is an undisputed heterogeneity in how patients develop symptoms and disease progresses, which results in numerous clinical phenotypes being described.

COPD can be categorised into patients who have predominantly emphysematous changes or clinical symptoms of chronic bronchitis. However there are also patients who suffer with more frequent exacerbations, some that respond better to treatments, and others who have an accelerated disease progression and subsequent mortality [113]. Furthermore, the severity of airflow limitation does not necessarily correlate with the degree of architectural distortion within the lung, highlighted by patients who have vastly differing levels of emphysema being classified within the same COPD severity [114]. The change in inflammation within the lung, and particularly within the small airways, appears to be an important component in the progression and severity of COPD [51]. Patients with stable COPD have consistently elevated levels of inflammatory cells and cytokines compared to healthy non-smokers, and during an exacerbation the levels of these inflammatory makers are significantly increased further [115].

ILD encompasses a large number of different diseases, however clinical phenotypes are increasingly being used to describe commonalities between different sub-groups of the disease according to severity of disease, symptoms, progression and response to treatment [116]. Progressive fibrosing-ILD (PF-ILD) is defined as progressive lung fibrosis with worsening lung function, and is characteristic of patients with IPF, but not limited to that aetiology [117]. ILD patients with connective tissue disease backgrounds are also at risk of developing PF-ILD, as are those with hypersensitivity pneumonitis and exposure related ILDs. The grouping of patients by their clinical symptoms and treatment responses hold promise for expanding the use of anti-fibrotic drugs, namely Nintedanib and Pirfenidone [116] [117]. However, it is important to bear in mind that the use of these treatments in different ILD sub-groups does not mitigate the necessity to delineate

the molecular pathways that underpin the development and progression of each individual disease, and specifically the contribution of inflammatory processes.

Whilst the specific mutations of the CFTR gene are well characterized, and the pathogenic outcomes associated with each class of mutation are well known, there is significant phenotypical variation in patients with the same mutation. This manifests as a broad age of disease onset, with different levels of disease activity across multiple organ systems and subsequent associated symptoms It is thought that this disease variability can reflect differences in environmental influences such as the exposure to different pathogens, and other modifier genes that individual patients might possess [118, 119]. Polymorphisms in upper airway proteins, such as members of the BPI fold containing family A member 1 (BPIFA1), have been shown to have immunomodulatory effects that could influence the pulmonary severity observed between different patients [120]. However, further clinical phenotyping of those with extensive pulmonary disease is still being established [121, 122].

Despite there being thousands of publications regarding inflammation in lung disease, there is a continued lack of knowledge correlating inflammatory endotypes to clinical manifestations [123], [116]. The notion of inflammatory endotypes for different clinical phenotypes has only been considered in recent years. However, in the strictest sense, the term endotype cannot be applied to most COPD or ILD clinical phenotypes given the lack in understanding of the molecular mechanisms driving disease. In contrast, CF has a clearly defined genetic aetiology, however, further research is required to delineate the relationships between individual CFTR mutations, tissue specific polymorphisms in modifier genes, and subsequent clinical phenotypes [124].

A major challenge to understanding the inflammatory processes driving chronic lung diseases, is that within each disease, the lungs are not uniformly affected and there is often regional variation within the same clinical phenotypes. For example, emphysema can manifest in three distinct forms that affect regions of the lung differently [125]. Centriacinar emphysema predominantly affects the upper lobes destroying alveoli in an inconspicuous nature, whilst panacinar emphysema uniformly destroys alveoli across the entirety of the lower lobes [126] [125]. The third form is paraseptal

emphysema, which is a distal form of the disease limiting itself to the peripheral airways. Furthermore, within the same region of the lung, there could be spatial and temporal disease heterogeneity, whereby normal tissue is interspersed with pathological tissue at various stages of the disease process. Although these features are more extensively described within ILD sub-groups [127] they may also be seen in COPD and CF.

As disease severity progresses, the regional changes in the structure and function of the lung, have largely been characterised by imaging studies using techniques such as computed tomography (CT) (Figure 1.4). In COPD, CT imaging is one of the most sensitive tools for identifying emphysema, but it can also diagnose bronchiectasis in those patients presenting with chronic cough [128-130]. Determining the extent and pattern of emphysema in patients with COPD can be vital for delivering effective treatments such as LVRS. It is important to evaluate ventilation and perfusion in order to target a lobe or area for reduction and then also assess the success of the intervention. Recent studies have evaluated new CT technologies and imaging software for these specific purposes, successfully and reliably measuring lobar volumes and performances before and after surgical intervention [131, 132]. Valipour et al. (2015) describe the existence of both inter-lobar and intra-lobar heterogeneity in a high proportion of patients with emphysema [133], suggesting the importance of a segmental approach to LVRS. Yet despite the recognised use of CT imaging for determining regional heterogeneity in the COPD lung, there is still a lack of a gold standard method for defining this heterogeneity within the lung and the potential impact on treatment options [133].

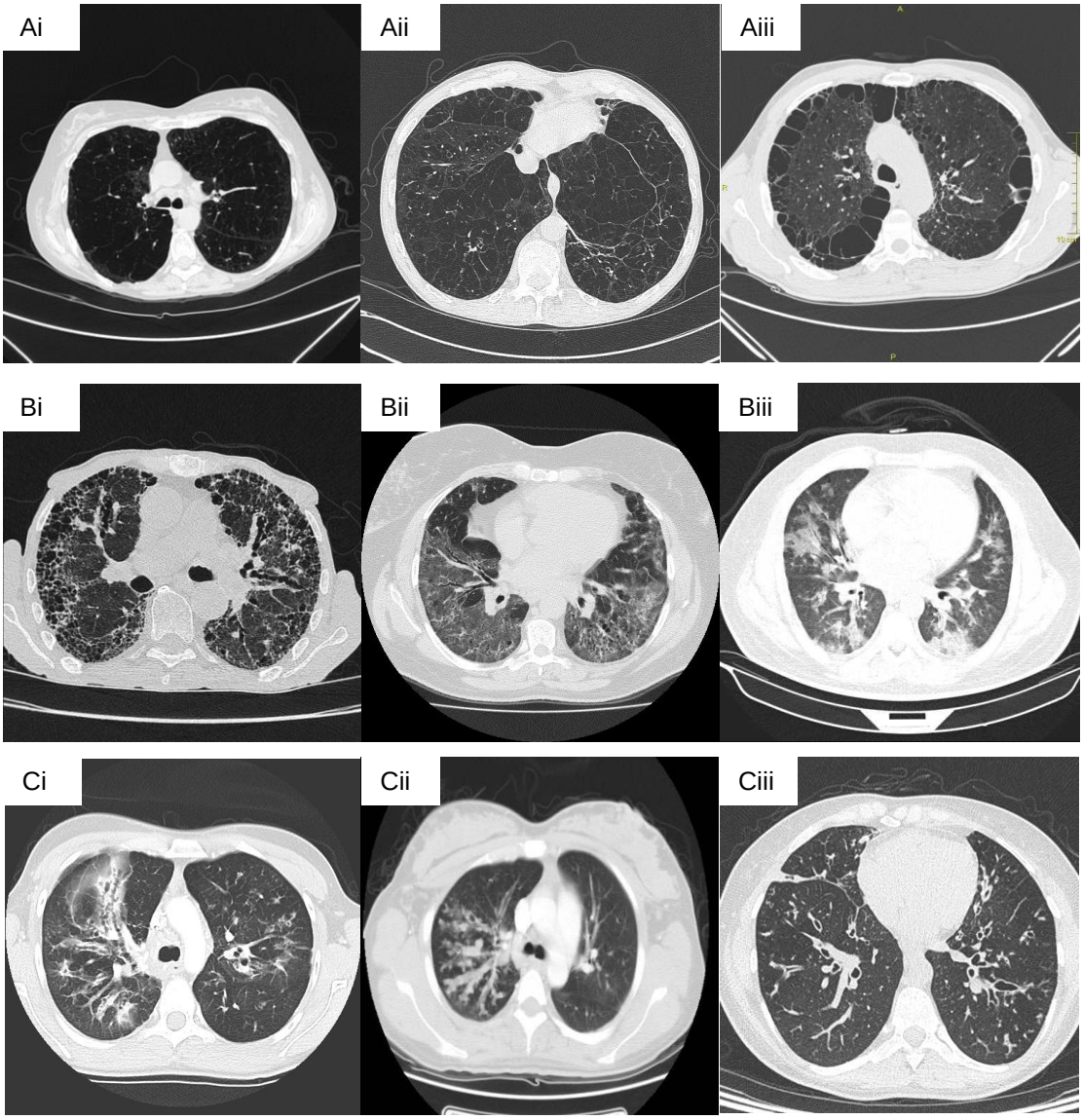

Figure 1.4 The Regional Heterogeneity Observed in Chronic Lung Disease on Computed Tomography (CT) Images. Axial planes in lung windows of different regions of the lung in COPD (A), ILD (B) and CF (C) to demonstrate some of the radiological differences observed between and within phenotypes. (Ai) Centrilobular emphysema with extensive destruction of the lung parenchyma with an upper lobe predilection. (Aii) Panlobular emphysema, with a characteristic basal predominance with increased lung volumes and severe destruction of the basal segments. (Aiii) Paraseptal emphysema with a peripheral distribution, adjacent to the pleura and septal lines, with bullae in the periphery of the secondary pulmonary lobule. (Bi) Usual interstitial pneumonia (UIP) whereby there is advanced pulmonary fibrosis with extensive sub-pleural interlobular septal thickening and marked peripheral honey-combing, more pronounced basally. There is widespread traction bronchiectasis throughout. (Bii) Non-specific interstitial pneumonia (NSIP) with bibasilar ground-glass opacities associated with reticulation and traction bronchiectasis, with evidence of some sub-pleural sparing. (Biii) Cryptogenic organising pneumonia (COP) with alveolar ground-glass opacities with a predominantly peripheral and peri-bronchial distribution, particularly within the middle and lower lobes of both lungs. (Ci) Cystic fibrosis with cylindrical and varicose bronchiectasis in the central and upper lobes, associated with centrilobular nodular opacities and background mild mosaic attenuation. (Cii) Cystic fibrosis with extensive mucus plugging in the right lung. (Ciii) Cystic fibrosis with bilateral cylindrical bronchiectasis, predominantly in the lower, lingula and middle lobes, associated with peri-bronchial thickening and mucus plugs, especially in the lower lobes. Images from Radiopaedia [134], full image credits in Appendix 1.

The severity of disease, and primary endpoints for drug trials, are commonly determined by clinical parameters such as lung function testing. However these parameters do not determine the actual cause of lung dysfunction or quantify the contribution of inflammation to reduced lung function [135]. In order for effective therapies to be developed, a firmer understanding of the inflammatory contribution across different areas of the lung is essential, and imaging techniques can be utilized for this purpose in addition to quantifying lung destruction. Inflammation in non-infectious respiratory diseases can be identified by characteristic alterations in lung density, which can be visualized through CT imaging [135]. However these characteristic density changes are not specific for inflammation and more definitive measurements of inflammation have recently been characterised. These include molecular functional imaging techniques such as positron emission tomography (PET) with fluorodeoxyglucose (^{18}F-FDG) uptake, ^{67}Gallium-Citrate (Ga) and ^{68}Ga-Citrate localization, leukocyte radiolabelling, and somatostatin receptor (SSTR) and translocator protein imaging [135]. An increase in lung ^{18}F-FDG uptake has previously been correlated as a measure of inflammatory response within the lung, and a marker of neutrophil recruitment [136, 137], as well as the activation of macrophages, eosinophils and lymphocytes [138-140]. There have been a number of small ^{18}F-FDG uptake studies involving CF patients, establishing it as an effective measure of lung inflammation [141] as well as correlating the uptake rate with lung function decline and exacerbation [141-143].

^{67}Ga-Citrate and ^{68}Ga-Citrate have been utilised in pre-clinical models to measure inflammation, with ^{67}Ga-Citrate thought to bind lactoferrin within neutrophils [144], whilst ^{68}Ga-Citrate is thought to enhance spatial resolution of inflammation as well as aid quantifiable uptake [145]. In recent years, radiolabelled neutrophils have been used to quantify neutrophil migration in a small number of patients with COPD [146], with a significant increase observed in accumulation of labeled neutrophils in the lungs of COPD patients compared to healthy controls. SSTR expression has previously been described on endothelial cells and fibroblasts isolated from IPF tissue samples [147], and is also expressed on other leukocytes such as monocytes and macrophages, although not neutrophils [148]. Given SSTR imaging has been a commonly used technique in other disciplines such as the imaging of neuroendocrine tumours, agents such as ^{68}Ga-DOTANOC and ^{68}Ga-DOTATATE could be used to image various isoforms of SSTR across the lung. Finally, the

translocator protein, previously peripheral benzodiazepine receptor, can be bound and visualized by radiolabeled isoquinoline, which has been demonstrated in a rabbit model to correlate with macrophage recruitment to the lungs following artificially induced lung injury [149]. Each of these techniques presents an opportunity to visualise inflammation across the lungs, particularly in diseases that are inherently so heterogenous. Whilst some of these techniques are currently limited to animal models only, they present an opportunity to understand how inflammation may manifest regionally and therefore evaluate the efficacy of existing therapies and identify new therapeutic targets.

Although lung disease heterogeneity has been widely demonstrated using imaging techniques, there have only been a handful of supporting articles considering the prospect of regional variation in lung immunology at a tissue level. Baharom et al. (2016) demonstrated differences in monocyte and DC density between different compartments by performing sampling of the healthy lung [150]. They found these cells increased as they sampled further into the airway, demonstrating that regional differences, even in healthy lungs, are integral to consider for inflammation research. Regional variation of leukocyte content is unsurprisingly not restricted to healthy lung tissue. It has also been demonstrated in lung diseases such as CF, not only between upper and lower lobes [151], but also between the middle regions of the left and right lungs [152]. Battaglia *et al.* (2007) explored the distribution of inflammatory cells in both the small and large airways in cancer resection patients who were current or ex smokers [153]. Utilising immunohistochemistry, they found that neutrophils and mast cells had a non-uniformed distribution across the bronchial tree, with significantly more of each cell type present in the small, peripheral airways than the large airways. The notion of regional variation is also not limited to leukocytes, but supported by factors such as microbiota distribution. There have been spatially heterogenous microbiota characterized across the lungs of CF patients, as part of a case study of a child undergoing lobectomy [154], as well as a larger study utilising multiple sampling methods [155].

Armstrong et al (2017) reported regional variation in the lung via microRNA profiling of the upper and lower lobes of 16 healthy subjects [156]. Their findings support a divergence in microRNA expression between lobes, both within alveolar macrophages and the lavage fluid, that have

potential downstream impacts on inflammation. Indeed, microRNA has been implicated in the molecular pathogenesis of a number of lung diseases; miR-218-5p is expressed in the bronchial airway epithelium but downregulated in patients with COPD, resulting in a loss of protection from cigarette smoke induced inflammation (27409149). This could perhaps explain why the correlation of smoking and the development of COPD is somewhat variable between individuals. Aberrant microRNA expression including miR-126 [157] and miR-93 [158] have also been demonstrated in several studies concerning CF. However these studies are often limited to cell lines or isolated bronchial brush sampling [159] and therefore such aberrant microRNA expression cannot be reliably associated with the heterogeneity of CF disease.

The regional variation of leukocyte populations is an important aspect of lung disease, as various leukocyte subsets have been implicated in the pathogenesis of many diseases. Airway neutrophilia, neutrophil degranulation and altered functional activity are some of the commonly described attributes of chronic inflammatory lung diseases including COPD and CF, and are correlated with disease progression [160]. Macrophages have been shown to modulate the induction and resolution of inflammation, and play a role in neutrophil regulation. AMs are thought to limit the initial stages of neutrophil extravasation into tissue, whilst IMs have been shown to promote neutrophil removal from the lung [161]. However, impaired phagocytosis and aberrant polarisation of these key leukocytes have been shown to induce progressive lung inflammation in COPD and asthma [162]. Changes in the circulating frequency of some leukocytes have also been described as biomarkers for disease activity, clinical phenotypes of disease, treatment response or worsened severity. An imbalance in the frequency of natural killer (NK) cells and T cell subsets has correlated to increased risk of ILD occurrence and progression in patients with rheumatoid arthritis (RA) [163], whilst a low relative lymphocyte count is associated with severe COPD and mortality in elderly patients [164].

The heterogeneity of chronic lung diseases, their subsequent clinical phenotypes and the regional variation of disease within the lung are well established. However, the correlation between the regional variation of inflammatory patterns and the different phenotypical presentations within diseases has not been fully explored. Specifically, the identification of prominent leukocyte

populations within these different regions may give useful information regarding the upstream signaling processes that result in the different clinical phenotypes of chronic lung disease.

1.4 Limitations of Current Research Techniques

Imaging studies undoubtedly hold high potential for allowing visualisation of the whole lung, and in turn assessing regional inflammation, however there are a number of disadvantages to their use for this purpose. Firstly, the utilisation of this research technique requires a specialist radiologist to interpret the images obtained. Another major limitation is the exposure of patients to potentially harmful radiation for research purposes [165]. In the instance of CF, such cumulative radiation exposure is of great concern, given that this lung disease tends to manifest at a much younger age. Therefore any imaging techniques utilised for research assessments should correlate closely with the clinical need for imaging at that time. Finally, whilst imaging studies may allow visualisation of general inflammation, and in some instances enable specific cell types such as neutrophils to be identified, this type of research lacks the ability to truly phenotype the different leukocyte subsets residing within a region. There is also a lack of tangible sample to enable *ex vivo* and *in vitro* analysis that may yield important mechanistic insights into a disease.

Given the value of obtaining physical samples to facilitate extensive analysis, it is no surprise the majority of research into the inflammatory profile of lung disease has been carried out using techniques such as BAL, bronchial biopsies, sputum sampling and peripheral blood collection [166].

BAL in particular has been established as a key tool in the advancement of pulmonary research over the past 50 years [167]. The technique involves the introduction of sterile saline into an area of the lung and subsequent fluid removal to analyse the cellular, bacterial and viral content of the airway. The right middle lobe and the left lingula are heavily favoured for BAL because maximal recovery of fluid is aided by the anatomy of these lung regions [168]. Given that they are anteriorly projected, when a patient is lay on their back during bronchoscopy, fluid return is assisted by gravity [169]. Whilst BAL is a highly accessible tool for researchers, this sampling method has been

criticised for a lack of reproducibility and accuracy [166]. This may in part be due to the recovery of fluid during BAL sampling being inhibited by the extent of disease [170], increasing the variability of sampling and restricting reliable sample returns to mild or moderate phenotypes.

Bronchoscopy with bronchial biopsies allow sampling of airway tissue to facilitate insight into airway morphology in health and disease, however the technique is limited. Firstly, sampling is confined to the larger airways and as such may not be reflective of inflammatory processes occurring within the periphery of the lungs [39]. Furthermore it is not possible to sample the entire airway, and given regional heterogeneity within disease is widely recognised, it could lead to the under- or over-representation of disease burden. This is of specific relevance to ILD, whereby the National Institute for Health and Care Excellence (NICE) recommends at least 5-6 transbronchial lung biopsies (TBLB) are taken from multiple sites in ILD patients suitable for the procedure, to improve the diagnostic yield of the samples [171]. Bronchial biopsies are also limited by their size and subsequent quality. Samples are often small (0.3 – 0.5 mm^2) and desquamation by forceps may lead to inadequate sampling of the epithelium, so called crush artefact. Furthermore, the high degree of variation in the depth of each biopsy obtained can lead to inadequate sampling of the subepithelial compartment [172]. These limitations can often lead to ambiguous histological profiles between samples and lobes, which can result in little diagnostic value.

Given that many diseases manifest in destruction of the lung parenchyma, particularly in peripheral areas, access to such samples is paramount to further delineate the mechanisms that underpin the disease process. Research bio-banks have improved access to much larger lung tissue samples from patients undergoing thoracic surgery for confirmed or suspected lung cancers, with or without underlying chronic inflammatory lung conditions. However, there are major limitations to utilising such tissue for the immune characterisation of chronic inflammatory lung disease. Firstly, although tissue for research is taken distal to the tumour, the influence of cancer on leukocyte phenotypes isolated from the same lobe must be questioned. Shimizu et al. (2007) demonstrated an increased frequency of NK cells in the lung interstitium of patients with lung cancer, postulating that this increase was secondary to the presence of malignancy within the same region [173]. A second limitation is the amount of time between procurement of tissue from the patient and the subsequent

analysis of immune content. In order to accurately immunophenotype and provide meaningful quantitative and qualitative data regarding leukocyte populations within a disease, leukocytes should be isolated from fresh lung tissue [173]. Whilst many groups utilise tissue resections from cancer surgeries to study leukocytes [153] [174] [173] the tissue is dependent upon release from a histopathologist. Samples obtained from patients who undergo surgery late into the afternoon are often left overnight in the fridge, without media, before review by a histopathologist. Finally, lung tissue samples procured through biobanks are taken from an isolated region of the lung dependent upon the location of malignancy. As such, the sampling sites not only differ between patients but also may not be entirely reflective of disease across the whole lung.

Whilst the described sampling techniques have facilitated the research of chronic lung conditions and their associated inflammatory processes, their limitations have led to inconsistencies within the literature. Baharom et al (2016) and Rutgers et al (2000) have highlighted how isolated sampling can inhibit immunological investigation as the identification of different cell populations have been shown to be dependent upon the sampling technique used and the subsequent compartment of the lung from which they are derived [175, 176]. Given that the performance of these sampling techniques may also be limited due to underlying disease severity, as well as the diverse methodologies used to analyse samples, the characterisation of inflammation in chronic lung diseases has become increasingly difficult [177].

An improved platform to characterise inflammation in lung disease may be to obtain whole tissue samples from the explanted lungs of patients undergoing transplantation for end-stage lung disease [178], [179], [180]. Multi-lobar whole tissue samples from explanted lung tissue would enable multi-lobe interrogation and facilitate the assessment of lung inflammation across the lung as a whole, a process that is not possible with other sampling techniques. Furthermore, the procurement of samples immediately upon lung explantation would ensure accurate immunophenotyping by reducing the attrition of cells during storage. However, the accessibility of obtaining explanted lung tissue has limited its use, compared to other lung sampling techniques. This is in part due to the specialist nature of transplantation and the limited number of sites at which they are performed, but also, the erratic, unpredictable nature of when transplants may occur.

Given that lung transplantation is predominantly performed in patients with more severe, chronic lung disease, the relevance of characterising the lung in such patients may also be questioned. However, although viable lung tissue is greatly reduced in explanted lungs prior to transplantation when compared to earlier stages of the disease, it is still important to understand the natural history of disease from beginning to end [181]. Furthermore, patients on the waiting list for transplant will often continue to deteriorate clinically, with frequent exacerbations, suggesting that the inflammatory processes are on-going. Indeed, patients who then progress to a more advanced, end stage disease, may then be deemed unsuitable for transplantation.

In chronic lung disease there is a recognised regional variation in underlying inflammatory processes. The use of multi-lobar tissue samples from explanted lungs may help to characterise the different regional inflammatory phenotypes and determine whether this contributes to the marked heterogeneity within each disease group. Given the fundamental lack of information regarding leukocyte distribution and phenotype of the lung as a whole, this would be an essential first step for the characterisation in chronic lung disease.

1.5 Hypothesis and Aims

The regional variation of leukocytes and cytokines across the chronically diseased lung are poorly understood. As such, the hypothesis and aims of the project will largely be led by fundamental discovery and will allow the project to be determined by key findings with a continuous evolution of aims. However a broad hypothesis for the project can be considered as;

There are fundamental differences in inflammation across the lungs of patients with end stage chronic lung disease (COPD, CF and ILD) requiring transplantation that can be characterised by regional sampling of different lobes of the lungs.

The initial aims of the project will be to achieve the following objectives:

1) Establish a protocol to enable the collection of regional lung samples from the native lung during transplantation
2) To characterise immune cell populations residing within different peripheral regions of the COPD, ILD and CF lung
3) To characterise other inflammatory markers across the same regions
4) To explore the loss of homeostatic mechanisms that may drive lung heterogeneity in disease

Chapter Two: Methodology

2.1 Ethical Approval and Patient Recruitment

The research study 'Exploring the mechanisms of homeostasis and disease before and after lung transplantation' was approved by the North West Liverpool Central Research Ethics Committee (14/NW/0260) and carried out at Manchester University NHS Foundation Trust (MFT). Patient inclusion criteria required patients to be 16-80 years old, active on the lung transplantation waiting list or a previous recipient of a lung transplant, and able to provide informed consent. Patients listed for either double (DLTx) or single (SLTx) lung transplantation were considered for the study, and all disease diagnoses were included. Eligible patients were identified with the help of the MFT transplant coordinators and approached upon admittance to MFT for transplant, or during routine pre-transplant clinic visits, and consented to the study. Due to the unpredictable nature of transplant, patients were given participant information sheets and consent was taken immediately following a discussion about the study. Patients who had already undergone lung transplantation were approached during routine post-transplant clinic visits. These patients were given the option to provide same-day consent or take home an information sheet for reflection. Patients who consented to take part in the study were given a unique identifying code (LTx-01, 02, 03 etc.), which referenced the order they were consented, not necessarily the order they received a transplant. These LTx codes are referenced throughout the thesis to describe and link patient data.

From April 2016 to June 2019, there were 118 patients recruited to the research study. During this time period, there was 224 donor offers, of which 86 went ahead to transplant. This study utilised samples from 49 different patients, 36 of whom had samples taken at the time of transplant.

2.2 Procurement of Fresh Explanted Lung Samples

The human biological samples were sourced ethically, and their research was used in accordance with the terms of informed consent. Fresh lung tissue was collected from cardiothoracic surgeons in theatre immediately following native lung explant; samples were taken from the upper lobe, middle lobe (or lingula) and lower lobe from peripheral areas of each explanted lung. These samples are referred to throughout the thesis as left upper (LU), lingula (Ling), left lower (LL), right upper (RU),

right middle (RM) and right lower (RL). The samples were taken directly to the transplant research laboratory for immediate processing, or snap frozen and stored at -80°C for later use. A detailed summary of how the tissue was used will be provided in the appropriate analytical methodologies.

2.3 Histological Analysis

Following tissue collection, the explanted lungs were all processed for clinical histopathology at MFT as part of routine clinical practice. An explant histopathology report was generated for each patient and made available to the research team upon request.

2.4 Clinical History

All clinical history was collected retrospectively for patients who went on to have samples that were actively used in some form of analysis. Clinical notes were scribed to cover clinical diagnosis and progression, smoking history or other relevant exposures, lung function testing, medications and any co-morbidity. In the COPD group, the most recent lung function was reviewed and FEV_1 was used to determine the severity of disease in accordance with the Global Initiative for Chronic Obstructive Lung Disease (GOLD) classification (Table 2.1).

Table 2.1 The classification of airflow limitation severity in chronic obstructive pulmonary disease (COPD). The spirometric cut-points for classifying COPD severity based on post-bronchodilator forced expiratory volume in one second (FEV_1) in patients who have a FEV_1/forced vital capacity (FVC) of < 0.70 as determined by the Global Initiative for Chronic Obstructive Lung Disease (GOLD) [182].

GOLD Classification	Description
GOLD 1 (Mild)	FEV_1 > 80%
GOLD 2 (Moderate)	FEV_1 50% - 79%
GOLD 3 (Severe)	FEV_1 30% - 49%
GOLD 4 (Very Severe)	FEV_1 <30%

2.5 Flow Cytometry

2.5.1 Single Cell Suspension

The primary objective of the study was to characterise leukocyte content across different regions of the lungs using flow cytometry. In order to achieve this, a single cell suspension was generated from the tissue samples and a broad leukocyte panel was utilised to identify major leukocyte subsets. The disassociation of cells from whole tissue to generate a single cell suspension can be achieved by numerous approaches, such as enzymatic or mechanical methods, either in combination or separately. Liberase is a refined cocktail of purified collagenase and protease enzymes intended to reduce the variable nature of crude collagenase digestion so that cell disassociation becomes a reproducible, high quality process [183]. Liberase blended with a low concentration of thermolysin (TL), is a product that was already utilised by another group in the Manchester Collaborative Centre for Inflammation Research (MCCIR) for human and mice lung tissue disassociation and has been used for lung digestion by other groups in a variety of species [184-186]. The following methodology is an established technique within the MCCIR and was scaled appropriately for 1g of tissue. A detailed list of the reagents and consumables used throughout this study can be found in Appendix 2.

After obtaining samples, 1 g of each sample was processed immediately into a single cell suspension. Fresh tissue was diced and digested with an enzyme cocktail of Liberase TL (Roche, Switzerland) (0.8 U/ml) and DNAse (Sigma Aldrich, UK) (80 U/ml) in Hank's buffered saline solution (HBSS) (+Mg +Ca) (Thermo Fisher Scientific, US) for 45 minutes at 37°C in a rocking water bath. After 20 minutes samples were gently mixed by inversion and then incubation continued. An EDTA stop solution (2 mM in phosphate buffered saline solution (PBS) containing 2% fetal calf serum (FCS)) was then added to the samples to cease enzyme activity, and filtered through 500 µm (Cambridge Bioscience, UK) then 70 µm (Falcon™, Corning, US) cell strainers before undergoing a red blood cell lysis step (BD Pharm Lyse^{TM}, Becton Dickinson, US). A wash step consisting of adding 2 ml PBS and centrifugation for 10 minutes at 700 x *g* was then performed. Finally, the cells were counted using trypan blue on a haemocytometer and re-suspended at 2 x 10^6 cells/100 µl for

flow cytometry staining or cryopreserved for later use. Cells requiring cryopreservation were centrifuged at 700 x *g* for 5 minutes at 4°C and suspended in FCS containing 10% dimethyl sulfoxide (DMSO) at a concentration of 10 x 10^6 cells/ml. These samples were then placed into a Nalgene® Mr Frosty (Thermo Scientific, US) filled with propan-2-ol for controlled freezing down to -80°C.

2.5.2 Phenotype Staining

Cells were stained with a broad leukocyte panel to allow the detection of T cells (CD3, CD4, CD8, FOXP3), B cells (CD19), NK/NKT cells (CD56, CD16, CD3), Granulocytes (CD66b, CD117, Siglec-8), mononuclear phagocyte system cells (MPS: monocytes and macrophages) (CD64 against fluorescein isothiocyanate (FITC), CD16, CD14, Human leukocyte antigen-DR isotype (HLA-DR)) in additional to a pan leukocyte marker (CD45) and a viability stain (Zombie UV™ (ultraviolet)). All antibodies were purchased from BioLegend (US) except for CD8 (eBioscience, US), and used at a 1:200 PBS staining dilution except for HLA-DR at 1:150 and Zombie UV at 1:100. A list of the antibodies, clones, suppliers and catalogue numbers can be found in Appendix 3. The panel design and antibody optimisation was performed in house at the MCCIR by Dr Anu Goenka/ Dr Peter Cook and shared collaboratively with members of the MCCIR. An antibody cocktail was made up for the appropriate number of samples (n=6 or n=3) upon the transplant being confirmed, and kept at 2-8°C until required. To determine viability, 1 µl of Zombie UV™ was added to 2 x 10^6 cells in 100 µl PBS and incubated in the dark at room temperature for 30 minutes as per the manufacturers protocol (BioLegend, Appendix 4). Following a wash step that consisted of 500 µl flow buffer and centrifugation at 700 x *g* for 5 minutes, the cell pellet was re-suspended in 50 µl of antibody cocktail and incubated for 15 minutes at 2-8°C. The cells were then washed again and an intracellular protocol was commenced (BioLegend, US, Appendix 4). Following fixation and permeation steps, the cells were stained with FOXP3 for 30 minutes at room temperature in the dark. Finally, cells were washed twice, as directed in the intracellular staining protocol, and then re-suspended in 200 µl of flow buffer. Cells were covered in parafilm to prevent evaporation, and stored at 2-8°C to be run within 48 hours. To allow ratiometric enumeration of cells, 20 µl of 123count eBeads

(ThermoFisher, US) were added to each sample immediately prior to running. Samples were run on a BD LSRFortessa for 3 minutes and analysed using FlowJo V.10.1. (TreeStar Inc, US).

In flow cytometry, best practice recommends running all samples alongside fluorescence minus one (FMO) controls to ensure accurate accounting of fluorescence spillover. However, given the unpredictable nature of transplant, and the time-consuming task of generating FMO's combined with long on call and processing hours, a set of FMO's were carried out only once for each disease group. Given the panel design and marker selection was largely restricted to exclusive or brightly-expressed surface markers, discontinuance of FMOs was deemed acceptable.

2.5.3 Analysis

After performing the gating strategy in FlowJo to identify major leukocyte subsets (Figure 2.1), data was exported to excel and total cell numbers were calculated using the following formula;

$$\frac{\left(\frac{C_c eB_v}{eB_c V_s}\right) eB_{conc} V_{ts}}{T_w} = Cells/gram$$

$C_c = Cell\ count$

$eB_v = eBead\ volume$

$eB_c = eBead\ count$

$V_s = Staining\ volume$

$eB_{conc} = eBead\ concentration$

$V_{ts} = Total\ sample\ volume$

$T_w = Tissue\ weight$

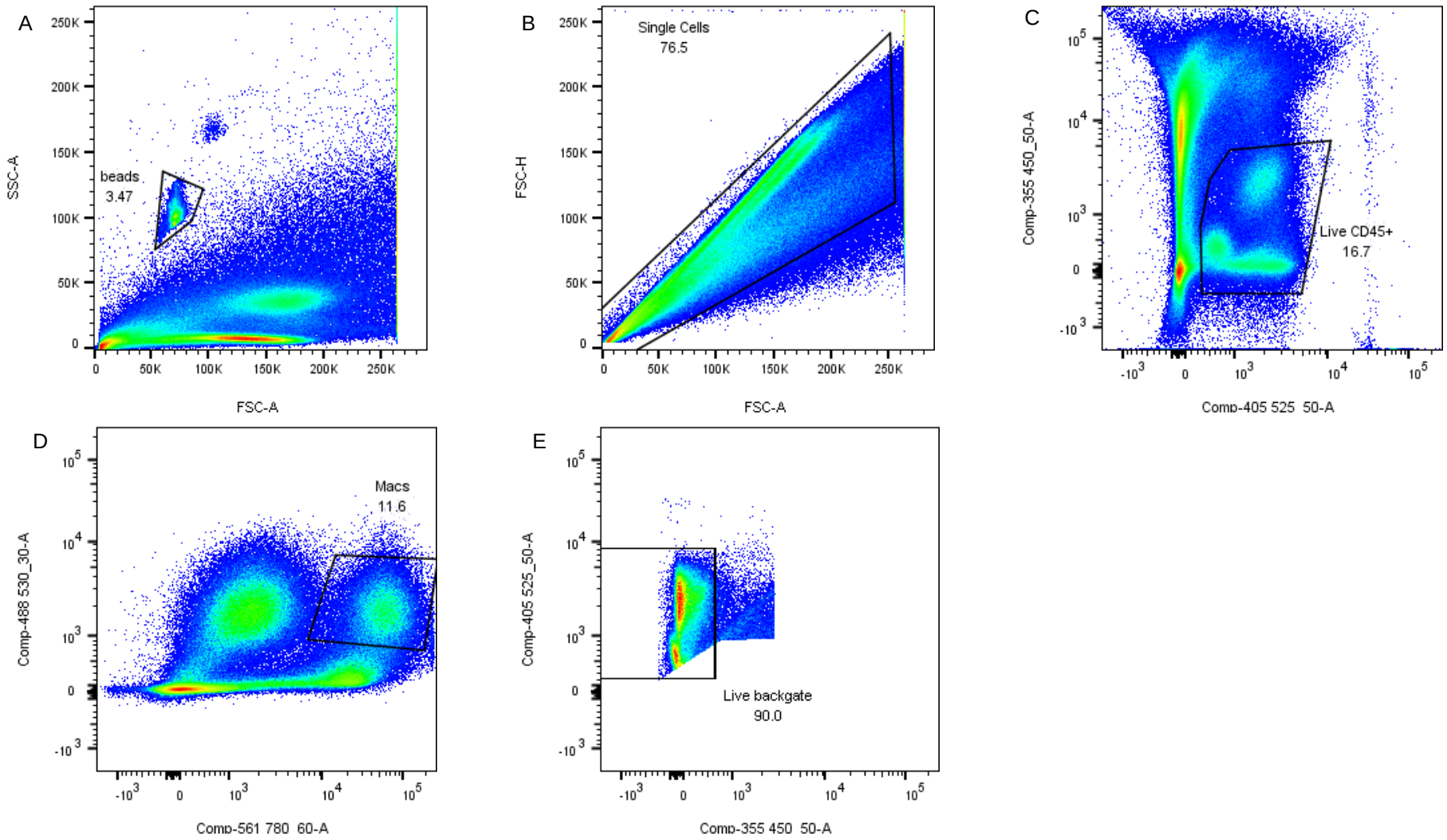

Figure 2.1 Representative images of the gating strategy for identifying leukocytes in lung tissue. The initial steps required the exclusion of counting beads (A), removal of doublets (B) and identification of live CD45+ cells (C). Macrophages were gated on their expression of CD64 vs autofluorescence in the FITC channel (D) before a live back gate was performed on remaining cells (E).

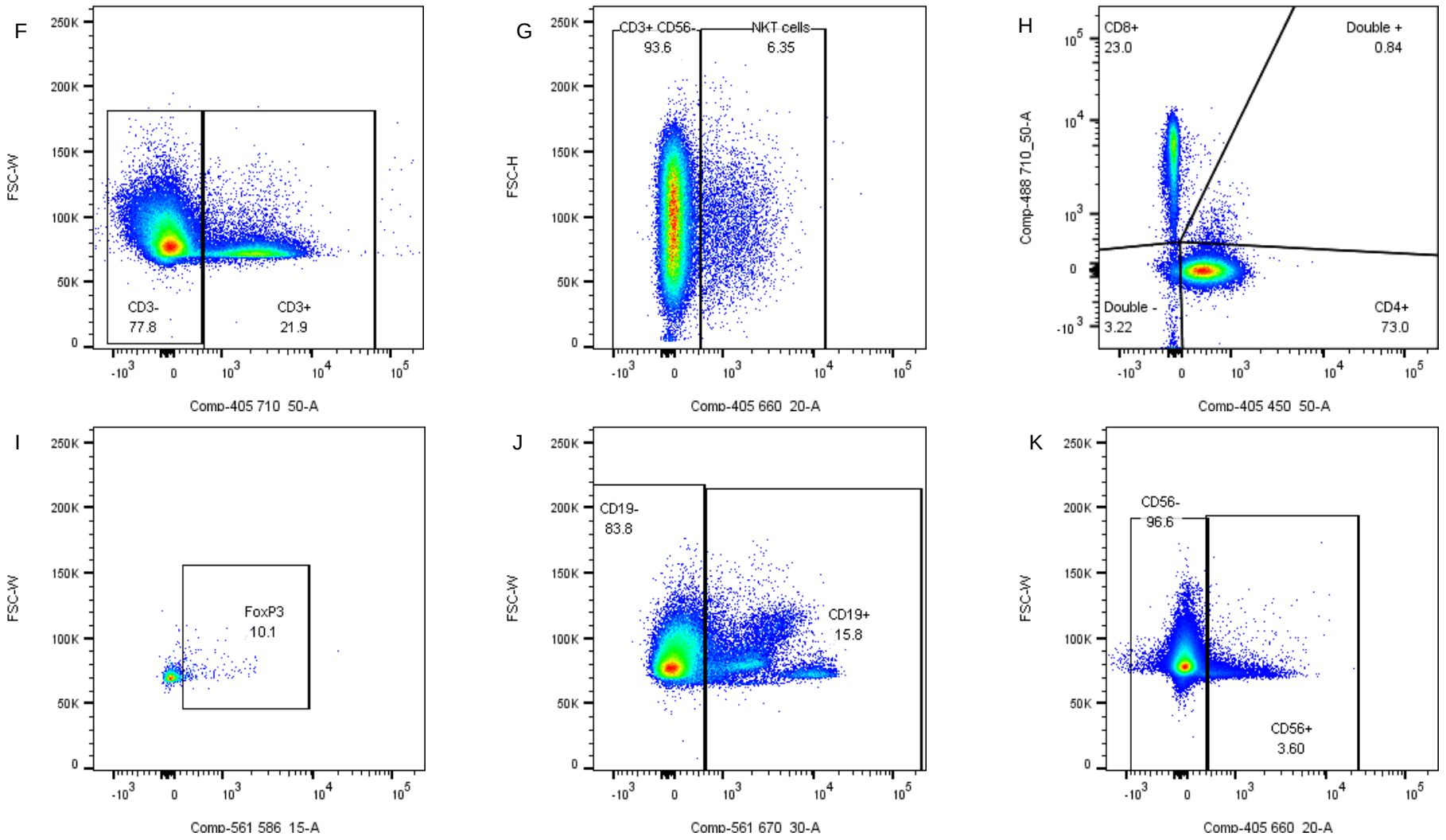

Figure 2.1 Representative images of the gating strategy for identifying leukocytes in lung tissue continued. CD3+ cells were identified and categorised into NKT, CD4+, with and without FOXP3 expression, and CD8+ cells (F-I). CD3- cells were further categorised into CD19+ (J) and NK (K) populations.

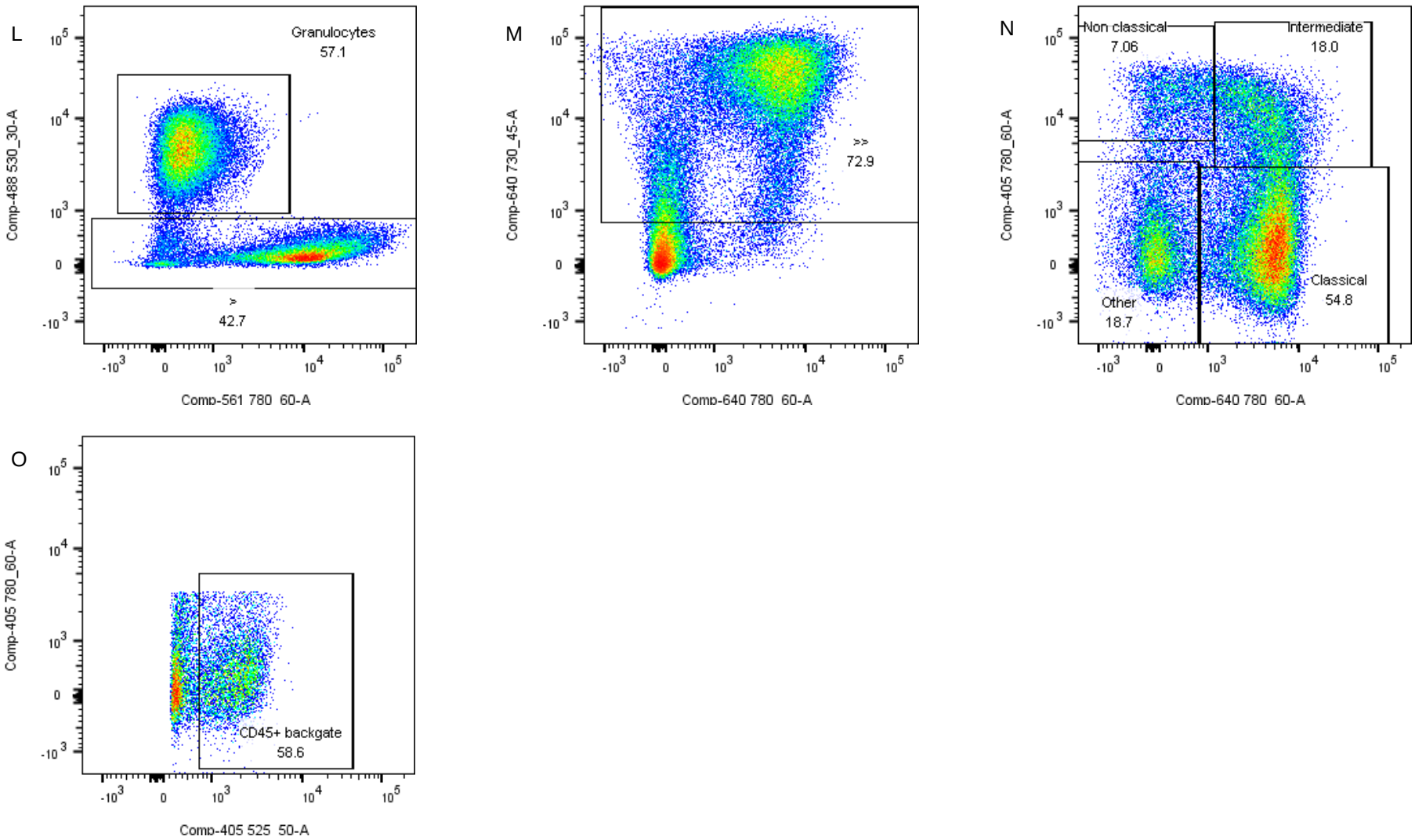

Figure 2.1 Representative images of the gating strategy for identifying leukocytes in lung tissue continued. Granulocytes were then identified (L) before the remaining cells were assessed on MHC-II expression (M) and monocyte subsets were gated (N). Remaining cells were re-gated on CD45+ expression to leave leukocytes unable to be identified within the scope of the panel (O).

2.6 Luminex Analysis

The concentration of 13 cytokines and chemokines within the regional tissue samples were measured in tissue lysate generated from snap frozen tissue (Section 2.2). Approximately 80-120 mg of tissue was mechanically dissociated in 500 µl of radioimmunoprecipitation (RIPA) buffer plus cOmplete protease inhibitor cocktail (one tablet/10 ml, Roche, Switzerland) using a handheld homogeniser (Polytron® PT1200E, Kinematica Inc). Samples were incubated on ice for 1 hour, and then centrifuged at 14,000 x *g* for 3 minutes and supernatant stored at -20°C until processing. This methodology was derived from GBiosciences (Appendix 4), but to increase the protein concentration of the tissue lysate and allow further downstream dilution, the volume of RIPA buffer was reduced by half.

Total protein content was determined using a bicinchoninic acid (BCA) protein assay (Pierce™, Thermo Scientific, US) as directed by manufacturers protocol (Appendix 4). Briefly, 25 µl of bovine serum albumin (BSA) standards and samples diluted at 1:10, 1:100 and 1:200 were plated onto a 96 well plate then 200 µl of working reagent (BCA reagent A plus BCA reagent B, 50:1) was added. The plate was mixed thoroughly then incubated at 37°C for 30 minutes before being read using an Infinite® 200 PRO plate reader (Tecan, Switzerland) at an absorbance of 562 nm. Samples were adjusted with assay buffer to 1 mg/ml total protein in a total volume of 75 µl to immediately perform the assay.

A commercially available human 13-plex magnetic bead panel (Merck Millipore, US) was utilised, following the manufacturer's protocol (Appendix 4). Briefly, 200 µl of wash buffer was added to all wells of a 96 well plate prior to use and incubated on a plate rocker for 10 minutes at room temperature. During this time, the 13 individual magnetic bead bound antibodies were prepared by thoroughly vortexing each vial for 1 minute then adding 60 µl of each antibody into a mixing bottle containing 2.22 ml of bead diluent. The buffer was decanted from the 96 well plate and 25 µl of assay buffer was added to all wells, then 25 µl of samples, standards or controls were added to

appropriate wells. Finally, 25 µl of the antibody bead cocktail was added to all wells and the plate was covered in foil and incubated on a plate shaker at room temperature for 2 hours. The plate was decanted and washed twice with 200 µl wash buffer using a magnet plate holder. The procedure for washing required the plate to rest on the magnet for 60 seconds before removing plate content by decantation and blotting. The plate was then removed from the magnet before the second wash volume was added, shook for 30 seconds and placed back onto the magnet to repeat the steps. This process was carried out for each wash step. Next, 25 µl of detection antibodies were added to all wells, covered in foil and incubated on a plate shaker at room temperature for 1 hour. Directly after incubation, and without aspiration, 25 µl of Streptavidin-Phycoerythrin was added directly to all wells. The plate was covered and incubated on a plate shaker for a further 30 minutes at room temperature. The plate was decanted and washed twice with 200 µl wash buffer using the magnet as directed, then re-suspended in 150 µl of sheath fluid. The plate was then read using a Bio-Plex 200 system which had passed QC test controls prior to use (Bio Rad, Hertfordshire, UK).

2.7 Semi-Quantitative Histological Analysis

The extent of fibrosis, inflammation and fibroblastic foci was semi quantitatively assessed across three regions of the ILD lung (n=13) to evaluate disease severity. A consultant histopathologist performed the assessment using a scoring system of one-three for mild, moderate or severe (Table 2.2). This analysis was performed retrospectively after an ILD specific finding, to relate those findings back to specific regions of the lung more accurately than the routine histological report allowed. To this end, samples from COPD and CF patients were not analysed further in this way.

Table 2.2 Semi-quantitative scoring system for histological assessment of disease severity. The extent of fibrosis, mononuclear inflitration and fibroblastic foci were assessed and given a semi-quantitative score based on the described severity of each parameter.

Score	*Established Fibrosis (EF)*	*Mononuclear Infiltration (MI)*	*Fibroblastic Foci (FF)*
Magnification	*x4*	*x4*	*x10 (10 fields)*
1 – Mild	*Patchy fibrosis/Subpleural*	*Patchy aggregates*	*0-2*
2 – Moderate	*Centrilobular fibrosis bridging to pleura*	*Patchy & extending to septa*	*2-4*
3 – Severe	*Honeycomb lung*	*Diffuse inflammation*	*>4*

2.8 Immune Checkpoint Analysis

2.8.1 Tissue Lysate

The concentrations of 10 different immune checkpoint co-stimulatory molecules of the B7/CD28 family were measured using the same tissue lysate samples generated for Luminex analysis (Section 2.6). Using the results of the previous BCA protein assay, samples were adjusted with sample diluent (RayBiotech, Norcross, GA) to 0.6 mg/ml total protein in a total volume of 150 µl to immediately perform the immune checkpoint array.

The Quantibody® Human Immune Checkpoint Molecule Array 1 (RayBiotech, Norcross, GA) was carried out as per manufacturer's instructions (Appendix 4), with all reagents included within the kit. All washes and incubations were carried out under gentle rocking, and covered in adhesive film if incubation was longer than 2 hours. Slides were air dried prior to use then all wells were blocked by adding 100 µl of sample diluent and incubated for 30 minutes at room temperature. This was then decanted and 100 µl of samples, standards or a negative control were added to the appropriate wells then incubated overnight at 2-8°C. The wells were decanted and washed five times with wash buffer 1, and twice with wash buffer 2. The biotinylated antibody cocktail was reconstituted in 1.4 ml of sample diluent, 80 µl was added to every well, and then incubated at room temperature for 2 hours. After decanting and washing as previously described, the Cy3 equivalent dye-conjugated streptavidin was reconstituted in 1.4 ml of sample diluent and 80 µl was added to all wells and incubated in the dark at room temperature for 1 hour. The wells were then decanted and washed

five times with wash buffer 1, before dismantling the slide from its holder. Slides were then placed into a chamber filled with wash buffer 1 for 15 minutes, then the buffer was replaced with wash buffer 2 and repeated for 5 minutes. Slides were centrifuged at 1000 x rpm for 3 minutes to dry, and then stored in a dry slide chamber wrapped in foil until sent back to the manufacturer for scanning and data extraction.

2.8.2 Immunohistochemistry (IHC)

2.8.2.1 Immunohistochemistry Processing

The expression of programmed death ligand-1 (PD-L1) and B7-H3 were assessed in different regions of the lung. Paraffin blocks generated by histopathology at MFT were available to the research study. Due to the importance of preserving clinical blocks for future diagnostic work, an experienced senior biomedical scientist (BMS) at MFT performed all microtome sectioning and staining. All antibody optimisation, isotype and antibody control conditions were manually performed and reviewed by the senior BMS, but the complete sample set were stained using a fully automated system. Briefly, samples were sectioned at 4 µm using a Thermo Shandon Finesse microtome (Thermo Scientific, US) then stained the same day using a fully automated Benchmark ULTRA (Roche) to preserve staining standardisation and prevent sample variation introduced by human error. Staining control tissue was included on every slide and consisted of placenta, tonsil, a PD-L1+ tumour and a PD-L1- tumour (Figure 2.2). The protocol for PD-L1 staining consisted of 32 minutes of antigen retrieval using cell conditioning 1 solution (CC1, Roche) pH 8 at 95°C followed by incubation with anti-PD-L1 (clone 28-8, ab205921, Abcam) for 32 minutes at RT. An OptiView DAB IHC detection kit (Roche) was used to identify the primary antibody, and then slides were counterstained with haematoxylin for 8 minutes at RT before bluing for 4 minutes. The B7-H3 protocol was similar to PD-L1 with the following modifications; the antigen retrieval step was increased to 64 minutes, incubation with anti-B7-H3 (ab219648, Abcam) was for 24 minutes, and the detection kit used was ultraView Universal DAB. Images were acquired on a 3D-Histech Pannoramic-250 microscope slide-scanner using a *20x/ 0.80 Plan Apochromat* objective (Zeiss,

Germany) and the *DAPI* filter set. Snapshots of the slide-scans were taken using the Case Viewer software (3D-Histech, Hungary).

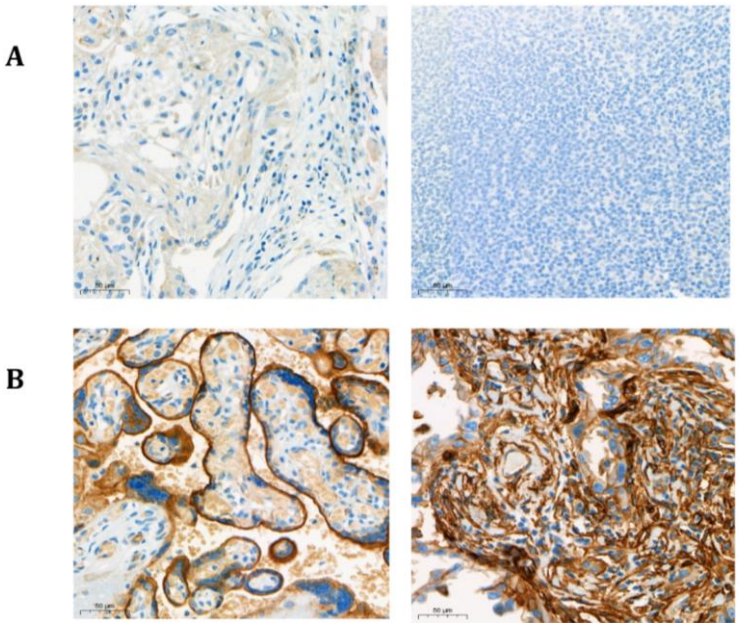

Figure 2.2 Negative and positive control tissue for programmed death ligand-1 (PD-L1) and B7-H3 immunohistochemistry. Control tissue from a PD-L1 negative tumour, a PD-L1 positive tumour, human tonsil and human placenta were included on every slide to act as negative (A) and positive controls (B). All scale bars represent 50 µm.

2.8.2.2 Immunohistochemistry Analysis

Bronchioles and lung interstitium were quantitatively assessed for PD-L1 and B7-H3 staining using the digital microscope application CaseViewer and QuantCenter (3D-Histech, Hungary). Briefly, three (one-three if bronchioles were limited) bronchioles closest to the top, right and bottom of the slide were selected (Figure 2.3.A), and three (one-three depending on size of bronchiole) random field of view (FOV) (20x) were annotated (Figure 2.3.B). Following three lines that dissected the slides into thirds (Figure 2.4.A), the interstitium was analysed by selection of nine random FOV circles (20x) across the slide (Figure 2.4.B). In QuantCenter, colours were selected to represent mild, moderate or intense staining (Figure 2.5), and all annotations on each slide were then run through the software for analysis.

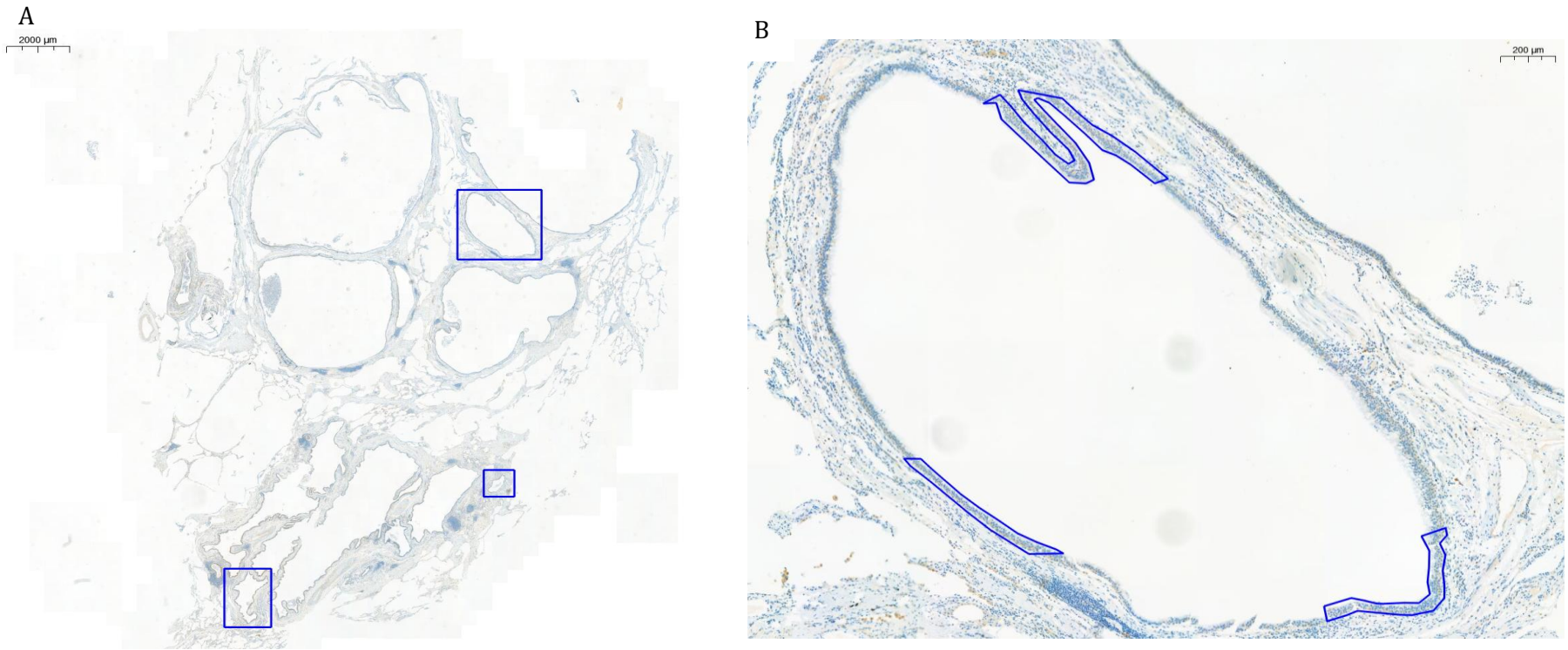

Figure 2.3 Selection of bronchioles and 20x field of views (FOV) for immunohistochemistry analysis. Three bronchioles were selected per slide (A) and then three random FOV at 20x magnification were selected per bronchiole (B). These annotations selected in blue then underwent quantitative analysis. The scale bars represent 2000 µm (A) and 200 µm (B).

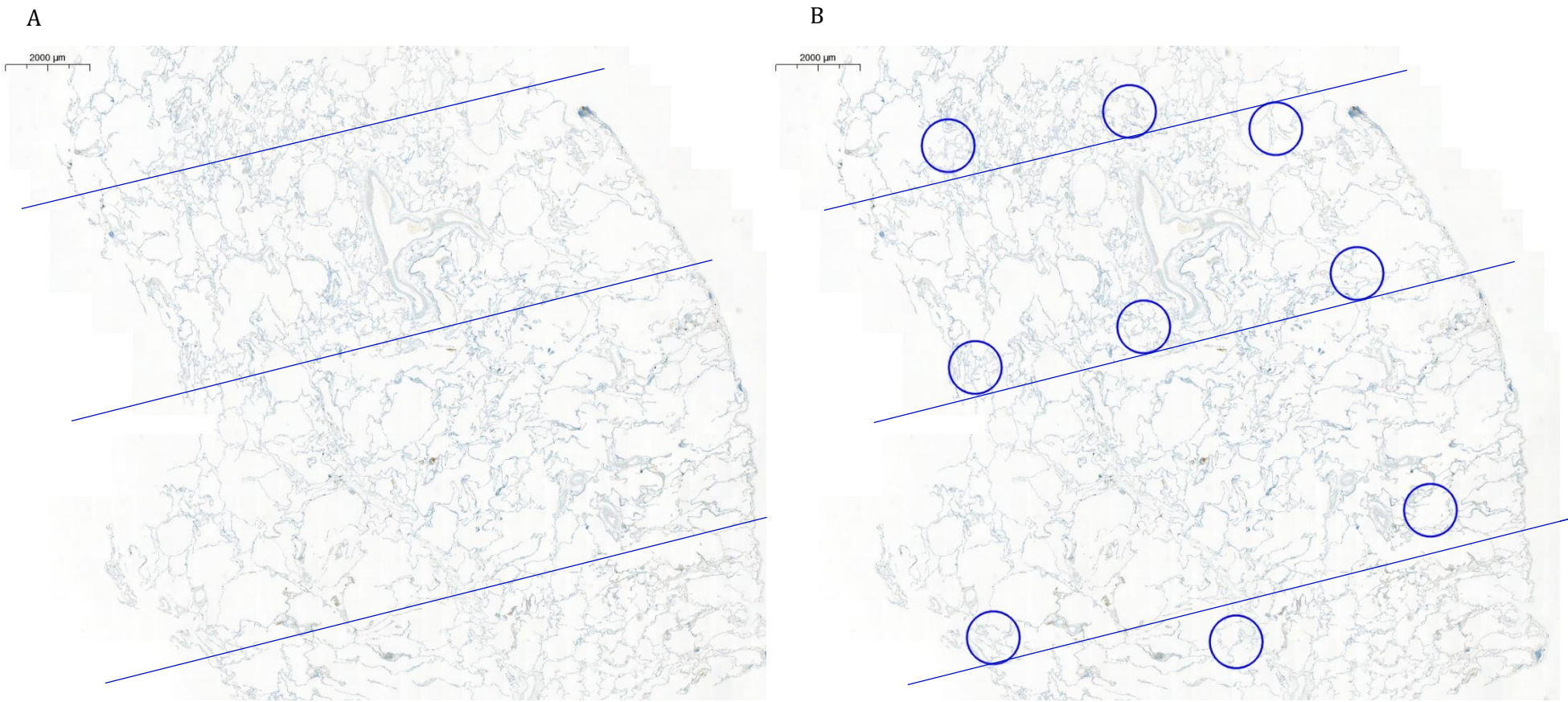

Figure 2.4. Selection of nine interstitium 20x fields of view (FOV) for immunohistochemistry (IHC) analysis. Three lines were annotated across each slide (A) and then nine random FOV circles at 20x magnification were distributed across these lines (B) to ensure uniform coverage across each slide section. These annotations then underwent quantitative analysis. The scale bars represent 2000 µm.

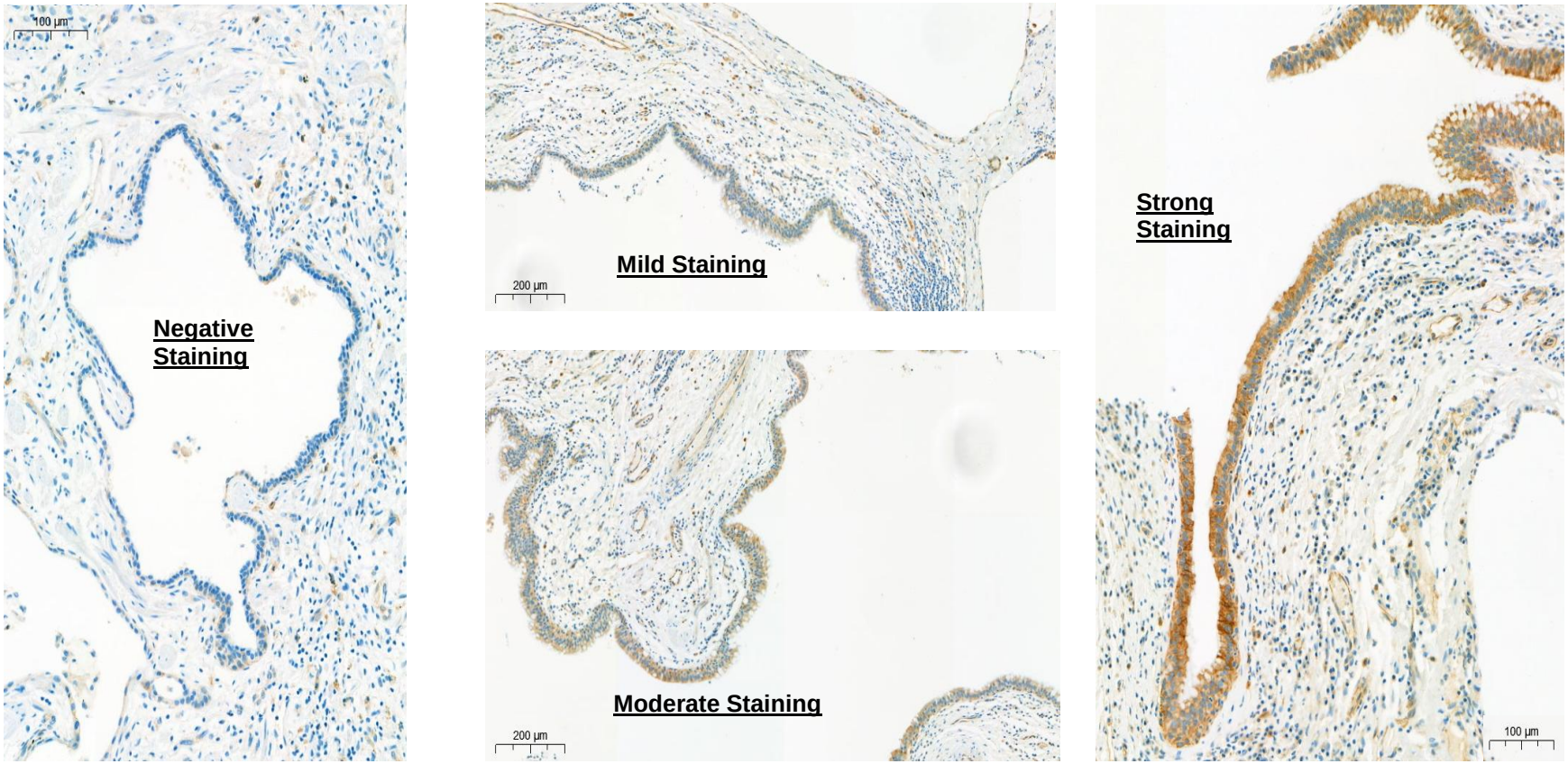

Figure 2.5 Staining intensity methodology for immune checkpoint molecules, programmed death ligand-1 (PD-L1) and B7-H3, for immunohistochemistry analysis. Representative images of the negative, mild, moderate and strong staining intensities used to guide QuantCenter during quantitative analysis of PD-L1 and B7-H3 IHC. Scale bars represent 100 µm for negative and strong staining images, and 200 µm for mild and moderate staining images.

2.9 Cytometry by Time Of Flight (CyTOF)

2.9.1 Sample Thawing

Cytometry by time of flight (CyTOF) was performed on excess cells that had been cryopreserved at the time of transplant and stored at -80°C (Section 2.5.1). Cell samples were rapidly thawed in a water bath at 37°C until only a small ice crystal remained in the sample. Each sample was then transferred to 9 ml of post-thaw solution of equal parts FCS to Roswell Park Memorial Institute (RPMI) media which was pre-warmed to 37°C. Samples were centrifuged at 700 x *g* for 5 minutes at 4°C and then cell pellets were re-suspended in 80 µl of buffer consisting of PBS with 0.5% BSA and 2 mM EDTA.

2.9.2 CD45 Enrichment

CD45+ cells were labeled by adding 20 µl of CD45 microbeads (Miltenyi Biotech, Germany) into the cell suspension, vortexing and incubating for 15 minutes at 2-8°C. Samples were then washed with 2 ml of MACS buffer and centrifuged at 300 x *g* for 10 minutes at 4°C. Samples were then passed through Miltenyi LS columns on a strong magnet to capture CD45+ cells as per Miltenyi LS column protocol. After CD45+ enrichment, samples were cell counted using a NC-250 (Chemometec, Denmark) for total number and viability. Samples were adjusted with cell staining buffer (CSB) (Fludigm, US) to allow staining of 2 x 10^6 cells for CyTOF.

2.9.3 Staining

Cells were stained with comprehensive myeloid and lymphoid panels (Table 2.3) to enhance characterisation performed during flow cytometry. All antibodies were purchased from the MCCIR CyTOF antibody bank and used at a 1:100 staining dilution. Barcoding of samples was performed to maximize the efficiency of antibody availability, by staining individual samples with different CD45 conjugations. CD45 was bound to metals 89, 115 and 198 and were used singularly or in combination. Cells were stained following a Fluidigm (US) CyTOF staining protocol (Appendix 4). Briefly, cell pellets were stained for viability with 1 µl of Rhodium 103 in 500 µl CSB and incubated for 20 minutes at room temperature before quenching with 2 ml of CSB (Fluidigm, US). Cells were centrifuged at 700 x *g* for 5 minutes, resuspended in 100 µl of CSB and then incubated with 5 µl of

FC block (BioLegend, US) for 10 minutes before CD45 barcode staining commenced. After samples were incubated with appropriately labelled CD45 antibodies for 20 minutes at 2-8°C, they were washed and pooled together for panel staining. The pooled samples were divided into two and stained with 25 µl antibody cocktail to 25 µl cell suspension. Where appropriate, individual primary antibodies were added prior to cocktail staining. All staining steps were incubated for 20 minutes at 2-8°C, and washing was performed between stains as required. Finally, cells were fixed with 200 µl of intercalation solution containing iridium (1:1000) and left at 2-8°C overnight.

2.9.4 Acquisition and Analysis

After overnight incubation, cells were washed with 200 µl Maxpar water (Fluidigm, US) and centrifuged at 800 x *g* for 5 minutes at room temperature. This wash step was performed a total of three times before a final re-suspension in Milli-Q distilled water (Merck Millipore, US). The samples were passed through a 50 µm filter and then 200 µl of EQ beads (Fluidigm, US) were added for processing normalisation. The samples were run at a rate of 500 events per second on a Fluidigm Helios CyTOF until the samples were depleted.

All data was first analysed using FlowJo V.10.1. (TreeStar Inc, US) to identify viable, single cells (Figure 2.6) and separate barcoded samples by CD45+ expression (Figure 2.7). Samples were then analysed using cytofKit V.3.7 (Chen, Bioconductor) operated through R studio V.1.1.463 (R Studio, US). All cytofKit parameters remained as default with the following exceptions; the ceil merge method was adjusted to 7500 cells per samples, and the transformation method was switched to cytofAsinh.

Table 2.3 Cytometry by time of flight (CyTOF) panel design for lymphoid and myeloid cells. A breakdown of the lymphoid and myeloid cell surface markers and the mass and metal tag they were conjugated to. All antibodies were purchased from the Manchester Collaborative Centre for Inflammation Research (MCCIR) CyTOF antibody bank, which were purchased ready to use from Fluidigm or conjugated in-house at the MCCIR.

Mass and Metal Tag	Lymphoid Marker	Myeloid Marker
89 Y	CD45	CD45
103 Rh	Live/Dead	Live/Dead
107/109 Ag-Strept		CD14-Bio
112 Qd	CD8/CD19	CD8/CD19
115 In	CD45	CD45
141 Pr	CCR6	
142 Nd	CD62L	CD40
143 Nd	CD117	CD117
145 Nd	CD4	FcεR1
146 Nd	CCR5	CD64
147 Sm		CD11c
148 Nd		CD66b
149 Sm	CD127	CD303
150 Nd	CD44	CD86
151 Eu	CD2	CD123
152 Sm	TCRgd	CD2
153 Eu	CD45RA	MerTK
154 Sm	CD73	CD163
155 Gd	CD56	CD7
156 Gd		CD24
158 Gd	CCR4	
159 Tb		PDL2
161 Dy		PDL1
162 Dy		CD80
163 Dy	CXCR3	CD200R
164 Dy	CD161	Siglec8
165 Ho		CD16
166 Er		CD141
167 Er	CCR7	CD33
168 Er	CD206	CD206
169 Tm	CD25	CX3CR1
170 Er	CD3	CD3
171 Yb	CRTh2	CD169
172 Yb	CD38	CD1a
173 Yb		CLEC9a
174 Yb	HLADR	HLADR
175 Lu	PD1	SIRPa
191 Ir	DNA 1	DNA 1
193 Ir	DNA 2	DNA 2
198 Pt	CD45	CD45
209 Bi		CD11b

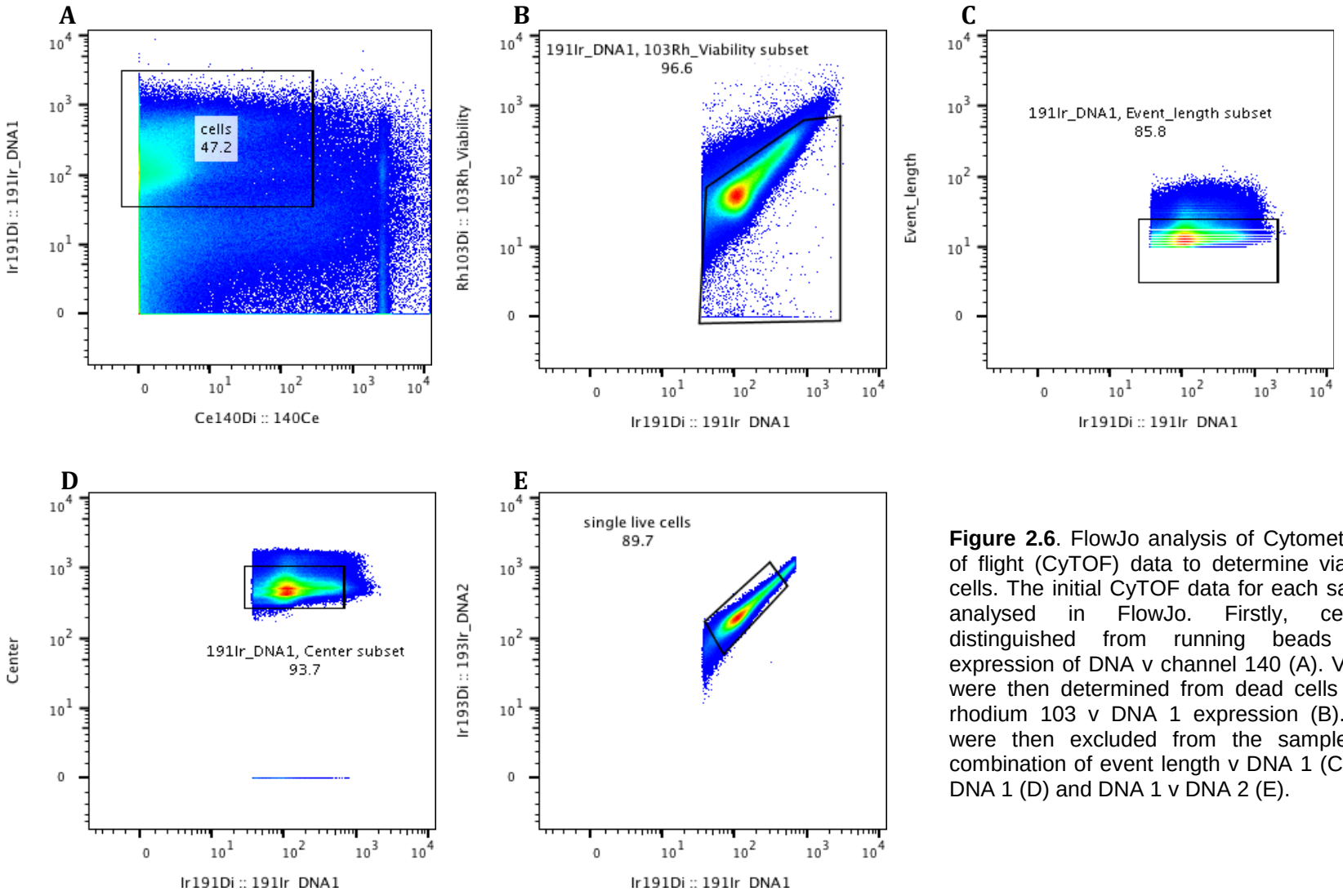

Figure 2.6. FlowJo analysis of Cytometry by time of flight (CyTOF) data to determine viable single cells. The initial CyTOF data for each sample was analysed in FlowJo. Firstly, cells were distinguished from running beads via the expression of DNA v channel 140 (A). Viable cells were then determined from dead cells based on rhodium 103 v DNA 1 expression (B). Doublets were then excluded from the sample using a combination of event length v DNA 1 (C), centre v DNA 1 (D) and DNA 1 v DNA 2 (E).

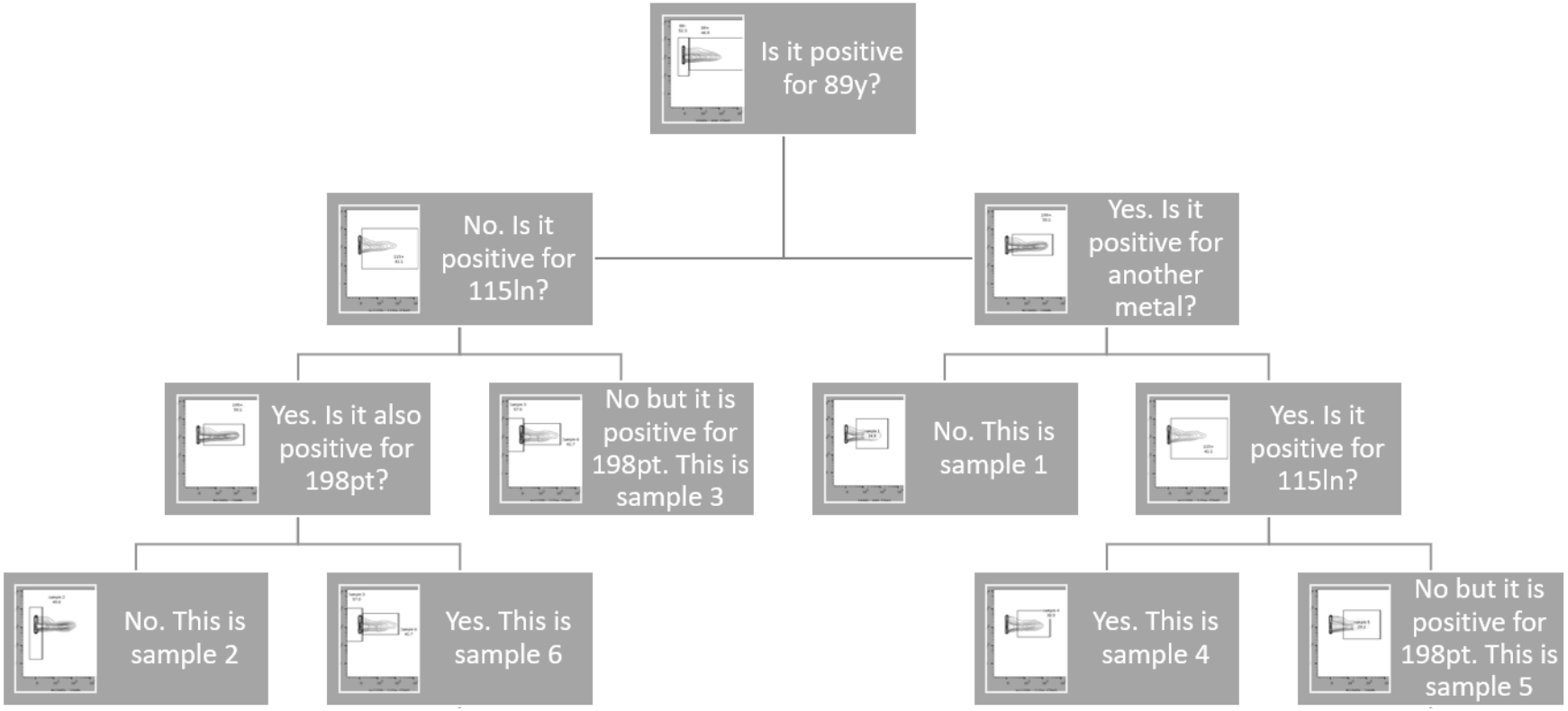

Figure 2.7. Process chart for the separation of samples bar coded for cytometry by time of flight antibody panel staining. Following data acquisition, samples that were labeled by individual combinations of CD45 on metals 89, 115 and 198 required identification. Samples one, four and five were identified from cells positive for metal 89 (right-hand side of the flow chart), whilst samples two, three and six were from cells negative for metal 89 (left hand side of the flow chart).

2.10 Statistical Analysis

All statistical analysis was performed using SPSS version 22.0 or GraphPad Prism 8 version 8.2.0. Data normality was determined by assessing mean, standard deviation, skewness and kurtosis. Formal evaluation was performed using the Shapiro-Wilk test.

To interrogate regional heterogeneity, data that was severely different to normal distribution were log transformed, and then all data underwent generalized estimating equation (GEE) analysis. The relationship between leukocyte number in different clinical parameters was examined by two-way ANOVA of grouped data. Bonferroni was used as the post-test correction in both circumstances.

To explore the relationship between disease cohorts or subsets of cells, normally distributed data underwent independent t tests or ANOVA, whilst data that was not normally distributed underwent Mann-Whitney U or Kruskal-Wallis tests.

All data figures presented throughout this thesis were created in Prism V.7 and V.8 (GraphPad, US). Statistical significance was demonstrated using the American Psychological Association (APA) asterisk style; * = $p \leq 0.05$, ** = $p \leq 0.01$ and *** = $p \leq 0.001$.

Chapter Three: The Regional Heterogeneity of Lung Disease

3.1 Introduction

Lung disease is rarely homogenous across the entirety of lung, but rather severely diseased regions are interspersed throughout healthier tissue. Often these diseases have common risk factors, primarily smoking, yet result in significantly different pathological outcomes. Indeed, COPD is an inherently heterogeneous disease. The clinical manifestations of chronic bronchitis and emphysema, which itself has three distinct patterns, and even aetiologies, such as α1-antitrypsin deficiency, all display diverse pathophysiology [125] [187]. The same is true of ILD, with over 300 different sub-classifications that despite radiological similarities can present phenotypically very differently, and vice versa, rendering differential diagnosis extremely challenging. In addition, in CF, some pathological findings can have a regional predominance, with hyperinflation more common in the lower lobes and atelectasis more common to upper and middle lobes [188].

The factors driving disease heterogeneity within the lung are unknown, however inflammation is a common feature. Despite this, conclusions relating to the contribution of the immune system to the pathology of lung disease are often generated from airway samples, which may not be representative of the diseased area [51, 189]. The same is true of indiscriminate cancer tissue resections [190] [191].

Therefore, it is essential to describe the distribution and characteristics of the residing immune system in prevalent lung conditions. This could potentially advance treatment options and provide insight into whether current diagnostics have the propensity to misdiagnose or provide incorrect pathological grading, which could impact treatment decisions. Current therapeutic agents target very specific mechanisms that may not occur uniformly across the lung, and as such may lead to a varied clinical response. Characterising the leukocyte populations within different regions of the lung may help to elucidate the inflammatory processes occurring across the lung as a whole, and how they may drive the heterogenic patterns observed in disease.

A fundamental limitation to lung inflammation research is the access to reproducible multi-layer tissue sampling from all lobes of the lung in patients with lung disease. However, patients with end-

stage lung disease who are listed for lung transplantation represent a unique opportunity to study fully phenotyped patients, without any co-morbidities such as cancer.

The aim of this chapter was to characterise the regional immune and inflammatory profile of COPD, ILD and CF lungs. This fundamental discovery research would then dictate the direction and hypothesis of the remainder of the project.

3.2 Methods

All patients described in this chapter underwent a DLTx except for the cohort of patients with ILD, who all underwent SLTx with one exception (LTx-51). A detailed methodology for the collection, processing and analysis of lung tissue is provided in Chapter Two, Sections 2.1 to 2.6. Briefly, wedge biopsy samples from six uniform areas of the lungs (or three for a SLTx) were collected at the time of transplant and 1 g per sample was processed for leukocyte analysis via flow cytometry (Chapter Two, Section 2.5). The remaining tissue was snap frozen and stored for future use. A tissue lysate was generated from stored tissue and used in a Luminex assay to determine cytokine and chemokine quantities within the tissue (Chapter Two, Section 2.6). The total number of cells per gram of tissue was calculated for a broad panel of leukocyte subsets. The contribution of each cell population to the total leukocyte pool was then determined and presented as a percentage. Clinical data was collected from all patients who had explanted tissue samples analysed, as described in the methodology Section 2.4.

3.3 Results

3.3.1 The Distribution of Leukocytes in the Lobes of 28 Diseased Human Lungs

The total number of $CD45^+$ leukocytes within 1 g of lung tissue ranged from 4.79×10^5 to 1.54×10^7 in COPD (n=59 lobe samples obtained from n=10 individuals), 7.01×10^5 to 1.33×10^7 in CF (n=29 lobe samples obtained from n=5 individuals), and 1.96×10^5 to 5.96×10^6 in ILD (n=41 lobe samples obtained from 13 individuals) (Figure 3.1A). Both COPD and CF lung tissue samples had marked variation in leukocyte numbers between patients, whilst variability in leukocyte numbers was homogenous from ILD lungs. The degree of variation persisted at a regional level across the different lung lobes in COPD and CF, and there was limited variation in the upper left and right lobes of the ILD lungs (Figure 3.1B). This inter-lobe variation was not driven by individual patients possessing homogenously higher or lower leukocyte numbers across their lungs, but instead continued at an intra-patient level in each disease (Figure 3.1C).

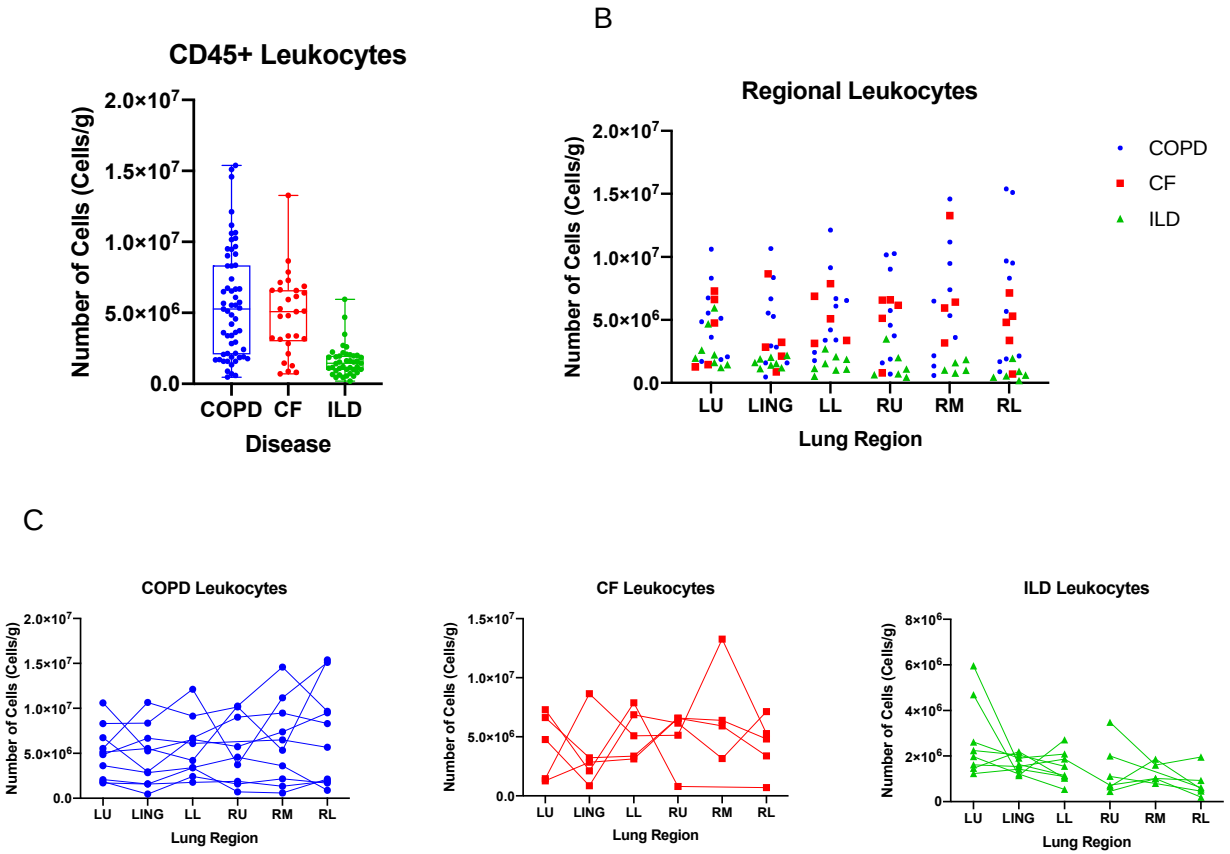

Figure 3.1 The heterogeneity of leukocyte numbers in lung tissue samples from patients with chronic obstructive pulmonary disease (COPD), cystic fibrosis (CF) and interstitial lung disease (ILD). (A) The number of leukocytes within 1 g of tissue (n=129) was determined for patients with COPD (n=59 obtained from n=10 patients), CF (n=29 obtained from n=5 individuals), and ILD (n=41 obtained from 13 individuals). Box and whisker plots represent the interquartile range (box) whilst the line shows the median and the whisker the full range of the data. (B) The individual samples were then categorised by the area of the lung they were acquired from (LU; left upper, LING; lingula, LL; left lower, RU; right upper, RM; right middle, RL; right lower). n=10 per region for COPD (except RU, n=9), n=5 per region for CF (except RM, n=4), and n=13 in the ILD cohort (left lung; n=8* for all regions, right lung; n=6* for all regions except RM, n=5*). *One patient had a double lung transplant and has data points for both lungs. (C) The intra-patient variation in leukocyte number was then demonstrated by region and disease type (repeated measures plot with symbols representing individual sample data, and the lines to correlate regional samples from each patient).

3.3.2 Chronic Obstructive Pulmonary Disease

3.3.2.1 Patient Demographics and Clinical History

Patient demographics, lung function, clinical history and explant histology of n=10 COPD patients were summarised in Tables 3.1 to 3.2. Samples were obtained from seven female and three male patients, with an average age of 57.7 years (range of 49-64 years) at the time of transplant. All patients had emphysema, two of which had AATD. Three patients also had documented bronchiectasis. Eight patients were classified as very severe COPD and two as severe COPD in accordance with the GOLD classification [182]. Three patients had type II respiratory failure. Nine patients were previous smokers, with a pack year history ranging from 17-55 pack years. The most common co-morbidity was pulmonary hypertension (PH), with other co-morbidities consisting of diabetes, arthritis, asthma, left ventricular (LV) impairment, dyslipidemia, and mitral regurgitation (Table 3.1). Histopathology reports confirmed that disease severity was not confined to one region of the lung in all patients. Instead four patients had severe disease in the upper lobes, two in the lower lobes, and four patients had diffuse emphysematous changes throughout the lobes of each lung (Table 3.2)

Table 3.1 Chronic obstructive pulmonary disease cohort demographics, pulmonary function and clinical history. The clinical history of each patient (n=10) was obtained from the transplant medical records held by Manchester University NHS Foundation Trust and key parameters pertaining to the patients' demographics, lung function and clinical history were summarised.

LTx Code (Colour)	*COPD Phenotype*	*Gender*	*Age at Tx*	*FEV_1, L (% Predicted)*	*FVC, L (% Predicted)*	*GOLD Classification*	*Interval from diagnosis to Tx (years)*	*Exacerbation Hx (no. of events in year prior to Tx)*	*Co-morbidities*	*Smoking Hx (pack years)*
29 (Cyan)	Emphysema	F	49	0.5 (20%)	1.44 (49%)	Very severe	6	1	PH Diabetes	Yes – 30 years
61 (Orange)	Emphysema	F	62	0.49 (23%)	1.75 (70%)	Very severe	10, 18 month deterioration	3-4	Basal cell carcinoma (2016)	Yes (NA)
69 (Purple)	Emphysema	M	63	NA (22%)	NA	Very severe	8	6		Yes (30)
79 (Red)	Emphysema	F	55	0.54 (25%)	1.84 (73%)	Very severe	5 year deterioration	0 (Hx of)	Mild mitral regurgitation End stage RF	Yes (40)
83 (Yellow)	Emphysema	F	54	0.52 (22%)	2.54 (92%)	Very severe	4	0 (Hx of)	Type II RF	Yes (30)
92 (Blue)	Emphysema	F	64	0.55 (25%)	1.73 (67%)	Very severe	NA	On going for 11 months prior	Hypertension Dyslipidaemia	Yes (55)
37 (Green)	Emphysema & Bronchiectasis	M	53	1.42 (40%)	2.96 (68%)	Severe	7	1-2	PH Diabetes Asthma	No
45 (Magenta)	Emphysema & Bronchiectasis	M	63	0.47 (16%)	1.64 (46%)	Very severe	12	4	Arthritis	Yes – 20 a day
80 (Black)	Emphysema & Bronchiectasis : AATD (M2)	F	58	1.03 (45%)	2.12 (79%)	Severe	NA	0	LV impairment	Yes (NA)
96 (Brown)	Emphysema: AATD (Z)	F	56	0.69 (28%)	1.95 (68%)	Very severe	1 year deterioration	1	PH Eosinophilic asthma Type II RF Hypothyroidism	Yes (17)

Abbreviations: LTx= Lung transplant, COPD= chronic obstructive pulmonary disease, Tx= transplant, Hx= history, NA=not available in medical records, FEV_1= Forced expiratory volume in one second, FVC= Forced vital capacity, L= liter, M= male, F= female, AATD= Alpha-1 antitrypsin deficiency, M/Z= allele variant of the AATD gene, PH= pulmonary hypertension, RF= respiratory failure, LV= left ventricular

Table 3.2 A summary of explanted lung histopathology reports for patients with chronic obstructive pulmonary disease. A histopathology report for each patients' (n=10) explanted lungs were obtained following examination by a histopathologist at Manchester University NHS Foundation Trust and the key observations were summarised. Particular attention was paid to any reference of disease heterogeneity across the lungs, and the area(s) of the lung most affected were identified.

LTx Code (Colour)	***COPD Phenotype***	***Summary of Histology Report (R; right lung, L; left lung, O; overall analysis)***	***Area of lung most affected?***
29 (Cyan)	*Emphysema*	R: Homogeneously emphysematous. Fibrosis between lobes L: Prominent towards apex. O: Prominence slightly towards upper lobes. Mixed centriacinar/pan-acinar pattern. Patchy peri-bronchiolar chronic inflammation. Secondary PH changes	Upper lobes
61 (Orange)	*Emphysema*	R: upper lobe has severe emphysema. L: Upper lobe and apex of lower lobe show moderate emphysema. O: Both lungs have severe emphysema.	Upper lobes
69 (Purple)	*Emphysema*	R: severely emphysematous, large bullae up to 25mm. No normal lung identified L: severe emphysema in both lobes, worse in upper lobe and apex of lower lobe. Comparatively preserved lung at base of lower lobe. O: Extensive destruction of parenchyma throughout, numerous fibrous-walled bullae. Secondary PH changes.	Right lung and Left Upper Lobe
79 (Red)	*Emphysema*	R: Pan-acinar emphysematous changes. Upper lobe could have obstructive pneumonitis. Mucus plugging & patchy inflammation. PH changes L: Both lobes have emphysematous changes. O: Moderate emphysematous changes. Evidence of bronchiectasis.	All lobes
83 (Yellow)	*Emphysema*	R: Severe widespread emphysematous change L: Emphysematous changes less prominent. O: Moderate chronic bronchiolitis.	All lobes
92 (Blue)	*Emphysema*	R: Bullae across all lobes. Severely emphysematous, particularly upper lobe. L: Bullae on upper lobe. Emphysema upper lobe, to an extent in lower. O: Severely emphysematous, focal chronic inflammation. Focal sub-pleural fibrosis. Some necrosis in upper lobes. PH changes. Dilated bronchi(oles)	Upper lobes
37 (Green)	*Emphysema & Bronchiectasis*	R: Dilated large bronchi extending to periphery, mucus plugs. Emphysematous change in apex of upper lobe L: Apex has emphysematous change. Abnormally dilated large bronchi, patchy areas of mucus plugging. O: Similar across both lungs, most advanced in lower lobes. Bronchiectasis most prominent feature. Mild to moderate emphysematous change in peripheral lung.	Upper lobes Emphysema Lower lobes Bronchiectasis
45 (Magenta)	*Emphysema & Bronchiectasis*	R: All lobes have emphysematous changes, more prominent in upper lobe. Bronchiectasis mainly confined to lower lobe. L: Prominent emphysematous change in upper lobe. Bronchiectasis mainly involving lower lobe. O: Patchy interstitial fibrosis. Ectatic bronchi contain inflammatory debris with chronic inflammation. Organising pneumonia & PH also present.	Upper lobes Emphysema Lower lobes Bronchiectasis
80 (Black)	*Emphysema & Bronchiectasis: AATD (M2)*	R: Marked emphysematous change, sub pleural bullae. L: Marked emphysematous change, sub pleural bullae. O: Diffuse and severe emphysema. Consistent with *AATD*	All lobes
96 (Brown)	*Emphysema: AATD (Z)*	R: Lower diffuse emphysematous change and bronchi filled with secretion. Middle mild emphysematous change, upper relatively normal. L: Lower lobe diffusely abnormal with necrosis, reduced volume and marked emphysematous change. O: Severe widespread emphysema and bronchiectasis. Consistent with *AATD.*	Lower lobes

Abbreviations: LTx= Lung transplant, COPD= chronic obstructive pulmonary disease, R= right lung, L= left lung, O= overall, AATD= Alpha-1 antitrypsin deficiency, PH= pulmonary hypertension, RF= respiratory failure, LV= left ventricular, M/Z= allele variant of the AATD gene

3.3.2.2 Distribution of Leukocytes Across the Chronic Obstructive Lung Disease Lung

There was an error during the processing of lung samples for flow cytometry from LTx-45 (magenta symbol in figures) and subsequently, flow cytometry could not be performed on the RU sample. Therefore this data set consisted of five samples instead of six, resulting in n=9 for RU samples and n=10 for the remaining regions. This error only affected flow cytometry data, as other analysis was performed on snap frozen tissue.

3.3.2.2.1 Leukocyte Numbers

Using a generalised estimating equation, macrophage ($p=0.024$), NK cell ($p<0.001$) and B cell ($p=0.028$) distribution was highly variable across different areas of the COPD lung (Figure 3.2B, E and F). In macrophages, these differences were confined within the left lung, but for NK and B cells intra- and inter-lung differences were observed. There were no differences detected in overall leukocyte, monocyte, granulocyte or T cell numbers between lobes ($p>0.05$) (Figure 3.2A, C, D and G). However, the high inter-patient variation observed in Figure 1 persisted within individual leukocyte subsets.

3.3.2.2.2 Leukocyte Proportions

The contribution of each cell population to the total leukocyte pool was determined and presented as a percentage for each subset and region (Figure 3.3). The same assessment of regional heterogeneity found that macrophages ($p=0.015$), monocytes ($p<0.001$), granulocytes ($p=0.023$), B cells ($p<0.001$) and a population of CD4+ regulatory T cells (Tregs) ($p<0.001$) had significantly different proportions (as a percentage of total leukocytes) between lobes of the lung (Figure 3.3B, C, D, F and Gc). The differences in monocyte proportion were confined to the right lung, but all other subsets were highly variable at intra- and inter-lung levels. Interestingly, the proportion of CD4+ T cells was significantly higher compared to the proportion of CD8+ T cells (Figure 3.3Gb, also see Appendix 5). A number of subsets, most evident in granulocytes and T cells, were highly variable between patients.

A summary of all statistical results for GEE analysis of regional leukocyte number and proportion can be found in Appendix 6.

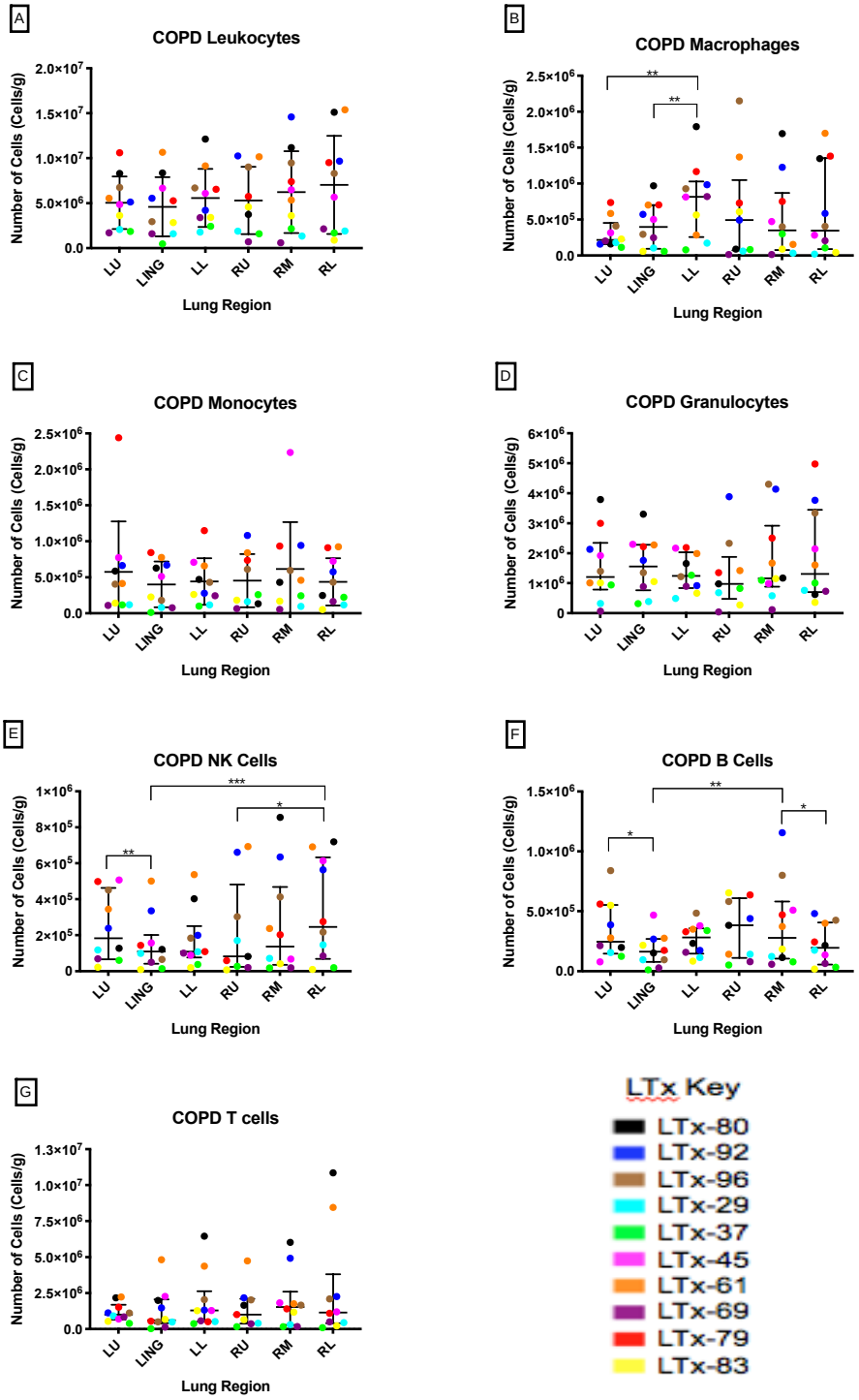

Figure 3.2 The regional number of key leukocyte subsets within the chronic obstructive pulmonary disease lung. Each patient in the cohort is characterised by a distinct colour (see key, refer to Table 3.1-3.2 for clinical information), demonstrating the total number of cells per gram of tissue for the overall number of CD45+ leukocytes (A) and six major leukocyte subsets (B-G) (n=10 for all regions except RU, n=9). On scatter plots A and C, bar and lines represent mean ±SD, on scatter plots B, D, E, F and G bar and lines represent median + IQR (data log transformed for statistical analysis). All differences between regions determined by a generalized estimating equation with Bonferroni post-test correction, * = $p \leq 0.05$, ** = $p \leq 0.01$, *** = $p \leq 0.001$, significance $p > 0.05$ not reported.

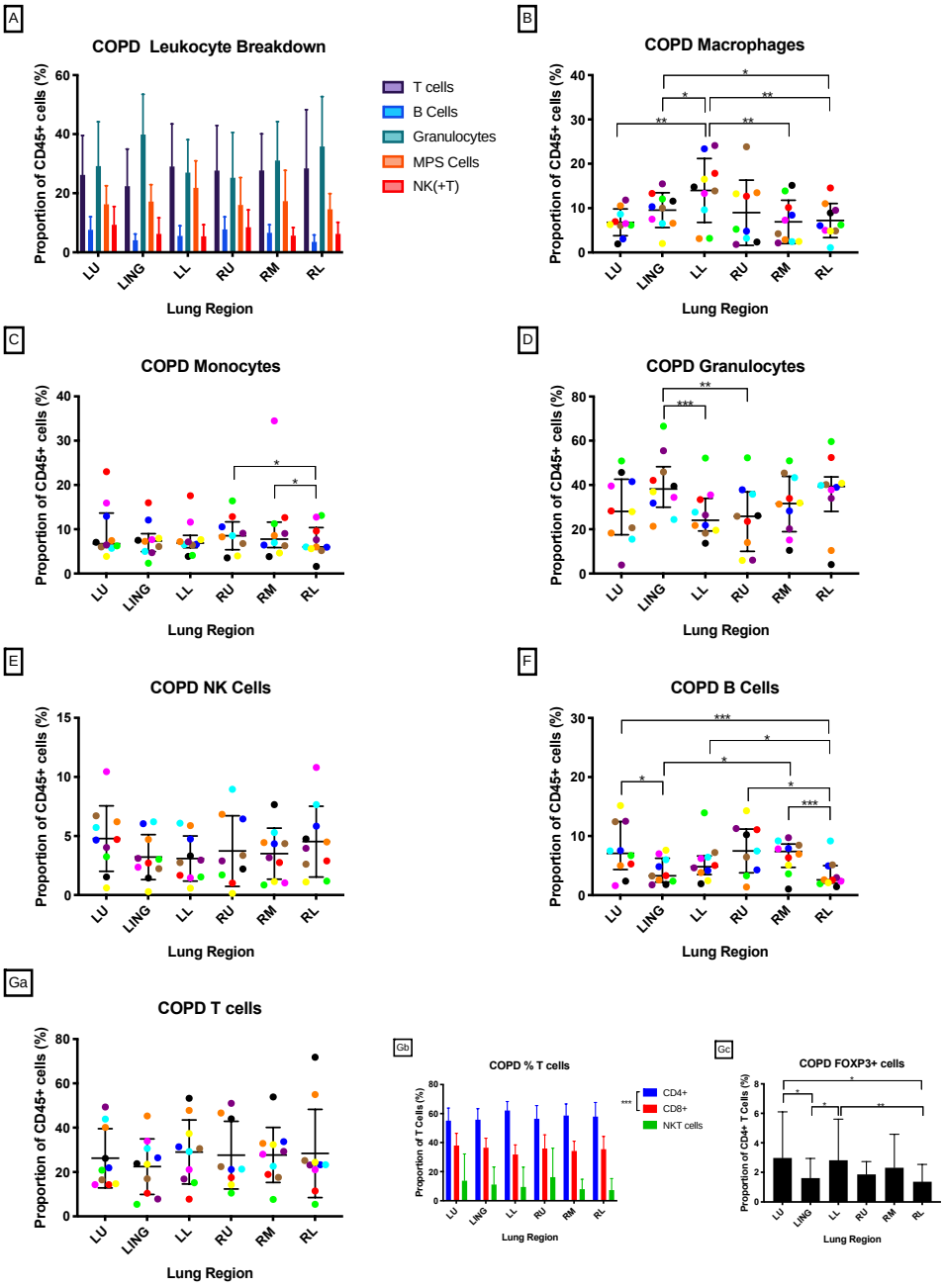

Figure 3.3 The regional proportion of key leukocyte subsets to the total leukocyte pool within the chronic obstructive pulmonary disease lung. The contribution of each cell population to the total leukocyte pool in each region of the lung was determined and presented as a percentage for major subsets (A). Each patient in the cohort is characterised by a distinct colour, demonstrating the proportion per gram of tissue for six major leukocyte subsets (B-G). Gb shows the proportion of CD3+ cells that were CD4+, CD8+ or CD56+ (NKT cells) across each region, and Gc shows the proportion of CD4+ cells that were also FOXP3+ (n=10 for all regions except RU, n=9). Bars on A, Gb and Gc represent mean +SD, and on scatter plots B, E and Ga the bars and lines represent mean ± SD. On scatter plots C, D and F, the bar and lines represent median + IQR (data log transformed for statistical analysis). All differences between regions determined by a generalized estimating equation with Bonferroni post-test correction, * = $p \leq 0.05$, ** = $p \leq 0.01$, *** = $p \leq 0.001$, significance $p > 0.05$ not reported. A paired samples T test was performed to test the difference between CD4+ and CD8+ proportions, *** = $p \leq 0.001$.

3.3.2.3. The Intra-Patient Regional Heterogeneity in Leukocyte Subsets Across the Chronic Obstructive Lung Disease Lung

Given the high degree of inter-patient variability, leukocyte number and proportions were then determined within individual COPD lungs.

3.3.2.3.1 Leukocyte Numbers and Proportions

In n=5 explanted lungs (LTx-29, -45, -69, -83 and -37), the number of leukocytes between lobes remained homogenous. However, leukocyte populations were highly heterogeneous in the remaining lungs (LTx-80, -96, -61, -79, -92) (Figure 3.4). This pattern of heterogeneity was predominantly driven by lobar variability in either T cell or granulocyte subsets. Based on observational analysis, lungs from male recipients had conserved leukocyte populations across each lobe, whilst the patients with the most heterogeneous and elevated leukocyte counts were all female with emphysema (Figure 3.4).

The evaluation of regional variation in leukocyte subset proportions at an intra-patient level demonstrated that the immunophenotype of the lung tissue varied according to the region the sample was taken (Figure 3.5). In particular, the proportion of T cells and granulocytes differed substantially in different regions of samples from patients LTx-80, -29, and -69. Although some increases in T cell proportion appeared to correlate with areas of greatest severity interpreted from their histopathology reports (LTx-29 LU, LTx-69 LU and RU, Table 3.2), this was not uniform across all patients or every region.

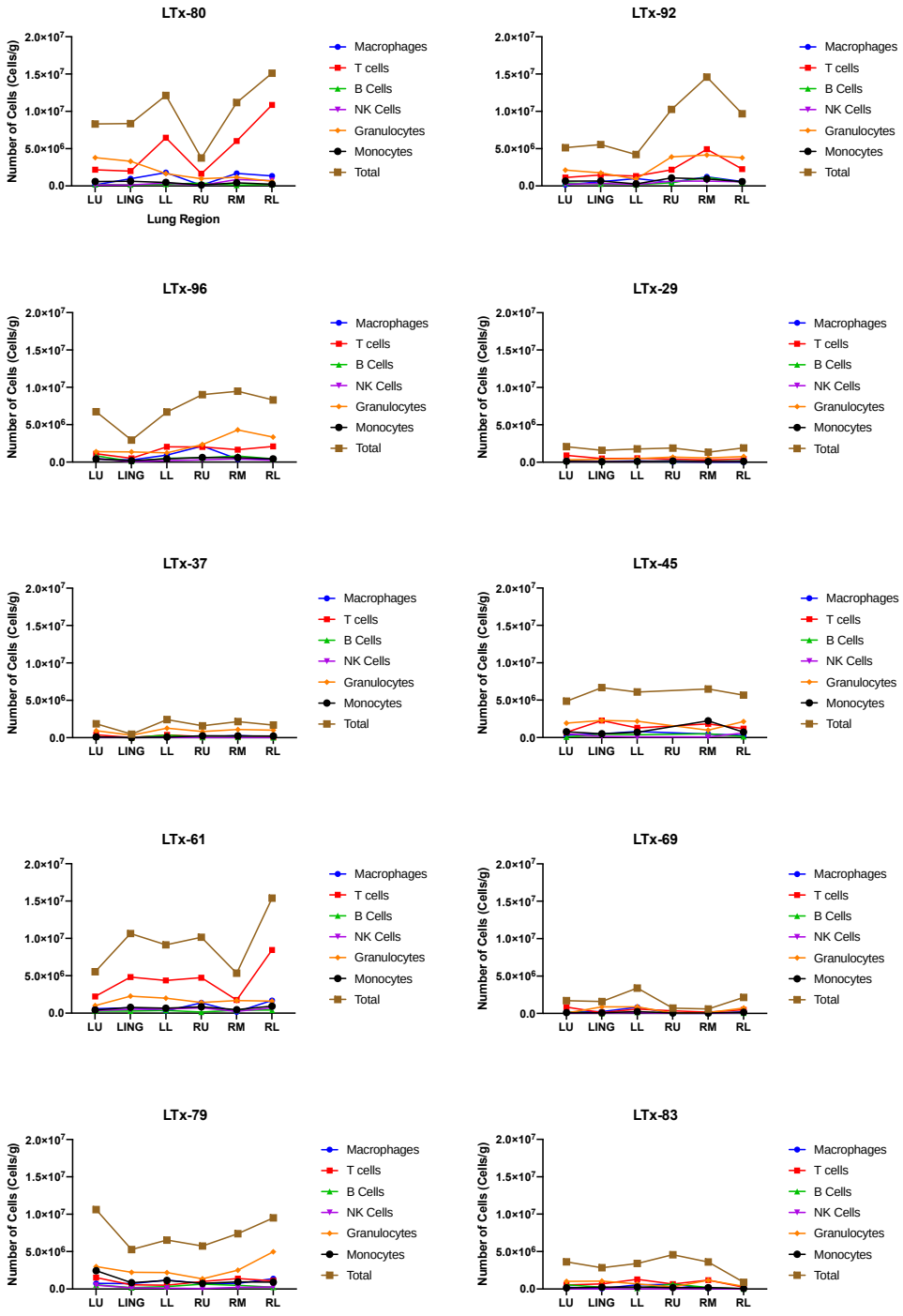

Figure 3.4 Quantifying the regional variation in leukocyte subset numbers in chronic obstructive pulmonary disease (COPD) at an intra-patient level. Each graph represents the total number of leukocytes (brown) and six major subsets per gram of tissue across different lobe regions in patients with COPD (n=10). There is a data point for each patient at every region, except LTx-45 who did not have a right upper (RU) lobe sample. The lines on each graph help visualise the increases or decreases in each subset across the six regions of the lung. The scale bars on each graph are the same and range from zero to 20 million cells per gram of tissue.

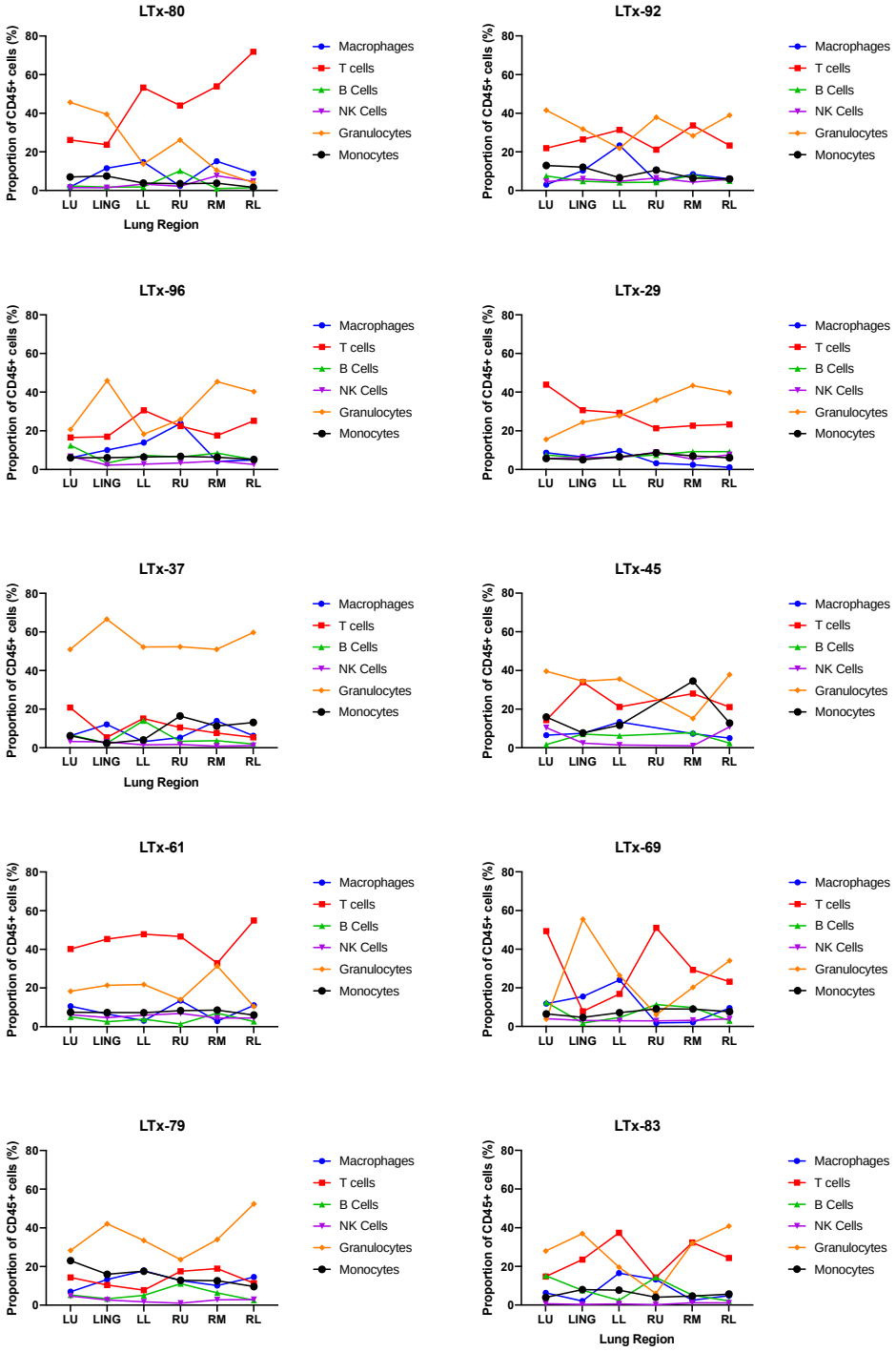

Figure 3.5 Quantifying the regional variation in leukocyte subset proportions in chronic obstructive pulmonary disease (COPD) at an intra-patient level. Each graph represents the contribution of six leukocyte subsets to the total leukocyte pool per gram of tissue as a percentage, across different lobe regions in patients with COPD (n=10). There is a data point for each patient at every region, except LTx-45 who did not have a right upper (RU) lobe sample. The lines on each graph help visualise the increases or decreases in proportion of each subset across the six regions of the lung. The scale bars on each graph are the same and range from zero to 80%.

3.3.2.4 The Relationship Between Total Leukocyte Number and Clinical Parameters in Chronic Obstructive Lung Disease

The total number of leukocytes across the COPD lung was examined within different clinical parameters, phenotypes and clinical history (Figure 3.6). There was a significant difference in leukocyte number determined by clinical phenotype, demonstrating patients with AATD had significantly more leukocytes across the lung compared to those without AATD (Figure 3.6A, p=0.0134). Significant differences were also evident based on gender (Figure 3.6B, p=0.007) and smoking history (Figure 3.6C, p=0.013). However there was no significant difference in the number of leukocytes when correlated to exacerbation frequency or disease severity as classified by GOLD based on FEV_1 grading (Figure 3.6D & E, p>0.05).

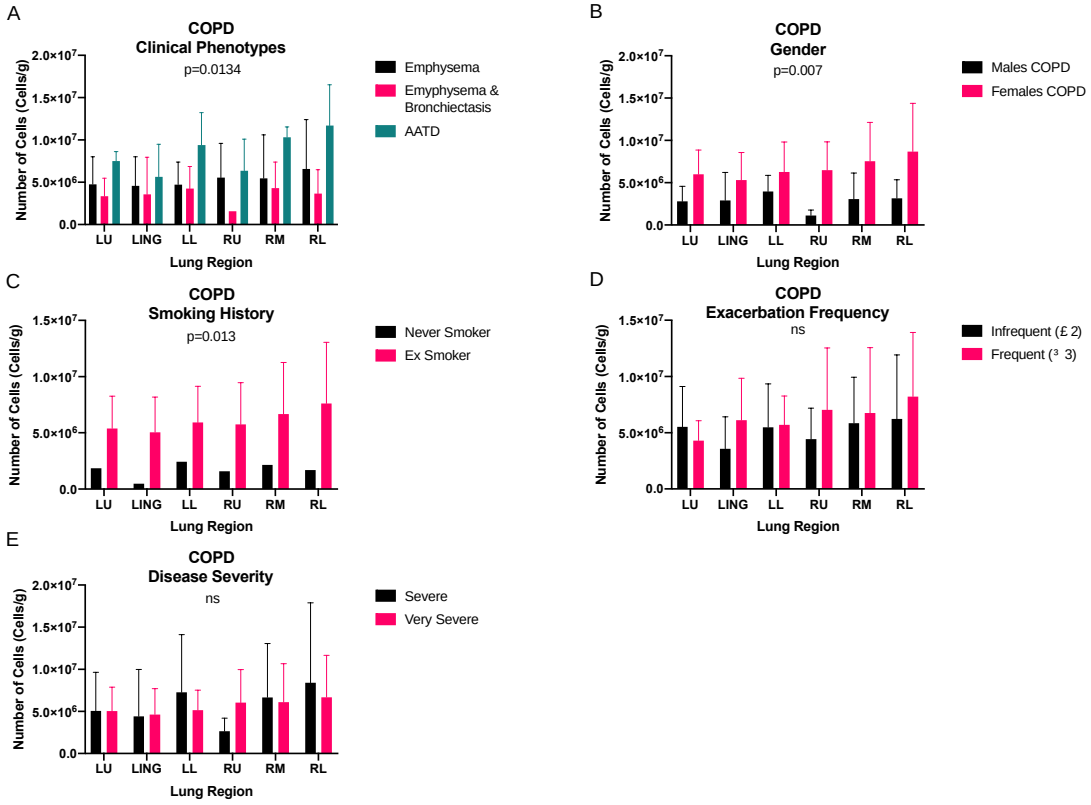

Figure 3.6 Correlating the total number of leukocytes in chronic obstructive pulmonary disease (COPD) to clinical parameters. The total number of leukocytes per gram of tissue in each region was assessed based on (A) COPD phenotype (emphysema; n=6, emphysema with bronchiectasis; n=2, AATD; n=2), (B) patient gender (female vs male; n=7v3), (C) patient smoking history (ex smoker; n=9, never smoker; n=1), (D) the frequency of exacerbations in the year preceding transplant (infrequent; n=6, frequent; n=4) and (E) the severity of disease as assessed by forced expiratory volume in one second (FEV_1) per the Global Initiative for Chronic Obstructive Lung Disease classification (severe; n=2, very severe; n=8). All bars represent mean +SD, statistical differences between parameters were determined by a two-way ANOVA of grouped data, significant p value reported, significance p > 0.05 reported as ns.

3.3.2.5 Cytokine and Chemokine Profiling

The concentration of 13 cytokines and chemokines was assessed across six different regions of the COPD lung (n=6) (Figure 3.7). The concentrations of granulocyte macrophage colony stimulating factor (GM-CSF), interferon gamma (IFNγ), IL-10, IL-12p70, IL-1β, and IL-2 were below the limit of detection (3.2 pg/ml) for most samples. IL-12p40, IL-1α, IL-4 and TNFα had detectable levels in approximately half the samples, however the levels in remaining samples were extrapolated. This data has been included in the Appendix 7 for reference, but given some levels were extrapolated, statistical analysis was not performed. Cytokines that did exceed the assays limit of detection for all samples were IL-1 receptor antagonist (IL-1RA), IL-6 and IL-8. Each of these was found in significantly different quantities across the six lung regions (IL-1RA; p=0.043, IL-6; p=0.003 and IL-8; p<0.001).

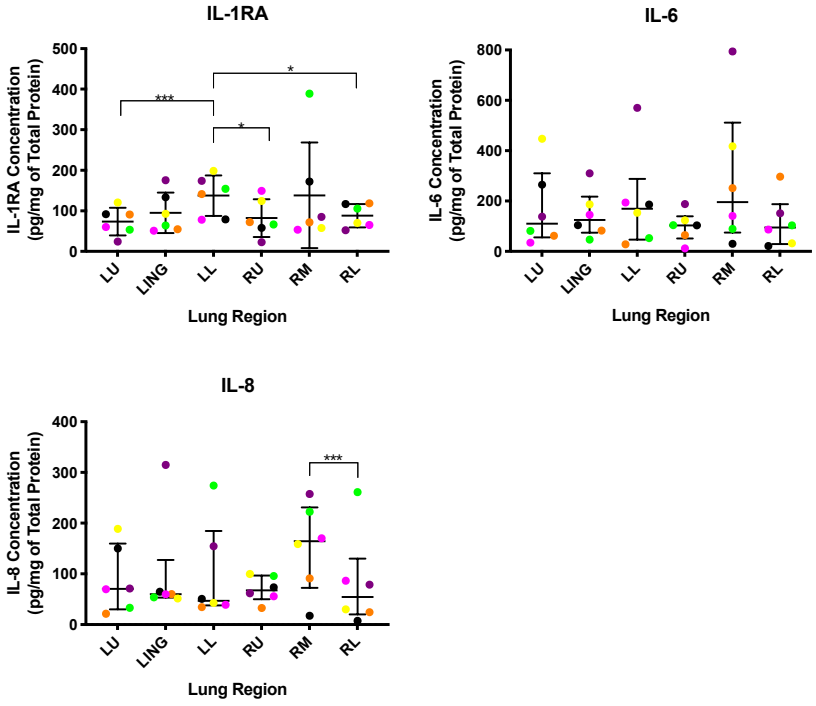

Figure 3.7 The regional concentration of interleukin-1 receptor antagonist, interleukin-6 and interleukin-8 within the chronic obstructive pulmonary disease lung. The concentration of interleukin- (IL-) 1RA, IL-6 and IL-8 was measured per milligram of total protein in lung tissue lysate from six regions of the lung (n=6). Each patient in the cohort is characterised by a distinct colour, representing the cytokine concentrations in each region per patient, and correlate to six of the 10 patients in figures 3.2 to 3.3. The IL-1RA scatter plot bar and lines represent mean ±SD, the IL-6 and IL-8 scatter plots represent median + IQR (data log transformed for statistical analysis). All differences between regions determined by a generalized estimating equation with Bonferroni post-test correction, * = $p \leq 0.05$, *** = $p \leq 0.001$, significance $p > 0.05$ not reported. Overall, generalized estimating equation determined the regions of IL-6 were statistically different (p=0.003) but no specific post-test corrections were found.

3.3.3 Interstitial Lung Disease

3.3.3.1 Patient Demographics and Clinical History

Demographics, clinical history, pulmonary function and explant histology of ILD patients are summarised in Tables 3.3 to 3.4. Samples were obtained from four female and nine male patients, with an average age of 59.3 years (range of 45-65 years) at the time of transplant (Table 3.3). The clinical diagnosis of patients prior to transplant comprised of nine patients with confirmed IPF, two patients with NSIP and two with atypical ILD, of which one had a differential diagnosis of cryptogenic organising pneumonia. The pulmonary function tests were the most recently reported results prior to transplant, with a patient FEV_1 range of 38% to 86% predicted. Eight of the 13 patients were previous smokers, with a pack year history ranging from 18-34 pack years. The most common co-morbidities were related to the heart, including coronary artery disease, atrial fibrillation, mitral regurgitation and tachycardia and heart failure. Other co-morbidities included diabetes and hypercholesterolemia. The histopathology reports demonstrated that seven of the patients were most severely affected in their lower lobes, two had basal predominance, one was most severely affected in their upper lobe, two displayed a heterogeneous pattern of disease with distorted architecture throughout the lung, whilst one displayed a homogeneous pattern of disease throughout (Table 3.4).

Table 3.3 Interstitial lung disease cohort demographics, pulmonary function and clinical history. The clinical history of each patient was obtained from the transplant medical records held by Manchester University NHS Foundation Trust and key parameters pertaining to the patients demographics, lung function and clinical history were summarised.

LTx Code (Colour)	***ILD Phenotype***	***Gender***	***Age at Tx***	***Lung Tx***	***FEV_1, L (% Predicted)***	***FVC, L (% Predicted)***	***Interval from diagnosis to Tx (years)***	***Co-morbidities***	***Smoking Hx (pack years)***
42 (Brown)	*Atypical PF*	*F*	*62*	*L*	*1.99 (46%)*	*1.32 (52%)*	*11*	*NA*	*No*
41 (Blue)	*IPF*	*M*	*60*	*L*	*1.91 (NA)*	*2.10 (NA)*	*2*	*Coronary artery disease Hypertension Hypercholesterolemia*	*Yes - 15/day)*
44 (Cyan)	*IPF*	*M*	*65*	*L*	*2.33 (70%)*	*2.65 (63%)*	*2*	*Osteoarthritis*	*Yes (34)*
51 (Purple)	*PF (NSIP)*	*F*	*45*	*DL*	*2.37 (84%)*	*3.27 (100%)*	*8*	*Hypertension*	*Yes (NA)*
55 (Magenta)	*Cryptogenic organisimg pneumonia vs atypical ILD*	*M*	*58*	*L*	*2.84 (86%)*	*3.44 (83%)*	*3*	*NA*	*No*
52 (Green)	*IPF*	*M*	*55*	*L*	*2.14 (53%)*	*2.59 (51%)*	*9 months*	*NA*	*Yes (30)*
58 (Orange)	*IPF*	*F*	*51*	*L*	*2.26 (79%)*	*2.76 (76%)*	*1*	*IBS*	*Yes – 10/day*
13 (Black)	*IPF (atypical PF)*	*F*	*63*	*L*	*1.47 (NA)*	*1.64 (NA)*	*9*	*NA*	*No*
65 (Asparagus)	*IPF*	*M*	*61*	*R*	*2.63 (78%)*	*NA (NA)*	*2*	*Atrial Fibrillation Mitral regurgitation LV hypertrophy Haemoptysis*	*Yes (18)*
53 (Yellow)	*NS ILD*	*M*	*64*	*R*	*NA (84%)*	*NA (88%)*	*2*	*Type II diabetes*	*Yes (NA)*
60 (Nickle)	*IPF*	*M*	*64*	*R*	*1.62 (51%)*	*1.76 (43%)*	*7, progressive 2 years*	*Tachycardia Atrial dysrhythmia Pulmonary oedema Heart failure*	*No*
59 (Teal)	IPF	*M*	*62*	*R*	*1.27 (38%)*	*1.49 (35%)*	*2*	*Pulmonary hypertension Reflux*	*Yes (25)*
43 (Red)	*IPF (Family Hx)*	*M*	*61*	*R*	*1.84 (59%)*	*2.05 (52%)*	*1.5*	*Hypercholesterolemia Haemoptysis*	*No*

Abbreviations: LTx= Lung transplant, ILD= interstitial lung disease, Tx= transplant, Hx= history, NA=not available in medical records, FEV_1= Forced expiratory volume in one second, FVC= Forced vital capacity, (in relation to lung function) L= liter, (in relation to lung Tx) L= left, R= right, F= female, M= male, IPF = idiopathic pulmonary fibrosis, NS= non specific, PF= pulmonary fibrosis, NSIP= nonspecific interstitial pneumonia, IBS= irritable bowel syndrome, LV= left ventricular

Table 3.4 A summary of explanted lung histopathology reports for patients with interstitial lung disease. A histopathology report for each patients' explanted lung(s) were obtained following examination by a histopathologist at Manchester University NHS Foundation Trust and the key observations were summarised. Particular attention was paid to any reference of disease heterogeneity across the lungs, and the area(s) of the lung most affected were identified where relevant information was available.

LTx Code (Colour)	***Lung Tx***	***Summary of Histology Report***	***Area of lung most affected?***	***Pattern of Fibrosis?***
42 (Brown)	*L*	Fibrosing ILD with chronic inflammation. Scattered areas of parenchymal firmness & pleural thickening, predominantly UL.	Upper lobe	NSIP
41 (Blue)	*L*	Areas of fibrosis with honeycombing. Lobes similar but advancing in LL. Heterogeneous interstitial fibrosis, sub-pleural dominance.	Lower lobe	UIP
44 (Cyan)	*L*	Heterogeneous fibrosis with honeycombing, most severe towards bases. Mild chronic inflammation. Limited number of FF.	Lower lobe	UIP
51 (Purple)	*DL*	UIP changes with areas of advanced fibrosis, worsened in LL's, and towards Apex. Cystic dilation.	Lower lobes	UIP
55 (Magenta)	*L*	UL normal with basal fibrosis. Apex of LL normal, but elsewhere severe fibrosis with honeycombing. Some bronchiolar metaplasia. No FF.	Lower lobe	Limited information
52 (Green)	*L*	Preserved UL with peripheral fibrosis, confluent fibrosis in LL with honeycombing. FF largely confined to LL.	Lower lobe	UIP
58 (Orange)	*L*	Limited sub-pleural fibrosis, heterogeneous with basal dominance. Mild chronic inflammation & bronchiolar metaplasia. FF present.	Basal dominant	Limited information
13 (Black)	*L*	Diffuse fibrosis with honeycombing in LL, with active remodelling. FF & mild chronic inflammation. Preserved areas in UL.	Lower lobe	UIP
65 (Asparagus)	*R*	Basal dominant fibrosis with moderate chronic inflammation and some bronchiolar metaplasia. FF present.	Bases of all lobes	UIP
53 (Yellow)	*R*	Sub-pleural fibrosis with hypertensive changes. Honeycombing in UL. All lobes similar, with some preserved architecture. Severe welders siderosis.	Lobes homogenous	Limited information
60 (Nickle)	*R*	Diffuse fibrosis with some bronchiectasis. Honeycombing and FF, with mild-moderate chronic inflammation.	Heterogeneous	UIP
59 (Teal)	*R*	Consolidated fibrosis and honeycombing in LL, with preserved areas in UL. Sub-pleural fibrosis most prevalent showing temportal heterogeneity. FF present.	Lower lobe	UIP
43 (Red)	*R*	Minor areas of preserved lung, but largely distorted architecture. Mucus within airspace, and FF prominent.	Heterogeneous	UIP

Abbreviations: LTx= Lung transplant, Tx= transplant, ILD= interstitial lung disease, L= left, R= right, ILD= interstitial lung disease, UL= upper lobe, LL= lower lobe, UIP= usual interstitial pneumonia, PF= pulmonary fibrosis, NSIP= nonspecific interstitial pneumonia, FF= fibroblastic foci

3.3.3.2 Distribution of Leukocytes Across the Interstitial Lung Disease Lung

Patient LTx-43 (red symbol in figures) had an incomplete fissure between the upper and middle lobes, meaning only samples from the upper and lower lobe were obtained from the surgical team. This resulted in n=5 samples from the RM and n=6 for the RU and RL regions for flow cytometry analysis. LTx-51 (purple symbol in figures) received a double lung transplant and therefore has data points for both left and right lungs, which is reflected in the reported n number where relevant and denoted by an asterisk.

3.3.3.2.1 Leukocyte Numbers

At an inter-lung level, there were significantly higher numbers of total leukocytes (p=0.015), macrophages (p=0.015), monocytes (p=0.015) and T cells (p=0.032) isolated from the left lung (i.e. patients receiving a left SLTx, n=8*) than the right lung (i.e. from patients receiving a right SLTx, n=6*) (Figure 3.8). However, the distribution of granulocytes, NK cells and B cells were not significantly different between lungs.

There was also a variable distribution of cells at an intra-lung level. In the left lung, the distribution of total leukocytes (p=0.006), granulocytes (p<0.001), NK cells (p<0.001), and T cells (p<0.001) were highly variable, specifically between the upper lobe and the remaining lobes (Figure 3.8A, D, E & G). The same subsets were also variable in their distribution within the right lung (total leukocytes granulocytes, p=0.004, NK cells p=0.010, and T cells p<0.001). However, differences in distribution were also identified between the middle and lower lobe (Figure 3.8D & G).

3.3.3.2.2. Leukocyte Proportions

The contribution of each cell population to the total leukocyte pool was determined and presented as a percentage for each subset and region (Figure 3.9). The same assessment of regional heterogeneity (generalized estimating equation) found that in the left lung, monocytes (p=0.003), NK cells (p<0.001), T cells (p<0.001) and Tregs (p<0.001) had significantly different proportions between lobes of the lung, and these differences persisted in the right lung (p=0.015, p<0.001,

p=0.002 and p<0.001, respectively) (Figure 3.9B, C, D, F and Gc). The proportion of CD4+ T cells was significantly higher compared to the proportion of CD8+ T cells (p=0.024) (Figure 3.9Gb).

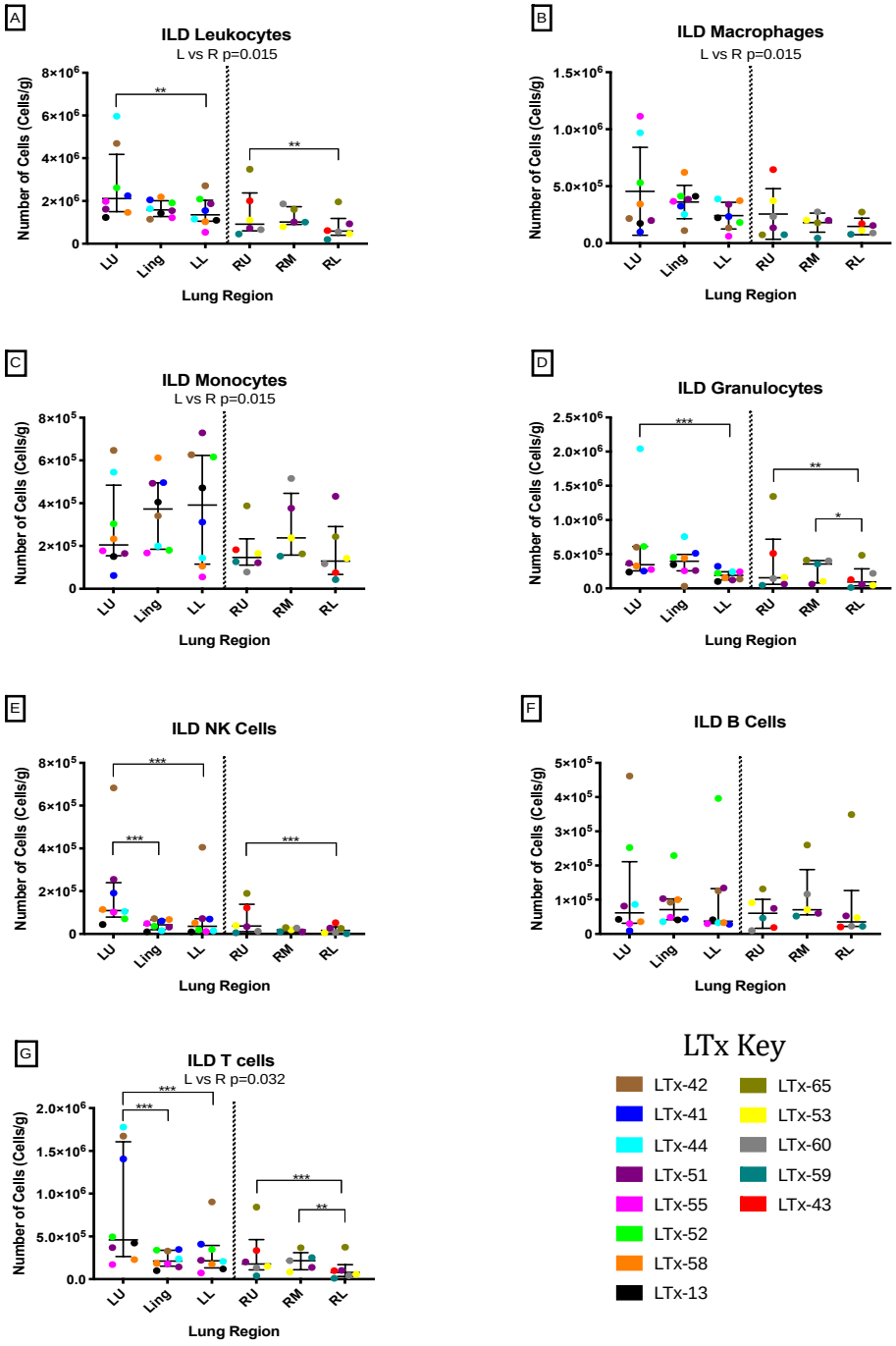

Figure 3.8 The regional number of key leukocyte subsets within the interstitial lung disease lung. Each patient in the cohort is characterised by a distinct colour (see key, refer to Table 3.3-3.4 for clinical information), demonstrating the total number of cells per gram of tissue for the overall number of CD45+ leukocytes (A) and six major leukocyte subsets (B-G) (left; n=8*, right; n=6*, for all regions except RM, n=5*). On scatter plot A and C-G, bar and lines represent median + IQR (data log transformed for statistical analysis), on scatter plots B they represent mean ±SD. All differences between regions determined by a generalized estimating equation with Bonferroni post-test correction, * = $p \leq 0.05$, ** = $p \leq 0.01$, *** = $p \leq 0.001$, significance $p > 0.05$ not reported. The p value reported below the subset graph title represents an overall difference between the number of leukocytes in the left and right lung (two-way ANOVA of grouped data, significant p value reported, significance $p > 0.05$ not reported.). The dotted line separates the data sets to distinguish between patients who received a left or right single lung transplant. *LTx-51 (purple) received a double lung transplant and therefore has data points on both sides of the dotted line.

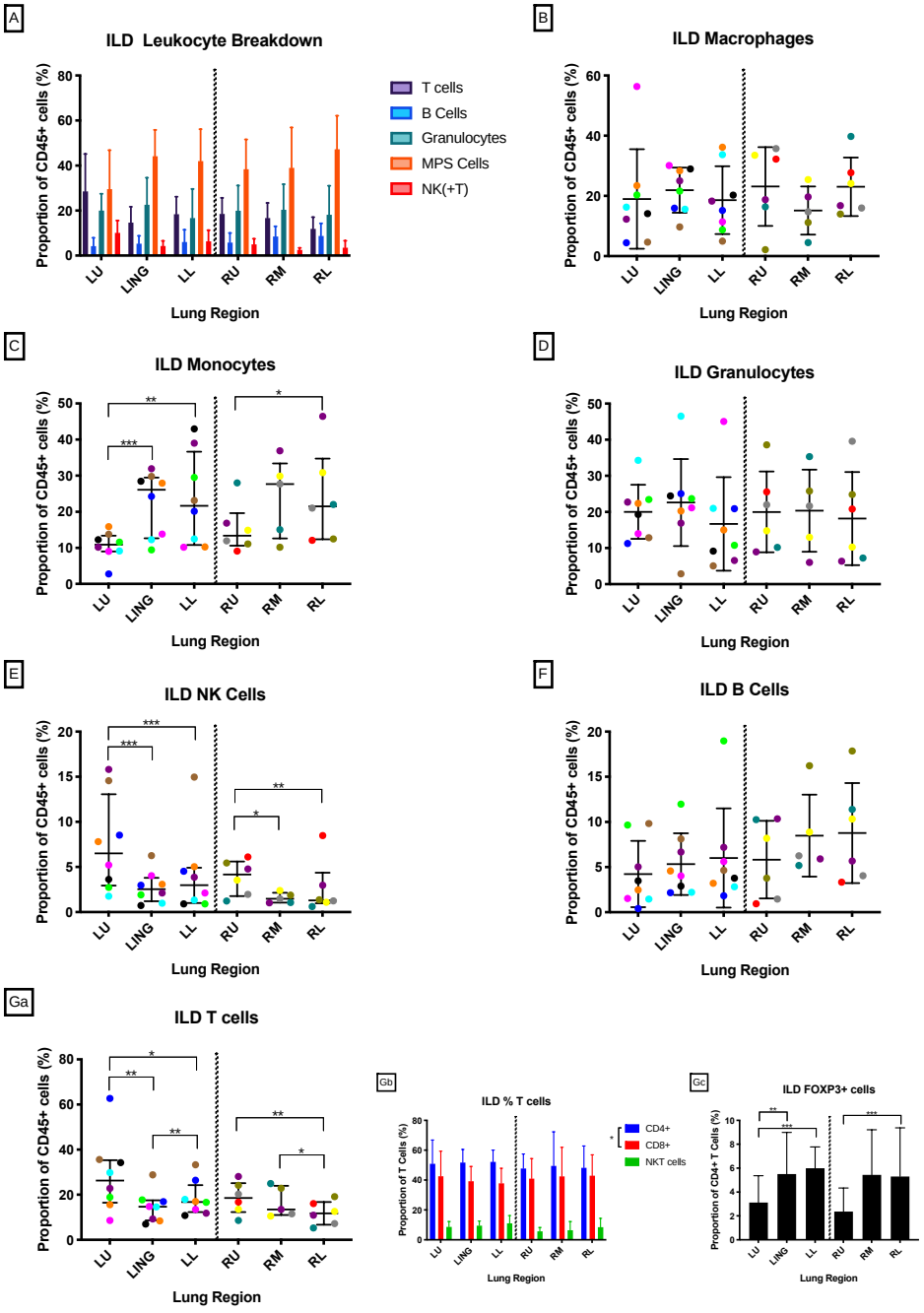

Figure 3.9 The regional proportion of key leukocyte subsets to the total leukocyte pool within the interstitial lung disease lung. The contribution of each cell population to the total leukocyte pool in each region of the lung was determined and presented as a percentage for major subsets (A). Each patient in the cohort is characterised by a distinct colour, demonstrating the proportion per gram of tissue for six major leukocyte subsets (B-G). Gb shows the proportion of CD3+ cells that were CD4+, CD8+ or CD56+ (NKT cells) across each region, and Gc shows the proportion of CD4+ cells that were also FOXP3 positive (left; n=8*, right; n=6*, for all regions except RM, n=5*). Bars on A, Gb and Gc represent mean +SD, and on scatter plots B, D & F the bars and lines represent mean ±SD. On scatter plots C, E & Ga, the bar and lines represent median + IQR (data log transformed for statistical analysis). All differences between regions determined by a generalized estimating equation with Bonferroni post-test correction, * = $p \leq 0.05$, ** = $p \leq 0.01$, *** = $p \leq 0.001$, significance $p > 0.05$ not reported. A paired samples T test was performed to test the difference between CD4+ and CD8+ proportions, * = $p \leq 0.05$. The dotted line separates the data sets to distinguish between patients who received a left or right single lung transplant. *LTx-51 (purple) received a double lung transplant and therefore has data points on both sides of the dotted line.

3.3.3.3 The Intra-Patient Regional Heterogeneity in Leukocyte Subsets Across the Interstitial Lung Disease Lung

The high degree of intra-patient variability in leukocyte number (Figure 3.10) and proportions (Figure 3.11) were determined within individual ILD lungs (n=12). LTx-43 was disregarded from this analysis, as a RM sample was not obtained from the surgical team at the time of transplant due to an incomplete fissure between their upper and middle lobe.

3.3.3.3.1 Leukocyte Numbers and Proportions

Three patients had homogenous leukocyte numbers between lobes, with only minor variation in cell number (LTx-13, -53 and -52). In three different patients, the number of total leukocytes was higher in the upper lobe compared to the middle and lower lobe regions, particularly driven by increases in T cell, granulocyte and macrophage number (LTx-44, -65, and -55). However histologically, each of these patients had disease that was most extensive in the lower lobes with basal dominance (Table 3.4). Conversely, leukocyte numbers were higher in the lingula or RM lobe of three ILD lungs (LTx-58, -59, and -60).

The proportion of T cells, granulocytes, macrophages and monocytes exhibited high intra-patient variation within the lung. Although an increase in monocyte proportion in the middle to lower lobes was evident in a large number of patients, changes in the other subsets across different regions were more difficult to generalise.

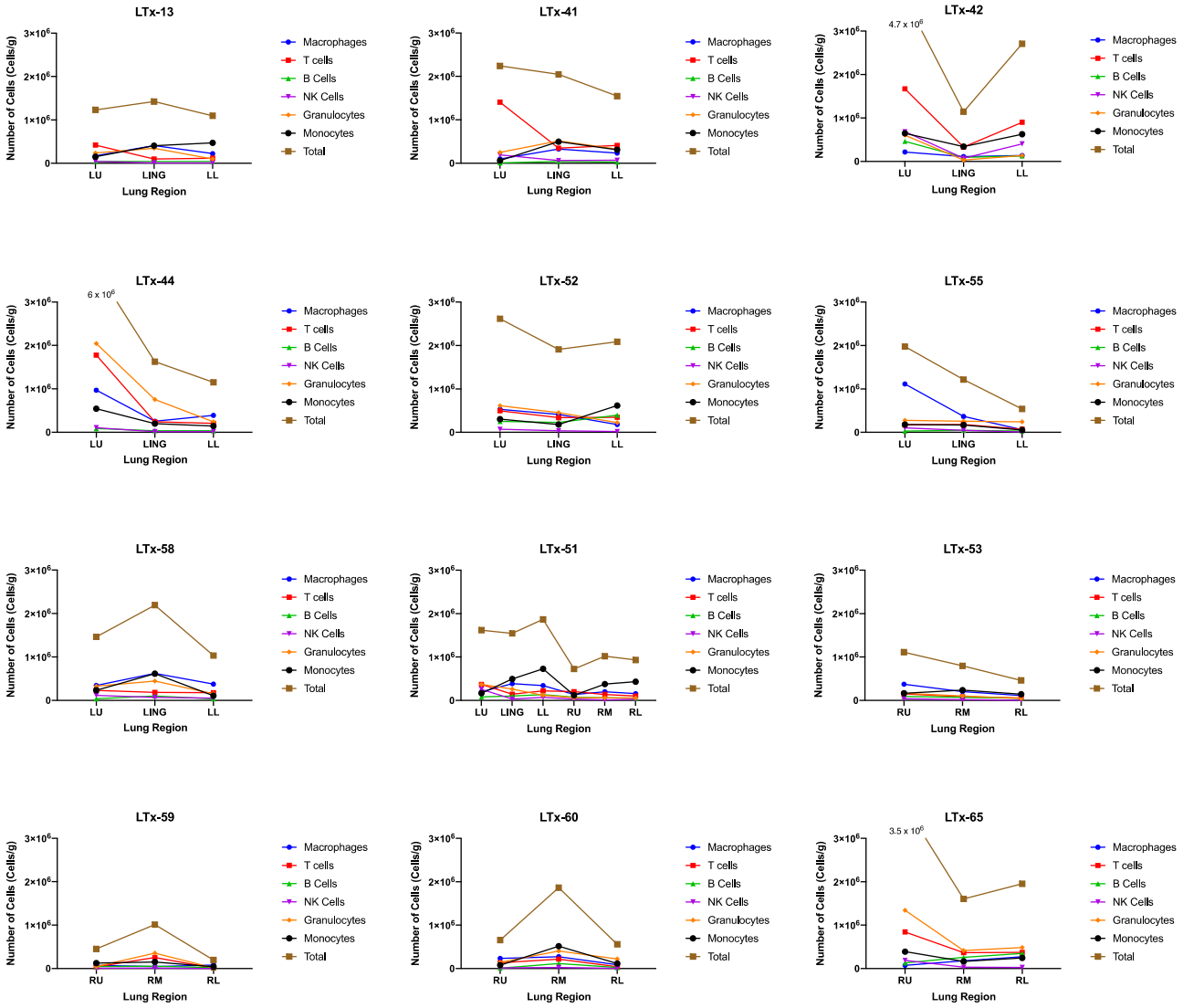

Figure 3.10. Quantifying the regional variation in leukocyte subset numbers in interstitial lung disease (ILD) at an intra-patient level. Each graph represents the total number of leukocytes (brown) and six major subsets per gram of tissue across different lobe regions in patients with ILD (n=12). The lines on each graph help visualise the increases or decreases in each subset across the three regions of the lung, determined by the side of the lungs undergoing transplant. One patient, LTx-51, received a double lung transplant and therefore has six samples. The scale bars on each graph are the same and range from zero to 3 million cells per gram of tissue, given the predominantly low leukocyte number in the majority of samples. However, in three of the patients, one of their samples exceeded 3 million and the actual value of the data point has instead been written next to the missing point.

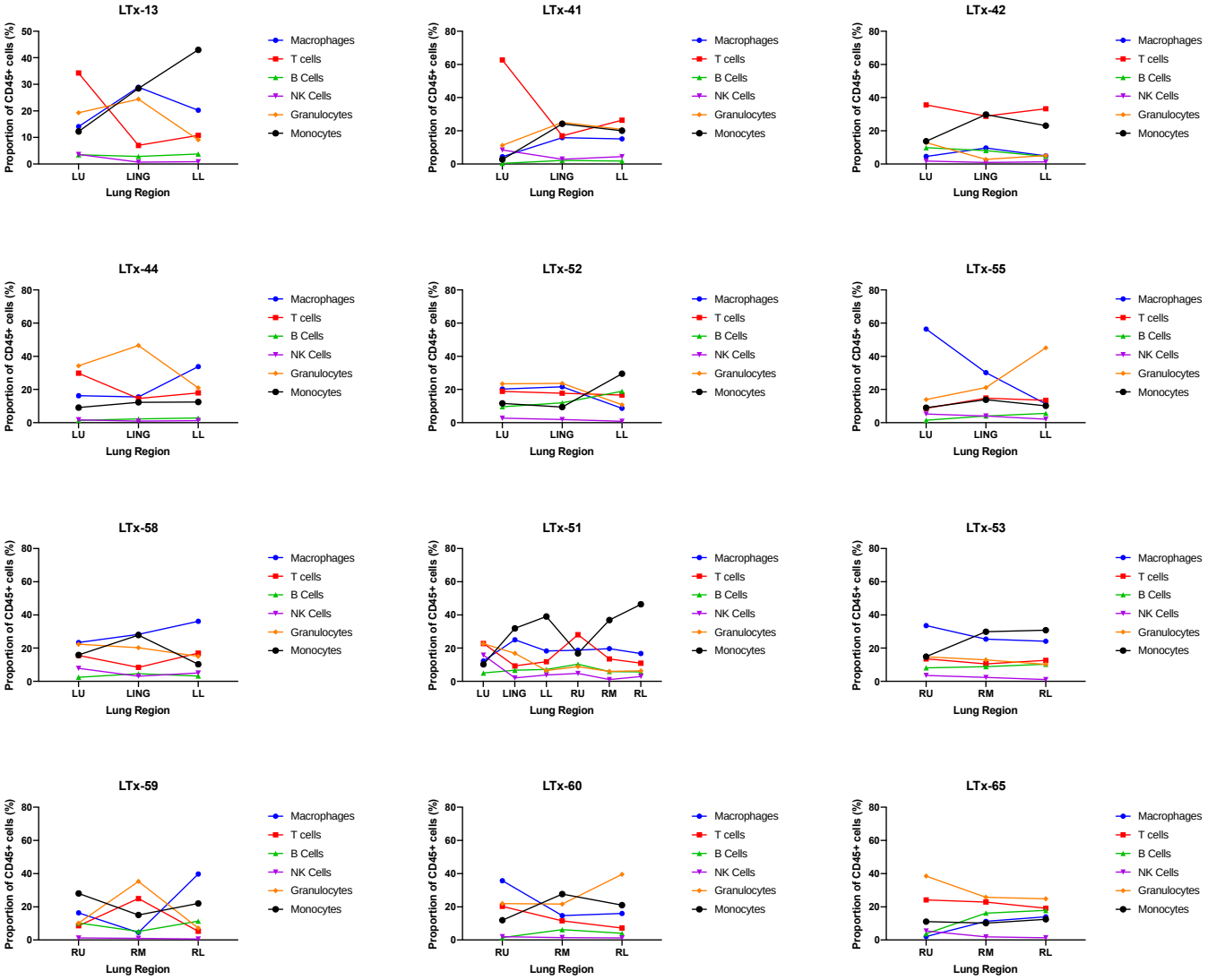

Figure 3.11 Quantifying the regional variation in leukocyte subset proportions in interstitial lung disease (ILD) at an intra-patient level. Each graph represents the contribution of six leukocyte subsets to the total leukocyte pool per gram of tissue as a percentage, across different lobe regions in patients with ILD (n=12). The lines on each graph help visualise the increases or decreases in each subset across the three regions of the lung, determined by the side of the lungs undergoing transplant. One patient, LTx-51, received a double lung transplant and therefore has six samples. The scale bars on each graph are the same and range from zero to 80%.

3.3.3.4 The Relationship Between Total Leukocyte Number and Clinical Parameters in Interstitial Lung Disease

The total number of leukocytes across the ILD lung was examined within different clinical parameters, phenotypes and clinical history (Figure 3.12). This included analysis between patients that had IPF or another form of ILD (Figure 3.12A), between males and females (Figure 3.12B), smoking history (Figure 3.12C), disease progression (determined as the time between diagnosis and transplant) (Figure 3.12D) and lung function, specifically difference in FEV_1 and FVC (Figure 3.12E and F). There was no significant difference in the number of leukocytes when correlated to any of these parameters ($p>0.05$), with the exception of FVC which demonstrated patients with an FVC between 50-80% of their predicted grade had the highest number of leukocytes in all regions ($p=0.0075$).

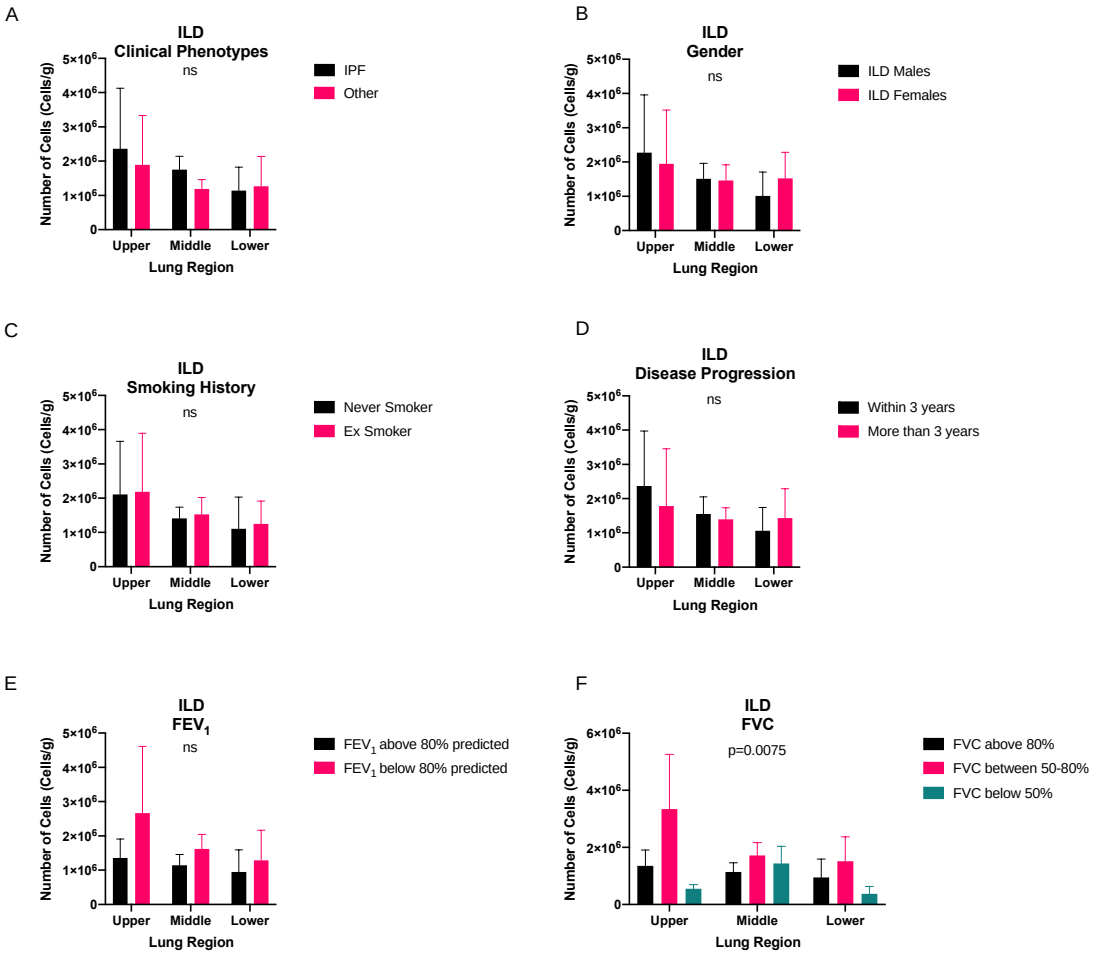

Figure 3.12 Correlating the total number of leukocytes in interstitial lung disease (ILD) to clinical parameters. The total number of leukocytes per gram of tissue in each region was assessed based on (A) ILD phenotype (IPF; n=8, other; n=6*), (B) patient gender (female vs male; n=5*v9), (C) patient smoking history (ex smoker; n=9*, never smoker; n=5), (D) the time in which someone progressed from diagnosis to transplant (within three years; n=9, more than three years; n=5*), (E**) the severity of disease as assessed by forced expiratory volume in one second (FEV_1) (FEV_1 above 80% predicted; n=4*, FEV_1 below 80% predicted; n=8) and (F**) disease severity by FVC grading (FVC above 80%; n=4*, FVC between 50-80%; n=5, FVC below 50%; n=2). All bars represent mean +SD, statistical differences between parameters were determined by a two-way ANOVA of grouped data, significance $p > 0.05$ reported as ns. *Patient LTx-51 underwent a double lung transplant, and has leukocyte data from both lungs. **This data was not available for all patients and subsequently the n numbers are lower for these parameters.

3.3.4.6 Cytokine and Chemokine Profiling

The concentration of 13 cytokines and chemokines were quantified across the three different regions of the fibrotic lung (left; n=8*, right; n=5*) (Figure 3.13). LTx-43 (red symbol in figures) was not included in Luminex analysis because of the missing RM sample point as previously described. The concentrations of GM-CSF, IFNγ, IL-10, IL-12p70, IL-1β, IL-2 and TNFα were below the limit of detection (3.2 pg/ml) for most samples, whilst IL-12p40, IL-1α and IL-4 had detectable levels in approximately half the samples, however the levels in remaining samples were extrapolated. This

data has been included in Appendix 7 for reference, but statistical analysis was not performed due to low concentrations of these cytokines. Cytokines that did exceed the assays limit of detection for all samples were again IL-1RA, IL-6 and IL-8 and differences between regions of each lung were examined. IL-1RA and IL-6 demonstrated significant heterogenic differences within the right lung (p=0.005, p=0.004 respectively). There was no significant difference within the left lung in both IL-1RA and IL-6. The concentration of IL-8 was not different across either lung (p>0.05).

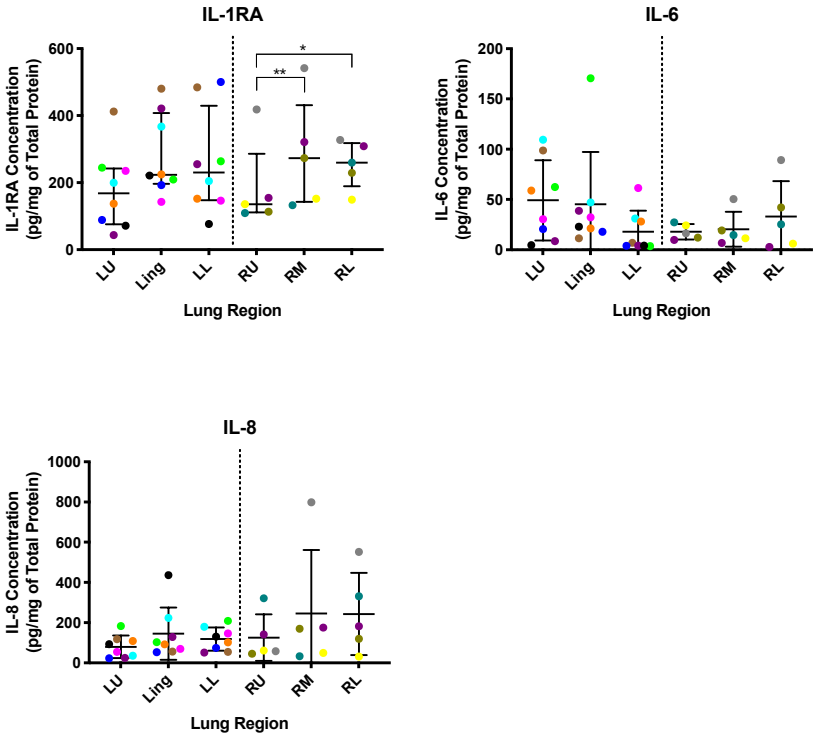

Figure 3.13 The regional concentration of interleukin-1 receptor antagonist, interleukin-6 and I interleukin-8 within the interstitial lung disease lung. The concentration of interleukin- (IL-) 1RA, IL-6 and IL-8 was measured per milligram of total protein in lung tissue lysate from three regions of each lung (left; n=8*, right; n=5*). Each patient in the cohort is characterised by a distinct colour, representing the cytokine concentrations in each region per patient, and correlate to 12 of the 13 patients in figures 3.8 to 3.9. The IL-1RA scatter plot bar and lines represent median + IQR (data log transformed for statistical analysis), the IL-6 and IL-8 scatter plots represent mean ±SD. All differences between regions determined by a generalized estimating equation with Bonferroni post-test correction, * = $p \leq 0.05$, ** = $p \leq 0.01$, significance $p > 0.05$ not reported. Overall, generalized estimating equation determined the right lung regions had significantly different levels of IL-6 (p=0.01) but no specific post-test corrections were found. The dotted line separates the data sets to distinguish between patients who received a left or right single lung transplant. *LTx-51 (purple) received a double lung transplant and therefore has data points on both sides of the dotted line.

3.3.4 Cystic Fibrosis

3.3.4.1 Patient Demographics and Clinical History

Demographics, pulmonary function, clinical history and explant histology of CF patients are summarised in Tables 3.5 to 3.6. Samples were obtained from two female and three male patients, with an average age of 34.6 years (range of 27-53 years) at the time of transplant (Table 3.5). The most recent pulmonary function tests performed prior to transplant were collected where possible, with FEV_1 falling below 15% predicted and FVC below 30% predicted for the majority of patients. All patients had a history of exacerbations and had ward admissions in the year prior to Tx, with four of the five patients being in-patients at the time of Tx. All patients also had microbial colonisation, most commonly with species of *Pseudomonas* or *Aspergillus.* One patient also had MRSA infection as well as *M. Abscessus.* All but one patient had a co-morbidity of CF-related diabetes, with osteo-related disorders or the need for an ileostomy also common. Histopathology reports confirmed that bronchiectasis was generally widespread throughout the lungs with a homogenous pattern, although other features such as fibrosis or emphysema were heterogeneous (Table 3.6).

Table 3.5 Cystic fibrosis cohort demographics, pulmonary function and clinical history. The clinical history of each patient (n=5) was obtained from the transplant medical records held by Manchester University NHS Foundation Trust and key parameters pertaining to the patients demographics, lung function and clinical history were summarised.

LTx Code (Colour)	***Gender***	***Age at Tx***	***FEV_1, L (% Predicted)***	***FVC, L (% Predicted)***	***Co-morbidities***	***Smoking Hx***	***Colonisation Hx***	***Exacerbation Hx***
68 (Blue)	*F*	*31*	*0.47(NA)*	*1.14 (NA)*	*CF related diabetes* *Mild haemoptysis*	*NA*	*Aspergillus*	*Frequent 2016/2017, ward admissions*
72 (Brown)	*M*	*28*	*0.39 (8.5%)*	*0.98 (17.5%)*	*CF related diabetes* *Osteopenia* *Ileostomy*	*Never smoked*	*P. aeruginosa*	*3-4 per year, ward admissions*
87 (Cyan)	*M*	*34*	*0.57 (13.4%)*	*1.36 (26.5%)*	*CF related diabetes* *Ileostomy* *Respiratory failure* *Talc pleurodesis*	*Never smoked*	*Pseudomonas*	*Ward admission August 2017*
118 (Green)	*M*	*53*	*1.07 (28%)*	*3.2 (65.6%)*	*Gastro oesophageal reflux disease* *Pancreatic insufficiency*	*Never smoked*	*MRSA* *P. aeruginosa* *M. abscessus*	*7 ward admissions in pre Tx year*

Abbreviations: LTx= Lung transplant, Tx= transplant, Hx= history, NA=not available in medical records, FEV_1= Forced expiratory volume in one second, FVC= Forced vital capacity, F= female, M= male, L= liter, CF= cystic fibrosis, SVC= superior vena cava, *P.*= *Pseudomonas, A.*= *Aspergillus, MRSA*= meticillin-resistant Staphylococcus aureus.

Table 3.6. A summary of explanted lung histopathology reports for patients with cystic fibrosis. A histopathology report for each patients' explanted lungs were obtained following examination by a histopathologist at Manchester University NHS Foundation Trust and the key observations were summarised. Particular attention was paid to any reference of disease heterogeneity across the lungs, and the area(s) of the lung most affected were identified where relevant information was available.

LTx Code (Colour)	***Summary of Histology Report (R; right lung, L; left lung, O; overall analysis)***	***Area of lung most affected?***
47 (Black)	R: Fibrosis in lower region of upper lobe and parts of lower lobe, with bullous lesions. Dilated pus filled bronchioles. Worse in lower lobes. L: Fibrosis in lower lobe, and lower region of upper lobe. Widespread bronchiectasis & bronchiole dilation. Worse in lower lobes. O: Similar, widespread bronchiectasis, inflammatory debri. Acute inflammation extending to lung parenchyma. Features of PH. Changes prominent within the lower lobes.	Lower lobes
68 (Blue)	R: Small upper lobe, adherent to middle lobe. Cystic bronchiectasis of upper lobe with purulent material. Middle & lower lobes relatively spared, dark nodule at base of lower lobe. L: Pale pleural surface, nodular over lower lobe. Dilated bronchi filled with green mucus in apex of both lobes, lower lobe central bronchiectasis with empty bronchi O: Similar, range of bronchi dilation and plugging with acute chronic inflammation to chronic inflammation and fibrosis. Left lower lobe has some normal lung. PH features.	Mixed
72 (Brown)	R: Entire lobes show obstructive pneumonitis in a background of bronchiectasis L: Widespread bronchiectasis, more prominent in upper lobe and upper region of lower lobe. O: Similar pattern, extensive bronchiectasis involving hilar. Lower lobe inflammation extends into parenchyma with prominent bronchitis and bronchiolitis. Emphysematous changes in lower lobes	Mixed
87 (Cyan)	R: Upper and lower lungs adherent to each other. Fluid filled bullae at base. Cystic areas containing purulent debris, bronchiectasis secondary to CF. Relatively normal background tissue. L: Solid area at apex, possible infarct. Diffuse bronchiectasis and cystically dilated spaces containing purulent debris. O: Generalised bronchiectasis and bronchiolectasis with some purulent secretions. Centrilobular fibrosis and elastosis, a probable consequence of recurrent infection.	Mixed
118 (Green)	R: Pleural surface unremarkable, no lesions, bronchiectatic changes L: No lesions, but parenchyma has broncciectatic changes O: Moderate to severe emphysematous change with bullae formation. Bronchiectasis with acute inflammatory cell infiltration of bronchi to adjacent alveoli.	Not specified

Abbreviations: LTx= Lung transplant, R= right lung, L= left lung, O= overall, PH= pulmonary hypertension

3.3.4.2 Distribution of Leukocyte Across the Cystic Fibrosis Lung

During the acquisition of the sample on the flow cytometer, the RM sample for patient LTx-87 (cyan symbol in figures) was lost when the cytometer malfunctioned. This resulted in an n=4 for RM and n=5 for the remaining regions for the flow cytometry data in the CF cohort.

3.3.4.2.1 Leukocyte Numbers

Total leukocyte ($p<0.001$), monocyte ($p<0.001$), granulocyte ($p<0.001$), NK cell ($p<0.001$) and T cell ($p<0.001$) distribution was highly variable across different areas of the CF lung (Figure 3.14A, C, D, E and G). These differences were inter-lung for total leukocytes, specifically between the lingula and RM, but each of the other subsets had both inter- and intra-lung differences. Interestingly, a number of post-hoc differences in these subsets were also between the two middle regions of the lung. There were no differences detected in macrophage or B cell numbers between lobes ($p>0.05$) (Figure 3.14B and F). The high inter-patient variation observed in Figure 3.1 persisted within individual leukocyte subsets.

3.3.4.2.2 Leukocyte Proportions

The contribution of each cell population to the total leukocyte pool was determined and presented as a percentage for each subset and region (Figure 3.15). Monocytes, ($p=0.015$), NK cells, ($p<0.001$), T cells ($p<0.001$) and Tregs ($p<0.001$) each had significantly different proportions between lobes of the lung (Figure 3.15C, E, Ga and Gc). These differences were evident at both an inter- and intra-lung level.

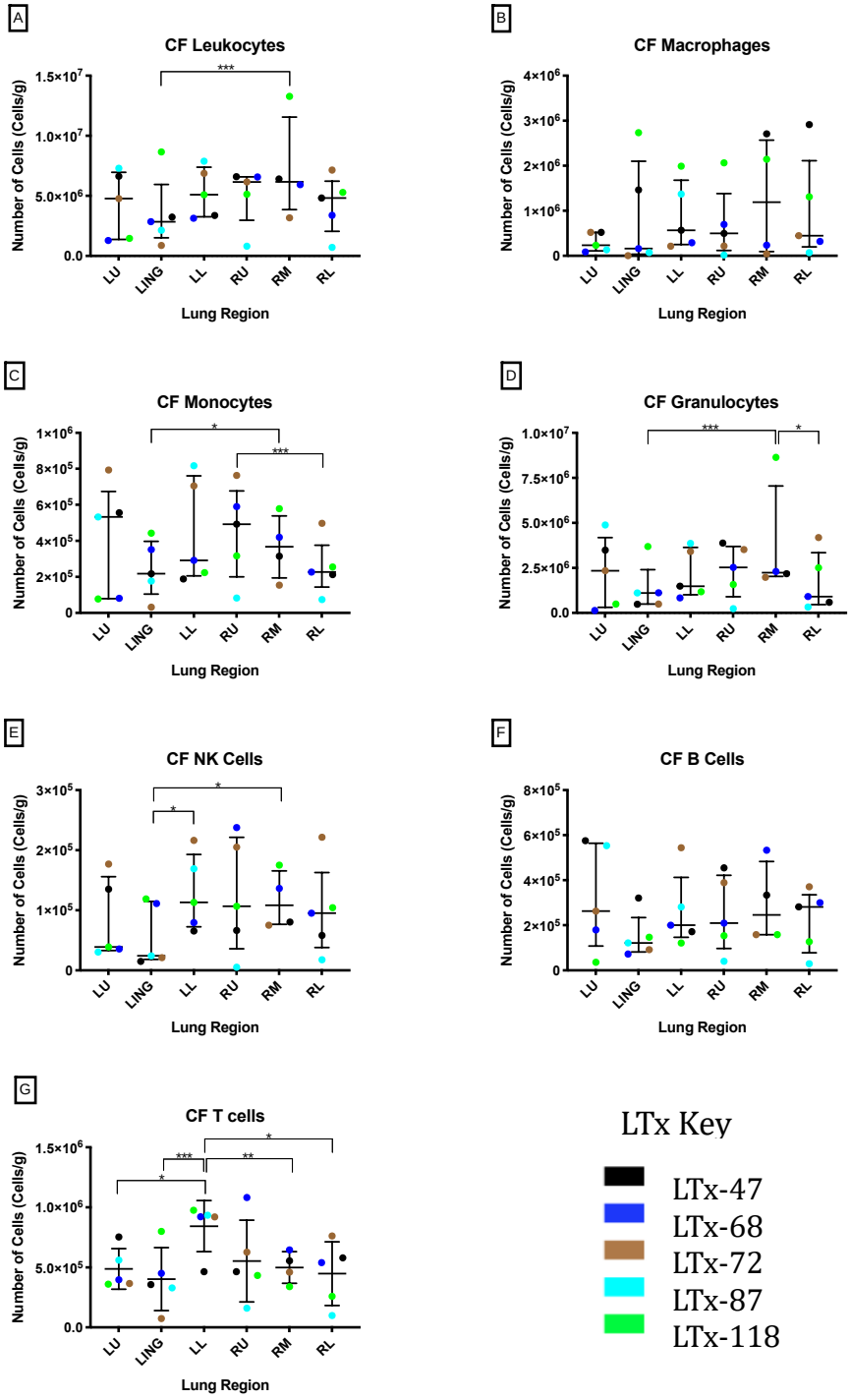

Figure 3.14 The regional number of key leukocyte subsets within the cystic fibrosis lung. Each patient in the cohort is characterised by a distinct colour, demonstrating the total number of cells per gram of tissue for the overall number of CD45+ leukocytes (A) and six major leukocyte subsets (B-G) (n=5 for all regions except RM, n=4). On scatter plots A-F, bar and lines represent median + IQR (data log transformed for statistical analysis), whilst scatter plot G, bar and lines represent mean ±SD. All differences between regions determined by a generalized estimating equation with Bonferroni post-test correction, * = $p \leq 0.05$, ** = $p \leq 0.01$, *** = $p \leq 0.001$, significance $p > 0.05$ not reported.

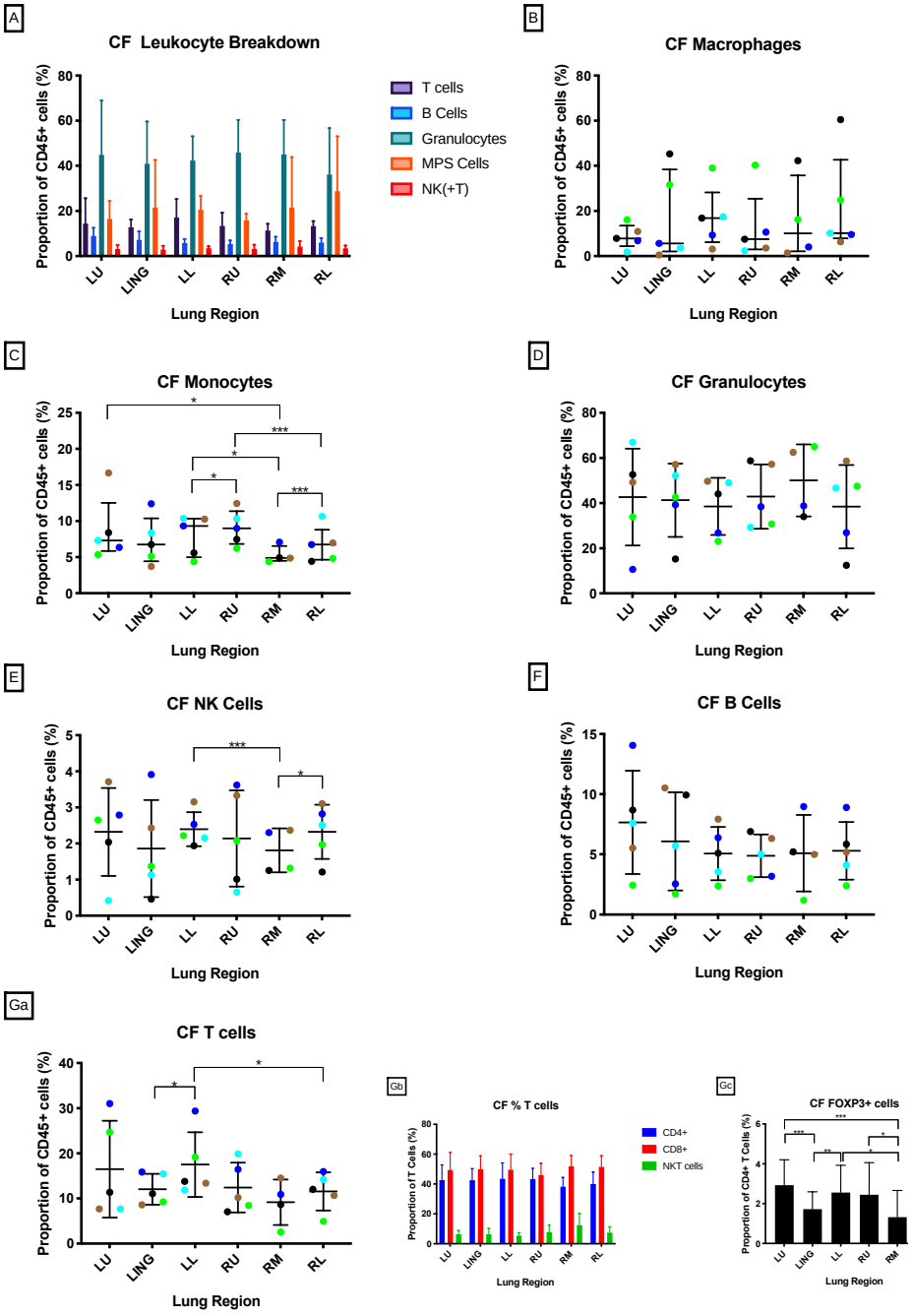

Figure 3.15 The regional proportion of key leukocyte subsets to the total leukocyte pool within the cystic fibrosis lung. The contribution of each cell population to the total leukocyte pool in each region of the lung was determined and presented as a percentage for major subsets (A). Each patient in the cohort is characterised by a distinct colour, demonstrating the proportion per gram of tissue for six major leukocyte subsets (B-G). Gb shows the proportion of CD3+ cells that were CD4+, CD8+ or CD56+ (NKT cells) across each region, and Gc shows the proportion of CD4+ cells that were also FOXP3 positive (n=5 for all regions except RM, n=4). Bars on A, Gb and Gc represent mean +SD, and on scatter plots C-G the bars and lines represent mean ±SD. On scatter plots B & C, the bar and lines represent median + IQR (data log transformed for statistical analysis). All differences between regions determined by a generalized estimating equation with Bonferroni post-test correction, * = $p \leq 0.05$, ** = $p \leq 0.01$, *** = $p \leq 0.001$, significance $p > 0.05$ not reported. A paired samples T test was performed to test the difference between CD4+ and CD8+ proportions, significance $p > 0.05$ not reported.

3.3.4.3 The Intra-Patient Regional Heterogeneity in Leukocyte Subsets Across the Cystic Fibrosis Lung

Given the high degree of inter-patient variability, leukocyte number and proportions were then determined within individual CF lungs (Figures 3.16 and 3.17).

3.3.4.3.1 Leukocyte Numbers and Proportions

Granulocytes were the most prevalent leukocyte for all patients across most regions, although macrophages were elevated to similar levels in LTx-47 and -118 in a limited number of areas. In patients that had increased variability across their lungs (LTx-72, -87 and -118), this was often manifested by large upward or downward deviations in leukocyte numbers in the right middle or left lingula regions in comparison to the remaining regions of the lung.

The proportion of leukocyte subsets varied within different CF patients. In LTx-72 and -87, granulocytes were the dominant subset across all regions. However, for the other three patients, the subset of leukocyte was much more variable within different regions. An increase in macrophage proportion, observed in LTx-47 and -118, correlated with multi-pathogen colonisation (Table 3.5).

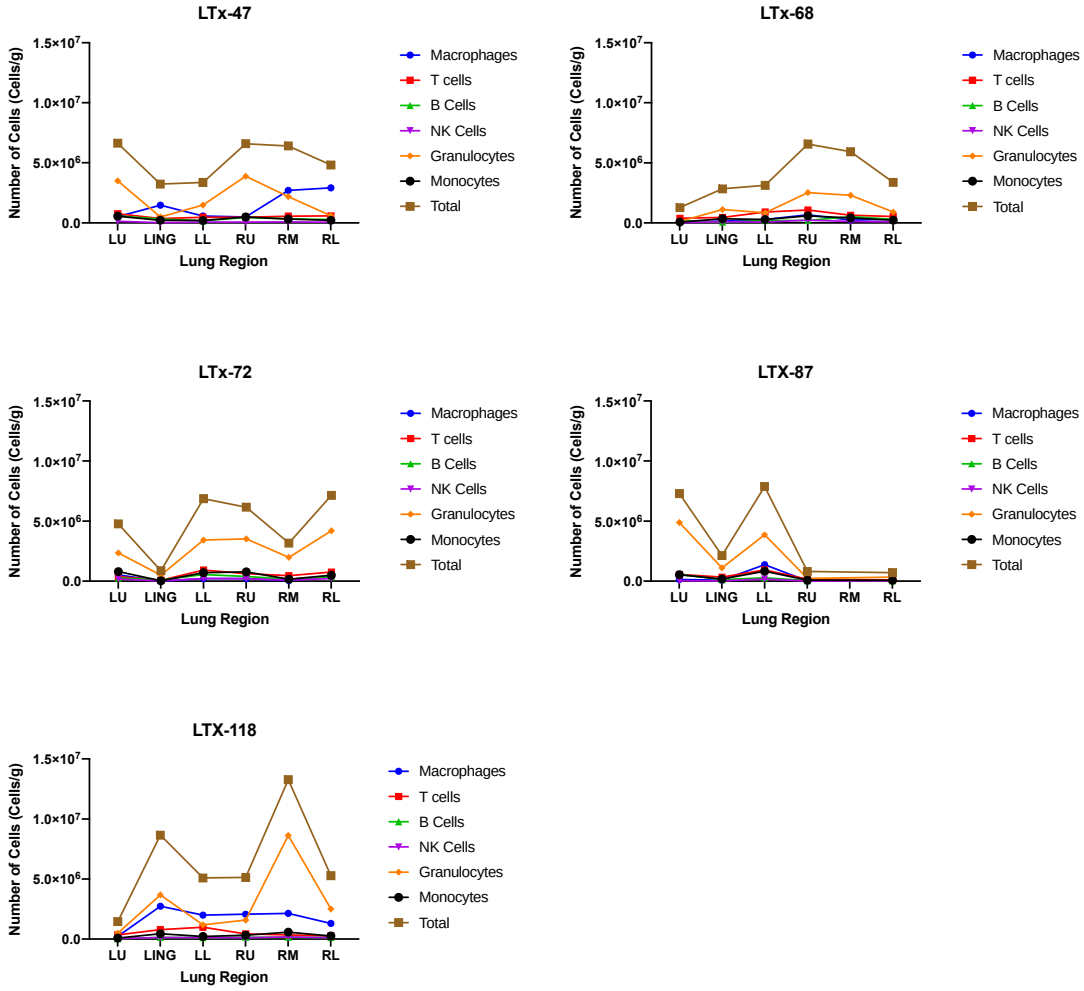

Figure 3.16 Quantifying the regional variation in leukocyte subset numbers in cystic fibrosis at an intra-patient level. Each graph represents the total number of leukocytes (brown) and six major subsets per gram of tissue across different lobe regions in patients with cystic fibrosis (n=5). There is a data point for each patient at every region, except LTx-87 who does not have a right middle (RM) lobe result for any leukocyte. The lines on each graph help visualise the increases or decreases in each subset across the six regions of the lung. The scale bars on each graph are the same and range from zero to 15 million cells per gram of tissue.

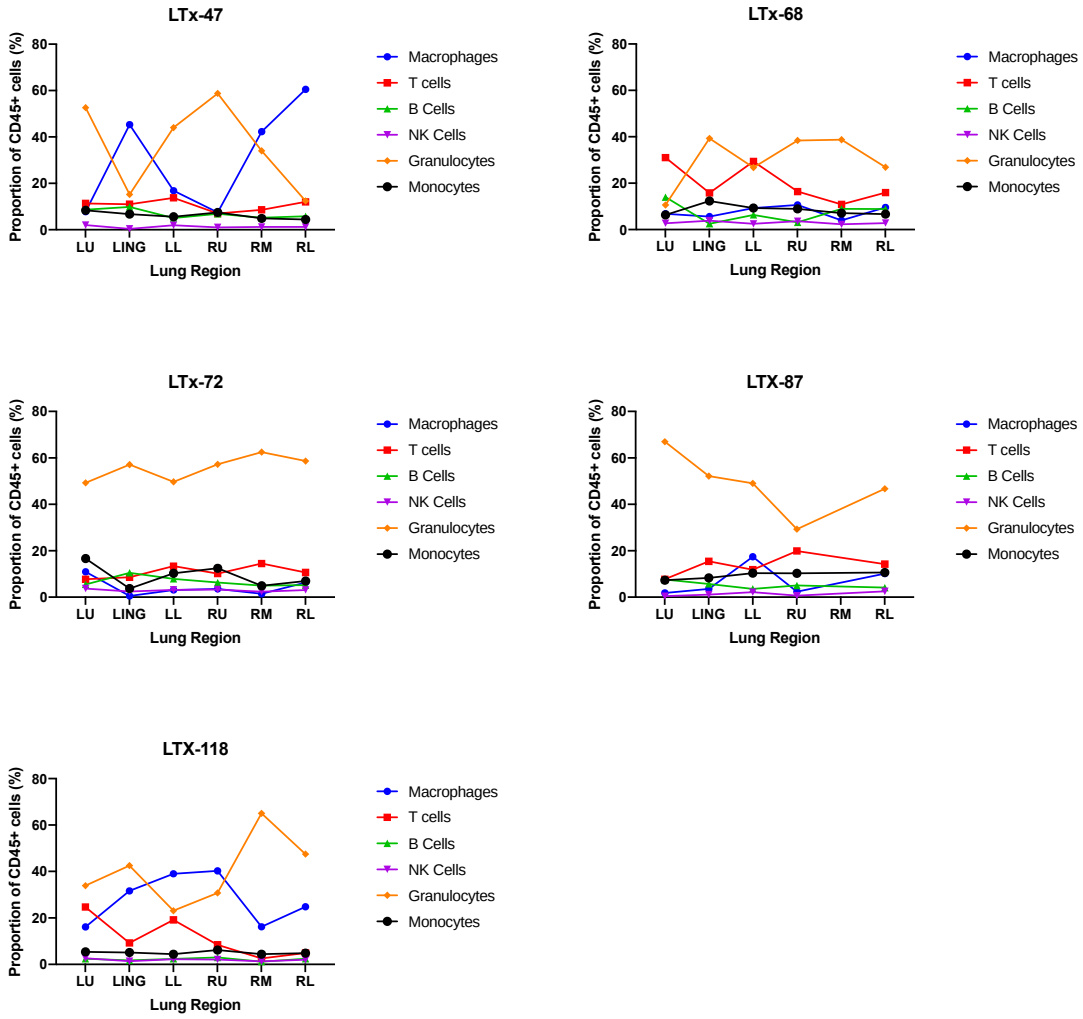

Figure 3.17 Quantifying the regional variation in leukocyte subset proportions in cystic fibrosis at an intra-patient level. Each graph represents the contribution of six leukocyte subsets to the total leukocyte pool per gram of tissue as a percentage, across different lobe regions in patients with cystic fibrosis (n=5). There is a data point for each patient at every region, except LTx-87 who does not have a right middle (RM) lobe result for any leukocyte. The lines on each graph help visualise the increases or decreases in proportion of each subset across the six regions of the lung. The scale bars on each graph are the same and range from zero to 80%.

3.3.4.4 The Relationship Between Total Leukocyte Number and Clinical Parameters in Cystic Fibrosis

Given the already small n= number of CF lungs, it was not appropriate to further divide the group to compared immune data with different clinical parameters, severity or clinical history.

3.4 Discussion

Chronic lung disease is inherently heterogeneous, given the role of gravity on perfusion-ventilation [192] and the natural hypoxic gradient, where O_2 percentage differs between the apex and the base of the lungs by up to 10% [193]. However, this presents a major challenge in understanding the inflammatory processes driving chronic lung disease, because in each disease, the lungs are not uniformly affected and there is often regional variation within the same clinical phenotype. This is confounded by limitations in isolated tissue sampling, and specifically how they may not be representative of the entire lung. Given these challenges, the correlation between the regional variation of inflammatory patterns and the different phenotypical presentations within diseases have not been fully explored. Specifically, the identification of prominent leukocyte populations within these different regions are the first step to understanding the upstream signalling processes that result in the different clinical phenotypes of chronic lung disease.

This study aimed to characterise the immune content of regional samples from lungs with end-stage COPD, CF or ILD. The samples were collected from peripheral sections of each lobe, containing parenchymal tissue, vasculature and small airway, and major leukocyte subsets were quantified. There was widespread heterogeneity in the numbers and proportions of leukocytes, evident at a cohort, regional and individual level. This heterogeneity also persisted for cytokines within the lung tissue. Despite this, there were a number of disease specific findings that were clinically relevant. In COPD, granulocytes and T cells were the most predominant cell types, and an increase of CD4+ T cells was observed compared to CD8+ T cells. The absolute number of leukocytes was significantly lower in COPD males, whilst COPD females, particularly with emphysema, had increased numbers that were highly variable across the lung. In ILD, there were significantly more leukocytes in the left lung than in the right, and the most prevalent cells were MPS cells. In particular, monocytes were increased in the middle and lower lobes for most patients. Finally, in CF, granulocytes were the dominant subset and major variations in leukocyte number occurred most frequently in the middle lobes. This was interesting given that bronchiectasis is a predominant feature in CF, and high granulocyte numbers were also noted in the lungs of COPD patients who had evidence of bronchiectasis upon histological analysis. Although the low n number of CF patients prevented

formal clinical correlation, a trend of increased macrophage proportion was associated with multi-colonisation.

3.4.1 Factors That May Influence Regional Heterogeneity

Clearly, caution should be taken when interpreting leukocyte data based on a single sample point, particularly in diseases such as COPD and CF, due to the intra-cohort and intra-patient variability. Conversely, the variationin leukocytes from ILD lung samples was relatively conserved. This may be driven by the differences in inflammatory mediators within the local tissue environment; in COPD the cohort demonstrated a pro-inflammatory state with elevated levels of IL-6 and IL-8, whilst ILD patients had lower levels of these inflammatory cytokines and instead had increased levels of the inflammatory inhibitor IL-1RA. The extent of regional heterogeneity in different leukocyte subsets will be discussed at a disease specific level in the proceeding sections. The findings will be related to clinical phenotypes of disease, patient demographics and other relevant clinical history where possible. However, there are broad physiological factors that may affect leukocyte movement within the lung, such as gravitational blood flow and ventilation pressures, vascular structure, size and density. There are also a number of transplant related factors such as the timing and length of the transplant and any circadian influences of leukocyte migration. Finally, microbial colonisation across the lung may also influence the number and population prevalence in different regions.

The lungs have grossly different vasculature to other organs given their unique dual blood supply via bronchial and pulmonary circulation [194]. These circulatory systems supply different areas of the lung; the bronchial arteries supply oxygen rich blood to the bronchial wall whilst the pulmonary arteries provide blood to the lung interstitium and alveoli. The structure of the vessels, their size and haemodynamics, as well as adhesion molecules and their expression within each of the circulatory systems can all impact leukocyte migration [195]. Despite the large degree of heterogeneity in chronic lung disease, conditions can often be grouped into those that primarily impact on the large airways, such as chronic bronchitis and cystic fibrosis, or those that affect the alveoli and interstitium as in emphysema and ILD [195]. Certain subsets of lymphocytes, effector T cells in particular, are more likely to amass in regions of the lung that receive bronchial blood [196], rather

than areas that receive a pulmonary supply such as the lung parenchyma. It could be speculated that lungs with large airway disease would be associated with larger numbers of T cells, as a possible contributor to disease pathology.

Another factor that can affect leukocyte margination within the lung is the size and density of the alveolar capillaries and venules, with 15% of functional capillary segments thought to be obstructed by leukocytes at any given time [197]. Given that the concentration of leukocytes during passage through the lungs is 1.5 times greater in capillaries than in the venules [198, 199], the proportion of these vascular structures within the sample could have a bearing on leukocyte numbers. Indeed, capillary density is different across the lung; there is a lower density of capillary segments within the subpleural microcirculation than in central regions of the lung [197]. Given all samples in this study were procured from peripheral sections, this will have been somewhat normalised across the samples. However, changes in lung vasculature occur in chronic lung disease, and this may be different between patients with the same condition. Regional differences in both ventilation and perfusion have also been characterised within the lung, identifying differences between the apex and base of the lungs [200]. These topographical differences, driven by hydrostatic pressure within the pulmonary blood vessels, result in an ascending reduction in blood flow towards the apices of the lungs. This in theory could alter the number and proportion of leukocytes residing within the upper and lower lobes of each lung, and provide an argument for the regional differences that were observed. However, given heterogeneity was not limited to upper and lower lobes in this study, topographical differences in blood flow perhaps have limited relevance.

The migratory pattern of leukocytes in circulation and their infiltration into surrounding organ tissue is modulated by the time of day and circadian rhythm, although this phenomenon has most extensively been studied in murine models [201, 202]. Pick *et al.* (2019) reviewed recent evidence regarding the mechanisms that govern leukocyte migration in both steady state and inflammation, highlighting that neutrophils in particular can change the phenotypic fingerprint of different tissues throughout the course of a 24-hour period [203]. Neutrophils were observed to migrate to the lung during the evening, which is the onset of the active phase in mice [201]. However, how comparative this is to human diurnal variation is currently unclear. Given the unpredictable nature of transplant, it

is no surprise the patients enrolled in this study underwent transplants at vastly different times of the day. Despite the small n= numbers for each cohort, an attempt was made to compare leukocyte numbers between patients who had a transplant during the day or at night in the COPD and ILD cohorts (Appendix 8). Although there were no significant differences in this analysis, the results should be taken with caution. The use of day or night is highly arbitrary for an operation that can last over eight hours, and many patients bridged the two. The time at which samples were received is also highly variable from when the operation began, and when the patients were put onto bypass, essentially halting pulmonary circulation within the lungs. However, these respective timings and further segmentation of the 24-hour day could be factored into future statistically powered studies.

A second transplant factor that could influence leukocyte heterogeneity observed between patients in particular, but also intra-patient variation, is the time taken to perform the surgery. Specifically, the time of patients were commenced on bypass to the time taken to explant the lungs and sample the different regions, and the subsequent ischaemic insult to the native lung/s. During a transplant, one native lung is explanted, the corresponding new donor lung is transplanted, and then the process begins again for the second native lung. The average time between obtaining samples from each of the lung explants was approximately two hours, although this was highly dependent on the surgical team and the difficulty in performing the procedure for each patient. Other surgeries that utilise cardiopulmonary bypass have observed an activation of the circulating neutrophil pool within 15 minutes of bypass commencing, demonstrated by elevated expression of CD11b/CD18 integrin [204]. The ischemic insult during bypass promotes endothelial cell activation leading to rapid expression of adhesion molecules, such as P-selectin and intercellular adhesion molecule 1, which facilitate the process of cell extravasation into tissues [205]. However, given that immunophenotyping of lung tissue often occurs from surgical resections that undergo significantly longer and more varied periods of ischaemic time, the ischaemic time between the two lungs was relatively small (one to four hours) and standardised by being on-site to collect the samples immediately following explant. This could therefore be relatively inconsequential to the research.

Respiratory infections are a common contributor to exacerbations in patients with chronic lung disease, particularly in COPD and CF, although patients with ILD also experience periods of acute

exacerbations that have been correlated to the lung microbiome [206]. Pathogen-associated molecular patterns (PAMPs) drive inflammation through the activation of macrophages, T cells and B cells, which augments chronic respiratory disease [207]. In turn, the destruction of normal airway and the development of bronchiectasis perpetuates pathogen colonisation. An analysis of the microbiome in explanted COPD lungs identified gross differences in the regional composition of bacterial communities across the same lung [208]. Given bacterial colonies regulate the local immune environment, it is quite feasible they contribute to the variability of leukocytes observed across the lung.

3.4.2 Clinical Correlation with Regional Heterogeneity

Absolute leukocyte counts and proportions were examined between disease groups and between individual lungs within each disease cohort. Pre-transplant clinical data was then compared to determine if leukocyte characteristics were controlled or influenced by clinical factors.

3.4.2.1 Chronic Obstructive Pulmonary Disease

During the intra-COPD lung analysis, it was apparent that some lungs had comparably low and homogenous numbers of leukocytes across the different lung regions, whilst other patients were profusely more variable. This appeared to be a gender associated difference; three lungs explanted from male COPD patients were regionally homogenous in terms of absolute leukocyte numbers, whilst the patients with greatest variability were all female and had emphysema. The number of leukocytes isolated from lung samples was also significantly increased in female patients. This could be reflective of an active verses static diseased state in females and males, with the larger degree of inflammatory heterogeneity in the lung indicative of disease severity and clinical instability. The gender difference in cytokine expression of IL-6, IL-8 and IL-1RA was also examined, and conversely found that COPD lungs explanted from male patients had significantly higher levels of inflammatory chemokine IL-8 compared to female COPD lungs (Appendix 8). However, this analysis was significantly underpowered (n=3 per gender) and should be viewed with caution. Tam *et al.* (2015) demonstrated increased oxidative stress and activation of TGF- β1 (a

pro-inflammatory cytokine previously discussed in Chapter One, Section 1.2.1) in females compared to males in a mouse model of COPD, which was inhibited when an ovariectomy was performed [209]. This suggests female hormones could play a role in the increase of inflammation in the female COPD lung. In turn, this could lead to impaired responses to treatment in women; perpetuating the poorer outcomes described in other COPD gender based studies [210-212]**.** There has been a marked rise in the prevalence of women diagnosed with inflammatory lung disease, and despite COPD being more common in males than females, during this study samples were collected from a higher proportion of women than men (n= 7 vs n=3). Indeed, the precedent of women being more severely affected by the condition may lead to an increase in their need for transplantation, perhaps explaining the increased sampling from female patients in this study. However, the gender profiles of the transplant waiting list were not analysed over the course of the 3.5 years of collection in this study, and the greater number of female COPD patients could equally be random.

T cells were one of the predominant leukocyte subsets in COPD, which is not unexpected given CD8+ T cells have been linked to disease pathogenesis in a number of studies obtaining samples from airway or tissue resections [51], [213] [190]. However, in this study there were significantly more CD4+ than CD8+ T cells, and interestingly this was evident across all regions of the lung (Figure 3.3Gb). Although rare in the literature, and perhaps due to sampling limitations, CD4+ T cell prevalence has previously been described in the emphysematous lung, due to clonal expansion in response to an antigen-specific stimuli [214]. T cell numbers were generally well conserved between patients and across each of the regions, with the exception of LTx-61, LTx-80, and in one instance LTx-92 (Figure 3.4). These patients all had a markedly elevated CD4 to CD8 ratio compared to the rest of the cohort (Appendix 5), so whilst most patients did have marginally higher CD4:CD8 ratios, it is likely these outliers drove a significant difference. They were all female patients with emphysema, although one also had bronchiectasis with an AATD diagnosis, all were previous smokers, and at the upper age range of the group. CD4+ T cells have previously been described as a useful biomarker in differentiating COPD phenotypes [215], and identifying patients with a history of exacerbations. Interestingly, two of the three patients had frequent exacerbations in the year prior to transplant (Table 3.1), and the number of CD4+ T cells were significantly increased

in patients that experienced more frequent exacerbations (Appendix 8). Exacerbations in COPD are predominantly infection driven, and the increase of foreign antigen could perpetuate antigen-specific clonal expansion of CD4+ cells as previously described [214]. CD4+ cells express increased levels of signal transducer and activator of transcription 4 (STAT4), which drives Th1-polarisation [216]. In turn, Th1 associated cytokines influence macrophage derived products such as matrix metalloprotease 12, which has been correlated with alveolar degradation [217].

Another interesting finding was the predominance of granulocytes within COPD subjects who had histological evidence of bronchiectasis (Tables 3.1-3.2, Figures 3.2-3.3). Although the acute inflammatory response is essential to deal with microbial infection, it should be self-limiting and result in the resolution of inflammation as well as the infection [218]. However in bronchiectasis, excessive neutrophilic airway inflammation and colonisation perpetuate a cause and effect cycle that culminates in damage to the airways. Neutrophil lifespan is highly dependent on cues from the local environment such as that of epithelium derived factors like GM-CSF, and yet in bronchiectasis this increased lifespan results in an impaired ability to perform phagocytosis, which further promotes bacterial infection [219, 220]. This is supported by the increased prevalence of granulocytes in the CF lung, where bronchiectasis is a common pathological process. The paradoxical feedback loop between localised epithelial signals, prolonged neutrophil survival and persistent microbial infection may be a driver for the heterogeneous pattern of disease and observations of granulocytes across the lungs.

As described earlier, chronic lung disease can alter the lung vasculature, and a number of patients, particularly in the COPD cohort, had evidence of PH. COPD results in poorly ventilated areas of the lung, and pulmonary vasoconstriction is a physiological response to hypoxia in the pulmonary arterioles, redirecting blood flow to areas of superior ventilation within the lung. However, the exaggerated occurrence of this reflex can contribute to PH, and result in further systemic consequences [221]. Given the large number of leukocytes, and neutrophils in particular, that reside within the blood, the act of vasoconstriction shunting blood indiscriminately to other areas may drastically alter the immune composition within tissue from different lung regions. As such, PH is likely to be an important factor in this study. This was considered retrospectively for the COPD

patients enrolled in this study, comparing those patients who had reported PH in their clinical history or evidence of PH changes in their histology reports to those who did not (Appendix 8). The sources of clinical information regarding PH were conflicting between clinical history and histopathology reports (Table 3.1 vs Table 3.2), so analysis was performed on three scenarios. The separation of patients with PH based solely on their clinical history or histological report had no significant difference to patients without PH, although the average number of leukocytes trended lower overall in the PH groups. However, when grouping all patients with any reference to PH, there were significantly lower numbers of leukocytes compared to lungs without PH. The reduced numbers of leukocytes in the COPD-PH lung was surprising given that systemic inflammation has previously been found to be higher in COPD patients with PH [222, 223], and CD8+ T cell infiltration of the pulmonary arteries is associated with vascular abnormalities in earlier stages of COPD [224]. However, samples from this study were obtained from peripheral sections of the lung and as such may have missed areas with predominant PH features. The small n= numbers in this study may also have contributed to the confounding findings.

3.4.2.2 Interstitial Lung Disease

CD4+ were dominant in ILD, and also had an elevated proportion of FOXP3+ regulatory T cells (Tregs) (Figure 3.9Gc) compared to COPD and CF (Figures 3.3Gc and 3.15Gc). Tregs were most abundant in more severely diseased areas (Table 3.4), and decreased in the relatively conserved upper lobes of most patients. Tregs maintain homeostasis by suppression of immune responses such as T cell proliferation and cytokine production [225]. However, there are very few studies exploring the relationship of FOXP3+ Tregs in ILD. Patients with systemic sclerosis who had a high ILD score demonstrated an increased frequency of Tregs [226], although this remains contradictory throughout the limited literature [227]. Nevertheless this is an interested finding, discernible due to the regional sampling conducted during this study, and warrants further investigation of the role of Tregs in ILD.

In ILD, SLTx is a far more common procedure than in other chronic lung conditions, largely because of a reduction in lung compliance driven by disease pathology resulting in reduced operating lung volumes [228]. Whilst the most impaired lung would be the ideal explant for transplant, this is not always possible and the choice can frequently come down to which side of the chest has the capacity for the donor lung. It is therefore important to not infer that the data from these lung samples were derived from the patients' most grossly diseased lung. The lung samples were primarily analysed for heterogeneity within a single lung using a generalised estimating equation to take into account the inherent relatedness within the three lung samples. However, there are unique advantages in being able to explore the left and right lungs of patients with ILD so thoroughly. This is not only relevant for the clinical management of the remaining native lung, but to patients at much earlier stages of disease. During BAL, clinicians favour sampling from the right side of the lung, in either the middle or lower lobe, as this has largely been considered representative of inflammation in the lung as a whole [229, 230]. However, data from this study demonstrated that overall leukocytes, and in particular macrophages, T cells and monocytes were significantly higher in the left lung. Therefore information regarding inflammation in ILD could repeatedly be underestimated by sampling from the right lung alone. Given macrophages and monocytes are key leukocytes in the initiation of tissue repair and regeneration, and that a loss in the regulation of these cell types can consequently result in the aberrant repair process observed in ILD [231], it is essential to characterise these cell populations accurately across the lung. Interestingly, the middle lung regions produced the most consistent leukocyte numbers despite the cohort having multiple differential diagnoses. This was evident for all leukocyte subsets except monocytes, which had greater homogeny between patients in the upper lobes and far greater variation in the middle and lower regions. Given this coincides with areas of increased disease severity, further characterisation of monocytes may provide a useful insight to ILD pathogenesis.

Further clinical correlation of leukocyte numbers to factors such as gender, smoking history, disease progression and between IPF and other ILD phenotypes did not demonstrate any significant differences. However, the grouping of patients based on their FVC grading did demonstrate a significant difference. Patients with an impaired FVC of between 50-80% of their predicted normal value had increased numbers of leukocyte, particularly in the upper lobes, to both

those with preserved (>80% predicted) and severely impaired (<50%) FVC. Interestingly, a FVC of 50-80% is a clinical criterion for the use of both Nintedanib and Pirfenidone in IPF, which some of the patients within this study were taking prior to transplant (Appendix 9). These anti-fibrotic drugs are the only two approved drugs capable of slowing the progression of IPF. Nintedanib is a tyrosine kinase inhibitor, preventing the activation of pro-fibrotic mediators such as TNF-α, platelet-derived growth factor and TGF-β, which are thought to contribute to abnormal fibrotic processes [232]. In turn, this inhibits fibroblast functions such as proliferation, differentiation and extracellular matrix production. Pirfenidone has a broader, less specific mode of action, possessing anti-fibrotic, anti-inflammatory and anti-oxidant that targets not only lung, but also hepatic, kidney and cardiac fibrosis [232-234]. An association between increased leukocyte numbers in a patient group where some patients were taking pirfenidone is therefore surprising, given it has been correlated with a reduction in infiltrating leukocytes [235]. However, there are a number of other anti-inflammatory and immunosuppressant drugs, such as prednisolone and azathioprine, prescribed across the cohort that may further confound this analysis. FEV_1 and FVC data were also the most recent results within the transplant clinical files, and there was no reference to the clinical context of these results. Any number of factors such as infection, exacerbation or length of time between lung function and transplant may bias this analysis over such a small cohort.

3.4.2.3 Cystic Fibrosis

Neutrophils and macrophages are the leukocytes most extensively linked to CF, and were the most prevalent cell types described in the current study. Infiltrating neutrophils in CF have been described as having a large degree of plasticity, taking cues from the lung microenvironment to guide effector and regulatory functions [236]. Local hypoxia within diseased areas of the CF lumen has been shown to drive neutrophilic inflammation [237], and heterogenetic colonisations of microbial biofilms perpetuate a hypoxic microenvironment [238]. Local microbial colonisation within the lung could therefore support why granulocytes were extremely variable at both an inter- and intra-patient level. In hindsight, the characterisation of microbiota within the regional samples procured during this study would have complimented the inflammatory data. The clinical history of the patients allowed a retrospective analysis of previously known infections and the leukocytes

observed within their lungs. The CF patients within this study all had prior history of microbial colonisation, primarily with *Pseudomonas* and *Aspergillus* species, and a high degree of intra-patient heterogeneity in granulocyte numbers and proportions across the lung. Interestingly, an increased variability in macrophage proportion across the lung was identified in two patients (LTx-47 and -118, Figure 3.17) who were the only patients to have multiple colonisations documented in their clinical history. Macrophages within the CF lung have been suggested to increase pro-inflammatory activity and secretions, possess an over responsiveness to external stimuli and have a reduced capacity to deal with pathogenic infection [239]. Whilst the limited n numbers in this cohort, and a lack of regional knowledge relating to colonisation, prevent further postulation, this is an avenue that could be explored in future studies. This is particularly important given inflammation is known to drive lung damage in CF, but there are limited therapeutic options available to disrupt this [240], suggesting the most relevant targets are still unknown. This may in part be due to the fact that, despite the CF lung being associated with bacterial and fungal colonisation, there have been inconsistent findings regarding the microbiota of end-stage CF lungs [154, 241, 242], which in turn creates difficulty when drawing conclusions between the microbiota and inflammation. One study found that end-stage CF patients who underwent lung transplantation had monospecies microcolonies, in contrast to expectorates sampled from non-end stage CF patients who had multiple pathogens [242]. Yet, this was in discordance with another study that found end stage CF explanted lungs to be polymicrobial and that infections were spatially heterogeneous [241]. However, it is important to remember that CF has an inherent genetic component, both through primary mutations of the CFTR gene as well as polymorphisms in modifier genes, which could strongly influence findings at an inter-patient level.

Despite the heterogeneity of chronic lung disease being well characterised, CF is the only disease where regional variation of inflammatory content has previously been examined, albeit in a limited number of studies. In BAL fluid from CF patients, variability in inflammatory markers was demonstrated between the upper and lower lobes [151], as well as between the middle regions of the left and right lungs [152]. Comparably, the most variable regions of the CF lung in this study were also seen in the right middle and left lingula lobes. They were commonly identified by post-corrective statistical analysis, and also had evident variability in the intra-patient analysis. The

findings of this study add support to this, and build upon current knowledge with the utilisation of wedge biopsies that represent the full composite of the lung.

3.4.3 Limitations

The primary limitation to this study is the limited number of lungs that were analysed. Although an attempt was made to sub-categorise patients with COPD or ILD on the basis of clinically relevant factors, this analysis should be interpreted with caution due to the small n numbers. However, these disease cohorts were large enough to demonstrate the considerable heterogeneity in the numbers and proportions of leukocyte subsets, evident at a cohort, regional and individual level. A second limitation was the inability to analyse different lung compartments; parenchyma, airway and vasculature, in isolation. Whilst the study was able to map the overall inflammatory profile across 28 diseased lungs, the ideal scenario would have been to explore the inflammatory signature of each compartment to provide a complete picture of inflammation in each disease. Finally, although it recognized that other factors such as genetic variations, including circulating microRNA [156], and pathogenic colonisation can have a bearing on inflammation within the lungs, it is important that the concept of intra-lung analysis of inflammation is more widely considered.

3.4.4 Summary

The evidently heterogenic inflammation described between patients, lungs and lobes, in this study makes it clear that we should not generalise inflammation in lung disease. Isolated sampling techniques can place exorbitant or insubstantial importance to a finding that may not be relevant to the lung or disease as a whole. The collection of large, multi-site specimens in this study has led to several important observations. Firstly, female patients with emphysematous COPD have greater heterogeneity in leukocytes, compared to males. The proportion of CD4+ T cells was higher than CD8+ T cells in the end-stage COPD lung, which is in contradiction to existing reports in the literature, albeit in patients with mild disease. In ILD, there were significantly higher numbers of leukocytes isolated from the left lung than the right lung, and this pattern persisted for a number of subsets. Given clinical sampling is predominantly associated with the right side of the lung, this

could be of important clinical interest. Furthermore, monocytes were increased in the middle and lower lobes for most patients, and were highly heterogeneous. Given the CF cohort consisted of only 5 patients, it was difficult to interpret any meaningful patterns. However the frequency of significant differences in leukocyte number between the lingula and right middle corroborates previous findings for other sampling methods such as BAL.

Given the fundamental lack of research into immunophenotyping of the lung as a whole, this data presents an important first step in the characterisation of regional heterogeneity in chronic lung disease. The observations from these samples will be further interrogated in the proceeding chapters, particularly in patients with COPD and ILD where n= numbers enabled more detailed analysis. Further characterisation of T cells in COPD will be of interest, given the unexpectedly prevalent population of CD4+ T cells that were identified, especially if these can be further correlated to exacerbation frequency. In ILD, it is interesting that whilst most leukocyte subsets were homogenous across the lung, monocytes were highly variable. Given that increased variability corresponded to areas of worsened disease, the role of monocytes in ILD warrants further exploration.

Chapter Four: The Characterisation of Monocytes in Interstitial Lung Disease

4.1 Introduction

In chapter three, the left ILD lung had significantly higher numbers of leukocytes than the right lung, and this pattern persisted for a number of subsets. Unlike in COPD and CF, each region of the ILD lung had limited variation in leukocytes numbers, particularly in the middle lobes. However this was not the case for monocytes, which presented the most heterogeneous numbers across all patients and regions. The experiments in chapter three were specifically designed to generate fundamental observations, which would subsequently direct the proceeding research. This chapter will focus on a fundamental discovery from chapter three, that the ILD lung was dominated by intermediate monocytes, with comparably low populations of classical and non-classical monocytes.

ILD pathogenesis is most commonly associated with myofibroblasts and fibroblasts, whose roles in extracellular matrix (ECM) deposition and remodelling have been widely scrutinised and reviewed [243] [244] [245]. The underlying mechanisms of activation for these cells remain poorly understood, although interactions with leukocytes are likely to play a role [246]. Various leukocytes have been implicated in the pathogenesis of ILD; including T cells [247], B cells [248] and mast cells [249]. However, it is monocytes and macrophages [250] that have most commonly been associated with the disease.

Monocytes are not a uniform cell type, instead comprising of 3 different subsets; classical, intermediate and non-classical, which are characterised by their surface expression of markers CD14 and CD16 [251]. The $CD14^{++}$ CD16- classical monocyte is the most abundant and well characterised, contributing up 80-90% of the total monocyte population. $CD14^{+}$ $CD16^{++}$ non-classical monocytes and $CD14^{++}$ CD16+ intermediate monocytes are present at much lower frequencies, at 2-10% and 2-5% respectively [252]. Each subset has distinct and overlapping functions; classical monocytes play a major role in phagocytosis, can initiate a pro-inflammatory response via the secretion of numerous cytokines, and are thought to contribute to tissue repair [253]. Non-classical monocytes are highly motile, patrolling the endothelium for signs of tissue damage, whilst intermediate monocytes are thought to be highly inflammatory. However, the precise functions of intermediate monocytes are still widely conflicting [253], [254], [255].

Monocytes have been implicated in different ILD phenotypes, particularly IPF. Monocyte chemoattractant protein 1 (MCP-1) is highly expressed by lung epithelial cells in patients with IPF, driving increased monocyte recruitment and infiltration into the lung [256] [257]. Monocytes have been shown to remain within parenchymal tissue for up to two months [258], and it is thought that interactions between monocytes and fibroblasts contribute to MCP-1 production, further enhancing monocyte accumulation [259].

The aim of this chapter was to further characterise monocytes in different chronic inflammatory lung diseases, with a specific emphasis on ILD.

4.2 Methods

All data reported in this chapter was generated during the exploration of regional heterogeneity of lung disease discussed in chapter three. This is with the exception of the control subset, and a semi-quantitative histological analysis of disease severity in ILD.

Lung resection samples were obtained from MFT/North West Lung Centre under the framework of the Manchester Allergy, Respiratory and Thoracic Surgery (ManARTS) Biobank with ethical approval from the National Research Ethics Service (10/H1010/7). Observations in the control subset were made on non-cancerous lung tissue collected from patients undergoing surgery for suspected or confirmed cancer, who did not have a chronic inflammatory lung disease or severely impaired lung function (FEV_1/FVC >70%). These samples were collected and processed separately to the current study by Dr Anu Goenka, so analysis was retrospective and further clinical information was not available. However the samples were processed using the same methods as detailed in Chapter Two, Section 2.5.1-2. The flow cytometry files could therefore be retrospectively analyzed using the gating strategy detailed in Section 2.5.3 (Figure 2.1) to form a control group in this study.

A detailed methodology for the semi-quantitative scoring system can be found in Chapter Two, Section 2.7, although for reference the scoring system is detailed in Table 4.1.

Table 4.1 Semi-quantitative scoring system for histological assessment of disease severity. The extent of fibrosis, mononuclear inflitration and fibroblastic foci were assessed and given a semi-quantitative score based on the described severity of each parameter.

Score	***Established Fibrosis (EF)***	***Mononuclear Infiltration (MI)***	***Fibroblastic Foci (FF)***
Magnification	*x4*	*x4*	*x10 (10 fields)*
1 – Mild	*Patchy fibrosis/Subpleural*	*Patchy aggregates*	*0-2*
2 – Moderate	*Centrilobular fibrosis bridging to pleura*	*Patchy & extending to septa*	*2-4*
3 – Severe	*Honeycomb lung*	*Diffuse inflammation*	*>4*

4.3 Results

4.3.1 Patient Demographics and Clinical History

All data for ILD, COPD and CF was generated from patients described in detail in chapter three. Further clinical information was not available for the control group, beyond patients not having a form of chronic respiratory illness or impaired lung function.

4.3.2 Monocyte Subset Identification

The expression of CD16 against CD14 was used to identify classical (CD14++ CD16-), intermediate (CD14++ CD16+) and non-classical (CD14+ CD16++) monocytes in control, CF, COPD and ILD lungs (Figure 4.1). In blood, these markers traditionally form a waterfall pattern on flow cytometry density plots, enabling the separation of monocyte subsets. Overall, the proportions of monocytes in control, CF and COPD tissue were typical, with a dominant classical monocyte population identified. However, in many samples from the ILD cohort, there was a large population of intermediate monocytes observed. Given this observation, the proportion each subset contributed to total monocyte number was explored further.

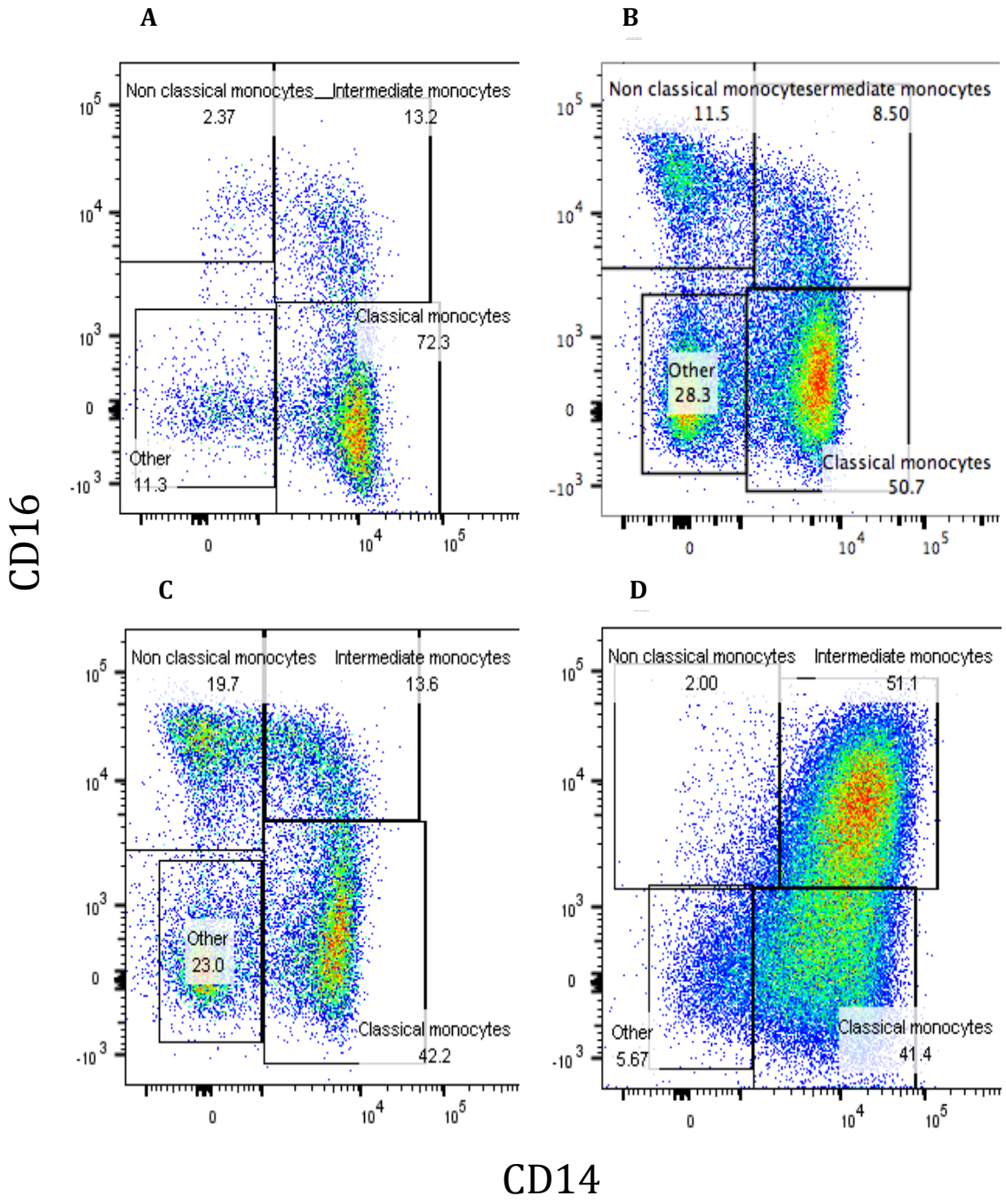

Figure 4.1 The monocyte waterfall in tissue samples from control, cystic fibrosis (CF), chronic obstructive pulmonary disease (COPD) and interstitial lung disease (ILD) lungs. Representative images of the density plots generated from (A) control, (B) CF and (C) COPD samples, demonstrating an evident waterfall pattern starting in the upper left box, flowing into the upper right box and then falling into the lower right box, and (D) ILD samples where the waterfall is less evident due to an abundance of intermediate monocytes in the upper right box.

4.3.3 Monocyte Populations in Different Disease Cohorts

In the COPD, CF, and control lung tissue, classical monocytes followed the traditional monocyte pattern being the dominant subset at 60-70%. (Figure 4.2.A-C). However, in ILD, classical monocytes only represented 40% of the total monocyte population. Instead, the average amount of intermediate monocytes increased to ~50%, although some patients ranged up to almost 80% (Figure 4.2.D). In contrast, the intermediate monocytes were approximately 20% in the COPD, CF and control lungs. Non-classical monocytes were the least frequent subset across all lungs, although control, CF and COPD patients averaged ~10% whilst ILD patients had ~5%. The proportion of monocytes described in lung tissue was atypical in all disease groups compared to the commonly described proportions within circulation (80-90% for classical, 2-10% for non classical and 2-5% intermediates). In blood, significant differences would be expected between classical monocytes to the other two subsets, but that intermediate and non-classical proportions would be comparable. Statistical analysis of the subsets in lung tissue demonstrated that only the control group met this expectation, demonstrating no statistical difference between intermediate and non-classical monocytes (figure 4.2.A). The other cohorts had significant differences between these two subsets ($p=<0.001$). The ILD cohort also deviated from the expected pattern, with no significant difference shown between classical and intermediate monocytes.

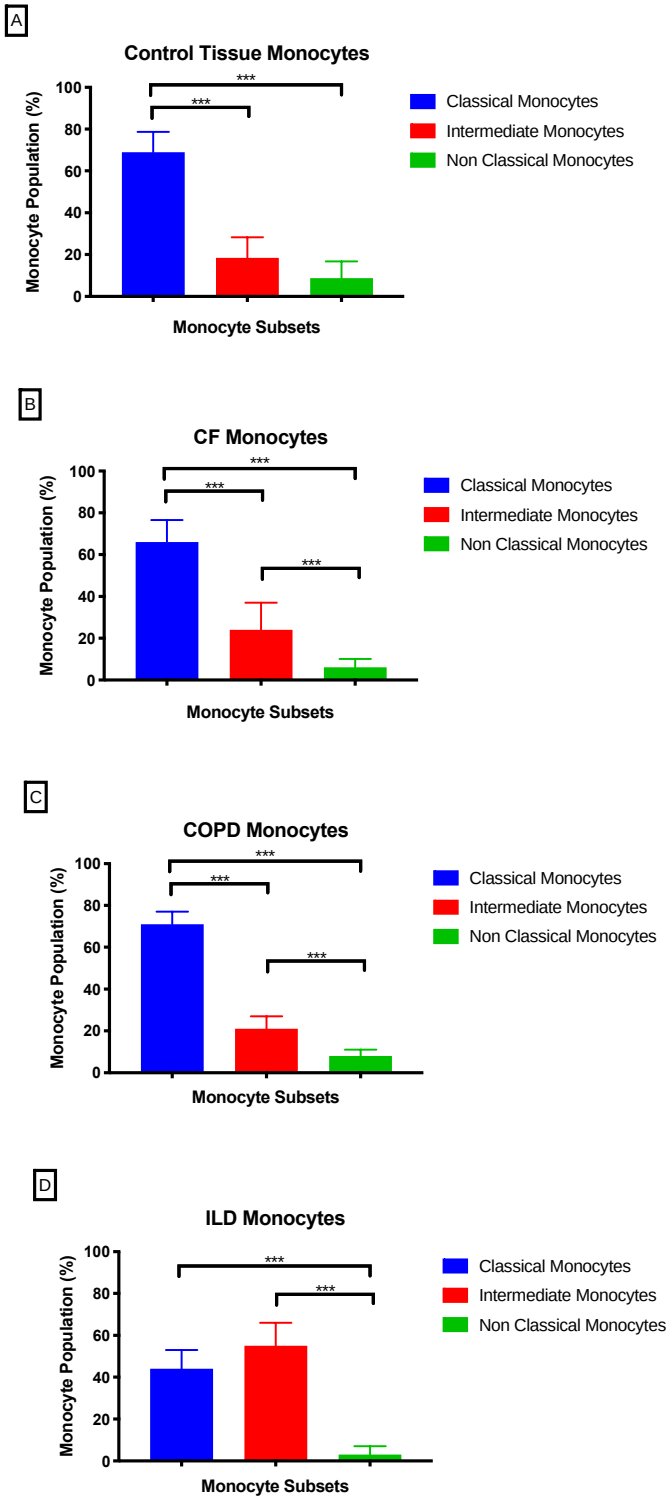

Figure 4.2 Monocyte subsets by disease group in control, cystic fibrosis (CF), chronic obstructive pulmonary disease (COPD) and interstitial lung disease (ILD) lungs. The percentage of total monocytes that classical, intermediate and non-classical monocyte subsets contribute in (A) control lung tissue (n=6), (B) CF (n=5), (C) COPD (n=10) and (D) ILD (n=13; 7 left SLTx, 5 right SLTx and 1 DLTx) lungs (bars represent median + IQR). All differences between monocyte subsets in each disease were determined by a Mann-Whitney U test, significance *** = $p \leq 0.001$, $p > 0.05$ not reported.

To explore these findings further, statistical analysis was also performed between the three disease groups and the control group (Figure 4.3). This confirmed that there were significant differences between the groups for classical monocytes ($p<0.001$), intermediate monocytes ($p<0.001$) and non-classical monocytes ($p=0.012$). Post-hoc analysis demonstrated classical monocytes were significantly lower in the ILD cohort compared to COPD and CF disease groups ($p<0.001$) and controls ($p=0.002$) (Figure 4.3.A). However, intermediate monocytes were significantly higher in the ILD group compared to COPD and CF ($p<0.001$) and controls ($p<0.001$) (Figure 4.3.B). There was also a significant difference between the cohorts for non-classical monocytes ($p=0.012$), which demonstrated that non-classical monocytes were present at a significantly higher frequency in COPD than the ILD cohort ($p=0.012$) (Figure 4.3.C).

There were no significant differences in monocyte populations between COPD, CF or controls lungs.

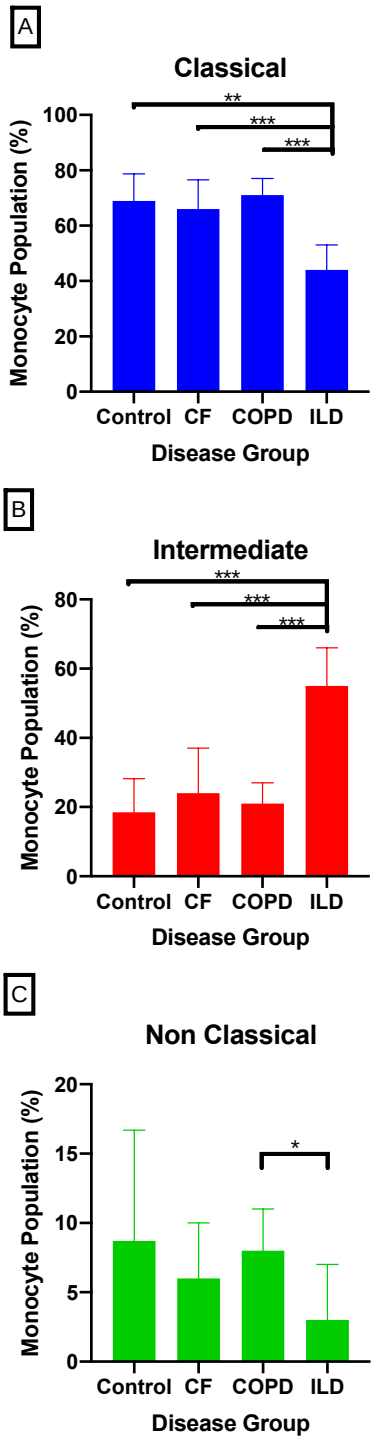

Figure 4.3 Monocyte subsets by cell type in control, cystic fibrosis (CF), chronic obstructive pulmonary disease (COPD) and interstitial lung disease (ILD) lungs. The percentage of total monocytes that (A) classical, (B) intermediate and (C) non-classical monocyte subsets contribute in control lung tissue (n=6), and in CF (n=5), COPD (n=10) and ILD (n=13; 7 left SLTx, 5 right SLTx and 1 DLTx) lungs (bars represent median + IQR). All differences between disease groups were determined by a Mann-Whitney U test, significance * = $p \leq 0.05$, ** = $p \leq 0.01$, *** = $p \leq 0.001$, $p > 0.05$ not reported. This data is the same as Figure 4.2, but reformatted to demonstrate statistical findings between disease groups instead of monocyte cell subsets in each disease cohort.

4.3.4 Regional Heterogeneity of Monocyte Subsets in Interstitial Lung Disease

Each of the monocyte subsets were examined across different regions of the ILD lung (Figure 4.4).

On average, classical monocytes were more prevalent in the upper lobe than in the middle or lower lobes, whilst intermediate monocytes demonstrated the reverse. However, despite quite clear clustering of intermediate monocytes across the majority of patients, high variability across the group prevented any significant differences being observed. In contrast, non-classical monocytes demonstrated significant difference in their prevalence in the upper lobe to both the middle ($p=0.042$) and lower ($p=0.039$) lobes.

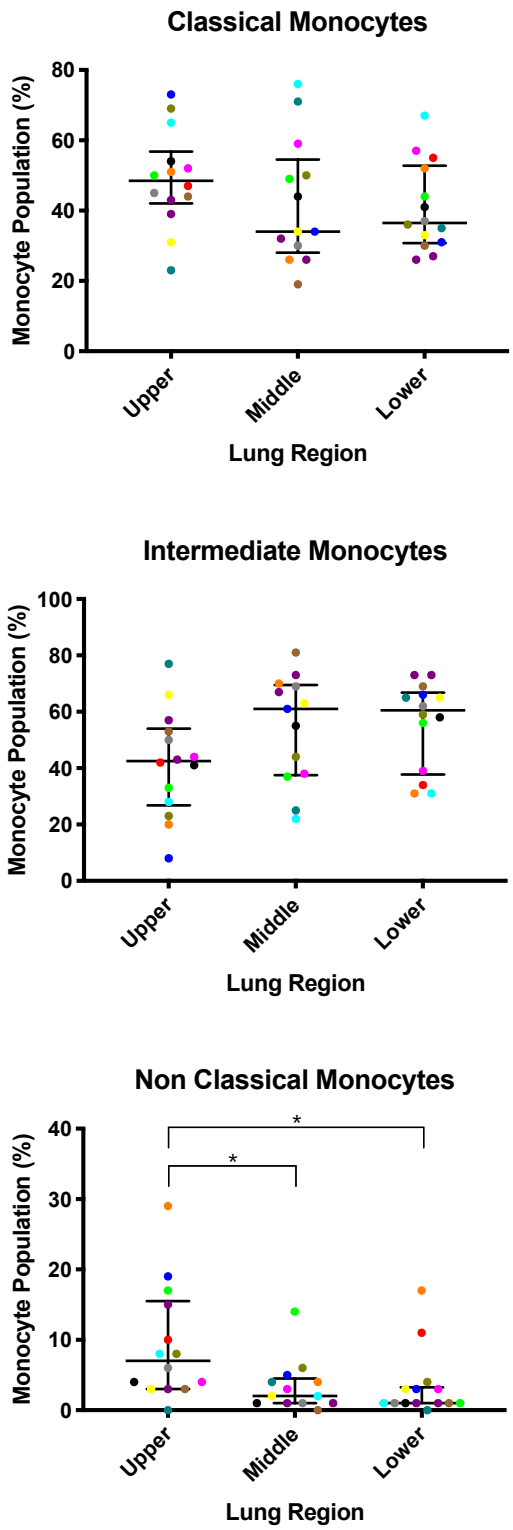

Figure 4.4 Regional proportion of monocyte subsets in interstitial lung disease (ILD). The proportion of classical, intermediate and non-classical monocytes that contributed to the total monocyte population were calculated across the ILD lung (n=14 upper, n=13 middle, n=14 lower, median ± IQR). All differences between lung regions were determined by a Mann-Whitney U test, significance * = $p \leq 0.05$, $p > 0.05$ not reported.

4.3.5 Histological Analysis of Disease Severity

The extent of fibrosis, inflammation and fibroblastic foci (FF) was semi quantitatively assessed across three regions of the ILD lung (n=13) (Figure 4.5). There were very few samples with only mild fibrosis, with the majority having at least a moderate level of fibrosis (Figure 4.5.A). There was an increase in fibrosis severity in the middle and lower regions of the lung, and this coincides with the increased frequency of intermediate monocytes, and the decreased frequency of non classical monocytes, in the middle and lower lobes (Figure 4.4).

Inflammation was largely moderate across all samples (Figure 4.5.B), with little difference observed between regions, and the extent of FF was mostly mild (Figure 4.5.C). Whilst FF is a hallmark of end stage ILD, the occurrence of mild FF is not in contradiction to the histopathology reports performed on the whole of the explanted lungs (Chapter Three, Section 3.3.3.1, Table 3.4). Approximately half of the patient's reports made reference to prominent FF, some reported a limited number or lack of FF altogether, and some reported that the occurrence of FF were localised to a specific area.

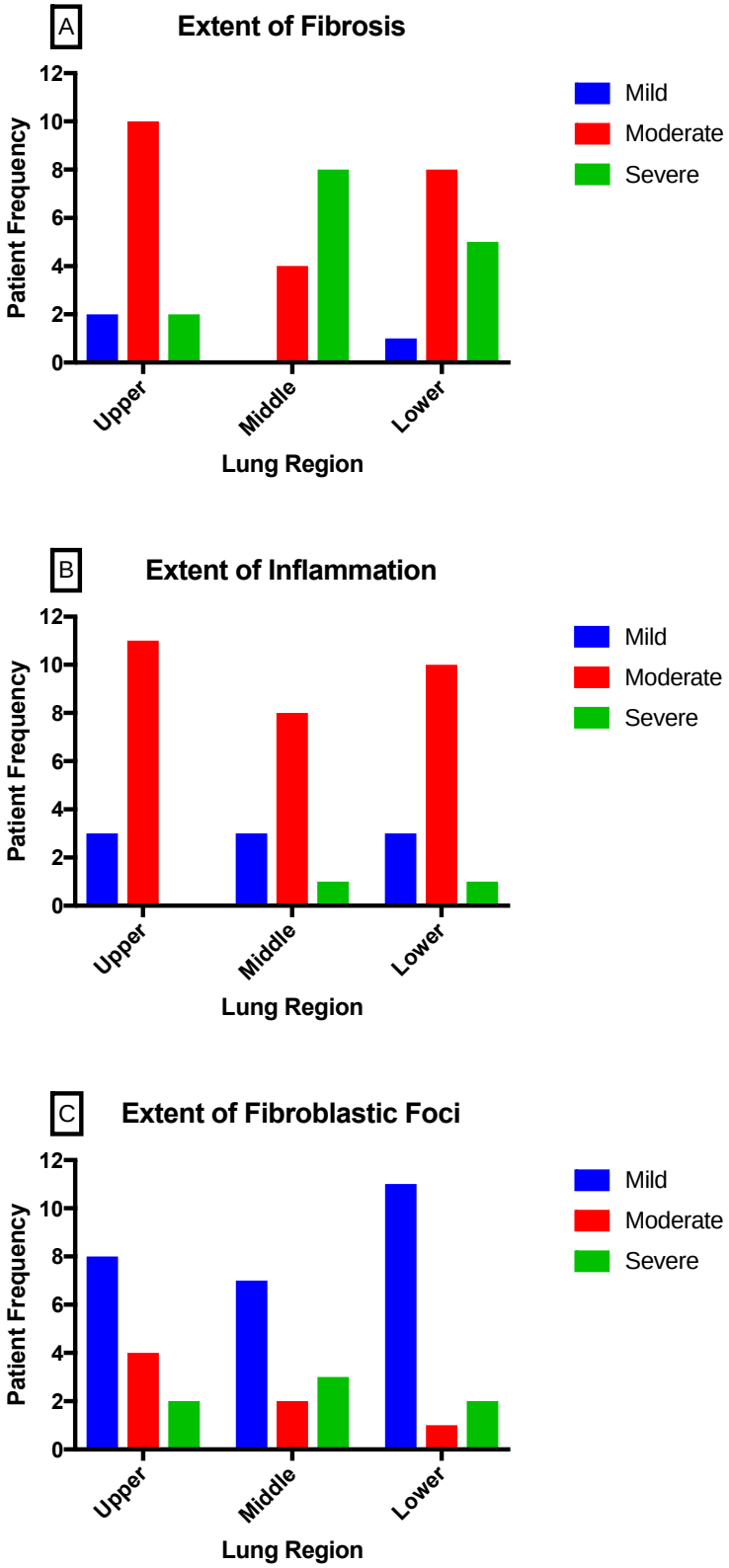

Figure 4.5. A semi quantitative histological analysis of regional disease severity. Three regions from each patient were assessed for the extent of fibrosis (A), inflammation (B) and fibroblastic foci (C) (n=13). Each histological parameter was given a grading of mild, moderate or severe, then the frequency of each was calculated.

4.4 Discussion

This chapter explored monocyte subsets in three disease groups; ILD, CF and COPD, and compared to control tissue from patients without chronic inflammatory lung disease or severely impaired lung function. The control, CF and COPD lung monocyte pattern was comparable to that described in blood, with classical monocyte dominance compared to intermediate and non-classical monocytes. Conversely, the ILD lung had a significantly decreased classical monocyte population compared to the other three cohorts. Non-classical monocytes were also significantly lower in comparison to COPD. Perhaps more interestingly, the ILD lung had significantly elevated intermediate monocyte populations. Given the disease specific finding that monocyte subsets were substantially altered in ILD compared to other lung diseases and control tissue, their relationship with disease severity was explored further. Using semi-quantitative histological analysis, severe fibrosis was more frequently reported in mid to lower regions of the lung, although this was not statistically different to the upper lobe. Intermediate monocytes were found to be elevated in areas of worsening fibrosis, whilst non-classical monocytes were significantly reduced.

Given the increased proportion of monocytes in ILD compared to other diseases (Chapter three, Figure 3.1.B, D & F), the presence of monocytes within the parenchymal tissue may not come as a surprise. However the distorted proportion of intermediate monocytes was unexpected and has not previously been reported. The phenomenon was ILD specific; the COPD, CF and control lungs had stereotypical classical monocyte dominance. In chapter three (Figure 3.1.F), MPS cells were uniform across the whole ILD lung. However, further characterisation of monocytes demonstrated that increased populations of intermediate monocytes correlated with ILD histological severity. The extent of disease was determined by a histopathologist (chapter three, Table 3.11), and fibrosis was found to be largely established in the lower lobes. This was supported by semi-quantitative analysis in this chapter and demonstrates the importance of considering the lung as a whole, rather than an isolated sampling point.

Historically it was thought that monocytes rapidly differentiate to macrophages or DCs when they leave the circulation and enter tissue [260, 261]. However, whilst monocytes are certainly not

terminally differentiated cells, there is increasing evidence to suggest their differentiation, or not, is driven by the surrounding environment [262], [263]. This is also supported by the discovery that tissue macrophages are not continuously renewed by blood monocytes as previously thought [264] [265]. However, this field of thought is relatively new, and many studies discuss the pro-fibrotic role of monocyte-derived macrophages in models of fibrosis [266], [267]. A transitional pro-fibrotic monocyte-derived macrophage was recently identified by gene expression, whose human counterparts were found to be up regulated in patients with IPF [268]. Despite the limited MPS markers utilised in the current study, the cells identified as monocytes displayed no characteristic sign of the autofluorescence that is typical of macrophages [269] (Figure 2.1L; the population monocytes derived from were negative for FITC). Given that cells such as granulocytes and NK cells were excluded prior to gating, the expression of CD14 and CD16 enabled identification of the specific monocyte subsets as approved by the Nomenclature Committee of the International Union of Immunological Sciences [251]. However whether driven by monocytes or macrophages, it is clear that MPS cells may have a role in the pathogenesis of ILDs.

The contribution of monocytes and macrophages to lung fibrosis is becoming increasingly recognised, particularly in IPF and connective tissue associated lung disease aetiologies [270-272], although the specific roles of these cell types continue to be elucidated. Monocytes act as a precursor for monocyte-derived alveolar macrophages, but differences in the behaviour of monocyte-derived compared to tissue resident- alveolar macrophages is only recently beginning to be explored with regards to ILD [273]. Misharin et al. (2017) utilised a murine model that enabled lineage tracking of cells, to distinguish between tissue resident and migratory monocyte-derived macrophages, and found that depletion of the latter ameliorated lung fibrosis in a bleomycin model of fibrosis, whilst depletion of tissue resident macrophages had no bearing on the subsequent fibrosis [273]. Circulating $Ly6C^{++}$ monocytes in mice have also been shown to direct pro-fibrotic activities in macrophages, and their ablation resulted in a reduction of pulmonary fibrosis [266]. However, there is a difficulty in relating the data presented in this results chapter to studies involving non-human sampling. In mice, there are only two described monocyte subsets and it is difficult to compare where human intermediate monocytes might fit in comparison. Nevertheless, there is a persuasive argument for the detrimental role monocytes and macrophages may play in the

pathogenesis of ILD, which transcends single species investigation. With specific regard to intermediate monocytes, which have become the population of interest within this body of work, there is still wide scale confusion over their exact role in immunity and disease [274]. In healthy lungs, intermediate monocytes are enriched in distal airways and produce less pro-inflammatory mediators than their peripheral blood counterparts, suggesting location driven function [175, 274]. In a study of 31 patients with IPF, patients with increased numbers of intermediate monocytes at baseline were shown to have increased disease progression despite comparable lung function parameters at the start of the study [275]. These patients were recruited at an earlier stage of the IPF disease trajectory, so it is therefore promising that information regarding intermediate monocytes at the end stage of disease could be utilised as a biomarker or prognostic tool at earlier stages. An increased yield of individual monocyte subsets can be obtained from much larger end-stage explant biopsies, allowing further downstream investigation that could later be applied for diagnostic and intervention purposes. An increased abundance of circulating monocytes in patients with IPF was also recently correlated to shortened patient survival times, and overall numbers of monocytes were significantly increased in IPF patients compared to the circulating levels in healthy controls [276]. However, this study did not provide a breakdown of each of the monocyte subsets.

Intermediate monocytes were discovered much later than classical and non-classical monocytes [277], and are still the subject of characterisation in recent years [254] [278] [279]. However this subset has been linked to a number of diseases, including severe asthma [280], rheumatoid arthritis [281] and liver fibrosis [282]. An increased accumulation of intermediate monocytes within organ tissue has previously been described by Liaskou et al. (2013), who report intermediate populations of up to 27% in the livers of patients with fibrotic liver disease, which was not observable in blood [282]. They did, however, find that a small increase in intermediate monocytes was not only restricted to diseased tissue, but also found in control tissue. It may be that the frequency of intermediate monocytes is naturally higher in tissue than in blood, which was demonstrated by the control, CF and COPD groups in this study at 20-25 percent. Liaskou et al. (2013) put forward two suggestions for the increase in intermediate monocytes; recruitment from blood via enhanced transendothelial migration, or the differentiation of classical monocytes into intermediates within the local tissue environment. Given that in this study, intermediate monocytes were found in

frequencies of between 40-80% in patients with ILD, their role in fibrosis is of great interest. Although other research has implicated monocytes as potential contributors to fibrosis or biomarkers of disease severity, there is paucity of knowledge characterising these cell types within lung tissue of ILD patients. It is this multi-regional sampling that enabled a link between increasing intermediate monocyte numbers in areas of more severe ILD. As yet we have no knowledge of the composition of these intermediate monocytes. They could be a homogenous population or a heterogeneous series of different groups all falling loosely under the classification of CD14++ CD16+. It is possible they are present in a regenerative capacity, ameliorating lung damage, although given their correlation with a loss of lung architecture this appears unlikely.

There was also a significant difference in non-classical monocytes between lungs from patients with ILD verses those with COPD. The proportion of non-classical monocytes in COPD (~10%) was similar to the CF cohort (~8%) and control group (~11%), whilst significant differences in non-classical monocytes were found across the ILD lung (9% in the upper lobes, down to ~3.5% in the middle to lower lobes). In blood, non-classical monocytes usually contribute ~10% of the monocyte population [251], and yet a decrease in non-classical monocyte proportion in this study was associated with areas of increased disease severity. Non-classical monocytes have multiple roles, including immune surveillance by patrolling the endothelium for injury [283], as well as roles in the resolution of inflammation. There have been a limited number of studies linking non-classical monocytes to various diseases, although the majority associate an increase of these cells with disease pathogenesis [284] [285] [286], rather than a decrease. However, a study characterising peripheral blood mononuclear cells (PBMCs) in ILD and a control group demonstrated a significant decline of non-classical monocytes in IPF and other ILDs compared to control [287]. It is difficult to suggest whether a decrease in the frequency of these cells is a consequence of ILD, or a by-product of the disease. A more in-depth characterisation of these monocytes within the lungs of both newly diagnosed as well as end stage ILD patients would therefore be warranted.

It is unsurprising that there was a large degree of variation in monocyte proportions between each of the ILD lungs, given the same heterogeneity was demonstrated in total monocyte numbers (chapter three). This was particularly evident in the upper lobe, although classical monocyte

proportions were extremely variable across all regions. Interestingly, there was a clear divide of patients above and below the lower lobe average for proportion of intermediate monocytes. A large number of the cohort had in excess of 55%, whilst four patients were below 40%. These four patients decreased the average proportion of intermediate monocytes in the lower lobe, and possibly influenced a lack of statistical significance, despite a 15% difference to the upper lobe. However, there was no commmon identifiable demographic or clinical features to this group (i.e. gender, age, disease phenotype, smoking history, disease trajectory and lung function). Despite a previous correlation between leukocyte number and left verses right sides of the lung, this was also not evident in this scenario.

Given there are over 300 different forms of ILD, it is feasible that the leukocyte compartment may vary between ILD aetiologies. However, the number of transplants performed limited this study and therefore all patients with any form of ILD were recruited. Despite an attempt to delineate any clinical phenotypes, small n= numbers and a number of inconclusive or atypical diagnoses prevented this. A second limitation was the retrospective analysis of paraffin histology blocks for semi-quantitative analysis. Every effort was made to match regional leukocyte data with blocks generated from the same region of the lung. However, regional sampling for leukocyte isolation was always taken from the peripheral areas of the lung, whilst clinical blocks were generated from both peripheral and central sections. So whilst this data in combination provides a rounder picture of the disease, how representative they are of each other should be considered with caution.

There is a substantial increase of intermediate monocytes within the ILD lung that correlates with regions of greatest disease severity. There was also a significant reduction in the proportion of non-classical monocytes in the ILD lung that again correlated with disease severity. These findings are particularly interesting given this phenomenom was specific to ILD and did not occur in the COPD, CFG or control lungs. A detailed characterisation of intermediate and non-classical monocyte populations is required to determine what role, if any, these cells may play in the pathogenesis of ILD. The application of a broader range of lineage, activation, adhesion and survival markers would greatly enhance this characterisation, and identify further monocyte heterogeneity and clustering within the three major subsets. Whilst flow cytometry could be further utilised for this purpose, mass

cytometry techniques are becoming an increasingly popular method to increase the number of markers and scope of immunophenotyping panels.

Chapter Five: Exploring the Capabilities of Cytometry by Time of Flight Technology

5.1 Introduction

The preceding chapters in this thesis have given evidence of the extensive heterogeneity of leukocytes across the lungs in three chronic lung diseases. The comprehensive exploratory nature of chapter three provided an avenue of interest regarding monocyte subsets in ILD, particularly intermediate and non-classical monocytes, which was explored further in chapter four. Whilst the methodology utilised in these chapters was appropriate to characterise different leukocyte subsets across the lung in a range of diseases, the markers used were restricted to key phenotypic identifiers. The expression of functional markers on these cell types would have been of great benefit to delineate the role each cell type may play in disease, and aid in identifying further disease or clinical phenotype specific phenomena. The potentially important finding that monocyte populations are altered in ILD was limited from further evaluation due to the small panel of monocyte markers incorporated within the broad leukocyte phenotyping panel. A deeper phenotypic and functional characterisation of monocytes in the ILD lung would be of obvious benefit. T cells were another cell type which were identified in large numbers, particularly in COPD and CF lungs. There were also differences in CD4+/CD8+ proportion; CD4+ cells were dominant in COPD and ILD, whilst CD8+ cells were more prevalent in CF (Chapter Three, Figures 3.3Gb, 3.9Gb and 3.15Gb). In addition to differences between diseases, CD4+/CD8+ proportion also has the potential to identify differences in clinical phenotypes within the same disease (Appendix 5, Appendix 8), so further exploration of lymphoid cells could also prove important.

Flow cytometry could be used for this purpose. However, fluorescently labeled antibodies used in flow cytometry emit a high degree of spectral overlap, which without new lasers and increasing fluorochromes, limit the routine use of flow cytometry to 18 colours [288]. In recent years, mass cytometry has been utilised as an alternative way to immunophenotype cells using isotope tags instead of fluorescent colour [289] [290]. Without the restrictions of spectral overlap, and the availability of many isotopes, it is easily possible to surpass 18-colour flow cytometry with 40 markers in one tube [291]. CyTOF was the first commercialised instrument to be utilised in this way [292], and this technology has great potential to supersede traditional flow cytometry over the upcoming years. However, as with any new technology, there are a number of disadvantages as

well as advantages. Fluorescently labelled antibodies are available in many fluorochrome forms and from many different companies, which strives to keep prices competitive. Conversely, antibodies labelled with isotopes, known as Maxpar antibodies, are currently only available from one company, Fluidigm. In acknowledgement of the potential mass cytometry holds for immunophenotyping, other companies have begun to generate 'Maxpar ready' antibodies for self-conjugation. However, without the years of supporting validation that fluorochromes offer, and the expense of in house conjugation kits, this route is not yet a feasible option for every laboratory. This is compounded by the significant investment in instrument technology to facilitate the technique in the first place. The inclusion of instruments like CyTOF within research core facilities and the implementation of antibody banks are two ways to offset this cost and increase the accessibility of CyTOF. Other caveats to mass cytometry are the restriction on further utilisation of samples, significantly slower acquisition rate and more complicated analysis [293]. Whilst fluorochrome conjugated cells can be sorted in a viable form, cells undergoing CyTOF must first be fixed and are then vaporised during the process of analysing the samples. The acquisition rate of CyTOF is only 500 cells/second, resulting in far longer run times than flow cytometry, which can acquire in excess of 10,000 cells/second. However, the enhanced ability of CyTOF to detect immune subsets from a starting sample of as little as 10,000 cells [290] and the frequent combining of samples with the use of barcoding systems offset this. The use of barcoding vastly reduces machine-induced variability between samples, and whilst this technique can now also be used in flow cytometry, it is not commonly used. Although flow and mass cytometry will more than likely co-exist for many years to come, it can be expected that mass cytometry will continue to improve as technological advances are made. This can only enhance the technology's utility and continue to minimize any current disadvantages compared to flow cytometry.

Given the enhanced multiplexing opportunities that CyTOF affords, the aim of this chapter was to perform preliminary testing of both lymphoid- and myeloid-specific CyTOF panels utilising cryo-preserved cells stored following lung explants prior to transplant. The capabilities of CyTOF to identify disease specific differences, and regional disease heterogeneity, were examined.

5.2 Methods

A detailed methodology for the preparation, processing and analysis of cells using CyTOF is described in Chapter Two, Section 2.8. Briefly, additional cells that were isolated at the time of lung explant but were surplus for flow cytometry were cryopreserved for future use. These cells were later thawed and CD45+ leukocytes were isolated by magnetic separation. The leukocytes were then stained with two separate panels, myeloid and lymphoid specific, before CyTOF was performed. All data analysis was performed in FlowJo and CyTOFkit.

5.3 Results

5.3.1 Sample Demographics and Clinical History

An overview of the five patients included in CyTOF analysis and their regional lung locations can be found in Table 5.1. Samples one and two are from patients previously described in Chapter Three; Sample one is COPD patient LTx-45 (Table 3.1), and sample two is ILD patient LTx-41 (Table 3.3). The remaining samples are from idiopathic PH patient LTx-35 (sample three) and samples four to six are from different lung regions of COPD patient LTx-105. The demographics and clinical history of these two patients is described in Tables 5.2 to 5.3.

Table 5.1 Overview of samples analysed by cytometry by time of flight (CyTOF). Six single cell suspensions generated from lung samples collected in the study were selected for further characterisation using CyTOF. These cells were from a range of disease types and regions to test the capability of CyTOF to determine both disease and regional differences in samples.

Sample (LTx)	*Disease Phenotype*	*Lung Region*
1 (LTx-45)	*COPD*	*Pooled*
2 (LTx-41)	*ILD*	*Pooled*
3 (LTx-35)	*Idiopathic PH*	*Pooled*
4 (LTx-105)	*COPD*	*Pooled Right lung*
5 (LTx-105)	*COPD*	*LU*
6 (LTx-105)	*COPD*	*LL*

Abbreviations: CyTOF= cytometry by time of flight, LTx= Lung transplant, COPD= chronic obstructive pulmonary disease, ILD= interstitial lung disease, PH= pulmonary hypertension, LU= left upper

Table 5.2 Overview of patient demographics and clinical history for LTx-35 and LTx-105 analysed by cytometry by time of flight (CyTOF). The clinical history of each patient was obtained from the transplant medical records held by Manchester University NHS Foundation Trust and key parameters pertaining to the patient's demographics, lung function and clinical history were summarised.

LTx Code (Colour)	***Gender***	***Age at Tx***	***Interval from diagnosis to Tx (years)***	***FEV_1, L (% Predicted)***	***FVC, L (% Predicted)***	***Co-morbidities***	***Smoking Hx***
LTx-35	*F*	*37*	*5-10*	*3.28 (105%)*	*4.3 (120%)*	*Heart & Lung Tx* *Iron deficiency anaemia* *Systolic mummer* *White cell neutropenia* *Atrial pace maker implant*	*NA*
LTx-105	*M*	*47*	*7*	*1.35 (39%)*	*2.99 (71%)*	*Itraconazole induced heart failure* *Secondary polycythaemia* *Diventricular disease* *Hypertension* *Osteopenia*	*Yes – 25/day*

Abbreviations: (L)Tx= (Lung) transplant, F= female, M= male, FEV_1= Forced expiratory volume in one second, FVC= Forced vital capacity, L= liter, Hx= history

Table 5.3 Summary of explant histology reports for patients LTx-35 and LTx-105 analysed by cytometry by time of flight (CyTOF). A histopathology report for each patients' explanted lungs were obtained following examination by a histopathologist at Manchester University NHS Foundation Trust and the key observations were summarised.

LTx Code	***Summary of Histology Report (R; right lung, L; left lung, O; overall analysis)***
LTx-35	*R; Prominent artiers, lung parenchyma slightly fibrotic* *L; Arteries markedly prominent in lower lobe, no areas of fibrosis* *O; Similar features, evidence of PA thickening. Plexiform & glomeruloid lesions in smaller arterioles. Scattered pigmented macrophages in alveoli, no evidence of chronic inflammation or emphysematous change*
LTx-105	*R; Severe emphysema, with upper lobe worst affected.* *L; External surface shows bullae formation in upper & lower lobes. Severe emphysema upon sectioning.* *O; Severe emphysema, worst in the upper lobes. Abundant pigment laden macrophages. Patchy interstitial inflammation. No infection or malignancy.*

Abbreviations: R= right (lung), L= left (lung), O= overall (analysis), PA= pulmonary artery

5.3.2 Delineation of Bar-Coded Samples

All six of the individual samples were successfully identified (after being pooled together for panel staining) during analysis of the CyTOF acquired data with the use of their bar coded CD45+ pattern. The frequency and total cell number for samples stained with the lymphoid panel or the myeloid panel are described below (Table 5.4). The variation between lymphoid samples of up to 5.6% was deemed acceptable given the preliminary nature of this study.

Table 5.4. Identification of samples using a CD45 bar-coding system within the lymphoid and myeloid marker tube. Samples labeled with unique combinations of anti-CD45 conjugated to 89Y, 115In and 198Pt mass tags were identified following CyTOF acquisition for cells labeled with lymphoid or myeloid markers. The proportion of the sample and total cell number that they represented was calculated.

	Sample (LTx)	CD45+ Bar Code Mass and Tag	Frequency of Single Live Cells	Cell number
Lymphoid Marker Samples	***1 (LTx-45)***	***89Y***	***11.6***	***50743***
	2 (LTx-41)	*115In*	*10.4*	*45660*
	3 (LTx-35)	*198Pt*	*16*	*70051*
	4 (LTx-105)	*89Y + 115In*	*14.3*	*62568*
	5 (LTx-105)	*89Y + 198Pt*	*13.7*	*59829*
	6 (LTx-105)	*115In + 198Pt*	*10.8*	*47378*
	Sample (LTx)	**CD45+ Bar Code Mass and Tag**	**Proportion of Total Sample**	**Cell number**
Myeloid Marker Samples	*1 (LTx-45)*	*89Y*	*16.3*	*30805*
	2 (LTx-41)	*115In*	*15.8*	*29968*
	3 (LTx-35)	*198Pt*	*15.8*	*29943*
	4 (LTx-105)	*89Y + 115In*	*18.3*	*34641*
	5 (LTx-105)	*89Y + 198Pt*	*18.4*	*34842*
	6 (LTx-105)	*115In + 198Pt*	*16.9*	*32030*

Abbreviation: LTx= lung transplant

5.3.3 Lymphoid Cell Characterisation

5.3.3.1 Capability of Cytometry by Time Of Flight

T-distributed stochastic neighbour embedding (t-SNE) is a stochastic process that requires the random sampling of individual samples to generate a t-SNE plot with consistently located cell populations. Data merging of the six samples stained with the lymphoid panel was performed by random sampling of 7500 cells per sample and generated a t-SNE plot comprising of 18 distinct cell populations (Figure 5.1). These cell islands consist of cells that uniformly express specific groups of markers. The individual samples could then be extracted into distinct t-SNE plots, whilst ensuring cell populations were in the same spatial alignment (Figure 5.2). There were evident differences in population density across samples; particularly in cluster 13, which showed a reduction in samples two and three compared to the COPD samples. Whilst t-SNE is visually informative, the software analysis provides other platforms to explore these differences further.

A heat map produced from t-SNE data enabled the comparison of individual cell clusters across the six different samples (Figure 5.3). The heat map aligns samples that have the most in common together, and identified the four COPD samples (samples one, four, five and six) separately to the patients with ILD (sample two) or PH (sample three). The software is also able to identify differences within a disease group, with a majority of clusters demonstrating differences between the four COPD samples. However, the data in the heat map is generated purely by cell number within a cell island. The accuracy of cells grouped within a cluster relies on the precision of the staining antibodies.

5.3.3.2 Evaluation of Cytometry by Time Of Flight Panel

This data set was a preliminary test of both the antibody panel and its ability to identify surface molecules in samples obtained from lung tissue (Figure 5.4). There were several molecules that were not detected; CD161, CD2, CRTh2 and CXCR3. These antibodies require evaluation using control samples positive for the specific molecule before deciding whether to alter the mass and tag they are bound to. Antibodies that worked well were CD3, CD117, CD4, CD127, CD45Rα, CD73,

CD56, CCR7, CD38, HLA-DR and PD-1. The remaining molecules were ambiguous; there was staining although the extent and specificity varied. The expressions of CD8/CD19, CCR6, CD44, TCRγδ, CCR4, CD206, CD62L and CD25 were largely non-specific, staining cell groups that should be mutually exclusive for certain markers, or did not stain expected cell clusters.

The next stages for analysis of CyTOF data would usually involve transportation of the t-SNE plots into traditional flow cytometry software such as FlowJo for further characterisation of each cluster. However, given 50% of the lymphoid panel was either not working or sub-optimal, this was not carried out at this stage.

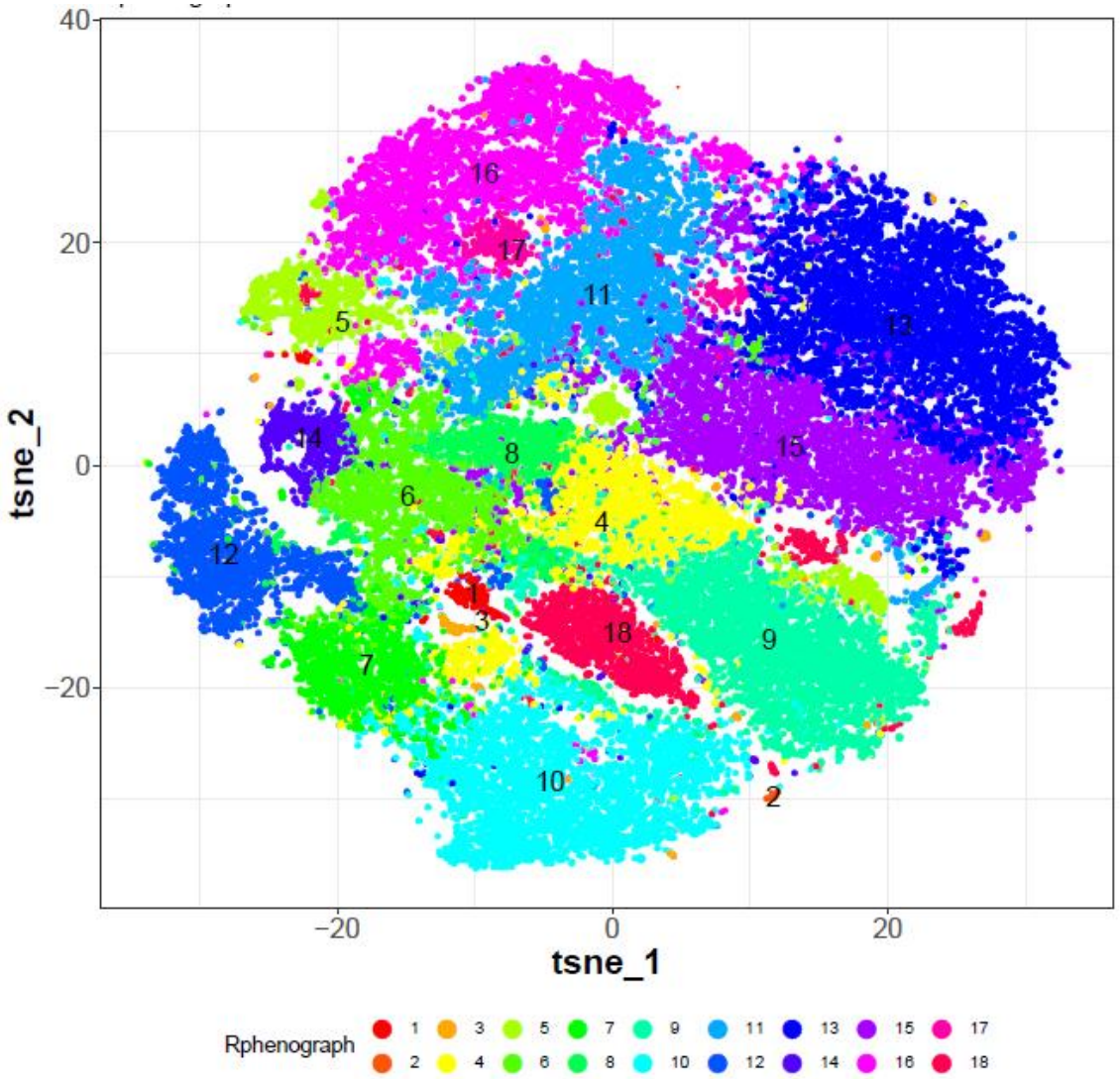

Figure 5.1 Lymphoid t-distributed Stochastic Neighbor Embedding (TSNE) plot of samples from interstitial lung disease (ILD), pulmonary hypertension (PH) and chronic obstructive pulmonary disease (COPD) as a collective. Following TSNE analysis of the six samples (ILD n=1, PH n=1, COPD n=4), as a collective the samples were determined to have 18 distinctive cell clusters based on the signal expression strength of markers within the myeloid panel.

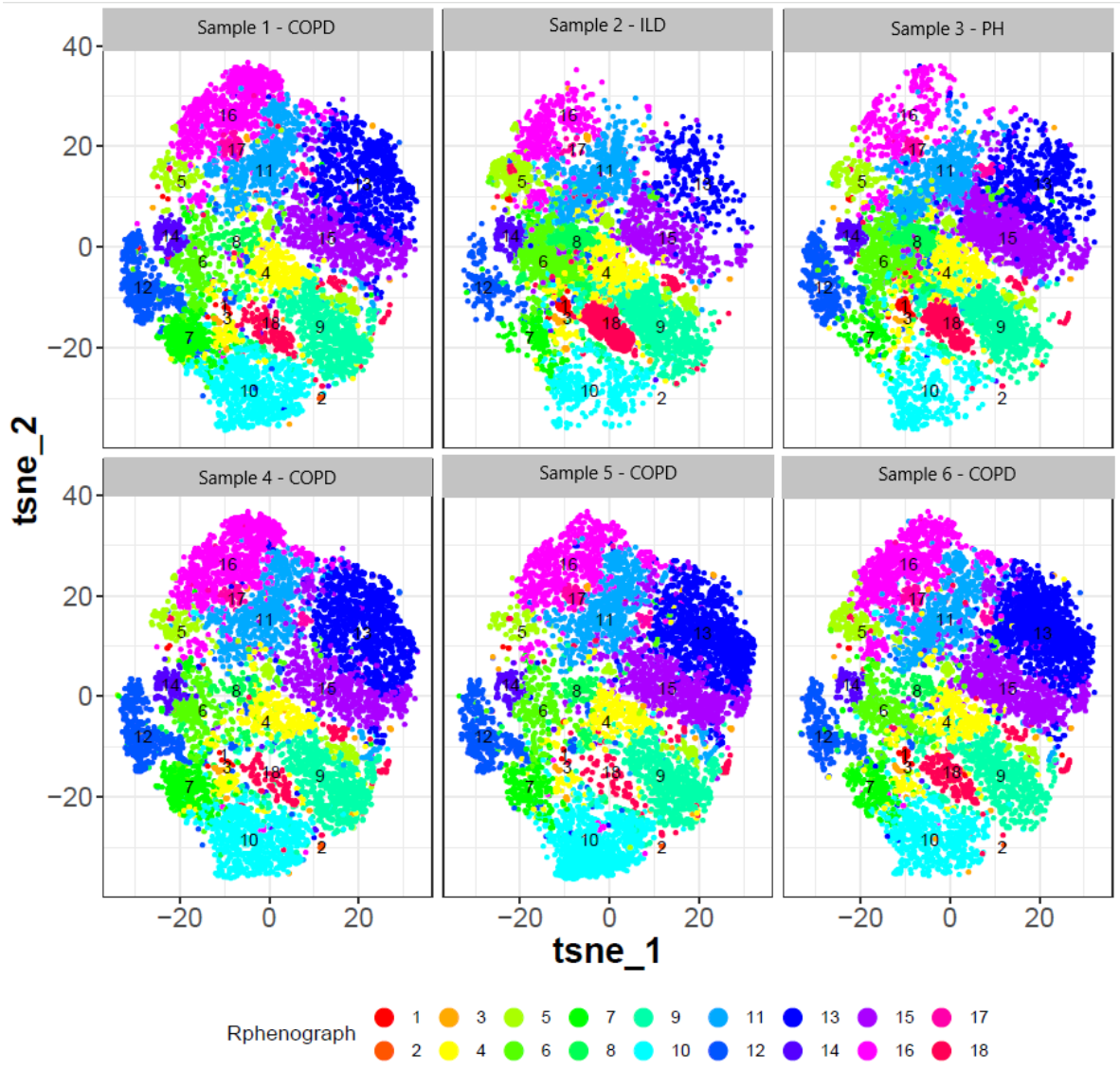

Figure 5.2 Lymphoid t-distributed Stochastic Neighbor Embedding (TSNE) plots of individual samples from patients with interstitial lung disease (ILD), pulmonary hypertension (PH) and chronic obstructive pulmonary disease (COPD). The TSNE plots are separated for each of the six individual samples (ILD n=1, PH n=1, COPD n=4) to enable identification of visual differences between cell clusters with regards to number density.

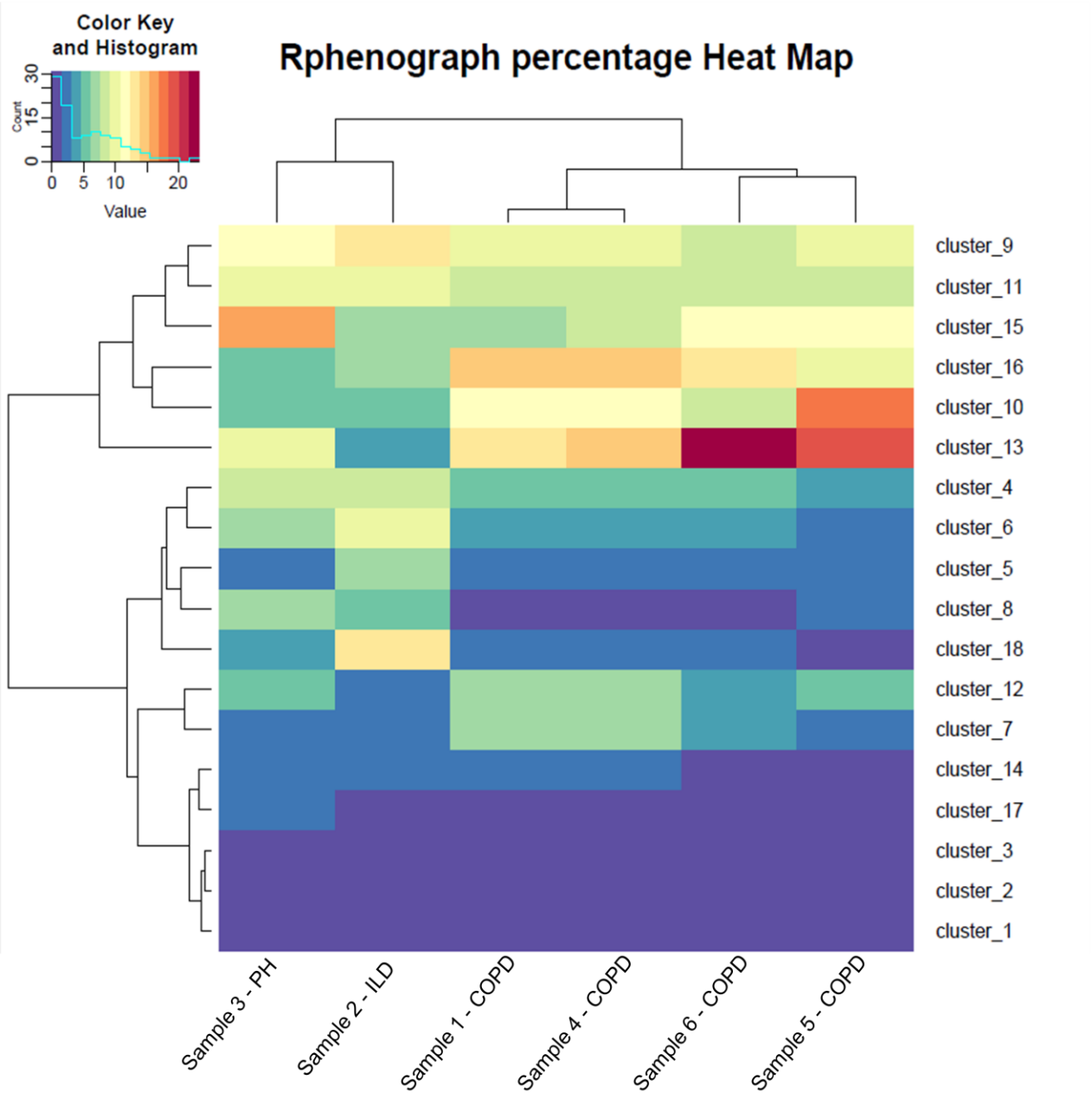

Figure 5.3 Lymphoid heat map of the relationship of cell clusters between samples from interstitial lung disease (ILD), pulmonary hypertension (PH) and chronic obstructive pulmonary disease (COPD). A heat map to demonstrate the relationship between the six samples (ILD n=1, PH n=1, COPD n=4) for each of the 18 clusters generated during t-distributed Stochastic Neighbor Embedding (TSNE) analysis. Data is grouped vertically based on the similarity of samples to one another, whilst the cell clusters are grouped horizontally by phenotypic relationship between the cells.

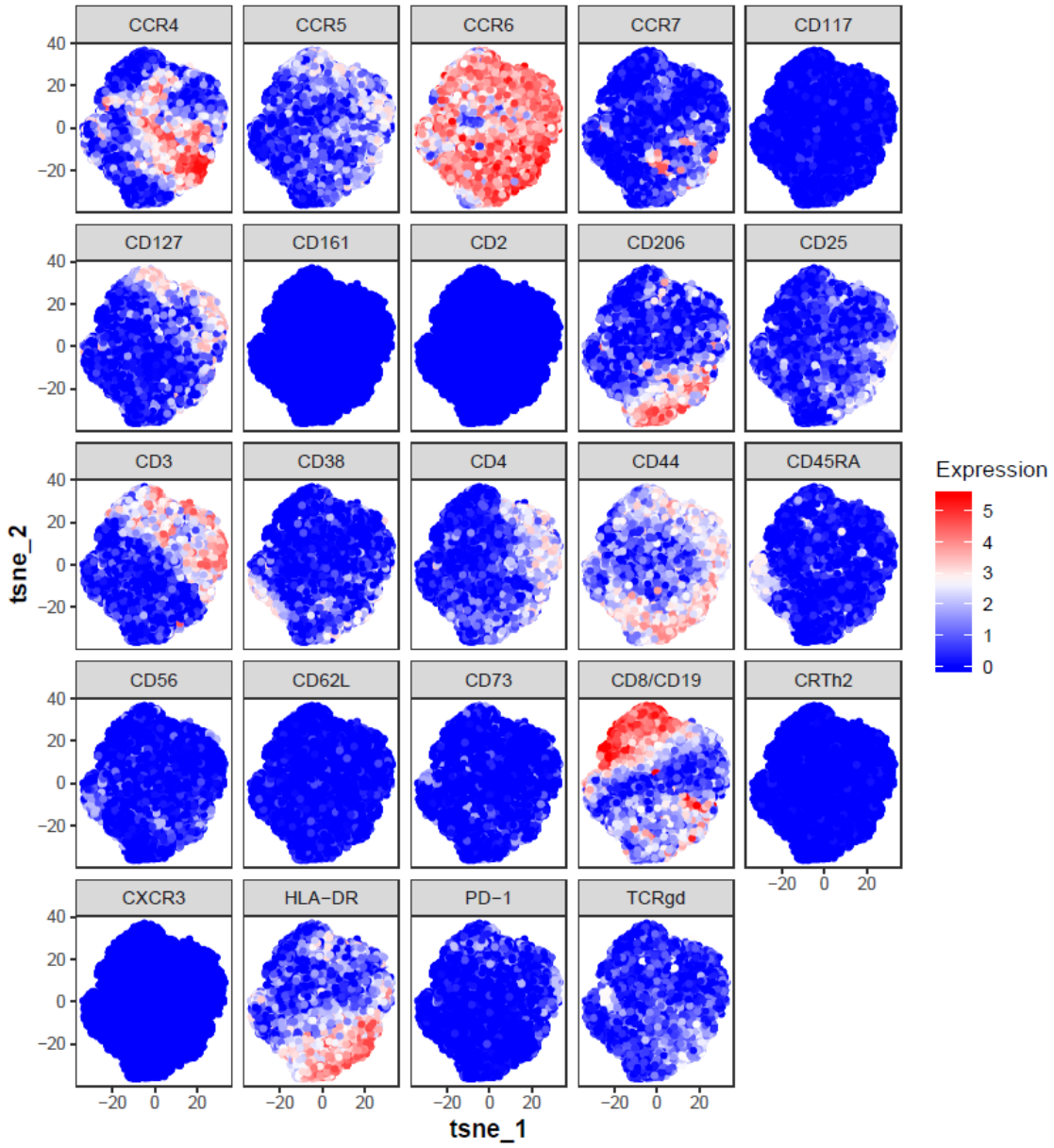

Figure 5.4 Lymphoid t-distributed Stochastic Neighbor Embedding (TSNE) plots for individual lymphoid markers. A visualisation of how each of the 24 individual markers contribute to the clustering of cells within the lymphoid panel, based on signal strength expression from 0 (blue) to 5 (red).

5.3.4 Myeloid Cell Characterisation

5.3.4.1 Capability of Cytometry by Time Of Flight

As previously described in the Section 5.3.3.1, data merging of the six samples stained with the myeloid panel was performed by random sampling of 7500 cells per sample and a t-SNE plot comprising of 20 distinct cell populations was generated (Figure 5.5). The individual samples were then extracted into distinct t-SNE plots (Figure 5.6). There were evident differences in population density across samples, particularly in clusters three, 14, 16 and 17.

The heat map of t-SNE data enabled the comparison of individual cell clusters across the six different samples (Figure 5.7). Similarly to the lymphoid panel, the heat map recognised that samples from patients with PH and ILD were fundamentally different to the COPD samples. However, the position of the ILD and PH samples in the heat map was different in the myeloid panel, with the ILD sample further distinguished from the COPD group. Although the data again marked samples one and four as most similar, there was an additional layer of differentiation between the four COPD samples than occurred in the lymphoid panel. There were also two extra cell clusters that demonstrated no difference across the samples; clusters 15, 13, six, 12 and 19, than in comparison to the lymphoid panel.

5.3.4.2 Evaluation of Cytometry by Time Of Flight Panel

An evaluation of the myeloid antibodies was also carried out (Figure 5.8), as previously described in Section 5.3.3.2. In the myeloid panel, only PD-L1failed to be detected. Antibodes that worked well were CD14, CD117, FcεR1, CD86, MerTK, CD7, CD24, PD-L2, CD80, CD200R, CD16, CD33, CX3CR1, CD169, CD1a, CLEC9a and HLA-DR. The remaining molecules were again ambiguous; there was positive staining although the extent and specificity varied. Some molecules, such as CD3, CD8/CD19, CD64, CD66b, CD123, CD163, CD303 and SIRPα had some non-specific staining, although their targeted cell types were evident. However, other antibodies had lots of non-specific staining that was difficult to interpret. Some molecules, such as CD11b and CD11c, were

expressed across many clusters but are generally expressed by many cell types, whilst CD40, CD2, siglec-8, CD141, CD206 were not comparable with the literature.

Again, given 50% of the myeloid panel was either not working or sub-optimal, transportation of the t-SNE plots into FlowJo for further characterisation of each cluster was not performed.

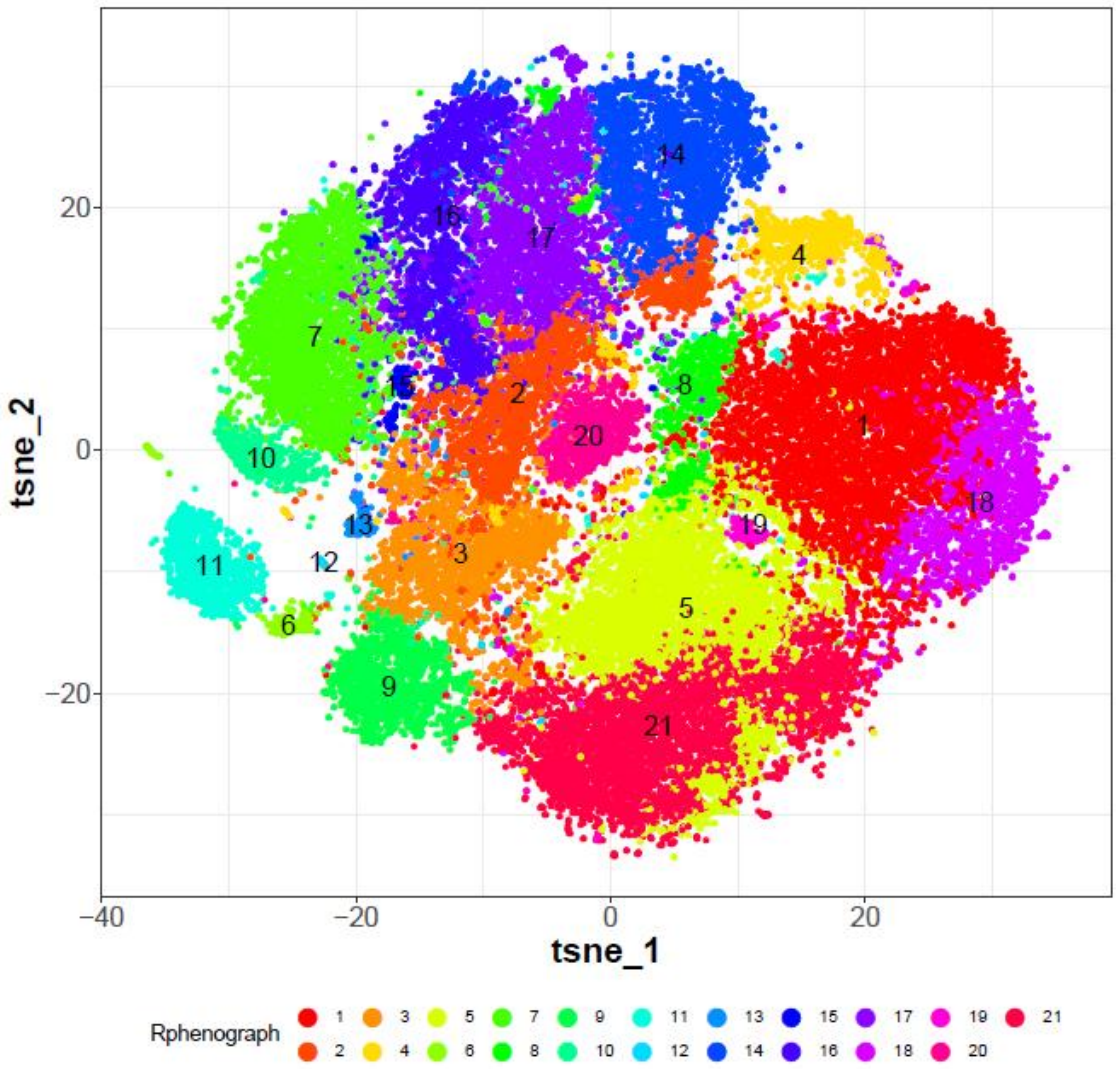

Figure 5.5 Myeloid t-distributed Stochastic Neighbor Embedding (TSNE) plot of samples from interstitial lung disease (ILD), pulmonary hypertension (PH) and chronic obstructive pulmonary disease (COPD) as a collective. Following TSNE analysis of the six samples (ILD n=1, PH n=1, COPD n=4), as a collective the samples were determined to have 21 distinctive cell clusters bases on expression of markers within the myeloid panel.

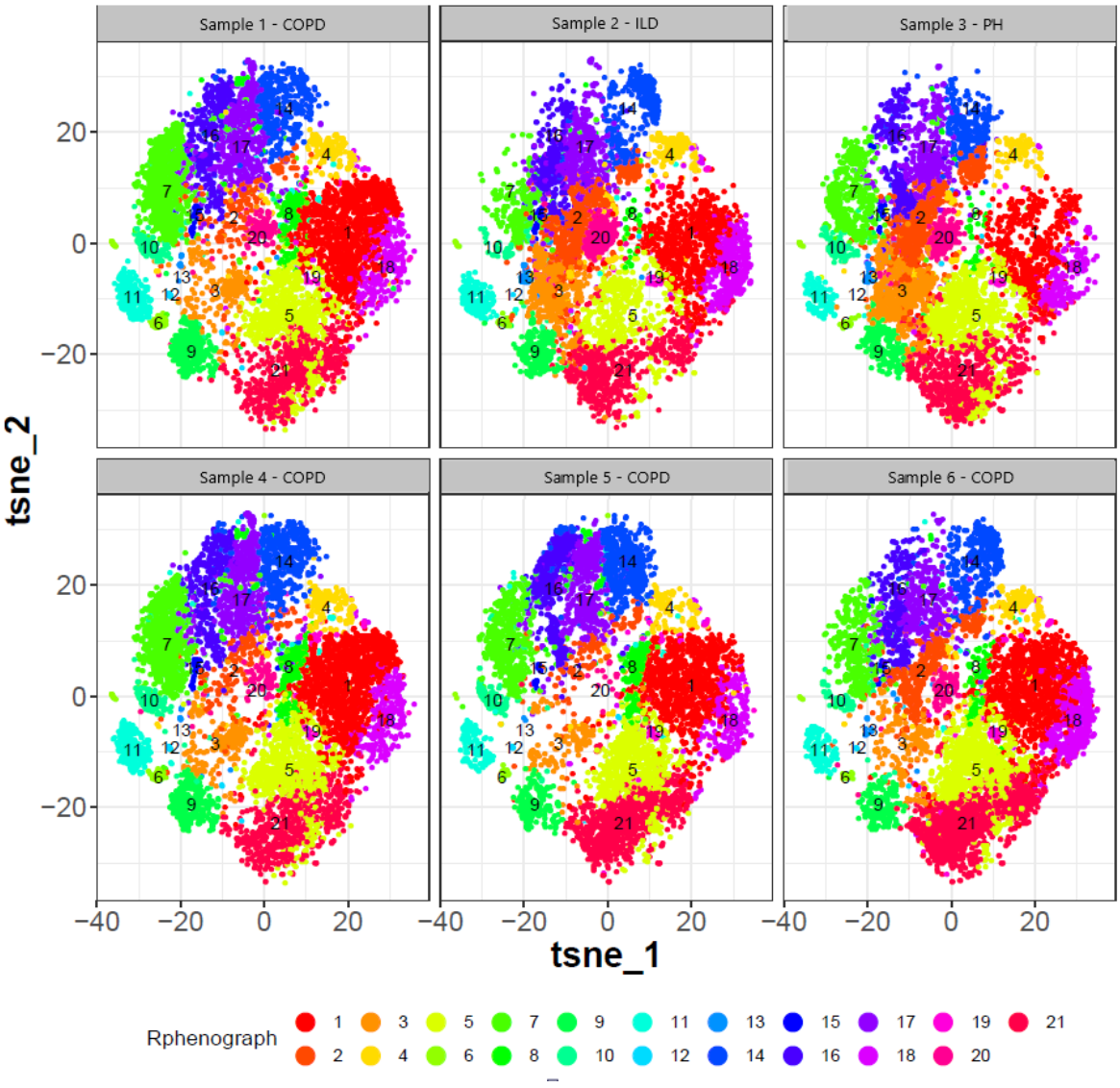

Figure 5.6 Myeloid t-distributed Stochastic Neighbor Embedding (TSNE) plots of individual samples from patients with interstitial lung disease (ILD), pulmonary hypertension (PH) and chronic obstructive pulmonary disease (COPD). The TSNE plots are separated for each of the six individual samples (ILD n=1, PH n=1, COPD n=4) to enable identification of visual differences between cell clusters with regards to number density.

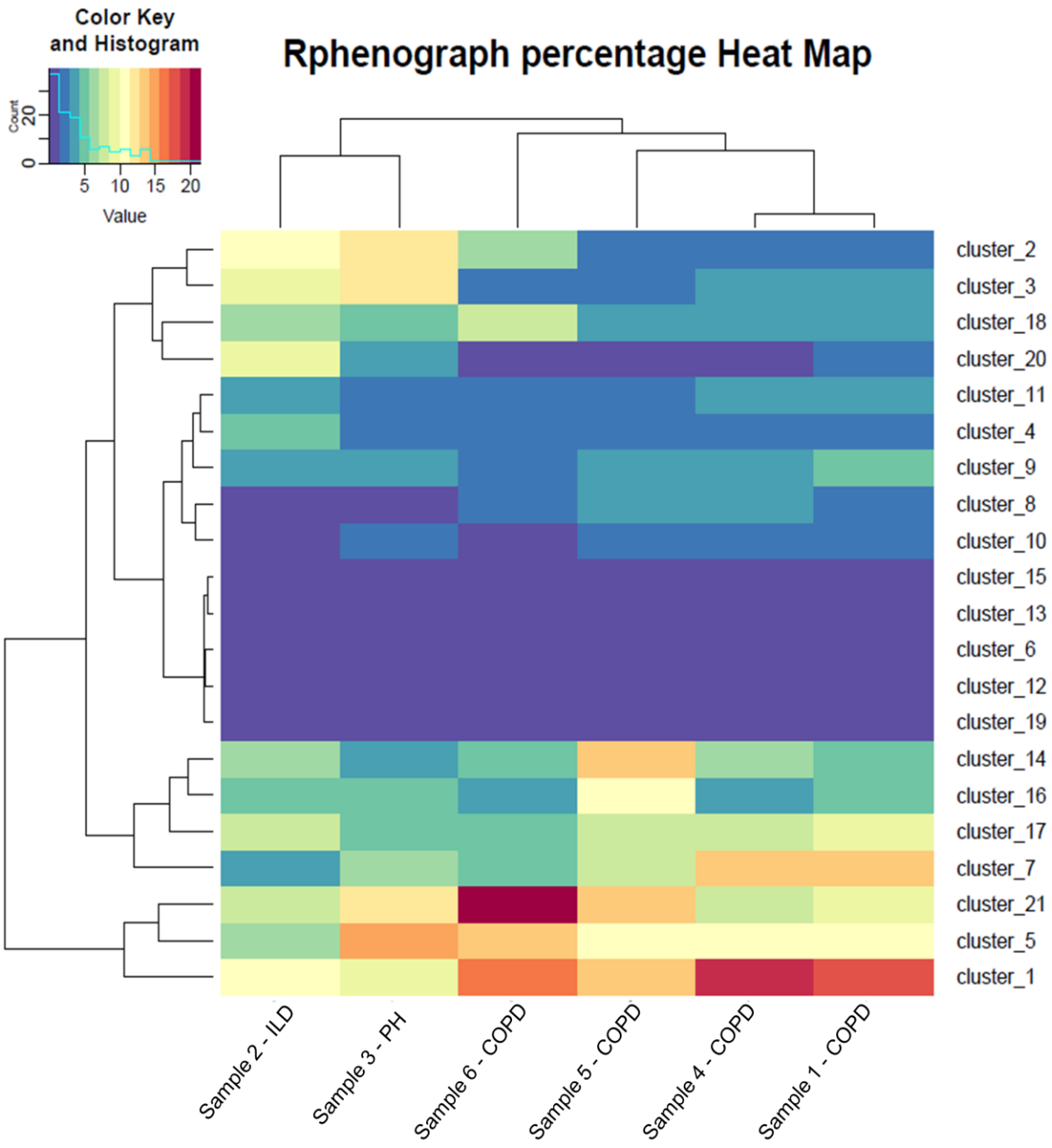

Figure 5.7 Myeloid heat map of the relationship of cell clusters between samples from interstitial lung disease (ILD), pulmonary hypertension (PH) and chronic obstructive pulmonary disease (COPD). A heat map to demonstrate the relationship between the six samples (ILD n=1, PH n=1, COPD n=4) for each of the 21 clusters generated during t-distributed Stochastic Neighbor Embedding (TSNE) analysis. Data is grouped vertically based on the similarity of samples to one another, whilst the cell clusters are grouped horizontally by phenotypic relationship between the cells.

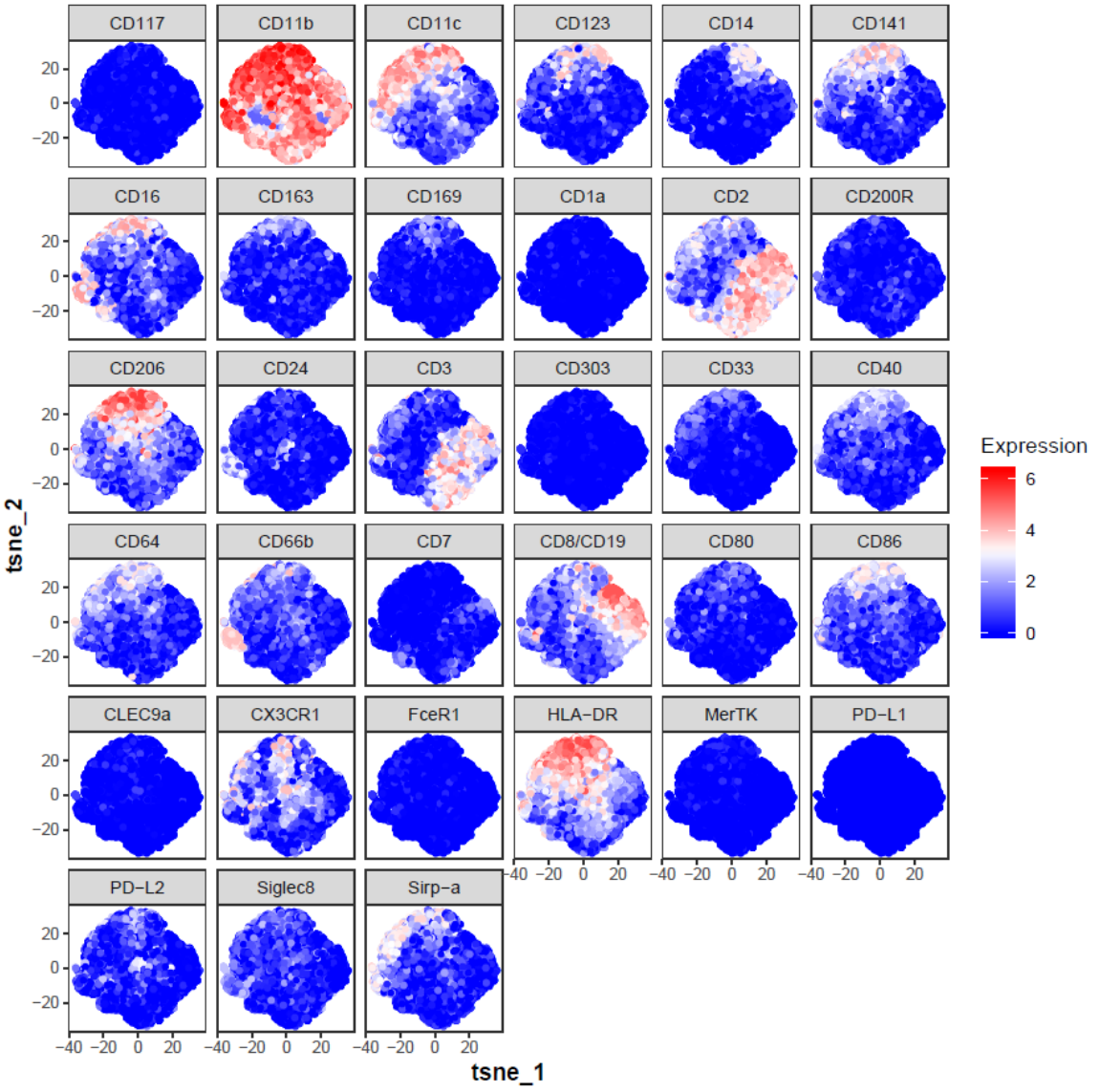

Figure 5.8. Myeloid t-distributed Stochastic Neighbor Embedding (TSNE) plots for individual myeloid markers. A visualisation of how each of the 33 individual myeloid markers contribute to the clustering of cells within the myeloid panel, based on signal strength expression from 0 (blue) to 6 (red).

5.4 Discussion

This chapter constituted a feasibility study to set up a detailed lymphoid and myeloid CyTOF panel for the purposes of immunophenotyping samples derived from lung tissue, to complement and enhance findings described in earlier chapters. The panels had previously been designed for collective use across the MCCIR, but their success in different tissue types was yet to be determined. The panels were able to provide a range of preliminary data that supports the use of this technology for immunological research, although optimisation is certainly required in the instance of lung tissue. However, due to the preliminary nature of these panels, further information could not be elucidated. Despite this, CyTOF technology demonstrated that differences between disease cohorts were easily detectable, and that regional differences within the same patient could also be identified. The comparison of individual cell clusters across the six different samples recognised that samples from patients with PH and ILD were fundamentally different to the COPD samples, but could also determine differences between the individual regional samples from the same COPD patient compared to the two COPD samples that both comprised of cells from multiple regions. The unbiased identification of different samples has clinical potential. This is particularly true for diseases such as ILD where differential diagnosis is incredibly difficult, and the propensity for misdiagnosis is often high using traditional methods such as CT scans and bronchoscopic biopsy [294]. CyTOF could prove beneficial in clinical trials of new therapies to identify biomarkers in responders and non-responders.

Given that CyTOF has only been used frequently in the last five years, the validity of its use is still being compared against traditional flow cytometry [295] [296]. However, there is now an increasing amount of literature regarding its use for the characterisation of leukocytes within different organs [297, 298] [299] as well as specific cell types such as NK cells [300], antigen specific T cells [301] and DCs [302]. There are also a limited number of studies that have used CyTOF to characterise COPD, ILD or CF in human samples. Yao et al (2017) performed single cell profiling of airway cells obtained from the induced sputum of patients with asthma or CF [298]. They quantified the frequency and activation status of major cell subset sets utilising a panel of 22 markers. Firstly, they found that the frequencies of major subsets in each condition complemented previous flow

cytometry knowledge [303]. Secondly, they identified distinct frequencies of cell populations that could identify disease cohorts, supported by the work in this thesis. Vasudevan et al (2018) characterised lung macrophages to determine phenotypes associated with exacerbation in COPD. The capability of CyTOF to increase the number of markers allowed the exploration of lineage, activating and inhibitory functions, adhesion, phagocytic, and chemokine markers to discover an imbalance between pro- and anti-inflammatory phenotypes in COPD exacerbates. These capabilities are essential to exploring the role of monocytes in ILD and interrogating the findings of flow cytometry further.

An obvious benefit of CyTOFs capability is the increased number of markers within a single tube, providing more in depth knowledge from samples of limited size. Human tissue for research is a precious artefact, and often available in a very limited quantity. This is particularly relevant to samples such a biopsies taken during bronchoscopy. The necessity for a small sample to be spread across different tubes of markers for basic characterisation is eliminated with CyTOF [290]. The samples used within this preliminary test were from previously cryopreserved cells, which are susceptible to impaired viability during the freeze-thaw process. To analyse these cells with flow cytometry for the markers incorporated in the CyTOF panels, it would have required samples being split over double, if not treble, the amount of tubes.

Although the results presented within this chapter are extremely preliminary and unable to convey quantifiable information, CyTOF shows promising potential to explore regional heterogeneity in a multitude of lung diseases. In order to advance this work, further optimisation of the markers is a critical first step. There is also a greater complexity to CyTOF analysis than is required with manual flow cytometry gating. It relies heavily on algorithms and programming to fully elucidate data in an unbiased manner, which is a limiting factor to many immunologists who are traditionally reliant on flow cytometry. The collaboration of immunologists and programmers has the potential to overcome this difficulty, and could see CyTOF rapidly overtake flow cytometry as a favoured research tool in the coming years.

The plan to develop this preliminary data into a larger study was severely limited by factors beyond the control of the project. Within the host institute, all investigators were expected to contribute to a communal library of antibodies for CyTOF (an approach commonly used by other CyTOF facilities). Hypothetically, this would enable researchers to access much larger panels without the need to purchase each antibody. Following completion of the preliminary study described above, an additional 25 lung samples from eight COPD, 13 ILD and four CF patients were prepared for CyTOF. Unfortunately it was at this point the host institute changed the policy and the antibody library was closed. As such, this work was not possible to complete within the timeframes of this PhD. Given the interesting preliminary observation that CyTOF may be able to diagnose different lung diseases based on phenotype, this work should be continued in the future.

Despite the limited nature of the results in this chapter, it does highlight the potential that CyTOF could hold for future clinical research. The unbiased assessment of sample similarities and differences proved capable of distinguishing between samples from ILD, COPD and PH patients. However, and arguably even more importantly, it was also able to identify similarities and differences within samples from the same cohort, and from different regions of the same lung. This is especially important for the increasingly variable clinical presentations in conditions such as ILD and COPD, and the responses and severities of patients within the same disease group. Further understanding of the similarities and differences of these patients will help guide clinical decisions and evaluation of new treatments within different clinical phenotypes. The clearer grouping of patients based on the active inflammatory profile of the lungs will ultimately lead to clearer delineation of potential mechanisms driving disease heterogeneity, which is currently inconclusive in all three of the diseases examined within this thesis. There are key regulatory processes that control homeostasis and immunological responses, and investigation of these mechanisms in well-defined groups of patients will be of great benefit.

Chapter Six: The Characterisation of Immune Checkpoints in Lung Disease

6.1 Introduction

The preceding chapters focused on characterising leukocytes across different regions of the chronically diseased lung. This is a fundamental step in advancing knowledge and enables discovery-led research. Flow cytometry, and advancements in mass spectrometry are important tools to allow immunophenotyping of leukocytes that may be critical to disease pathogenesis. Indeed, the utilisation of flow cytometry has led to potentially important observations in the frequency of monocyte subsets in ILD, and gender driven heterogeneity across the COPD lung. CyTOF technology has the potential to allow unbiased clustering of different clinical phenotypes based on increased scrutiny of leukocytes, their lineage and function, and where they might reside within the lung. However, it is also important to delineate the mechanisms that may be driving heterogeneity. This chapter will therefore seek to understand important factors involved in immune regulation in chronic lung disease.

In order for naïve T cells to be activated they must receive two independent signals; one of which is derived from the presentation of antigenic peptides via the major histocompatibility antigen on APCs to the T cell receptor (TCR), whist the second is a by-product of an antigen independent co-stimulatory signal [304]. Without the second signal, a T cell response is unable to be initiated. These co-stimulatory molecules are critical to adaptive immunity and T cell activation, playing a pivotal role between homeostasis and mounting an appropriate immune response [305] and are referred to as immune checkpoint molecules (ICM).

ICMs of the B7/CD28 family were the first to be described. B7 ICMs are co-signalling molecules responsible for the regulation of T cell activation or suppression [306]. B7 molecules are proteins located on the cell surface of activated APCs [307], but can also be found on the endothelium and epithelium. Conversely, CD28 family molecules are their receptor counterparts and are expressed on T cells during varying stages of maturity. In combination they provide a co-stimulatory signal, which depending on the molecule augments or dampens the activity between APCs and T Cells.

CD28 and cytotoxic T-lymphocyte-associated protein 4 (CTLA-4) are T cell receptors that can both bind to the CD80 (B7-1) and CD86 (B7-2) ligands on APCs [308]. However, CD28 and CTLA-4 have opposing roles on T cell immunity. CD28 is constitutively expressed on naïve and activated T cells, providing co-stimulatory signals for growth and survival [309], whilst CTLA is a receptor induced by T cell activation and drives an inhibitory response [310]. The ligands CD80 and CD86 are expressed in differing constitutive levels on a variety of APCs, and are considered primary co-stimulatory ligands. CD86 is constitutively expressed on DCs and resting monocytes, whose expression is up-regulated further after APC and lymphocyte activation [311], whilst CD80 demonstrates little constitutive expression prior to activation [312]. The functions enhanced by CD28 co-stimulation with B7 ligands are essential for antigen specific immune responses and the inhibitory effect of CTLA-4 co-stimulation prevents aberrant immune responses.

In addition to CD28 and CTLA-4, there are other T cell receptors that can mount a stimulatory or inhibitory T cell response. ICOS is a T cell receptor that shares functional and structural properties with CD28 but is not constitutively expressed [313]. In a similar manner to CD28, inducible T cell costimulator (ICOS) increases the response of T cells to antigens by promoting proliferation and cytokine secretion. ICOS ligand (ICOSL), also known as B7-H2, is an inducible ligand expressed on pulmonary DCs. Once induced, ICOSL expression remains high on mature DCs. This enables increased T cell costimulation via ICOS [314]. Another inhibitory receptor on T cells is programmed cell death protein 1 (PD-1), which can also bind to two co-ligands; programmed death-ligand 1 (PD-L1) (also known as B7-H1) and PD-L2 (B7-DC), which have an overlapping role in the regulation of T cell responses [315]. PD-L2 is a ligand predominantly expressed on DCs and macrophages, whilst PD-L1 has a more extensive expression profile [316], including APCs, T cells, B cells and endothelial cells. One of the least well-known molecules is B7-H3, whose role in immune regulation is less established than other members of the B7 family [317]. The receptor(s) that B7-H3 binds to is not yet known, but different groups have produced confounding results demonstrating the ligands role as a stimulatory [318] and suppressive [319] molecule.

Clinically, ICMs have emerged as an integral new concept for immuno-oncology [320], [321] but could also prove to be an important tool in inflammatory disease. Exploring the role of these checkpoint molecules in lung disease and examining their regional distribution may help delineate the mechanism behind aberrant inflammatory responses. This chapter seeks to define the relationship between inflammation and immune checkpoint molecules, by examining the expression of molecules from the B7/CD28 family in regional samples from diseased lungs explanted prior to lung transplantation.

6.2 Methodology

A detailed methodology for the generation of array and IHC data is provided in Chapter Two, Section 2.8. Briefly, the expression of 10 ICMs was examined in tissue lysate samples (Section 2.6) using a commercially available array (Section 2.8.1). IHC for PD-L1 and B7-H3 was performed on clinical paraffin sample blocks from the upper and lower lobes of lungs explanted during transplant (Section 2.8.2). The slides were stained using an automated stainer (Section 2.8.2.1) and analysed quantitatively using imaging software (section 2.8.2.2).

Relationships between leukocyte populations and ICM expression described in Section 6.3.3 was performed retrospectively. Given the heterogeneity of leukocyte numbers and ICM expression, a relevant scoring system was unable to be identified. The following scoring system was therefore created, and used impartially across the data sets. The data for each individual patient was explored by identifying the pattern of leukocytes across the lung regions (Figure 6.1A) and the pattern of each immune checkpoint molecule (Figure 6.1B). If the pattern on the immune checkpoint was opposite to the leukocyte region; for example the number of leukocytes increased between LU and LING, whilst there was an obvious decrease in B7-H1, B7-H2 and B7-H3 between the same regions, this was noted. If this pattern was identified three-four times (two in a SLTx) the checkpoint molecule pattern was scored as positive (+), if it was identified five-six times (three in a SLTx) it was scored as double positive (++). This method of analysis was performed for each patient included in the immune checkpoint array study (n=22).

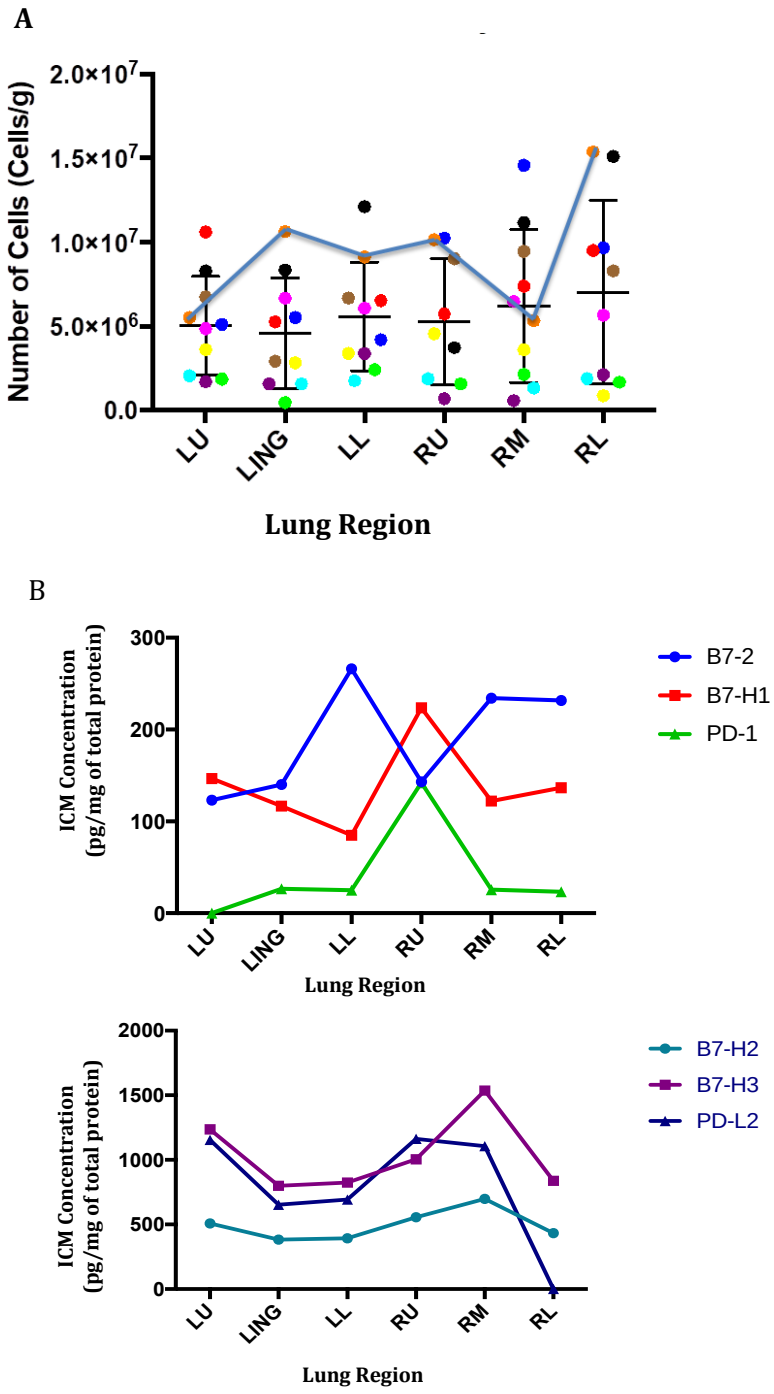

Figure 6.1 Methodology to correlate leukocyte number with immune checkpoint expression. A representative example using chronic obstructive pulmonary disease (COPD) LTx-61 to demonstrate the identification of the leukocyte pattern (A) and the subsequent immune checkpoint molecule (ICM) expression pattern (B).

6.3 Results

6.3.1 Patient Demographics and Clinical history

6.3.1.1 Immune Checkpoint Protein Array

All data in Sections 6.3.2-3 was generated from patients discussed in detail in chapter three, although not all patients were included in this study (COPD n=6, ILD n=12, CF n=4). This was due to insufficient sample remaining after 1g single cell isolation, or patient samples being collected after this part of the study was completed.

Table 6.1 Overview of patients in immune checkpoint array study. The expression of immune checkpoints was assessed in lung samples from six patients with chronic obstructive pulmonary disease, 12 patients with interstitial lung disease and four patients with cystic fibrosis. The clinical data for each of these patients can be found in Chapter Three, Sections 3.3.2, 3.3.3 and 3.3.4 (Tables 3.1-3.6).

COPD Patients	***ILD Patients***		***CF Patients***
LTx Code (Colour)	***LTx code (Colour)***		***LTx code (Colour)***
37 (Green)	*42 (Brown)*	*58 (Orange)*	*47 (Black)*
45 (Magenta)	*41 (Blue)*	*13 (Black)*	*68 (Blue)*
61 (Orange)	*44 (Cyan)*	*65 (Asparagus)*	*72 (Brown)*
69 (Purple)	*51 (Purple)*	*53 (Yellow)*	*87 (Cyan)*
83 (Yellow)	*55 (Magenta)*	*60 (Nickle)*	
80 (Black)	*52 (Green)*	*59 (Teal)*	

Abbreviations: COPD= chronic obstructive pulmonary disease, ILD= interstitial lung disease, CF= cystic fibrosis, Tx= transplant

6.3.1.2 Immune Checkpoint Immunohistochemistry Analysis

The demographic characteristics, clinical history, pulmonary function and explant histology of the patients are summarised in Tables 6.2 to 6.5. COPD samples were obtained from two female and five male patients, with an average age of 55.4 (range 44-63) at the time of transplant. ILD samples were also obtained from two female and five male patients, with an average age of 54.6 (range 38-65).

The clinical phenotypes of the seven COPD patients consisted of five with emphysema, three of which had AATD, whilst two patients had bronchiectasis, one of which also had obliterative bronchiolitis. The clinical diagnosis of the ILD patients prior to transplant comprised of three patients with confirmed IPF and a fourth UIP patient described as possible IPF, one patient with atypical NSIP, one patient with atypical sarcoidosis and one patient without a differential diagnosis.

The co- morbidities associated with the COPD group were varied between each patient, although a number of patients had conditions relating to the lungs such as asthma, hypercapnic respiratory failure, a previous pulmonary TB infection, PH and hyperinflation. Other co-morbidities included mild CAD, thyrotoxicosis and eosinophilia. In the ILD cohort, co-morbidities included diabetes, PH, inflammatory bowel syndrome (IBS) and osteoarthritis.

The majority of COPD patients were ex-smokers (six out of seven) whilst three of the seven ILD patients had a history of smoking. The pack year history ranged from 17-40 years across all patients that previously smoked. The most recent pulmonary function test results prior to transplant were collected, with a patient FEV_1 range of 18% to 30% predicted for COPD, whilst the ILD cohort had a FEV_1 range of 30% to 79%. The FVC results for COPD patients ranged from 43% to 83% predicted, and for ILD was 24% to 76% predicted.

Formal histological assessment reported heterogeneous emphysematous changes across the lungs of most COPD patients, although severity to particular regions differed between patients. Many patients also had bullae formation, whilst a number demonstrated evidence of interstitial fibrosis. In the ILD group, three patients were characterised as having a UIP pattern of fibrosis whilst two were described as NSIP. Fibroblastic foci were also evident in five of the seven ILD patients, whilst evidence of chronic inflammation was limited to four patients out of the total 14 within both groups. The same clinical blocks taken during formal clinical assessment were utilised in this study for immune checkpoint analysis. One block was taken per upper or lower region of the explanted lung.

Table 6.2 Overview of chronic obstructive pulmonary disease (COPD) immunohistochemistry patient demographics and pulmonary function. The clinical history of each patient was obtained from the transplant medical records held by Manchester University NHS Foundation Trust and key parameters pertaining to the patient's demographics, lung function and clinical history were summarised.

LTx Code	***COPD Phenotype***	***Gender***	***Age at Tx***	***FEV_1, L (% Predicted)***	***FVC, L (% Predicted)***	***Exacerbation Hx (in year pre Tx)***	***Interval from diagnosis to Tx (years)***	***Co-morbidities***	***Smoking Hx (pack years)***
15	*Emphysema: AATD (MZ)*	*F*	*52*	0.43 (18%)	1.20 (43%)	Recurrent	5	Concerns re Osteo	Yes – 40/day
75	*Emphysema*	*M*	*55*	*0.57 (18%)*	*2.40 (62%)*	*0*	*NA*	*Asthma* *Thyrotoxicosis* *Peripheral eosinophilia*	*Yes (30)*
28	*Bronchiectasis & Obliterative bronchiolitis*	*M*	*59*	*0.96 (30%)*	*3.26 (82%)*	*Recurrent*	*15, 5-6 year decline*	*Asthma* *Mild CAD*	*Yes (17)*
39	*Emphysema: AATD*	*F*	*55*	*0.62 (27%)*	*2.29 (83%)*	*0 (Hx of)*	*>3, 1 year decline*	*Hypercapnic Resp failure*	*Yes (17)*
63	*Emphysema*	*M*	*63*	*0.97 (32%)*	*3.14 (84%)*	*0 (Hx of)*	*>8 years, 1 year decline*	*PH (out of proportion to lung disease)* *Systemic hypertension* *Right lower lobe pneumonia* *Dupuytren's contracture*	*Yes*
33	*Bronchiectasis*	*M*	*44*	*1.03 (25%)*	*2.32 (46%)*	*Recurrent every 2-3 months*	*Childhood, 3-4 decline*	*Pulmonary TB* *Bowel surgery* *PH*	*No*
4	*Emphysema: AATD (MZ)*	*M*	*60*	*0.56 (19%)*	*2.38 (65%)*	*Frequent - ~9/year*	*5*	*Significant hyperinflation (181%)*	*Yes – 30/day*

Abbreviations: COPD= chronic obstructive pulmonary disease, Tx= transplant, FEV_1= Forced expiratory volume in one second, FVC= Forced vital capacity, L= liter, AATD= Alpha-1 antitrypsin deficiency, MZ= allele variant of the AATD gene, NA=not available in medical records, CAD=coronary artery disease, TB= tuberculosis, PH=pulmonary hypertension

Table 6.3 Overview of interstitial lung disease (ILD) immunohistochemistry patient demographics and pulmonary function. The clinical history of each patient was obtained from the transplant medical records held by Manchester University NHS Foundation Trust and key parameters pertaining to the patient's demographics, lung function and clinical history were summarised.

LTx Code	***ILD Phenotype***	***Gender***	***Age at Tx***	***FEV_1, L (% Predicted)***	***FVC, L (% Predicted)***	***Exacerbation Hx (in year pre Tx)***	***Interval from diagnosis to Tx (years)***	***Co-morbidities***	***Smoking Hx (pack years)***
74	*Hypersensitivity pneumonitis vs NSIP vs Sarcoid*	*F*	*57*	*1.65 (65%)*	*1.95 (65%)*	*Prolonged ~3*	*7, 1 year decline*	*Inconclusive ILD picture*	*No*
20	*IPF*	*M*	*59*	*NA*	*NA*	*1*	*2, rapid 3 month decline*	*Hip replacement*	*No*
19	*UIP – Classified as IPF*	*M*	*58*	*1.93 (55%)*	*2.11 (48%)*	*0*	*14, 3 year decline*	*Type II diabetes PH Hepatitis B antibodies*	*Yes (40)*
81	*Atypical sarcoidosis*	*M*	*38*	*2.71 (63%)*	*2.85 (54%)*	*3*	*>3,*		*No*
62	*Atypical ILD - NSIP*	*M*	*54*	*1.05 (30%)*	*1.05 (24%)*	*0*	*1.5*	*Hypothyroidism Oesophageal reflux Mild CAD*	*No*
58	*IPF*	*F*	*51*	*2.26 (79%)*	*2.76 (76%)*	*NA*	*1*	*IBS*	*Yes – 10/day*
44	*IPF*	*M*	*65*	*2.33 (70%)*	*2.65 (63%)*	*NA*	*2*	*Osteoarthritis*	*Yes (34)*

Abbreviations: ILD= interstitial lung disease, Tx= transplant, FEV_1= Forced expiratory volume in one second, FVC= Forced vital capacity, L= liter, NSIP= nonspecific interstitial pneumonia, UIP= usual interstitial pneumonia, IPF= idiopathic pulmonary fibrosis, NA=not available in medical records, PH=pulmonary hypertension, CAD=coronary artery disease, IBS=irritable bowel syndrome

Table 6.4 Summary of clinical histology reports for chronic obstructive pulmonary disease (COPD) immunohistochemistry patients. A histopathology report for each COPD patients explanted lungs were obtained following examination by a histopathologist at Manchester University NHS Foundation Trust and the key observations were summarised.

LTx Code	***Summary of Histology Report (R; right lung, L; left lung, O; overall analysis)***
15	R: Widespread fibrous adhesions, severe emphysema throughout all lobes. Lower lobe bronchiectasis. L: A few fibrous adhesions. Severe emphysema throughout both lobes and mild lower lobe bronchiectasis. O: Severe emphysema and mild bronchiectasis
75	R: Emphysematous changes to upper and lower lobes, predominant in upper lobe. Bullae present. L: Multiple emphysematous bullae in upper and lower lobes, with prominent emphysematous change in upper lobe. O: Similar across both lungs with widespread emphysematous changes. Scattered discrete granulomata with epithelioid cells and foreign body type giant cells. Suggests undiagnosed sarcoidosis presenting as emphysema.
28	R: Central dilatation and thickening of bronchi in lower lobe. Upper lobe bullae. L: Thickened and dilated bronchi in upper lobe. O: Similar, neutrophils within bronchial lumens. Mucus hyperplasia of bronchial walls, chronic inflammation. Right upper lobe has area of fibrosis with giant cells. Secondary PH changes.
39	R: Marked emphysema across all lobes, multiple bullae in middle and lower lobes. L: Multiple emphysematous bullae, predominantly upper lobe and apical/basal portion of lower lobe. O: Pan acinar emphysematous changes and bullae formation. Multiple, discreet granulomata along bronchovascular bundles – in keeping with secondary sarcoidosis.
63	R: Several bullae towards apex, with diffusely dilated airspace across all lobes. L: Diffusely dilated airspaces across both lobes. O: Centriacinar pattern of emphysema with increased anthracotic pigmentation in bronchioles & vessels. Paraseptal fibrosis.
33	R: Subpleural blebs on upper lobe but otherwise normal, middle lobe has moderate emphysema, lower lobe has severe emphysema and mild bronchiectasis. Mild interstitial fibrosis. L: Moderate emphysema in upper lobe, severe in the lower lobe. Mild interstitial fibrosis. O: Similar across both lungs, extensive bronchiectasis extending distally, devoid of cartilage. Suggestion of congenital abnormality of the airways.
4	R: Most of upper lobe has severe emphysema, upper part of lower lobe shows moderate emphysema. L: Upper half of upper lobe has severe emphysema, upper half of lower lobe has moderate emphysema. O: Gross emphysema of the upper lobes, moderate elsewhere.

Abbreviations: COPD= chronic obstructive pulmonary disease, R= right (lung), L= left (lung), O= overall (analysis), PH= pulmonary hypertension

Table 6.5 Summary of clinical histology reports for interstitial lung disease (ILD) immunohistochemistry patients. A histopathology report for each ILD patients explanted lungs were obtained following examination by a histopathologist at Manchester University NHS Foundation Trust and the key observations were summarised.

LTx Code	***Summary of Histology Report (R; right lung, L; left lung, O; overall analysis)***
74	R: Upper lobe is globally pale, middle lobe is densely fibrosed in core, lower part of lower lobe is densely fibrosed but the upper part has been relatively spared. O: Similar in upper and lower lobes but slightly more advanced in upper. Subpleural and centrilobular fibrosis. Evidence of constrictive bronchiolitis. Features consistent with chronic hypersensitivity pneumonitis.
20	R: Coarsely nodular pleura over lower lobe, with fibrosis along base of upper lobe and much of middle & lower lobes. O: Areas of preserved lung in upper lobe, with some mild fibrosis to middle/lower lobes. However majority of lung shows severe fibrosis with mild chronic inflammation. Fibroblastic foci are evident as well as bronchiolar metaplasia. Advanced stage UIP.
19	R: Pleural surface is fibrotic with cobblestone appearance. Extensive fibrosis and honeycombing. L: Cobble stone appearance with pleural adhesions. Extensive honeycombing and fibrosis. O: Similar in both lungs, little normal lung left. Dilated airspaces lined with bronchiolar-type epithelium. Fibroblastic foci present and patchy chronic inflammation. Appearance of NSIP but would be in keeping with long standing UIP.
81	R: Pale infiltrative nodules concentrated in the inferior aspect of the upper lobe, diffuse in the middle lobe and mainly superior in the lower lobe. Dilated bronchioles & vessels in lower lobe L: Patchy infiltrative nodules and dilated bronchioles & vessels in lower lobe. O: Similar across both lungs, areas of subpleural fibrosis with some normal lung parenchyma. Fibroblastic foci present. Patchy peribronchiolar metaplasia and bronchiolitis. Some focal honeycombing. NSIP with concerns re connective tissue disease.
62	L: Vague nodularity on pleural surface with dense adhesions between lobes. Densely fibrotic with some sup-pleural blood formation. O: Uniform fibrotic interstitial expansion with patchy chronic inflammation. Prominant squamous and bronchial metaplasia with mucus material in airway space. NSIP
58	R: Limited subpleural fibrosis in the base of the upper lobe and in the middle and lower lobes without honeycombing L: Limited subpleural fibrosis without honeycombing O: Heterogenous appearance with areas of normal lung and interstitial fibrosis with basal dominance. Mild chronic inflammation & bronchiolar metaplasia. FF present.
44	L: Fibrotic with honeycombing, most severe towards the bases. O: Heterogeneous fibrosis with areas of preserved lung. Most severe in lower lobe and towards bases. Mild chronic inflammation. Limited number of FF. Appearance in accordance with UIP.

Abbreviations: ILD= interstitial lung disease, R= right (lung), L= left (lung), O= overall (analysis), UIP= usual interstitial pneumonia, FF= fibroblastic foci, NSIP= nonspecific interstitial pneumonia

6.3.2 Heterogeneity of Immune Checkpoint Molecules Across the Chronic Obstructive Pulmonary Disease, Interstitial Lung Disease and Cystic Fibrosis Lung

The concentration of ICM per mg of total protein was quantified for 10 members of the B7/CD28 family across six different regions of COPD (n=6) (Figure 6.2) and CF (n=4) (Figure 6.3) lungs, and from three different regions of ILD lungs unless a DLTx was performed (n=11, n=1) (Figure 6.4). The expression of B7-1 and CTLA-4 were below the limit of detection (LOD) of the array for the majority of samples across all disease groups. This was also the case for ICOS in COPD and CF samples, and CD28 for COPD samples. Data relating to these molecules must therefore be examined with caution.

All molecules demonstrated significant differences between the regions of the lung for COPD (B7-H3 $p=0.018$, PD-L2 $p=0.005$, $p<0.001$ for remaining ICMs), although specific post-hoc differences were not observable for B7-H2, B7-H3 and ICOS (Figure 6.2). The CF cohort had significant differences across the lung for all molecules ($p<0.001$, and CD28 $p=0.003$) with the exception of B7-H2 ($p>0.05$) (Figure 6.3). However, the majority of molecules were not significantly different across the ILD lung (Figure 6.4); B7-1 was significantly different across both the left ($p=0.011$) and right ($p=0.007$) lungs, whilst B7-H3 was only different across the left lung ($p=0.032$) and CD28 and PD-1 different across the right lung ($p<0.001$ and $p=0.001$ respectively). A complete summary of statistical results can be found in Appendix 10.

A high degree of inter- and intra-patient variation was also evident across all three patient groups, in keeping with leukocyte and cytokine data reported in chapter three, and there were a number of outliers in each cohort. In COPD, patients LTx-80, LTx-83 and LTx-37 (black, yellow and green, respectively) were outliers with substantially higher checkpoint expression. There were no clinical features separating this group from the remaining COPD lungs.

In ILD, patients LTx-65 (asparagus) and LTx-13 (black) had consistently high expression of checkpoint molecules, and again there were no common clinical factors to link these two patients or differentiate them from the others in the cohort, beyond the fact they both had a UIP pattern of

fibrosis, which was not unique to those two patients. With regards to the CF cohort, the cohort too was limited in size and highly variable to identify any patterns. Patients who had an abnormally high expression of one checkpoint molecule were not the same outliers for other checkpoints.

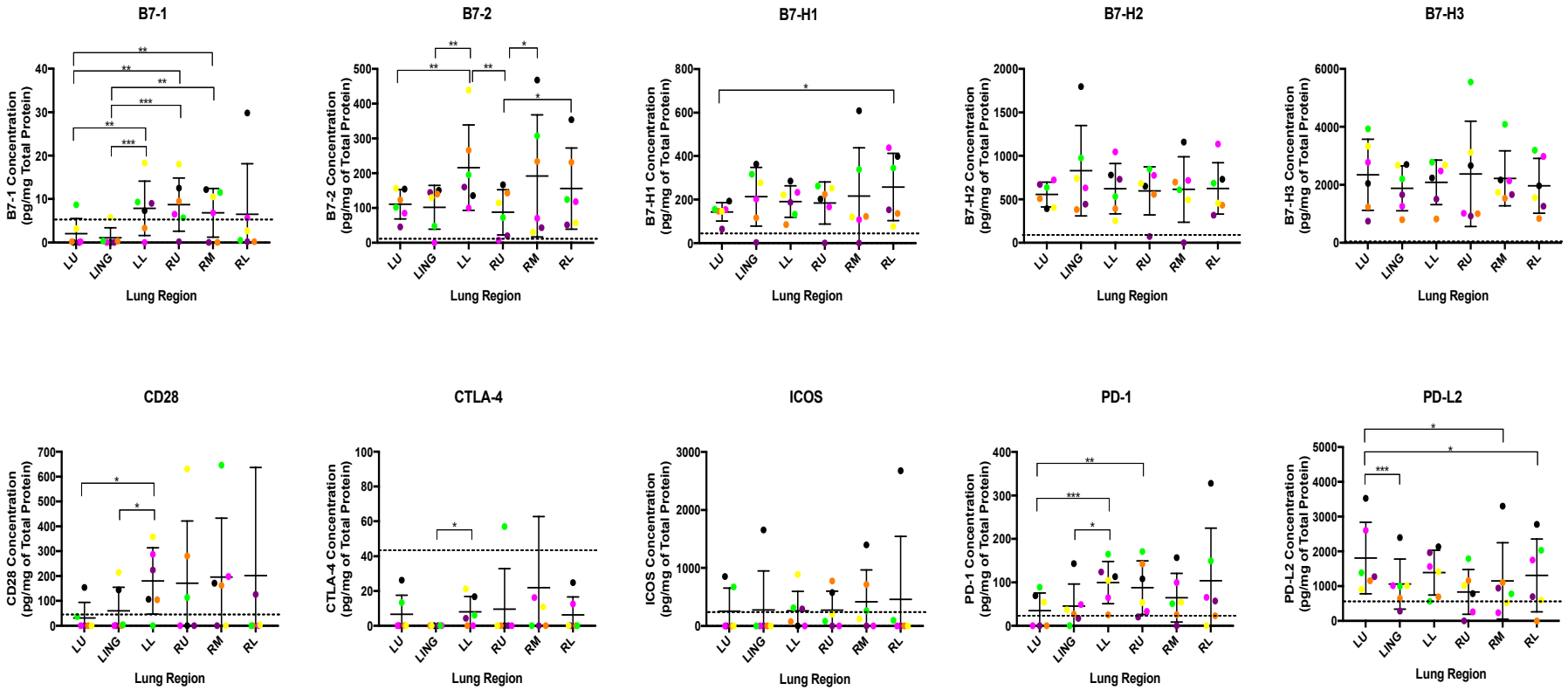

Figure 6.2 Expression of Immune Checkpoint Molecules across chronic obstructive pulmonary disease (COPD) lungs. The expression of B7-1, B7-2, B7-H1 (PD-L1), B7-H2, B7-H3, CD28, CTLA-4, ICOS, PD-1 and PD-L2 was examined across the different regions of COPD lungs (n=6, mean + SD). The dotted line represents the assay LOD. The coloured dots are representative of the same patients in previous chapters. All differences between regions determined by a generalized estimating equation with Bonferroni post-test correction, * = $p \leq 0.05$, ** = $p \leq 0.01$ and *** = $p \leq 0.001$, significance $p > 0.05$ not reported.

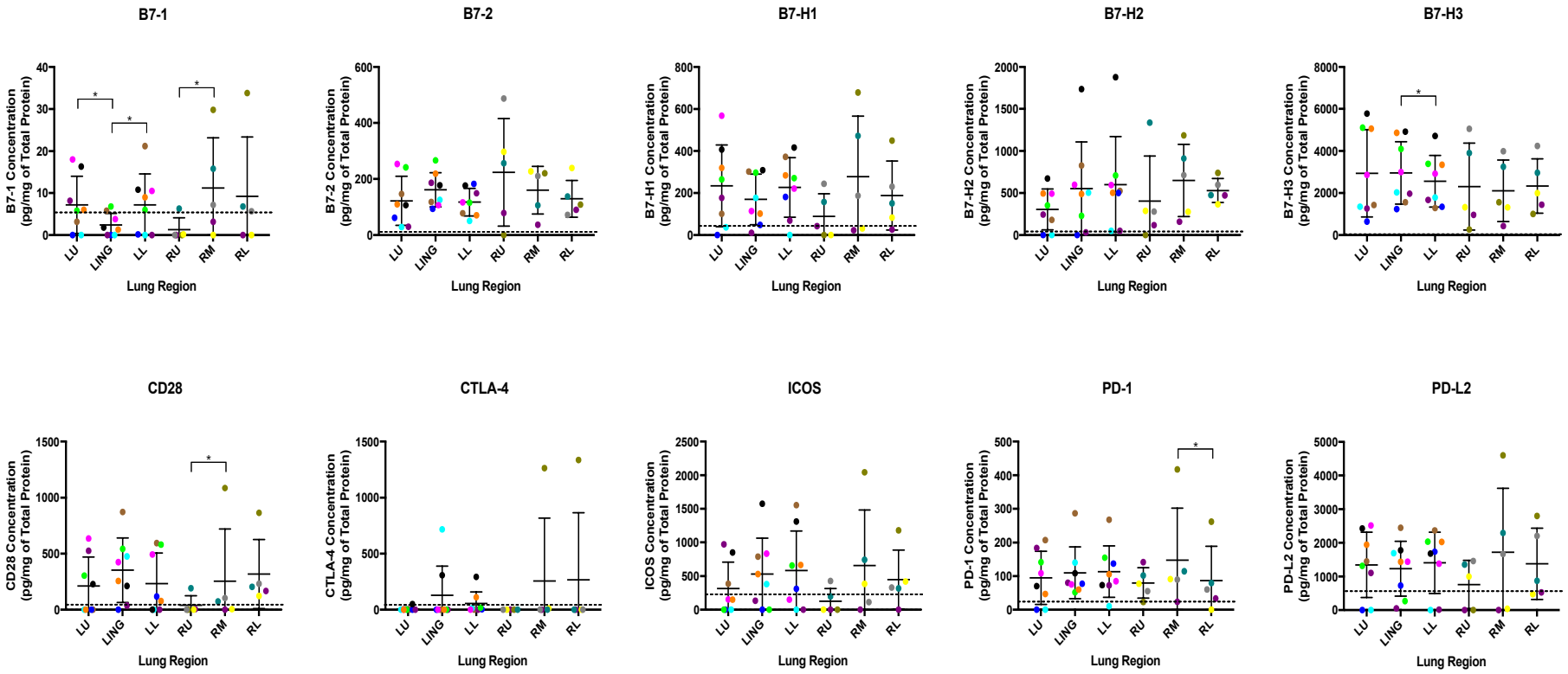

Figure 6.3 Expression of Immune Checkpoint Molecules across interstitial lung disease (ILD) lungs. The expression of B7-1, B7-2, B7-H1 (PD-L1), B7-H2, B7-H3, CD28, CTLA-4, ICOS, PD-1 and PD-L2 was examined across the different regions of ILD lungs (SLTx n=11, DLTx n=1, mean + SD). The dotted line represents the assay LOD. The coloured dots are representative of the same patients in previous chapters. All differences between regions determined by a generalized estimating equation with Bonferroni post-test correction, * = $p \leq 0.05$.

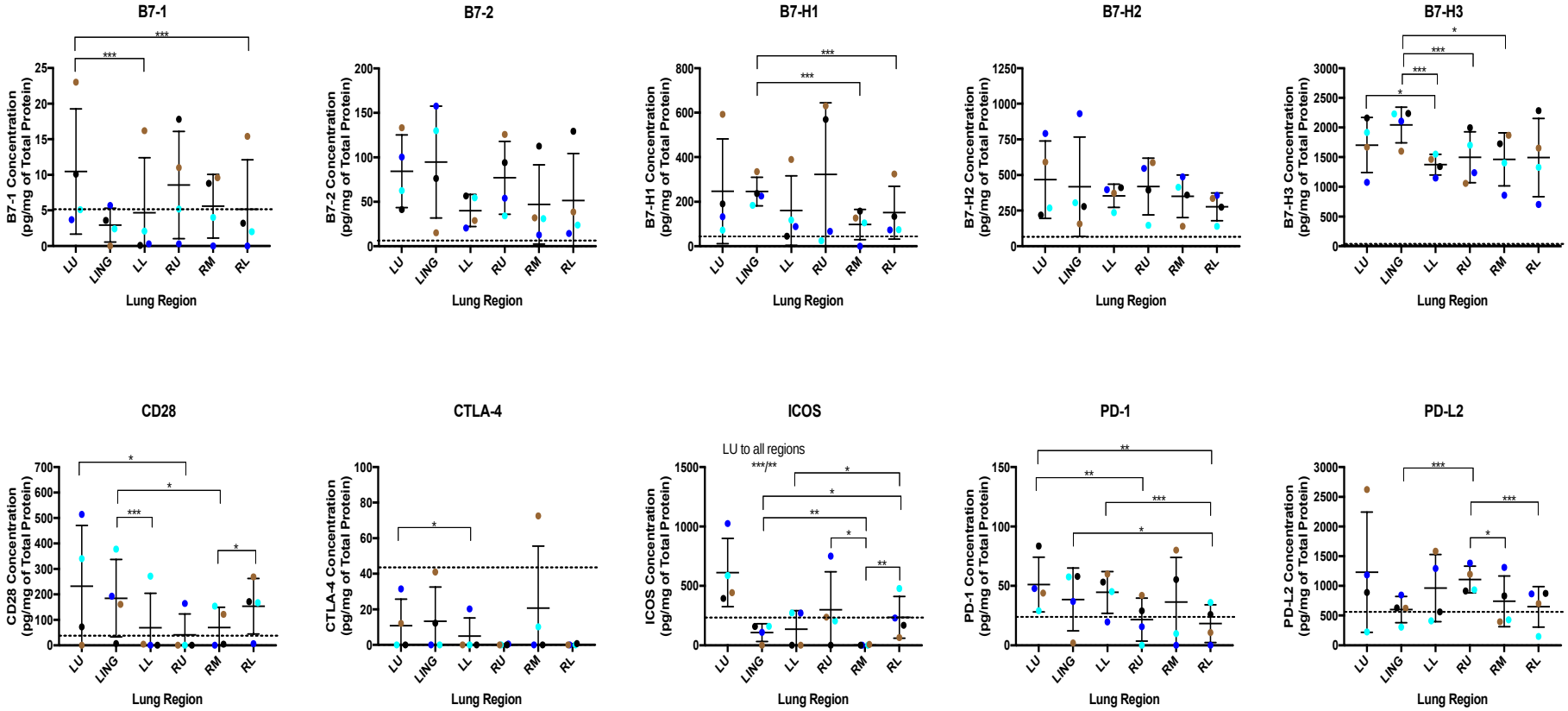

Figure 6.4 Expression of Immune Checkpoint Molecules across cystic fibrosis (CF) lungs. The expression of B7-1, B7-2, B7-H1 (PD-L1), B7-H2, B7-H3, CD28, CTLA-4, ICOS, PD-1 and PD-L2 was examined across the different regions of CF lungs (n=4, mean + SD). The dotted line represents the assay LOD. The coloured dots are representative of the same patients in previous chapters. All differences between regions determined by a generalized estimating equation with Bonferroni post-test correction, * = $p \leq 0.05$, ** = $p \leq 0.01$ and *** = $p \leq 0.001$, significance $p > 0.05$ not reported.

6.3.3 Pattern of Increased Immune Checkpoint Expression to Decreased Leukocyte Number Across the Chronic Obstructive Pulmonary Disease, Interstitial Lung Disease and Cystic Fibrosis Lung

The expression of immune checkpoints across the lung was compared to total leukocyte number within the same regions for COPD (n=6), CF (n=4) and ILD (n=12). An inverse pattern was observed between the expression of checkpoint molecules and leukocyte number in COPD lungs (Figure 6.5). This was also highly evident in the ILD lung (9/12 patients) although only in the upper lobe (Figure 6.6). Given the high degree of inter- and intra-patient variability, each patient data set was examined individually. The pattern of leukocytes across the different lung regions was compared to the expression pattern of each immune checkpoint (Figure 6.1).

ILD lungs demonstrated the largest number of inverse relationships between ICMs and leukocytes (Table 6.6). The two molecules that demonstrated the strongest inverse correlation with leukocytes were found to be PD-L1 (B7-H1) and B7-H3. These were also the molecules that had the strongest intra-patient sample correlation, with six of 14 and seven of 15 patients showing an inverse across five-six samples.

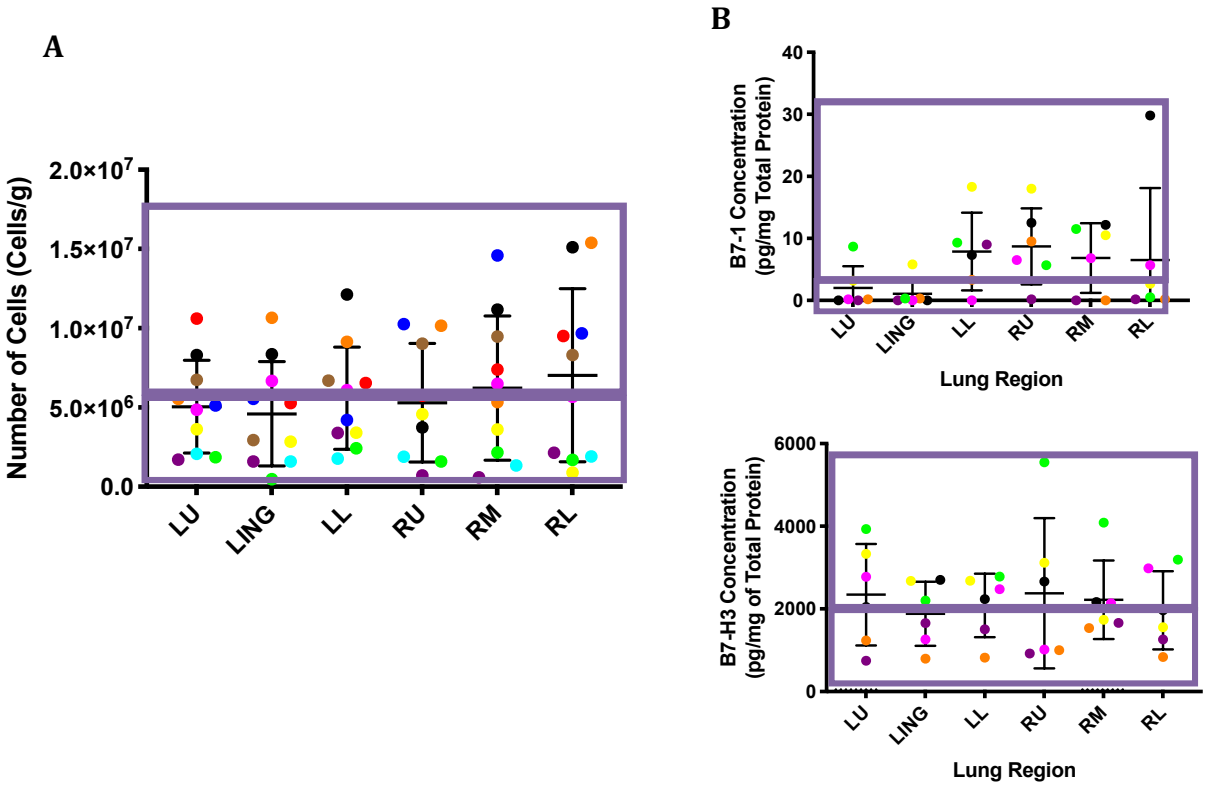

Figure 6.5. Inverse pattern between leukocyte number and immune checkpoint molecules (ICMs) in chronic obstructive pulmonary disease (COPD). The total number of CD45+ leukocytes in COPD (A) was compared to the expression of different ICMs in the same region (bars represents mean + SD). B7-H1 and B7-H3 (B) best represent the pattern of increased leukocyte number correlating with decreased ICM expression, and vice versa. The purple boxes represent patients residing above and below the mean, some of whom reside in the opposite location between separated scatter graph A and the graphs in part B.

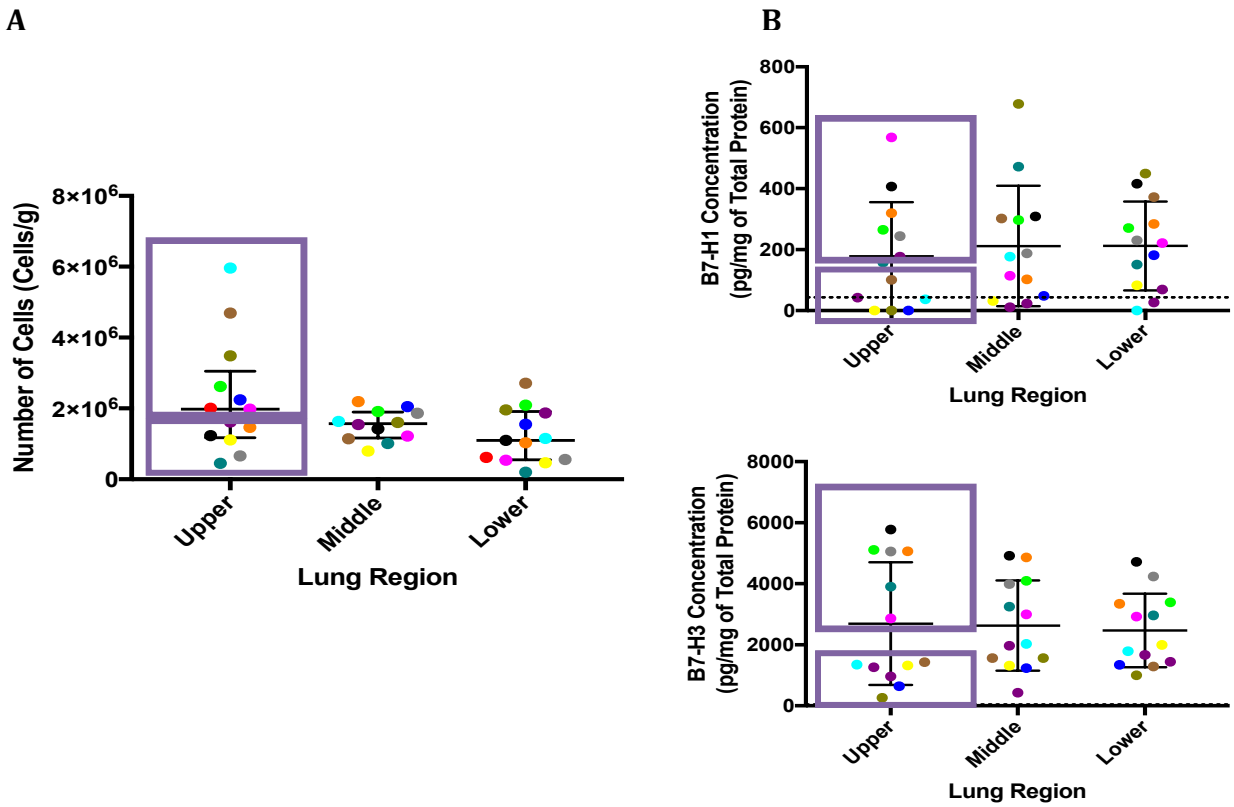

Figure 6.6 Inverse pattern between leukocyte number and immune checkpoint molecules (ICMs) in interstitial lung disease (ILD). The total number of CD45+ leukocytes in ILD (A) was compared to the expression of different ICMs in the same region (bars represents mean + SD). B7-H1 and B7-H3 (B) best represent the pattern of increased leukocyte number correlating with decreased ICM expression, and vice versa. The purple boxes represent patients residing above and below the mean, some of whom reside in the opposite location between separated scatter graph A and the graphs in part B.

Table 6.6 Inverse pattern between leukocyte number and immune checkpoint expression. The expression of immune checkpoints across the lung was compared to total leukocyte number within the same regions for chronic obstructive pulmonary disease, cystic fibrosis and interstitial lung disease. If a reverse correlation was identified three-four times (two in a SLTx) the checkpoint molecule pattern was scored as positive (+), if it was identified five-six times (three in a SLTx) it was scored as double positive (++).

COPD Patients	**B7-2**	**PD-L1**	**B7-H2**	**B7-H3**	**PD-1**	**PD-L2**
LTx-37		++				
LTx-45	+			+		+
LTx-61	+		+	++		++
LTx-69				+		
LTx-83		+	+			
LTx-80						
CF Patients	**B7-2**	**PD-L1**	**B7-H2**	**B7-H3**	**PD-1**	**PD-L2**
LTx-47		++		++		
LTx-68	+		++	+		
LTx-72						
LTx-87		+		+		
ILD Patients	**B7-2**	**PD-L1**	**B7-H2**	**B7-H3**	**PD-1**	**PD-L2**
LTx-42		+	++	+	+	++
LTx-41	+	+	+	++	+	+
LTx-44	+	+	+	++	+	+
LTx-51	+	+				
LTx-55				+		
LTx-52	++	++				
LTx-58		++			+	+
LTx-13		++		+		+
LTx-65	++	++	++	++	++	++
LTx-53	+	+		+		+
LTx-60		+		++		
LTx-59		++				
Total	**9**	**15**	**7**	**14**	**5**	**9**

Abbreviations: COPD= chronic obstructive pulmonary disease, CF= cystic fibrosis, ILD= interstitial lung disease, LTx=lung transplant, PD-L1= Programmed Death-Ligand 1, PD-1= programmed cell death protein 1, PD-L2= Programmed Death-Ligand 2,

6.3.4 Characterisation of Programmed Death-Ligand 1 and B7-H3 Across the Chronic Obstructive Pulmonary Disease and Interstitial Lung Disease Lung

Given the inverse correlation between increased PD-L1 and B7-H3 and decreased leukocytes, further characterisation across the bronchioles and interstitium of patients with COPD (n=7) and ILD (n=7) was performed. Each patient had an upper and lower lobe sample collected for routine histology These samples were obtained from clinical histology blocks generated as part of clinical practice following transplant. PD-L1 expression was examined in both the bronchioles and interstitium, but B7-H3 staining was only accurately detectable in the bronchioles. The proportion of each architecture that was stained mildly, moderately or intensely was evaluated.

The regional difference of PD-L1 and B7-H3 was examined in COPD (Figure 6.7A, C & E) and ILD (Figure 6.7B, D, & F). There were no significant differences in regional PD-L1 expression in COPD or ILD between the upper and lower lobes in either the bronchioles or the interstitium. The bronchioles also demonstrated no significant regional difference for B7-H1 in either disease cohort.

The difference in checkpoint expression between the disease groups was also examined. There were no significant differences in PD-L1 expression in the bronchioles between COPD and ILD lungs (Figure 6.8A & B), or in the interstitium of the upper lobes (Figure 6.7C). However, PD-L1 was significantly higher in the interstitium of the ILD cohort at both mild ($p=0.020$) and moderate ($p=0.002$) intensity (Figure 6.8D). B7-H3 expression and intensity was also significantly higher in the ILD bronchioles compared to COPD; in the upper lobes moderate ($p=0.001$) and intense ($p=0.001$) staining was significantly more prevalent, whilst in the lower lobes the proportion of mild ($p=0.037$) and moderate ($p=0.048$) staining was increased.

The source of PD-L1 expression in the interstitium of the lung was observationally different between COPD and ILD (Figure 6.9). A large number of ILD samples had prominent staining directly visible on the interstitium tissue, which was absent from COPD samples. Further interrogation of this observation was beyond the scope of the project, given the lack of endothelial specific markers.

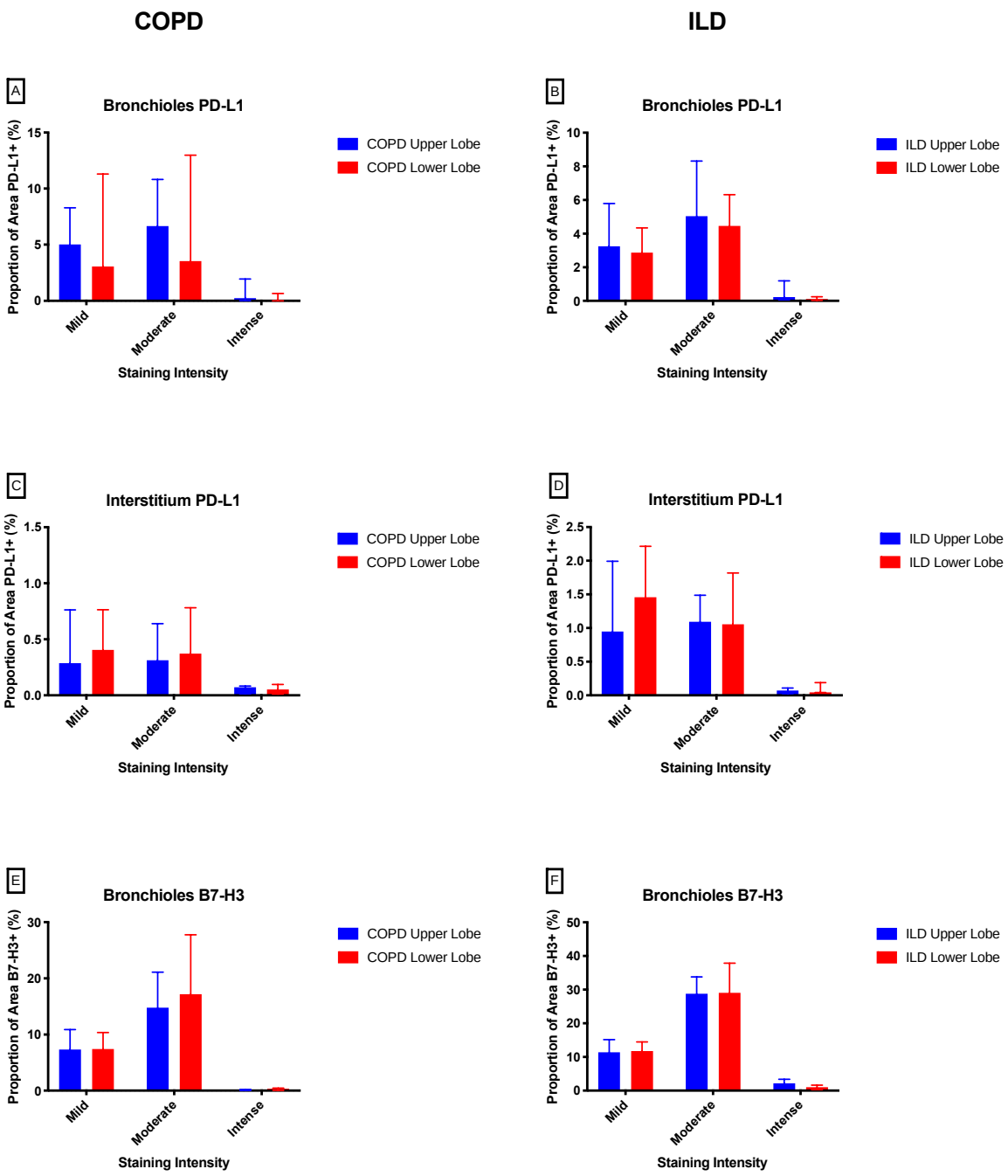

Figure 6.7 Regional expression of Programmed Death-Ligand1 (PD-L1) and B7-H3 across the lung in chronic obstructive pulmonary disease (COPD) and interstitial lung disease (ILD). Bar graphs (n=7 patients per cohort, median + IQR) show the expression and intensity of PD-L1 on the bronchioles (A-B) and interstitium (C-D) of patients with COPD (A, C) and ILD (B, D) in samples from the upper and lower regions of their lungs. The expression and intensity of B7-H3 was also examined in the same patients (E-F). Significant differences between lung regions were determined by a Mann-Whitney U test, significance $p > 0.05$ not reported.

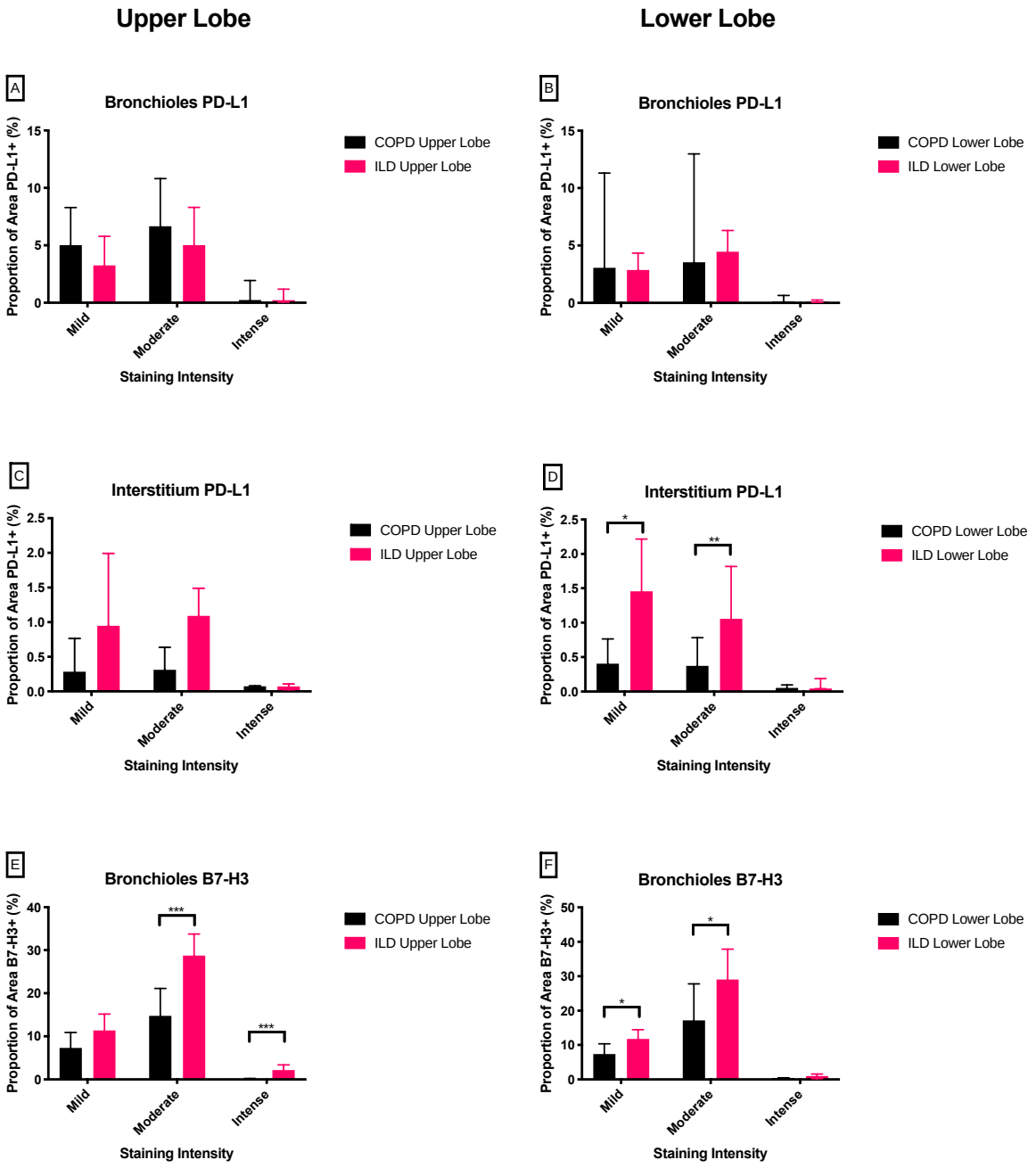

Figure 6.8 Comparison of Programmed Death-Ligand 1 (PD-L1) and B7-H3 expression between chronic obstructive pulmonary disease (COPD) and interstitial lung disease (ILD) across the lung. Bar graphs (n=7 patients per cohort, median + IQR) show the expression and intensity of PD-L1 on the bronchioles (A-B) and interstitium (C-D) of patients with COPD and ILD in samples from the upper (A, C) and lower (B, D) regions of their lungs. The expression and intensity of B7-H3 was also examined in the same patients (E-F). Significant differences in mild (* = $p \leq 0.05$) and moderate (** = $p \leq 0.01$) PD-L1 expression in the interstitium of the lower lobes were demonstrated between patients with COPD and ILD (D). Statistical differences were also identified in B7-H3 expression and intensity in the bronchioles of both the upper (E, moderate and intense, *** = $p \leq 0.001$) and lower (F, mild and moderate, * = $p \leq 0.05$) lobes.) All differences between cohorts determined by a Mann-Whitney U test, significance $p > 0.05$ not reported.

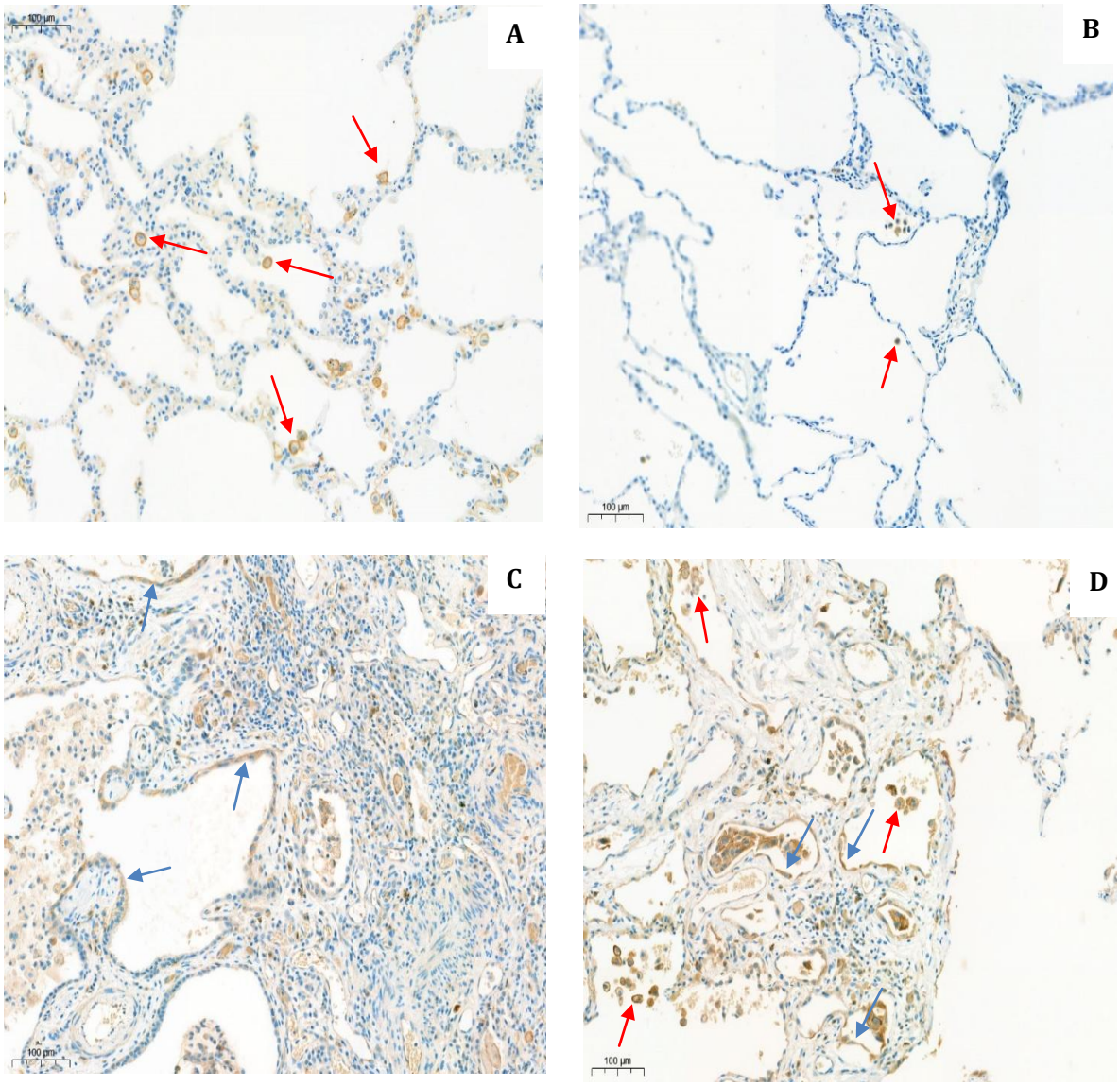

Figure 6.9 Programmed Death-Ligand 1 (PD-L1) staining of the lung interstitium. Representative images of PD-L1 staining of the interstitium for chronic obstructive pulmonary disease (COPD) (A & B) and interstitial lung disease (ILD) (C & D). The red arrows depict infiltrating cells positive for PD-L1, whilst the blue arrows depict moderate to intense staining directly on the interstitial tissue. Scale bars represent 100 µm.

6.4 Discussion

ICM targeted therapies have revolutionised the treatment of cancer, with improved survival of patients with previously unresponsive melanoma [322], as well as promising clinical trial results in a multitude of other tumour types [323]. As of 2018, there were six immune checkpoint blockade therapies with US FDA approval, targeting CTLA-4, PD-1 and PD-L1 [324]. However, despite their role in immune homeostasis, there is surprisingly little understanding regarding ICMs and lung diseases other than lung cancer. In fact, when common lung conditions such as COPD or ILD are described, it is usually in regards to the condition being a co-morbitity to lung cancer [325], [326]. Conversely, some studies have even linked these co-morbidities to a reduced efficacy during immune checkpoint blockade therapies [327], [328], or as a result of the cancer therapy [329]. The role of immune checkpoints in lung disease without cancer is therefore a vastly under-explored area that warrants investigation.

This chapter aimed to characterise the regional expression of B7/CD28 family molecules across different regions of the lung in COPD, ILD and CF. The expression of all of the molecules was highly heterogenous between lobes, irrelevant of the lung disease phenotype. There was also a high degree of heterogeneity between the lungs within each disease group, highlighting the difficulty in truly interpreting data generated from lung tissue. Despite this heterogeneity, significant differences were identified between regions of the COPD and CF lung for the majority of molecules, although regional differences in ILD were much more limited (Figure 6.3). It is possible this is a result of medication, as ILD patients often receive immunosuppressive drugs. In chapter three, male COPD patients generally had lower numbers of leukocytes, and a more homogenous pattern across the lung, whilst female patients with emphysema had consistently higher leukocyte numbers that were highly heterogeneous across the lung. The COPD data set of ICM expression was examined for a similar pattern, but this was not discernible. The was also no correlation between ICM expression and other demographic features, clinical phenotype, exacerbation history, lung function or histology. The ILD cohort also had two patients who were clear outliers across a number of different ICMs and regions; LTx-65 (asparagus) and LTx-13 (black), but beyond their shared UIP pattern of fibrosis, there were no other clinical factors that could link these two patients. Whilst it is probable these patients could have

influenced the statistical analysis of the regional ICM expression, the grossly heterogenic results within each cohort and region make it just as likely to reverse or create significant differences in other region. Given ICMs are commonly expressed on both T cells and APCs, it is also plausible that factors which may influence leukocyte numbers could also impact upon the expression levels of ICMs. These physiological, microbial and transplant related factors were discussed in greater detail in chapter three.

However, a increased expression of ICM, most evidently PD-L1 and B7-H3, correlated with lower leukocyte numbers (Table 6.7). Due to the nature of tissue lysate, further information regarding the location and expression of these markers was not possible to extract. As such, the aims of the study evolved to further characterise these molecules by performing immunohistochemistry on sample blocks collected for routine histology from patients with COPD or ILD who had previously undergone transplantation. This represents the first study to directly compare the expression of ICMs in two different lung conditions, without the co-morbidity of cancer. Although regional differences in the expression of PD-L1 or B7-H3 were not observed (Figure 6.6), significant differences were observed between COPD and ILD lungs (Figure 6.7), a novel finding that has yet to be described within the literature.

Given ICMs play a role in either the stimulation or inhibition of T cells, it is perhaps unsurprising that increases and decreases in their expression have an effect on leukocyte number. Indeed, PD-L1, and more controversially B7-H3, are inhibitory ICMs that prevent T cell proliferation and cytokine production [330] and were found to be the two molecules that correlated most with reduced leukocyte number (Table 6.7). However, the same pattern was also observed to a lesser extent in co-stimulatory molecules such as B7-2 (CD86) and B7-H2 (ICOSL), confounding the relationship between leukocyte recruitment and ICM. In the COPD lung, the inverse relationship between ICMs and leukocytes largely occurred over the entirety of the lungs; whereas in ILD, a large proportion (9/12) displayed this inverse relationship although only in the upper lobe (Figure 6.5). As previously discussed in chapter three, the majority of these patients had a UIP pattern of fibrosis, meaning the lower regions of the lungs were most severely affected by disease. It is interesting that an inverse relationship between leukocytes and ICMs was observed in areas that were disease free, and that the relationship was lost in lung regions of disease. During chronic inflammation, inhibitory ICMs can be excessively up-regulated to the point of

driving immune exhaustion [331]. Activities such as T cell proliferation and cytokine secretion are inhibited and the integrity of tissue is preserved. This may explain why the upper lobes of the ILD lung had increased ICM expression, lower populations of leukocytes, and less disease severity. If this is correct, up-regulation of inhibitory ICMs may represent a therapeutic mechanism for the treatment of ILD. However, the negative consequences of an impaired immune response must be considered.

Given the potentially critical role of PD-L1, its specific location within the lung was evaluated. In the COPD lung, PD-L1 was located in the bronchioles, whilst patients with ILD consistently expressed increased PD-L1 in the interstitium. PD-L1 is expressed on a range of leukocytes and parenchymal tissues [332], and is inducible on epithelial and endothelial cells in states of disease as a response to cytokines [333], [334]. However, precisely where PD-L1 resides in the interstitium of ILD and COPD is currently not described in the literature. There was a high proportion of PD-L1 staining in ILD that was observed directly on the interstitium (Figure 6.8), whilst the COPD lung was largely PD-L1+ as a result of infiltrating cells such as macrophages. The location of the interstitial staining suggests it is the capillaries within the ILD lung that are PD-L1+. However, the lack of an endothelial specific marker prevented confirmation that the capillaries, rather than the non-specific staining of erythrocytes, were truly PD-L1+. Whilst PD-L1 expression was higher in the bronchioles of COPD patients compared to ILD, this pattern was reversed for B7-H3 in the bronchioles. The precise role of B7-H3 remains unknown, with reports describing both activating and inhibitory properties as an ICM. B7-H3 is highly expressed on basal cells, one of the four major cell types of airway epithelium [335]. It is also expressed on fibroblasts [336], which have extensive interactions with the epithelium in ILD [337]. Therefore, the combination of epithelium, monocytes and fibroblasts in ILD may contribute to higher detectable levels of B7-H3 in the bronchioles of ILD patients.

A potential limitation to this finding is that the cellular location of B7-H3 cannot be determined. B7-H3 can be expressed on a range of cells as described above. In fact, a soluble form of B7-H3 can also be released from monocytes, DCs and activated T cells [338]. Whilst the negative control tissue did not express B7-H3 as a ‘background stain’, the interstitium of both ILD and COPD patients was moderately to intensely stained throughout. Given the tissue samples also contained residual blood, it was difficult to decipher blood against the expression of soluble and membrane bound B7-H3. The analysis of the

interstitium for B7-H3 therefore had to be omitted from this preliminary work until further optimisation of the samples could be performed. The immunohistochemistry element of the study was performed late into the project and was intended as preliminary work for future studies. Increasing patient numbers through the use of tissue microarrays (TMA) would be a fast and cost-effective way to progress the project. This would also allow for different disease aetiologies to be examined, which would be particularly useful for ILD patients who have such heterogeneous patterns of disease.

Increasing expressions of ICMs directly correlated with a localised decrease in leukocyte number, which was evident in COPD and CF lungs, but was particularly interesting in ILD. The relationship between increased ICM expression and lower populations of leukocytes occurred only in the upper lobes. In areas of increased disease severity, this pattern was lost, potentially highlighting a fundamental mechanism leading to leukocyte recruitment and increased severity. Whilst this data is observational, a preliminary study describing the specific locations of PD-L1 and B7-H3 expression within the ILD and COPD lung was provided for the first time. Given the capabilities of CyTOF to exponentially increase the number of markers that can be examined in one go, combining phenotypic markers and ICMs, and expanding to structural cells such as epithelial and endothelial cells, would provide further insight into the relationship between these cells types, immune checkpoint regulators and the loss of homeostasis in chronic lung disease.

Chapter Seven: Overall Discussion

7.1 Overall Discussion

Lung disease presents a major burden to the NHS, with approximately 12.7 million people currently diagnosed with some form of lung condition and over 500,000 new diagnoses each year [33, 339]. Lung disease, including lung cancers, respiratory infections and COPD, contributed to almost 25% of worldwide deaths in 2016 [340]. This proportion only accounts for conditions within the top 10 global causes of death, thus excluding ILDs and CF unless lower respiratory infections were the cause. In the UK, it is thought that a patient dies every 5 minutes from some form of lung disease [339]. However these conditions have equally alarming morbidity rates. This places immense pressure on the NHS, with over 700,000 hospital admissions, as well as six million inpatient bed stays each year. With this in mind, research into both underlying causes, as well as disease limiting and curative therapies, is essential to alleviate the mounting difficulties that pulmonary disease presents.

Given the complexity of the lung and the heterogeneous nature of lung disease, there are numerous limitations with current sampling methods, as detailed in Chapter one. Whilst BAL, biopsy, sputum, blood and resection sampling all have positive attributes, isolated sampling points restrict researchers from exploring the true extent of disease and inflammation across the lungs. Why is it that lung disease can so severely affect one region of the lung, whilst leaving other sections undisturbed? Can exploring such limited areas really advance therapeutic options for chronic lung diseases? With this in mind, the question is whether traditional sampling techniques inherently miss the signals and mechanisms at the sites of disease. This thesis intended to evaluate the inflammatory profile of major chronic lung conditions by performing multi-lobe wedge sampling across the native (diseased) lungs of patients undergoing lung transplantation. As such, it was anticipated that this project would focus on fundamental discovery, allowing early findings to dictate the future direction of the PhD.

This thesis hypothesised that there would be fundamental differences in inflammation across the lungs of patients with end stage chronic lung disease (COPD, CF and ILD). This indeed proved to be the case, demonstrated by a large number of cell types explored across different lobes of the COPD, CF and ILD lung in chapter three. In fact, the inflammatory heterogeneity that was hypothesised proved to be even more complex when considering patients as individuals, as well as part of a disease specific

group. The mean number of cells for some leukocyte subsets looked homogenous across the different lobes, particularly CD45+ leukocytes within COPD, but demonstrated vast intra- and inter-patient variation. In contrast, T cells from ILD patients demonstrated significant heterogeneity between lobes, but in reality this was driven by a small number of outliers. There were also some aspects of the study that reproduced and validated previously published research. The COPD lung contained a broad population of granulocytes and T cells, whilst leukocytes in CF tissue mainly consisted of granulocytes. These are both commonly associated findings with the two disease groups, particularly considering neutrophils contribute heavily to the marginated pool of leukocytes within the lung at any given time [341]. Given macrophages are commonly associated with pulmonary fibrotic processes [342], it was also not surprising that MPS cells were a dominant cell type within ILD. However, the collection of large, multi-site specimens in this study led to several important observations, which would not have been possible with routine sampling techniques. Firstly, female patients with emphysematous COPD have greater heterogeneity in leukocytes across the lung lobes, whilst male patients with COPD portrayed a significantly more homogenous pattern. An interesting increase in the ratio of CD4+ to CD8+ T cells was also observed in a number of patients, who each had greater heterogeneity in their total T cell numbers across different regions compared to the rest of the cohort. In ILD, there were significantly higher numbers of leukocytes isolated from the left lung than the right lung, and this pattern persisted for a number of subsets. Given clinical sampling is predominantly associated with the right side of the lung, this could be of important clinical interest as lung inflammation may be repeatedly underestimated in ILD. In general, each region of the ILD lung had limited variation in leukocytes numbers across the cohort, particularly in the middle lobes. However this was not the case for monocytes, which presented the most heterogeneous numbers across all patients and regions. This data was further interrogated in Chapter four, and demonstrated two ILD specific phenomena; firstly intermediate monocytes were disproportionally elevated in ILD, which coincided with areas of severe fibrosis. Secondly, non-classical monocytes were significantly decreased, with the largest decreases again occurring in areas of increased disease severity.

Chapter five aimed to provide a deep characterisation of lobar heterogeneity in lung disease, and understand the functional contributions of monocytes in ILD and T cells in COPD. Whilst the future capabilities on CyTOF were clearly demonstrated, the preliminary nature of the investigation prevented

any fundamental discoveries at the present time. Lastly, the project sought to examine mechanisms by which immune dysfunction could contribute to disease pathophysiology. Although there is a detailed understanding of ICMs in cancer immunotherapy research, there is a surprising lack of research into these molecules in chronic lung diseases (other than cancer). Given the role of ICMs in immune homeostasis, and the loss of immune tolerance in many lung diseases, increasing our understanding in this area could result in new therapies. The investigation began with the characterisation of 10 major ICMs across lobes of the lung, followed by the subsequent identification of an inverse relationship between leukocyte number and checkpoint expression. As PD-L1 and B7-H3 most commonly demonstrated this pattern, the expression of these molecules was characterised across key structures of the lung in COPD and ILD. The preliminary examination of the bronchioles and interstitium revealed significant differences between the two disease groups that warrant further investigation in an increased number of patients.

The disproportionate number of intermediates monocytes and ICM expression in ILD and compared to COPD are two of the novel findings from this thesis. Given that the discoveries both relate to the same disease, it is interesting to speculate if one had a bearing on the other. Epithelial to mesenchymal transition (EMT) has been linked to a role in the pathogenesis of lung fibrosis through a series of functions, albeit with controversial *in vivo* results [78]. Interestingly, previous studies have demonstrated that B7-H3 promotes EMT [343], and within this study the expression of this molecule was significantly higher in the bronchioles of ILD patients. Furthermore, monocytes express B7-H3, which can be cleaved by metalloproteinases (MMPs) into a functioning soluble form of the molecule [338]. A number of MMPs have been implicated in ILD, particularly IPF [344]. Although not possible to distinguish within the remit of this thesis, it could be that intermediate monocytes identified within ILD lungs are responsible for increased B7-H3. In a study of synovial monocytes in rheumatoid arthritis (RA), intermediate monocytes were shown to be elevated compared to classical monocytes [345]. These intermediate cells had increased expression of B7-H3 in comparison to the other subsets. However, whether B7-H3 mediated signalling played a pathogenic role in RA was not determined. Nevertheless, it is plausible that intermediate monocytes observed in ILD could be the contributor of increased B7-H3. As such, the increased expression of B7-H3 on the epithelium of the bronchioles, as

well as the increase in B7-H3 expressing monocytes within the lung tissue environment, requires further exploration as a potential contributor to ILD pathogenesis.

Whilst PD-L1 was not significantly different across the bronchioles of the disease groups, it was significantly elevated in the interstitium of ILD patients. PD-L1 plays a role in the expansion and maintenance of Tregs [346], which are an essential regulator of the adaptive immune response, and were examined as part of this thesis. There was increased expression of PD-L1 in the lower lobes that correlated with areas rich in Tregs. However, the findings of this study are controversial, as Tregs have also been shown to decreased in IPF [247]. This inconsistency in Treg proportions has also been documented for connective tissue disorders such as SSc, for which ILD is a common comorbidity [227]. Given the controversy within the field, it is unknown whether the presence of Tregs, PD-L1 mediated or otherwise, is a protective mechanism as seen in fibrotic mouse models [347] or alternatively a promoter of fibrosis as described in ILD relating to SSc [348]. In contrast to ILD, a second interesting finding regarding Tregs was that they were significantly decreased in the middle lobes of the CF lung. Decreases in Treg numbers within CF patients has previously been reported [349], although this remains a largely unexplored area. A CF mouse model of *A. fumigatus* infection demonstrated reduced Tregs compared to wild-type controls [350], resulting in amplified Th17 and Th2 responses. Given the decreased proportion of CD4+ cells in CF compared to the other disease groups, a subsequent reduction in Tregs may be a natural occurrence. Conversely, this finding is paradoxical to a study of CF biopsy samples where Th17 lymphocytes were characterised [351]. Significantly more CD4+ cells were present within the biopsy than CD8+ cells for both newly diagnosed and established CF. However, endobronchial biopsies provide information regarding the airway mucosa, whilst the current study utilised parenchymal tissue inaccessible to bronchoscopy. The increased ratio of CD8+ cells observed in this research is also supported by IHC from another study utilising CF samples obtained at transplant [352]. With regards to ICM expression, PD-L1 and B7-H3 expression was significantly higher in the lingual lobe of CF patients than in other regions and could perhaps impact on Treg numbers. However, this pattern was not observed in the right middle lobe where Tregs were also decreased. Unfortunately, because of low recruitment rates of CF patients to the study, the cohort were not included in the preliminary IHC examination of these molecules, preventing further delineation at this point in time.

One factor that must be discussed is the relevance of characterising the inflammatory profile of chronic lung diseases that have reached an end stage prognosis. All of the regional lung samples collected and analysed throughout this thesis were obtained from patients receiving a lung transplantation due to the significant pathology driven by their respective diseases. Each of the conditions result in dramatically remodeled lung architecture, gross destruction of functional tissue, and often long term compromise of sufficient ventilation and perfusion [353-355]. However, in order to fully understand a disease, it is important to understand the natural history of disease from beginning to end [181]. Although viable lung tissue is greatly reduced in these lungs compared to patients at earlier severities of the same disease, there was clearly still active inflammation occurring and the majority of these patients underwent periods of exacerbation and stability prior to transplant. Given COPD, ILD and CF continue to lack fundamental curative therapies, contributions of knowledge regarding all stages of severity continue to provide important insight. There is also a difficulty in standardising samples from patients at earlier disease severities, given patients may experience disease processes in varying orders and timeframes. It could be considered that patients on the transplant waiting list, who have all met pre-defined criteria including a cessation of smoking and a healthy BMI, have undergone every variability in their disease course at that end stage point and may be more representative of each other than a cohort of patients with a mild form of a disease. As previously discussed, patients with ILD more commonly receive a SLTx, leaving the patient with a diseased lung. It could be argued that a thorough understanding of this diseased lung, which cannot be sampled as rigorously or extensively as from an explanted lung, could be important for preserving the limited functionality it may retain. This in turn could be useful to help stabilise pre-transplant patients, who often spend a long time on the transplant waiting list because of the limited number of donor lungs that are actually suitable for transplant [356].

7.2 Limitations

Despite the many positives gained from working with samples obtained during transplant, there were also three major limitations to this study due to the nature of transplantation; the overall number performed, the unpredictability, and the frequency. Small n= numbers were a constant limitation throughout this PhD project, and drove the necessity for lung disease phenotypes to be grouped by

umbrella phenotypes rather than individual aetiologies. The very nature of transplantation dictates unpredictability, making it very difficult for an individual to collect samples every time an offer of a lung proceeds to transplantation. This is particularly true when there is a requirement to collect and process samples immediately, rather than during the working hours of histopathology. During the course of the study, 34 patients were transplanted in year one, 30 in year two and 22 in year three, totalling 86 lung transplants. The study required a number of patients to optimise the protocol (n=3), and fresh samples were also collected from other patients for different investigations that did not progress further (n=5). This equated to a collection rate of 42%, but does not account for the number of aborted transplants that were also prepared for. Aside from total number, there was no control over the frequency that each disease was transplanted. Whilst this did not impact the regional characterisation of disease groups, as flow cytometry can be performed immediately, it did impact some of the other analyses that were performed in this thesis. Cytokine, chemokine and immune checkpoint characterisation require batches of samples to be run, firstly to fully utilise an expensive kit and keep resource wastage to a minimum, and secondly to reduce assay variation influencing sample outcomes. The number of CF patients was by far the most restrictive during the four years, resulting in this group being omitted from Luminex cytokine analysis. In fact, the fifth CF patient was only collected in June 2019; despite an initial decision to cease further collections post January 2019 to enable other investigations to commence.

Another limitation is the study was largely observational, with little mechanistic investigation. This was the planned approach, as characterisation of inflammation across each lobe of a human lung had not been undertaken before. Although the work resulted in key observations such as disproportional frequencies of monocytes in ILD, the functional role these cells may perform was not elucidated further. ICM investigations were utilised to interrogate potential regulators or enhancers of inflammation, although these studies were again predominantly observational. The investigations could have been enhanced further with the use of *in vitro* cell culture models, or *in vivo* mouse models and porcine *ex vivo* perfusion.

There were also a number of circumstances and factors that may have contributed to the regional heterogeneity observed within this study, but were not accounted for within the aims of this project.

Such factors include the timing of the transplant and any circadian influences of leukocyte migration, bacterial or fungal colonisation, physiological factors that may affect leukocyte movement within the lung such as gravitational influences on blood flow and ventilation pressures, and vascular structure, size and density. The bearing that each of these factors may have had on the findings has been discussed in detail within chapter three.

7.3 Improvements & Future Work

If this body of work were to be completed again, better utilisation of histology expertise and clinical tissue blocks would be a first consideration. During the third year of the project, a collaborative partnership was developed with Dr Angeles Montero, consultant histopatholigist at MFT. Dr Montero was able to provide support regarding semi-quantitative analysis of disease severity in ILD, and the selection of suitable blocks for IHC staining of ICMs. This complemented work generated earlier in the project, and it was unfortunate Dr Montero only joined MFT in early 2018. Given there were 118 patients recruited to the study, IHC could have been utilised in other ways with greatly increased n numbers.

This work has only scratched the surface with regards to regional heterogeneity in lung disease. If this methodology were to be standardised across the five adult lung transplant centres in the UK, there could be a major increase in the number of lungs undergoing characterisation. This expansion has the potential to determine many more avenues of fundamental discovery, particularly those only evident when considering the lung as a whole rather than the areas accessible through isolated sampling techniques. This characterisation could only be further enhanced by collaboration with histopathologists, which would enable the study to be widened to include varying disease severities; areas of preserved architecture, moderate and severe disease across the lung. Patients could also be stratified based on factors such as their clinical phenotypes, transplant time and duration, as well as profiling the microbiota of each tissue sample and other inflammatory influencing factors such as microRNA.

There were a number of interesting results generated during this study, particularly with regards to ILD patients, that warrant further investigation. An attempt was made to perform RNA sequencing on intermediate monocytes in ILD, but unfortunately the number of cells limited the yield of RNA, which prevented this investigation at the first hurdle. Whilst the biopsy sizes were significantly larger than standard endobronchial biospies at approximately 5 g, it was not possible to take larger biopsies from the explanted lung, as the organ needed to be interrogated by clinical histology to ensure no ancillary diseases were present (i.e. infections, cancer) that would negatively impact on clinical outcome following transplantation. Although beyond the scope and budget of this project, there are numerous ways to overcome this barrier that could be explored going forward. This includes collecting fluorescence-activated cell sorting (FACS) cells directly into lysis buffer to increase RNA yield [357], or the use of RNA amplification kits prior to sequencing [358]. Besides RNA sequencing, *in vitro* cultures and stimulation assays are another way to assess functionality of monocytes in ILD. The key functions of monocytes include phagocytosis, chemotaxis and cytokine secretion, which are all able to be determined in a range of functional assays [359]. An evaluation of monocyte cytokine secretion during lipopolysaccharide (LPS) stimulation was attempted during the course of this research. However, due to the limited amount of each cell type acquired following FACS, an inadequate number of cells were proportioned between several investigations. Going forward, isolations from larger quantities of tissue are required, or the limited number of cells should be prioritised to only one investigation.

Given the success of the IHC staining of PD-L1, this is an obvious investigation that could easily be driven forward. The use of TMAs could rapidly scale up both the number of intra-patient samples investigated, as well as increase the overall n number. Finally, CyTOF has great potential to provide more in depth characterisation than flow cytometry using banked cells and future sample collections. The panels used in this project were dictated by collaborations with industrial partners across the MCCIR. Although they formed a good basis for myeloid and lymphoid investigation, there is still scope to expand on the markers currently used. A full workup and optimisation of these panels could be performed using currently banked cells, with the aim to replace flow cytometry with CyTOF for fresh processing in future study collections.

7.4 Conclusions

There is significant regional heterogeneity in leukocytes and other inflammatory mediators across a number of chronic lung diseases. The in-depth exploration of three different diseases allowed the discovery of a number of disease specific findings, the most interesting of which relating to monocyte subsets in ILD. The alteration in monocyte frequencies was evident in areas of severe disease in ILD, and further supports the benefits of multi-site sampling in lung inflammation research.

ICMs, such as PD-L1 and B7-H3, may play an integral role in driving leukocyte regional heterogeneity and were characterised across different lobes of the lung. The results of this examination established firm differences between COPD and ILD, which provides an excellent basis for future investigation. Monocytes and Tregs should also be considered within the context of ICMs.

More pertinently, although sampling from up to six different areas of the lung is clinically not feasible beyond studying explanted lungs, the results of this thesis suggest caution regarding generalised statements about inflammation in lung disease. The thorough examination of all native lungs removed during transplantation could provide greater insight into end stage inflammation in lung disease, particularly through the comparison of healthier and severely diseased tissue. In turn, this complete characterisation could eventually overcome the barriers of lobar heterogeneity and accelerate the effectiveness of lung specific inflammation treatments.

References

1. Crimeen-Irwin, B., et al., *Failure of immune homeostasis -- the consequences of under and over reactivity.* Curr Drug Targets Immune Endocr Metabol Disord, 2005. **5**(4): p. 413-22.
2. Moldoveanu, B., et al., *Inflammatory mechanisms in the lung.* J Inflamm Res, 2009. **2**: p. 1-11.
3. Raz, E., *Organ-specific regulation of innate immunity.* Nat Immunol, 2007. **8**(1): p. 3-4.
4. Holt, P.G., et al., *Regulation of immunological homeostasis in the respiratory tract.* Nature Reviews Immunology, 2008. **8**(2): p. 142-152.
5. Lloyd, C.M. and B.J. Marsland, *Lung Homeostasis: Influence of Age, Microbes, and the Immune System.* Immunity, 2017. **46**(4): p. 549-561.
6. Wissinger, E., J. Goulding, and T. Hussell, *Immune homeostasis in the respiratory tract and its impact on heterologous infection.* Seminars in Immunology, 2009. **21**(3): p. 147-155.
7. Spina, D., *Epithelium Smooth Muscle Regulation and Interactions.* American Journal of Respiratory and Critical Care Medicine, 1998. **158**(supplement_2): p. S141-S145.
8. Whitsett, J.A. and T. Alenghat, *Respiratory epithelial cells orchestrate pulmonary innate immunity.* Nat Immunol, 2015. **16**(1): p. 27-35.
9. Rogers, A.V., et al., *Identification of serous-like cells in the surface epithelium of human bronchioles.* Eur Respir J, 1993. **6**(4): p. 498-504.
10. Hong, K.U., et al., *Clara cell secretory protein-expressing cells of the airway neuroepithelial body microenvironment include a label-retaining subset and are critical for epithelial renewal after progenitor cell depletion.* Am J Respir Cell Mol Biol, 2001. **24**(6): p. 671-81.
11. Knight, D.A. and S.T. Holgate, *The airway epithelium: structural and functional properties in health and disease.* Respirology, 2003. **8**(4): p. 432-46.
12. Parker, D. and A. Prince, Innate immunity in the respiratory epithelium. Am J Respir Cell Mol Biol, 2011. **45**(2): p. 189-201.
13. Puttur, F., L.G. Gregory, and C.M. Lloyd, Airway macrophages as the guardians of tissue repair in the lung. Immunology & Cell Biology, 2019. **97**(3): p. 246-257.
14. BioRender. Respiratory Epithelium. 2020 [cited 2020; Available from: https://app.biorender.com/biorender-templates/t-5e2070c990315200865856f7-respiratory-epithelium.
15. Condon, T.V., et al., Lung dendritic *cells at the innate-adaptive immune interface.* J Leukoc Biol, 2011. **90**(5): p. 883-95.
16. Braciale, T.J., J. Sun, and T.S. Kim, *Regulating the adaptive immune response to respiratory virus infection.* Nature reviews. Immunology, 2012. **12**(4): p. 295-305.
17. Steinman, R.M., *The dendritic cell system and its role in immunogenicity.* Annu Rev Immunol, 1991. **9**: p. 271-96.
18. Wang, H.B., et al., *Airway eosinophils: allergic inflammation recruited professional antigen-presenting cells.* J Immunol, 2007. **179**(11): p. 7585-92.
19. Chen, X. and P.E. Jensen, *The role of B lymphocytes as antigen-presenting cells.* Arch Immunol Ther Exp (Warsz), 2008. **56**(2): p. 77-83.
20. Hussell, T. and T.J. Bell, *Alveolar macrophages: plasticity in a tissue-specific context.* Nature Reviews Immunology, 2014. **14**(2): p. 81-93.
21. Byrne, A.J., et al., *Pulmonary macrophages: key players in the innate defence of the airways.* Thorax, 2015. **70**(12): p. 1189-1196.
22. Franke-Ullmann, G., et al., *Characterization of murine lung interstitial macrophages in comparison with alveolar macrophages in vitro.* The Journal of Immunology, 1996. **157**(7): p. 3097-3104.

23. Bedoret, D., et al., *Lung interstitial macrophages alter dendritic cell functions to prevent airway allergy in mice.* The Journal of Clinical Investigation, 2009. **119**(12): p. 3723-3738.
24. Kuebler, W.M. and A.E. Goetz, *The marginated pool.* Eur Surg Res, 2002. **34**(1-2): p. 92-100.
25. Lien, D.C., et al., *Neutrophil kinetics in the pulmonary microcirculation. Effects of pressure and flow in the dependent lung.* Am Rev Respir Dis, 1990. **141**(4 Pt 1): p. 953-9.
26. Giacalone, V.D., et al., *Neutrophil Adaptations upon Recruitment to the Lung: New Concepts and Implications for Homeostasis and Disease.* Int J Mol Sci, 2020. **21**(3).
27. Kuebler, W.M., et al., *Contribution of selectins to leucocyte sequestration in pulmonary microvessels by intravital microscopy in rabbits.* J Physiol, 1997. **501 (Pt 2)**(Pt 2): p. 375-86.
28. Golubovskaya, V. and L. Wu, *Different Subsets of T Cells, Memory, Effector Functions, and CAR-T Immunotherapy.* Cancers (Basel), 2016. **8**(3).
29. Janeway CA Jr, T.P., Walport M, et al., *Immunobiology: The Immune System in Health and Disease.* 5th ed. T cell-mediated cytotoxicity. 2001, New York: Garland Science;.
30. Moore, B.B., T.A. Moore, and G.B. Toews, *Role of T- and B-;lymphocytes in pulmonary host defences.* European Respiratory Journal, 2001. **18**(5): p. 846-856.
31. Yagui-Beltrán, A., L.M. Coussens, and D.M. Jablons, *Respiratory Homeostasis and Exploitation of the Immune System for Lung Cancer Vaccines.* US oncology, 2009. **58**(1): p. 40-48.
32. Ferkol, T. and D. Schraufnagel, *The global burden of respiratory disease.* Ann Am Thorac Soc, 2014. **11**(3): p. 404-6.
33. Snell, N., et al., *Burden of lung disease in the UK; findings from the British Lung Foundation's 'respiratory health of the nation' project.* European Respiratory Journal, 2016. **48**(suppl 60).
34. Serhan, C.N., P.A. Ward, and D.W. Gilroy, *Fundamentals of Inflammation*. 2010: Cambridge University Press.
35. Galani, V., et al., *The role of apoptosis in the pathophysiology of Acute Respiratory Distress Syndrome (ARDS): An up-to-date cell-specific review.* Pathology - Research and Practice, 2010. **206**(3): p. 145-150.
36. (WHO), W.H.O. *Burden of COPD*. Chronic respiratory diseases 2020 [cited 2020; Available from: https://www.who.int/respiratory/copd/burden/en/ -:~:text=Burden%20of%20COPD.%20According%20to%20WHO%20estimates%2C%2065,which%20corresponds%20to%205%25%20of%20all%20deaths%20globally.
37. Foundation, B.L. *What is COPD*. 2019 [cited 2019 13/08/19]; Available from: https://www.blf.org.uk/support-for-you/copd/what-is-copd.
38. Celli, B.R., W. MacNee, and A.E.T. Force, *Standards for the diagnosis and treatment of patients with COPD: a summary of the ATS/ERS position paper.* Eur Respir J, 2004. **23**(6): p. 932-46.
39. Barnes, P.J., et al., *Pulmonary Biomarkers in Chronic Obstructive Pulmonary Disease.* American Journal of Respiratory and Critical Care Medicine, 2006. **174**(1): p. 6-14.
40. Ntritsos, G., et al., *Gender-specific estimates of COPD prevalence: a systematic review and meta-analysis.* Int J Chron Obstruct Pulmon Dis, 2018. **13**: p. 1507-1514.
41. Meek, P.M., et al., *Chronic Bronchitis Is Associated With Worse Symptoms and Quality of Life Than Chronic Airflow Obstruction.* Chest, 2015. **148**(2): p. 408-16.
42. Snider, G.L., et al., *The Definition of Emphysema.* American Review of Respiratory Disease, 1985. **132**(1): p. 182-185.
43. Ghattas, C., T.J. Barreiro, and D.J. Gemmel, *Giant bullae emphysema.* Lung, 2013. **191**(5): p. 573-4.
44. Mithieux, S.M. and A.S. Weiss, *Elastin*, in *Advances in Protein Chemistry*. 2005, Academic Press. p. 437-461.

45. Scoditti, E., et al., *Role of Diet in Chronic Obstructive Pulmonary Disease Prevention and Treatment.* Nutrients, 2019. **11**(6).
46. Ojo, O., et al., *Pathological changes in the COPD lung mesenchyme – Novel lessons learned from in vitro and in vivo studies.* Pulm Pharmacol Ther, 2014. **29**(2): p. 121-128.
47. Pugin, J., et al., *The alveolar space is the site of intense inflammatory and profibrotic reactions in the early phase of acute respiratory distress syndrome.* Crit Care Med, 1999. **27**(2): p. 304-12.
48. Pesci, A., et al., *Inflammatory cells and mediators in bronchial lavage of patients with chronic obstructive pulmonary disease.* Eur Respir J, 1998. **12**(2): p. 380-6.
49. Burnett, D., et al., *Neutrophils from subjects with chronic obstructive lung disease show enhanced chemotaxis and extracellular proteolysis.* Lancet, 1987. **2**(8567): p. 1043-6.
50. Senior, R.M., et al., *Human 92- and 72-kilodalton type IV collagenases are elastases.* J Biol Chem, 1991. **266**(12): p. 7870-5.
51. Hogg, J.C., et al., *The Nature of Small-Airway Obstruction in Chronic Obstructive Pulmonary Disease.* New England Journal of Medicine, 2004. **350**(26): p. 2645-2653.
52. Taggart, C.C., et al., *Elastolytic proteases: inflammation resolution and dysregulation in chronic infective lung disease.* Am J Respir Crit Care Med, 2005. **171**(10): p. 1070-6.
53. Helmy, T.A., et al., *Role of C-reactive protein and interleukin-6 in predicting the prognosis of ICU-admitted patients with acute exacerbation of COPD.* Egyptian Journal of Chest Diseases and Tuberculosis, 2014. **63**(4): p. 829-835.
54. Lee, S.H., et al., *Increased expression of vascular endothelial growth factor and hypoxia inducible factor-1α in lung tissue of patients with chronic bronchitis.* Clinical Biochemistry, 2014. **47**(7–8): p. 552-559.
55. Kim, V., et al., *Small airway mucous metaplasia and inflammation in chronic obstructive pulmonary disease.* COPD, 2008. **5**(6): p. 329-38.
56. Mannino, D.M. and A.S. Buist, *Global burden of COPD: risk factors, prevalence, and future trends.* Lancet, 2007. **370**(9589): p. 765-73.
57. Bosse, Y., *Updates on the COPD gene list.* Int J Chron Obstruct Pulmon Dis, 2012. **7**: p. 607-31.
58. Kalfopoulos, M., K. Wetmore, and M.K. ElMallah, *Pathophysiology of Alpha-1 Antitrypsin Lung Disease.* Methods Mol Biol, 2017. **1639**: p. 9-19.
59. Greene, C.M., et al., *α1-Antitrypsin deficiency.* Nat Rev Dis Primers, 2016. **2**: p. 16051.
60. Brøgger, J., et al., *Genetic association between COPD and polymorphisms in TNF, ADRB2 and EPHX1.* European Respiratory Journal, 2006. **27**(4): p. 682.
61. Cheng, S.L., et al., *Genetic polymorphism of epoxide hydrolase and glutathione S-transferase in COPD.* European Respiratory Journal, 2004. **23**(6): p. 818.
62. DeMeo, D.L., et al., *Genetic determinants of emphysema distribution in the national emphysema treatment trial.* Am J Respir Crit Care Med, 2007. **176**(1): p. 42-8.
63. Ho, L.-I., et al., *Polymorphism of the β2-Adrenoceptor in COPD in Chinese Subjects.* Chest, 2001. **120**(5): p. 1493-1499.
64. Yuan, C., et al., *Genetic polymorphism and chronic obstructive pulmonary disease.* International journal of chronic obstructive pulmonary disease, 2017. **12**: p. 1385-1393.
65. Takizawa, H., et al., *Increased expression of transforming growth factor-beta1 in small airway epithelium from tobacco smokers and patients with chronic obstructive pulmonary disease (COPD).* Am J Respir Crit Care Med, 2001. **163**(6): p. 1476-83.
66. Celedón, J.C., et al., *The transforming growth factor-β1 (TGFB1) gene is associated with chronic obstructive pulmonary disease (COPD).* Human Molecular Genetics, 2004. **13**(15): p. 1649-1656.

67. Ogawa, E., et al., *Transforming growth factor-beta1 polymorphisms, airway responsiveness and lung function decline in smokers.* Respir Med, 2007. **101**(5): p. 938-43.
68. Ariel, A., et al., *Inhaled therapies in patients with moderate COPD in clinical practice: current thinking.* Int J Chron Obstruct Pulmon Dis, 2018. **13**: p. 45-56.
69. Sethi, S., et al., *Inflammation in COPD: Implications for Management.* The American Journal of Medicine, 2012. **125**(12): p. 1162-1170.
70. Siddiqui, F.M. and J.M. Diamond, *Lung transplantation for chronic obstructive pulmonary disease: past, present, and future directions.* Curr Opin Pulm Med, 2018. **24**(2): p. 199-204.
71. Fiddler, C. and H. Parfrey, *Diffuse parenchymal lung disease.* Medicine, 2016. **44**(6): p. 359-366.
72. Coultas, D.B., et al., *The epidemiology of interstitial lung diseases.* American Journal of Respiratory and Critical Care Medicine, 1994. **150**(4): p. 967-972.
73. Sgalla, G., A. Biffi, and L. Richeldi, *Idiopathic pulmonary fibrosis: Diagnosis, epidemiology and natural history.* Respirology, 2016. **21**(3): p. 427-437.
74. Tomassetti, S., et al., *The multidisciplinary approach in the diagnosis of idiopathic pulmonary fibrosis: a patient case-based review.* European Respiratory Review, 2015. **24**(135): p. 69.
75. Cottin, V., *Lung biopsy in interstitial lung disease: balancing the risk of surgery and diagnostic uncertainty.* European Respiratory Journal, 2016. **48**(5): p. 1274.
76. Ley, B., H.R. Collard, and T.E. King, *Clinical Course and Prediction of Survival in Idiopathic Pulmonary Fibrosis.* American Journal of Respiratory and Critical Care Medicine, 2011. **183**(4): p. 431-440.
77. Torday, J.S. and V.K. Rehan, *The evolutionary continuum from lung development to homeostasis and repair.* Am J Physiol Lung Cell Mol Physiol, 2007. **292**(3): p. L608-11.
78. Kage, H. and Z. Borok, *EMT and interstitial lung disease: a mysterious relationship.* Curr Opin Pulm Med, 2012. **18**(5): p. 517-23.
79. Glasser, S.W., W.D. Hardie, and J.S. Hagood, *Pathogenesis of Interstitial Lung Disease in Children and Adults.* Pediatr Allergy Immunol Pulmonol, 2010. **23**(1): p. 9-14.
80. Wells, A.U., V. Steen, and G. Valentini, *Pulmonary complications: one of the most challenging complications of systemic sclerosis.* Rheumatology (Oxford), 2009. **48 Suppl 3**: p. iii40-4.
81. Baumgartner, K.B., et al., *Cigarette smoking: a risk factor for idiopathic pulmonary fibrosis.* Am J Respir Crit Care Med, 1997. **155**(1): p. 242-8.
82. Vergnon, J.M., et al., *CRYPTOGENIC FIBROSING ALVEOLITIS AND EPSTEIN-BARR VIRUS: AN ASSOCIATION?* The Lancet. **324**(8406): p. 768-771.
83. Jakab, G.J. and D.J. Bassett, *Influenza virus infection, ozone exposure, and fibrogenesis.* Am Rev Respir Dis, 1990. **141**(5 Pt 1): p. 1307-15.
84. ATS, *Idiopathic Pulmonary Fibrosis: Diagnosis and Treatment.* American Journal of Respiratory and Critical Care Medicine, 2000. **161**(2): p. 646-664.
85. Hesselstrand, R., et al., *The association of antinuclear antibodies with organ involvement and survival in systemic sclerosis.* Rheumatology (Oxford), 2003. **42**(4): p. 534-40.
86. Prasse, A., G. Kayser, and K. Warnatz, *Common variable immunodeficiency-associated granulomatous and interstitial lung disease.* Curr Opin Pulm Med, 2013. **19**(5): p. 503-9.
87. Kalchiem-Dekel, O., et al., *Interstitial Lung Disease and Pulmonary Fibrosis: A Practical Approach for General Medicine Physicians with Focus on the Medical History.* J Clin Med, 2018. **7**(12).
88. Raghu, G., et al., *Treatment of idiopathic pulmonary fibrosis with ambrisentan: a parallel, randomized trial.* Ann Intern Med, 2013. **158**(9): p. 641-9.

89. Brown, A.W., H. Kaya, and S.D. Nathan, *Lung transplantation in IIP: A review.* Respirology, 2016. **21**(7): p. 1173-84.
90. Girgis, R.E. and A. Khaghani, *A global perspective of lung transplantation: Part 1 - Recipient selection and choice of procedure.* Glob Cardiol Sci Pract, 2016. **2016**(1): p. e201605.
91. CFT, *UK Cystic Fibrosis Registry Annual data report 2013*, in *Cystic Fibrosis Reports: United Kingdom*. 2014, Cystic Fibrosis Trust.
92. Kerem, B., et al., *Identification of the cystic fibrosis gene: genetic analysis.* Science, 1989. **245**(4922): p. 1073-1080.
93. Villanueva, G., et al., *Diagnosis and management of cystic fibrosis: summary of NICE guidance.* BMJ, 2017. **359**: p. j4574.
94. Sanders, D.B. and A.K. Fink, *Background and Epidemiology.* Pediatr Clin North Am, 2016. **63**(4): p. 567-84.
95. Trust, C.F., *UK Cystic Fibrosis Registry 2017 Annual Data Report*. 2017.
96. Pilewski, J.M. and R.A. Frizzell, *Role of CFTR in airway disease.* Physiol Rev, 1999. **79**(1 Suppl): p. S215-55.
97. Rafeeq, M.M. and H.A.S. Murad, *Cystic fibrosis: current therapeutic targets and future approaches.* J Transl Med, 2017. **15**(1): p. 84.
98. Orenstein, D.M., G.B. Winnie, and H. Altman, *Cystic fibrosis: a 2002 update.* J Pediatr, 2002. **140**(2): p. 156-64.
99. Boyle, M.P. and K. De Boeck, *A new era in the treatment of cystic fibrosis: correction of the underlying CFTR defect.* Lancet Respir Med, 2013. **1**(2): p. 158-63.
100. BioRender. 2020 [cited 2020; Available from: https://biorender.com/.
101. Quinton, P.M., *Viscosity versus composition in airway pathology.* American Journal of Respiratory and Critical Care Medicine, 1994. **149**(1): p. 6-7.
102. Chmiel, J.F. and P.B. Davis, *State of the Art: Why do the lungs of patients with cystic fibrosis become infected and why can't they clear the infection?* Respiratory Research, 2003. **4**(1): p. 8-8.
103. Bonfield, T.L., M.W. Konstan, and M. Berger, *Altered respiratory epithelial cell cytokine production in cystic fibrosis.* Journal of Allergy and Clinical Immunology, 1999. **104**(1): p. 72-78.
104. Cantin, A.M., et al., *Inflammation in cystic fibrosis lung disease: Pathogenesis and therapy.* J Cyst Fibros, 2015. **14**(4): p. 419-30.
105. Van Goor, F., et al., *Correction of the F508del-CFTR protein processing defect in vitro by the investigational drug VX-809.* Proc Natl Acad Sci U S A, 2011. **108**(46): p. 18843-8.
106. Wainwright, C.E., et al., *Lumacaftor-Ivacaftor in Patients with Cystic Fibrosis Homozygous for Phe508del CFTR.* N Engl J Med, 2015. **373**(3): p. 220-31.
107. Konstan, M.W., *Ibuprofen therapy for cystic fibrosis lung disease: revisited.* Curr Opin Pulm Med, 2008. **14**(6): p. 567-73.
108. Eigen, H., et al., *A multicenter study of alternate-day prednisone therapy in patients with cystic fibrosis. Cystic Fibrosis Foundation Prednisone Trial Group.* J Pediatr, 1995. **126**(4): p. 515-23.
109. Moss, R.B., et al., *Randomized, double-blind, placebo-controlled, dose-escalating study of aerosolized interferon gamma-1b in patients with mild to moderate cystic fibrosis lung disease.* Pediatr Pulmonol, 2005. **39**(3): p. 209-18.
110. McAllister, F., et al., *Role of IL-17A, IL-17F, and the IL-17 receptor in regulating growth-related oncogene-alpha and granulocyte colony-stimulating factor in bronchial epithelium: implications for airway inflammation in cystic fibrosis.* J Immunol, 2005. **175**(1): p. 404-12.
111. Paul, K., et al., *Effect of treatment with dornase alpha on airway inflammation in patients with cystic fibrosis.* Am J Respir Crit Care Med, 2004. **169**(6): p. 719-25.
112. Griese, M., et al., *alpha1-Antitrypsin inhalation reduces airway inflammation in cystic fibrosis patients.* Eur Respir J, 2007. **29**(2): p. 240-50.

113. Chai, C.S., et al., *Clinical phenotypes of COPD and health-related quality of life: a cross-sectional study.* Int J Chron Obstruct Pulmon Dis, 2019. **14**: p. 565-573.
114. Makita, H., et al., *Characterisation of phenotypes based on severity of emphysema in chronic obstructive pulmonary disease.* Thorax, 2007. **62**(11): p. 932-7.
115. Fujimoto, K., et al., *Airway inflammation during stable and acutely exacerbated chronic obstructive pulmonary disease.* European Respiratory Journal, 2005. **25**(4): p. 640-646.
116. Hoffmann-Vold, A.-M., et al., *Endotype–phenotyping may predict a treatment response in progressive fibrosing interstitial lung disease.* EBioMedicine, 2019. **50**: p. 379-386.
117. Kolb, M. and M. Vašáková, *The natural history of progressive fibrosing interstitial lung diseases.* Respiratory Research, 2019. **20**(1): p. 57.
118. Collaco, J.M. and G.R. Cutting, *Update on gene modifiers in cystic fibrosis.* Current opinion in pulmonary medicine, 2008. **14**(6): p. 559-566.
119. Taylor, C., et al., *A novel lung disease phenotype adjusted for mortality attrition for cystic fibrosis genetic modifier studies.* Pediatric pulmonology, 2011. **46**(9): p. 857-869.
120. Saferali, A., et al., *Immunomodulatory function of the cystic fibrosis modifier gene BPIFA1.* PloS one, 2020. **15**(1): p. e0227067-e0227067.
121. Shen, Y., et al., *Clinical Phenotypes and Genotypic Spectrum of Cystic Fibrosis in Chinese Children.* The Journal of Pediatrics, 2016. **171**: p. 269-276.e1.
122. Conrad, D.J. and B.A. Bailey, *Multidimensional Clinical Phenotyping of an Adult Cystic Fibrosis Patient Population.* PLOS ONE, 2015. **10**(3): p. e0122705.
123. Barnes, P.J., *Inflammatory endotypes in COPD.* Allergy, 2019. **74**(7): p. 1249-1256.
124. Gong, J., et al., *Genetic association and transcriptome integration identify contributing genes and tissues at cystic fibrosis modifier loci.* PLoS Genet, 2019. **15**(2): p. e1008007.
125. Takahashi, M., et al., *Imaging of pulmonary emphysema: a pictorial review.* Int J Chron Obstruct Pulmon Dis, 2008. **3**(2): p. 193-204.
126. Finkelstein, R., et al., *Morphometry of small airways in smokers and its relationship to emphysema type and hyperresponsiveness.* Am J Respir Crit Care Med, 1995. **152**(1): p. 267-76.
127. Nuovo, G.J., et al., *The distribution of immunomodulatory cells in the lungs of patients with idiopathic pulmonary fibrosis.* Modern pathology : an official journal of the United States and Canadian Academy of Pathology, Inc, 2012. **25**(3): p. 416-433.
128. Smith, I.E., et al., *Chronic sputum production: correlations between clinical features and findings on high resolution computed tomographic scanning of the chest.* Thorax, 1996. **51**(9): p. 914-918.
129. Currie, D.C., et al., *Interpretation of bronchograms and chest radiographs in patients with chronic sputum production.* Thorax, 1987. **42**(4): p. 278-284.
130. WEDZICHA, J.A., *The heterogeneity of chronic obstructive pulmonary disease.* Thorax, 2000. **55**(8): p. 631-632.
131. Kristiansen, J.F., et al., *Lobar Quantification by Ventilation/Perfusion SPECT/CT in Patients with Severe Emphysema Undergoing Lung Volume Reduction with Endobronchial Valves.* Respiration, 2019. **98**(3): p. 230-238.
132. Shen, M., et al., *Quantitative Evaluation of Lobar Pulmonary Function of Emphysema Patients with Endobronchial Coils.* Respiration, 2019. **98**(1): p. 70-81.
133. Valipour, A., et al., *Patterns of Emphysema Heterogeneity.* Respiration; international review of thoracic diseases, 2015. **90**(5): p. 402-411.
134. Radiopaedia. 2020 [cited 2020; Available from: https://radiopaedia.org/.
135. Scherer, P.M. and D.L. Chen, *Imaging Pulmonary Inflammation.* Journal of nuclear medicine : official publication, Society of Nuclear Medicine, 2016. **57**(11): p. 1764-1770.

136. Chen, D.L. and D.P. Schuster, *Positron emission tomography with [18F]fluorodeoxyglucose to evaluate neutrophil kinetics during acute lung injury.* Am J Physiol Lung Cell Mol Physiol, 2004. **286**(4): p. L834-40.
137. Jones, H.A., et al., *In vivo measurement of neutrophil activity in experimental lung inflammation.* Am J Respir Crit Care Med, 1994. **149**(6): p. 1635-9.
138. Boscá, L., et al., *Metabolic signatures linked to macrophage polarization: from glucose metabolism to oxidative phosphorylation.* Biochem Soc Trans, 2015. **43**(4): p. 740-4.
139. Ramsay, G. and D. Cantrell, *Environmental and metabolic sensors that control T cell biology.* Frontiers in immunology, 2015. **6**: p. 99-99.
140. Chen, D.L., et al., *Increased T cell glucose uptake reflects acute rejection in lung grafts.* American journal of transplantation : official journal of the American Society of Transplantation and the American Society of Transplant Surgeons, 2013. **13**(10): p. 2540-2549.
141. Chen, D.L., et al., *Quantifying Pulmonary Inflammation in Cystic Fibrosis with Positron Emission Tomography.* American Journal of Respiratory and Critical Care Medicine, 2006. **173**(12): p. 1363-1369.
142. Klein, M., et al., *18F-Fluorodeoxyglucose-PET/CT Imaging of Lungs in Patients With Cystic Fibrosis.* Chest, 2009. **136**(5): p. 1220-1228.
143. Chen, D.L., J.J. Atkinson, and T.W. Ferkol, *FDG PET Imaging in Cystic Fibrosis.* Seminars in Nuclear Medicine, 2013. **43**(6): p. 412-419.
144. Weiner, R., P.B. Hoffer, and M.L. Thakur, *Lactoferrin: its role as a Ga-67-binding protein in polymorphonuclear leukocytes.* J Nucl Med, 1981. **22**(1): p. 32-7.
145. Kumar, V. and D.K. Boddeti, *(68)Ga-radiopharmaceuticals for PET imaging of infection and inflammation.* Recent Results Cancer Res, 2013. **194**: p. 189-219.
146. Ruparelia, P., et al., *Quantification of neutrophil migration into the lungs of patients with chronic obstructive pulmonary disease.* Eur J Nucl Med Mol Imaging, 2011. **38**(5): p. 911-9.
147. Borie, R., et al., *Activation of somatostatin receptors attenuates pulmonary fibrosis.* Thorax, 2008. **63**(3): p. 251-8.
148. Ferone, D., et al., *Somatostatin receptor distribution and function in immune system.* Dig Liver Dis, 2004. **36 Suppl 1**: p. S68-77.
149. Jones, H.A., et al., *Kinetics of lung macrophages monitored in vivo following particulate challenge in rabbits.* Toxicol Appl Pharmacol, 2002. **183**(1): p. 46-54.
150. Baharom, F., et al., *Dendritic Cells and Monocytes with Distinct Inflammatory Responses Reside in Lung Mucosa of Healthy Humans.* The Journal of Immunology, 2016. **196**(11): p. 4498.
151. Meyer, K.C. and A. Sharma, *Regional variability of lung inflammation in cystic fibrosis.* Am J Respir Crit Care Med, 1997. **156**(5): p. 1536-40.
152. Gutierrez, J.P., et al., *Interlobar differences in bronchoalveolar lavage fluid from children with cystic fibrosis.* Eur Respir J, 2001. **17**(2): p. 281-6.
153. Battaglia, S., et al., *Differential distribution of inflammatory cells in large and small airways in smokers.* J Clin Pathol, 2007. **60**(8): p. 907-11.
154. Brown, P.S., et al., *Directly sampling the lung of a young child with cystic fibrosis reveals diverse microbiota.* Ann Am Thorac Soc, 2014. **11**(7): p. 1049-55.
155. Zemanick, E.T., et al., *Assessment of airway microbiota and inflammation in cystic fibrosis using multiple sampling methods.* Ann Am Thorac Soc, 2015. **12**(2): p. 221-9.
156. Armstrong, D.A., et al., *Pulmonary microRNA profiling: implications in upper lobe predominant lung disease.* Clin Epigenetics, 2017. **9**: p. 56.
157. McKiernan, P.J. and C.M. Greene, *MicroRNA Dysregulation in Cystic Fibrosis.* Mediators Inflamm, 2015. **2015**: p. 529642.
158. Fabbri, E., et al., *Expression of microRNA-93 and Interleukin-8 during Pseudomonas aeruginosa-mediated induction of proinflammatory responses.* Am J Respir Cell Mol Biol, 2014. **50**(6): p. 1144-55.

159. Oglesby, I.K., et al., *miR-126 is downregulated in cystic fibrosis airway epithelial cells and regulates TOM1 expression.* J Immunol, 2010. **184**(4): p. 1702-9.
160. Jasper, A.E., et al., *Understanding the role of neutrophils in chronic inflammatory airway disease.* F1000Research, 2019. **8**: p. F1000 Faculty Rev-557.
161. Misharin, A.V., et al., *Flow cytometric analysis of macrophages and dendritic cell subsets in the mouse lung.* American journal of respiratory cell and molecular biology, 2013. **49**(4): p. 503-510.
162. Groot, L.E.S.d., et al., *Oxidative stress and macrophages: driving forces behind exacerbations of asthma and chronic obstructive pulmonary disease?* American Journal of Physiology-Lung Cellular and Molecular Physiology, 2019. **316**(2): p. L369-L384.
163. Lai, N.-L., et al., *Risk Factors and Changes of Peripheral NK and T Cells in Pulmonary Interstitial Fibrosis of Patients with Rheumatoid Arthritis.* Canadian respiratory journal, 2019. **2019**: p. 7262065-7262065.
164. Acanfora, D., et al., *Relative lymphocyte count as an indicator of 3-year mortality in elderly people with severe COPD.* BMC pulmonary medicine, 2018. **18**(1): p. 116-116.
165. Raman, P., et al., *Development and validation of automated 2D-3D bronchial airway matching to track changes in regional bronchial morphology using serial low-dose chest CT scans in children with chronic lung disease.* J Digit Imaging, 2010. **23**(6): p. 744-54.
166. Leaker, B.R., et al., *Bronchoabsorption; a novel bronchoscopic technique to improve biomarker sampling of the airway.* Respir Res, 2015. **16**: p. 102.
167. Rose, A.S. and K.S. Knox, *Bronchoalveolar lavage as a research tool.* Semin Respir Crit Care Med, 2007. **28**(5): p. 561-73.
168. ATS, *Clinical Role of Bronchoalveolar Lavage in Adults with Pulmonary Disease.* American Review of Respiratory Disease, 1990. **142**(2): p. 481-486.
169. Patel, P.H., M. Antoine, and S. Ullah, *Bronchoalveolar Lavage*, in *StatPearls*. 2019: Treasure Island (FL).
170. Löfdahl, J.M., et al., *Bronchoalveolar lavage in COPD: fluid recovery correlates with the degree of emphysema.* European Respiratory Journal, 2005. **25**(2): p. 275.
171. Du Rand, I.A., et al., *British Thoracic Society guideline for diagnostic flexible bronchoscopy in adults: accredited by NICE.* Thorax, 2013. **68**(Suppl 1): p. i1.
172. Jeffery, P., S. Holgate, and S. Wenzel, *Methods for the assessment of endobronchial biopsies in clinical research: application to studies of pathogenesis and the effects of treatment.* Am J Respir Crit Care Med, 2003. **168**(6 Pt 2): p. S1-17.
173. Shimizu, T., et al., *Isolation and immunophenotyping of mononuclear cells from human lung tissue.* Intern Med, 2007. **46**(4): p. 163-9.
174. Demedts, I.K., et al., *Identification and characterization of human pulmonary dendritic cells.* Am J Respir Cell Mol Biol, 2005. **32**(3): p. 177-84.
175. Baharom, F., et al., *Dendritic Cells and Monocytes with Distinct Inflammatory Responses Reside in Lung Mucosa of Healthy Humans.* J Immunol, 2016. **196**(11): p. 4498-509.
176. Rutgers, S., et al., *Comparison of induced sputum with bronchial wash, bronchoalveolar lavage and bronchial biopsies in COPD.* European Respiratory Journal, 2000. **15**(1): p. 109-115.
177. O'Donnell, R., et al., *Inflammatory cells in the airways in COPD.* Thorax, 2006. **61**(5): p. 448.
178. Reimann, S., et al., *Increased S100A4 expression in the vasculature of human COPD lungs and murine model of smoke-induced emphysema.* Respiratory Research, 2015. **16**: p. 127.
179. Mets, O.M., et al., *Emphysema Is Common in Lungs of Cystic Fibrosis Lung Transplantation Patients: A Histopathological and Computed Tomography Study.* PLoS ONE, 2015. **10**(6): p. e0128062.

180. Deslee, G., et al., *Oxidative damage to nucleic acids in severe emphysema.* Chest, 2009. **135**(4): p. 965-74.
181. Jewell, N.P., *Natural history of diseases: Statistical designs and issues.* Clin Pharmacol Ther, 2016. **100**(4): p. 353-61.
182. Rabe, K.F., et al., *Global strategy for the diagnosis, management, and prevention of chronic obstructive pulmonary disease: GOLD executive summary.* Am J Respir Crit Care Med, 2007. **176**(6): p. 532-55.
183. Seach, N., et al., *Purified enzymes improve isolation and characterization of the adult thymic epithelium.* Journal of Immunological Methods, 2012. **385**(1–2): p. 23-34.
184. Fogli, L.K., et al., *T cell-derived IL-17 mediates epithelial changes in the airway and drives pulmonary neutrophilia.* J Immunol, 2013. **191**(6): p. 3100-11.
185. Goodyear, A., et al., *MyD88-Dependent Recruitment of Monocytes and Dendritic Cells Required for Protection from Pulmonary Burkholderia mallei Infection.* Infection and Immunity, 2012. **80**(1): p. 110-120.
186. Li, D., et al., *IL-33 promotes ST2-dependent lung fibrosis by the induction of alternatively activated macrophages and innate lymphoid cells in mice.* Journal of Allergy and Clinical Immunology, 2014. **134**(6): p. 1422-1432.e11.
187. Wedzicha, J.A., *The heterogeneity of chronic obstructive pulmonary disease.* Thorax, 2000. **55**(8): p. 631.
188. Friedman, P.J., I.R. Harwood, and P.H. Ellenbogen, *Pulmonary cystic fibrosis in the adult: early and late radiologic findings with pathologic correlations.* American Journal of Roentgenology, 1981. **136**(6): p. 1131-1144.
189. Pesci, A., et al., *Inflammatory cells and mediators in bronchial lavage of patients with chronic obstructive pulmonary disease.* European Respiratory Journal, 1998. **12**(2): p. 380.
190. Freeman, C.M., et al., *Cytotoxic Potential of Lung CD8⁺ T Cells Increases with Chronic Obstructive Pulmonary Disease Severity and with In Vitro Stimulation by IL-18 or IL-15.* The Journal of Immunology, 2010. **184**(11): p. 6504.
191. Utokaparch, S., et al., *Respiratory Viral Detection and Small Airway Inflammation in Lung Tissue of Patients with Stable, Mild COPD.* COPD: Journal of Chronic Obstructive Pulmonary Disease, 2014. **11**(2): p. 197-203.
192. Nemec, S.F., A.A. Bankier, and R.L. Eisenberg, *Upper Lobe–Predominant Diseases of the Lung.* American Journal of Roentgenology, 2013. **200**(3): p. W222-W237.
193. West, J.B., *Regional differences in gas exchange in the lung of erect man.* J Appl Physiol, 1962. **17**: p. 893-8.
194. Pabst, R. and T. Tschernig, *Perivascular capillaries in the lung: an important but neglected vascular bed in immune reactions?* J Allergy Clin Immunol, 2002. **110**(2): p. 209-14.
195. Doerschuk, C.M., *Leukocyte trafficking in alveoli and airway passages.* Respir Res, 2000. **1**(3): p. 136-40.
196. Luettig, B., et al., *Naive and memory T cells migrate in comparable numbers through the normal rat lung: only effector T cells accumulate and proliferate in the lamina propria of the bronchi.* Am J Respir Cell Mol Biol, 2001. **25**(1): p. 69-77.
197. Kuebler, W.M., G.E. Kuhnle, and A.E. Goetz, *Leukocyte margination in alveolar capillaries: interrelationship with functional capillary geometry and microhemodynamics.* J Vasc Res, 1999. **36**(4): p. 282-8.
198. Doerschuk, C.M., *Mechanisms of leukocyte sequestration in inflamed lungs.* Microcirculation, 2001. **8**(2): p. 71-88.
199. Kuhnle, G.E., et al., *Effect of blood flow on the leukocyte-endothelium interaction in pulmonary microvessels.* Am J Respir Crit Care Med, 1995. **152**(4 Pt 1): p. 1221-8.
200. West, J.B., *Regional differences in the lung.* Postgrad Med J, 1968. **44**(507): p. 120-2.
201. He, W., et al., *Circadian Expression of Migratory Factors Establishes Lineage-Specific Signatures that Guide the Homing of Leukocyte Subsets to Tissues.* Immunity, 2018. **49**(6): p. 1175-1190 e7.

202. Pick, R., et al., *Time-of-Day-Dependent Trafficking and Function of Leukocyte Subsets.* Trends Immunol, 2019. **40**(6): p. 524-537.
203. Casanova-Acebes, M., et al., *Neutrophils instruct homeostatic and pathological states in naive tissues.* J Exp Med, 2018. **215**(11): p. 2778-2795.
204. Asimakopoulos, G., et al., *Leukocyte integrin expression in patients undergoing cardiopulmonary bypass.* Ann Thorac Surg, 2000. **69**(4): p. 1192-7.
205. Kalawski, R., et al., *Soluble adhesion molecules in reperfusion during coronary bypass grafting.* Eur J Cardiothorac Surg, 1998. **14**(3): p. 290-5.
206. Invernizzi, R. and P.L. Molyneaux, *The contribution of infection and the respiratory microbiome in acute exacerbations of idiopathic pulmonary fibrosis.* European Respiratory Review, 2019. **28**(152): p. 190045.
207. Richardson, M., P. Bowyer, and R. Sabino, *The human lung and Aspergillus: You are what you breathe in?* Medical mycology, 2019. **57**(Supplement_2): p. S145-S154.
208. Erb-Downward, J.R., et al., *Analysis of the Lung Microbiome in the "Healthy" Smoker and in COPD.* PLOS ONE, 2011. **6**(2): p. e16384.
209. Tam, A., et al., *Sex Differences in Airway Remodeling in a Mouse Model of Chronic Obstructive Pulmonary Disease.* Am J Respir Crit Care Med, 2016. **193**(8): p. 825-34.
210. Olié, V., et al., *Changes in tobacco-related morbidity and mortality in French women: worrying trends.* European Journal of Public Health, 2019. **30**(2): p. 380-385.
211. Prescott, E., et al., *Gender difference in smoking effects on lung function and risk of hospitalization for COPD: results from a Danish longitudinal population study.* Eur Respir J, 1997. **10**(4): p. 822-7.
212. Tam, A., et al., *The role of female hormones on lung function in chronic lung diseases.* BMC Womens Health, 2011. **11**: p. 24.
213. Tzanakis, N., et al., *Induced sputum CD8+ T-lymphocyte subpopulations in chronic obstructive pulmonary disease.* Respir Med, 2004. **98**(1): p. 57-65.
214. Sullivan, A.K., et al., *Oligoclonal CD4+ T cells in the lungs of patients with severe emphysema.* American journal of respiratory and critical care medicine, 2005. **172**(5): p. 590-596.
215. Roberts, M.E.P., et al., *CD4+ T-Cell Profiles and Peripheral Blood Ex-Vivo Responses to T-Cell Directed Stimulation Delineate COPD Phenotypes.* Chronic Obstr Pulm Dis, 2015. **2**(4): p. 268-280.
216. Di Stefano, A., et al., *STAT4 activation in smokers and patients with chronic obstructive pulmonary disease.* Eur Respir J, 2004. **24**(1): p. 78-85.
217. Grumelli, S., et al., *An immune basis for lung parenchymal destruction in chronic obstructive pulmonary disease and emphysema.* PLoS medicine, 2004. **1**(1): p. e8-e8.
218. Mantovani, A., et al., *Neutrophils in the activation and regulation of innate and adaptive immunity.* Nature Reviews Immunology, 2011. **11**(8): p. 519-531.
219. Bedi, P., et al., *Blood Neutrophils Are Reprogrammed in Bronchiectasis.* Am J Respir Crit Care Med, 2018. **198**(7): p. 880-890.
220. Brach, M.A., et al., *Prolongation of survival of human polymorphonuclear neutrophils by granulocyte-macrophage colony-stimulating factor is caused by inhibition of programmed cell death.* Blood, 1992. **80**(11): p. 2920-4.
221. Khan M., B.S., Murray I., et al., *Physiology, Pulmonary Vasoconstriction.* 2020, Treasure Island: StatsPearls Publishing.
222. Joppa, P., et al., *Systemic inflammation in patients with COPD and pulmonary hypertension.* Chest, 2006. **130**(2): p. 326-33.
223. Kwon, Y.S., et al., *Plasma C-reactive protein and endothelin-1 level in patients with chronic obstructive pulmonary disease and pulmonary hypertension.* Journal of Korean medical science, 2010. **25**(10): p. 1487-1491.
224. Peinado, V.I., et al., *Inflammatory reaction in pulmonary muscular arteries of patients with mild chronic obstructive pulmonary disease.* Am J Respir Crit Care Med, 1999. **159**(5 Pt 1): p. 1605-11.

225. Kondelkova, K., et al., *Regulatory T cells (TREG) and their roles in immune system with respect to immunopathological disorders.* Acta Medica (Hradec Kralove), 2010. **53**(2): p. 73-7.
226. Ugor, E., et al., *Increased proportions of functionally impaired regulatory T cell subsets in systemic sclerosis.* Clin Immunol, 2017. **184**: p. 54-62.
227. Frantz, C., et al., *Regulatory T Cells in Systemic Sclerosis.* Front Immunol, 2018. **9**: p. 2356.
228. Plantier, L., et al., *Physiology of the lung in idiopathic pulmonary fibrosis.* Eur Respir Rev, 2018. **27**(147).
229. Garcia, J.G., et al., *Assessment of interlobar variation of bronchoalveolar lavage cellular differentials in interstitial lung diseases.* The American review of respiratory disease, 1986. **133**(3): p. 444-449.
230. Wells, A.U. and N. Hirani, *Interstitial lung disease guideline.* Thorax, 2008. **63**(Suppl 5): p. v1.
231. Wynn, T.A. and K.M. Vannella, *Macrophages in Tissue Repair, Regeneration, and Fibrosis.* Immunity, 2016. **44**(3): p. 450-462.
232. Wollin, L., et al., *Mode of action of nintedanib in the treatment of idiopathic pulmonary fibrosis.* European Respiratory Journal, 2015. **45**(5): p. 1434-1445.
233. Datta, A., C.J. Scotton, and R.C. Chambers, *Novel therapeutic approaches for pulmonary fibrosis.* British journal of pharmacology, 2011. **163**(1): p. 141-172.
234. Schaefer, C.J., et al., *Antifibrotic activities of pirfenidone in animal models.* Eur Respir Rev, 2011. **20**(120): p. 85-97.
235. Iyer, S.N., D.M. Hyde, and S.N. Giri, *Anti-Inflammatory Effect of Pirfenidone in the Bleomycin-Hamster Model of Lung Inflammation.* Inflammation, 2000. **24**(5): p. 477-491.
236. Margaroli, C. and R. Tirouvanziam, *Neutrophil plasticity enables the development of pathological microenvironments: implications for cystic fibrosis airway disease.* Mol Cell Pediatr, 2016. **3**(1): p. 38.
237. Fritzsching, B., et al., *Hypoxic epithelial necrosis triggers neutrophilic inflammation via IL-1 receptor signaling in cystic fibrosis lung disease.* Am J Respir Crit Care Med, 2015. **191**(8): p. 902-13.
238. Wu, Y., I. Klapper, and P.S. Stewart, *Hypoxia arising from concerted oxygen consumption by neutrophils and microorganisms in biofilms.* Pathog Dis, 2018. **76**(4).
239. Bruscia, E.M. and T.L. Bonfield, *Cystic Fibrosis Lung Immunity: The Role of the Macrophage.* Journal of innate immunity, 2016. **8**(6): p. 550-563.
240. Perrem, L. and F. Ratjen, *Anti-inflammatories and mucociliary clearance therapies in the age of CFTR modulators.* Pediatr Pulmonol, 2019. **54 Suppl 3**: p. S46-s55.
241. Willner, D., et al., *Spatial distribution of microbial communities in the cystic fibrosis lung.* Isme j, 2012. **6**(2): p. 471-4.
242. Rudkjøbing, V.B., et al., *The microorganisms in chronically infected end-stage and non-end-stage cystic fibrosis patients.* FEMS Immunol Med Microbiol, 2012. **65**(2): p. 236-44.
243. Kramann, R., D.P. DiRocco, and B.D. Humphreys, *Understanding the origin, activation and regulation of matrix-producing myofibroblasts for treatment of fibrotic disease.* J Pathol, 2013. **231**(3): p. 273-89.
244. Enomoto, N., et al., *Quantitative analysis of fibroblastic foci in usual interstitial pneumonia.* Chest, 2006. **130**(1): p. 22-9.
245. Hsu, E., et al., *Lung tissues in patients with systemic sclerosis have gene expression patterns unique to pulmonary fibrosis and pulmonary hypertension.* Arthritis Rheum, 2011. **63**(3): p. 783-94.
246. Bagnato, G. and S. Harari, *Cellular interactions in the pathogenesis of interstitial lung diseases.* Eur Respir Rev, 2015. **24**(135): p. 102-14.
247. Kotsianidis, I., et al., *Global impairment of CD4+CD25+FOXP3+ regulatory T cells in idiopathic pulmonary fibrosis.* Am J Respir Crit Care Med, 2009. **179**(12): p. 1121-30.

248. Xue, J., et al., *Plasma B Lymphocyte Stimulator and B Cell Differentiation in Idiopathic Pulmonary Fibrosis Patients.* The Journal of Immunology, 2013. **191**(5): p. 2089.
249. Brown, J.M., et al., *Silica-directed mast cell activation is enhanced by scavenger receptors.* Am J Respir Cell Mol Biol, 2007. **36**(1): p. 43-52.
250. Prasse, A., et al., *A vicious circle of alveolar macrophages and fibroblasts perpetuates pulmonary fibrosis via CCL18.* Am J Respir Crit Care Med, 2006. **173**(7): p. 781-92.
251. Ziegler-Heitbrock, L., et al., *Nomenclature of monocytes and dendritic cells in blood.* Blood, 2010. **116**(16): p. e74.
252. Wong, K.L., et al., *The three human monocyte subsets: implications for health and disease.* Immunol Res, 2012. **53**(1-3): p. 41-57.
253. Idzkowska, E., et al., *The Role of Different Monocyte Subsets in the Pathogenesis of Atherosclerosis and Acute Coronary Syndromes.* Scandinavian Journal of Immunology, 2015. **82**(3): p. 163-173.
254. Zawada, A.M., et al., *SuperSAGE evidence for CD14++CD16+ monocytes as a third monocyte subset.* Blood, 2011. **118**(12): p. e50-61.
255. Skrzeczynska-Moncznik, J., et al., *Peripheral blood CD14high CD16+ monocytes are main producers of IL-10.* Scand J Immunol, 2008. **67**(2): p. 152-9.
256. Antoniades, H.N., et al., *Expression of monocyte chemoattractant protein 1 mRNA in human idiopathic pulmonary fibrosis.* Proc Natl Acad Sci U S A, 1992. **89**(12): p. 5371-5.
257. Iyonaga, K., et al., *Monocyte chemoattractant protein-1 in idiopathic pulmonary fibrosis and other interstitial lung diseases.* Hum Pathol, 1994. **25**(5): p. 455-63.
258. Doherty, D.E., et al., *Prolonged monocyte accumulation in the lung during bleomycin-induced pulmonary fibrosis. A noninvasive assessment of monocyte kinetics by scintigraphy.* Lab Invest, 1992. **66**(2): p. 231-42.
259. Zickus, C., et al., *Differential regulation of C-C chemokines during fibroblast-monocyte interactions: adhesion vs. inflammatory cytokine pathways.* Mediators Inflamm, 1998. **7**(4): p. 269-74.
260. Ziegler-Heitbrock, L., *Blood Monocytes and Their Subsets: Established Features and Open Questions.* Front Immunol, 2015. **6**: p. 423.
261. Ginhoux, F. and S. Jung, *Monocytes and macrophages: developmental pathways and tissue homeostasis.* Nature Reviews Immunology, 2014. **14**: p. 392.
262. Jakubzick, C., et al., *Minimal differentiation of classical monocytes as they survey steady-state tissues and transport antigen to lymph nodes.* Immunity, 2013. **39**(3): p. 599-610.
263. Jakubzick, C.V., G.J. Randolph, and P.M. Henson, *Monocyte differentiation and antigen-presenting functions.* Nature Reviews Immunology, 2017. **17**: p. 349.
264. Hashimoto, D., et al., *Tissue-resident macrophages self-maintain locally throughout adult life with minimal contribution from circulating monocytes.* Immunity, 2013. **38**(4): p. 792-804.
265. van Furth, R. and Z.A. Cohn, *The origin and kinetics of mononuclear phagocytes.* J Exp Med, 1968. **128**(3): p. 415-35.
266. Gibbons, M.A., et al., *Ly6Chi monocytes direct alternatively activated profibrotic macrophage regulation of lung fibrosis.* Am J Respir Crit Care Med, 2011. **184**(5): p. 569-81.
267. Misharin, A.V., et al., *Monocyte-derived alveolar macrophages drive lung fibrosis and persist in the lung over the life span.* The Journal of Experimental Medicine, 2017. **214**(8): p. 2387.
268. Aran, D., et al., *Reference-based analysis of lung single-cell sequencing reveals a transitional profibrotic macrophage.* Nature Immunology, 2019. **20**(2): p. 163-172.
269. Njoroge, J.M., et al., *Characterization of viable autofluorescent macrophages among cultured peripheral blood mononuclear cells.* Cytometry, 2001. **44**(1): p. 38-44.

270. Trombetta, A.C., et al., *A circulating cell population showing both M1 and M2 monocyte/macrophage surface markers characterizes systemic sclerosis patients with lung involvement.* Respir Res, 2018. **19**(1): p. 186.
271. Scott, M.K.D., et al., *Increased monocyte count as a cellular biomarker for poor outcomes in fibrotic diseases: a retrospective, multicentre cohort study.* Lancet Respir Med, 2019. **7**(6): p. 497-508.
272. O'Dwyer, D.N. and B.B. Moore, *Ironing Out the Roles of Macrophages in Idiopathic Pulmonary Fibrosis.* Am J Respir Crit Care Med, 2019. **200**(2): p. 127-129.
273. Misharin, A.V., et al., *Monocyte-derived alveolar macrophages drive lung fibrosis and persist in the lung over the life span.* J Exp Med, 2017. **214**(8): p. 2387-2404.
274. Kapellos, T.S., et al., *Human Monocyte Subsets and Phenotypes in Major Chronic Inflammatory Diseases.* Front Immunol, 2019. **10**: p. 2035.
275. Moore, B.B., et al., *Inflammatory leukocyte phenotypes correlate with disease progression in idiopathic pulmonary fibrosis.* Front Med, 2014. **1**(56).
276. Liu, Y.Z., et al., *Proportions of resting memory T cells and monocytes in blood have prognostic significance in idiopathic pulmonary fibrosis.* Genomics, 2019. **111**(6): p. 1343-1350.
277. Passlick, B., D. Flieger, and H.W. Ziegler-Heitbrock, *Identification and characterization of a novel monocyte subpopulation in human peripheral blood.* Blood, 1989. **74**(7): p. 2527-34.
278. Wong, K.L., et al., *Gene expression profiling reveals the defining features of the classical, intermediate, and nonclassical human monocyte subsets.* Blood, 2011. **118**(5): p. e16-31.
279. Hijdra, D., et al., *Phenotypic characterization of human intermediate monocytes.* Front Immunol, 2013. **4**: p. 339.
280. Moniuszko, M., et al., *Enhanced frequencies of CD14++CD16+, but not CD14+CD16+, peripheral blood monocytes in severe asthmatic patients.* Clin Immunol, 2009. **130**(3): p. 338-46.
281. Rossol, M., et al., *The CD14(bright) CD16+ monocyte subset is expanded in rheumatoid arthritis and promotes expansion of the Th17 cell population.* Arthritis Rheum, 2012. **64**(3): p. 671-7.
282. Liaskou, E., et al., *Monocyte subsets in human liver disease show distinct phenotypic and functional characteristics.* Hepatology, 2013. **57**(1): p. 385-98.
283. Auffray, C., et al., *Monitoring of Blood Vessels and Tissues by a Population of Monocytes with Patrolling Behavior.* Science, 2007. **317**(5838): p. 666.
284. Thomas, G., et al., *Nonclassical patrolling monocyte function in the vasculature.* Arterioscler Thromb Vasc Biol, 2015. **35**(6): p. 1306-16.
285. Misharin, A.V., et al., *Nonclassical Ly6C(-) monocytes drive the development of inflammatory arthritis in mice.* Cell Rep, 2014. **9**(2): p. 591-604.
286. Krychtiuk, K.A., et al., *Small high-density lipoprotein is associated with monocyte subsets in stable coronary artery disease.* Atherosclerosis, 2014. **237**(2): p. 589-96.
287. Greiffo, F., et al., *Circulating monocytes from interstitial lung disease patients show an activated phenotype.* European Respiratory Journal, 2016. **48**(suppl 60): p. PA3894.
288. O'Donnell, E.A., D.N. Ernst, and R. Hingorani, *Multiparameter flow cytometry: advances in high resolution analysis.* Immune Netw, 2013. **13**(2): p. 43-54.
289. Ornatsky, O., et al., *Highly multiparametric analysis by mass cytometry.* J Immunol Methods, 2010. **361**(1-2): p. 1-20.
290. Yao, Y., et al., *CyTOF supports efficient detection of immune cell subsets from small samples.* J Immunol Methods, 2014. **415**: p. 1-5.
291. Spitzer, M.H. and G.P. Nolan, *Mass Cytometry: Single Cells, Many Features.* Cell, 2016. **165**(4): p. 780-91.
292. Bjornson, Z.B., G.P. Nolan, and W.J. Fantl, *Single-cell mass cytometry for analysis of immune system functional states.* Curr Opin Immunol, 2013. **25**(4): p. 484-94.

293. Krams, S.M., et al., *Applying Mass Cytometry to the Analysis of Lymphoid Populations in Transplantation.* American Journal of Transplantation, 2017. **17**(8): p. 1992-1999.
294. Cosgrove, G.P., et al., *Barriers to timely diagnosis of interstitial lung disease in the real world: the INTENSITY survey.* BMC Pulm Med, 2018. **18**(1): p. 9.
295. Gadalla, R., et al., *Validation of CyTOF Against Flow Cytometry for Immunological Studies and Monitoring of Human Cancer Clinical Trials.* Frontiers in Oncology, 2019. **9**(415).
296. Gondhalekar, C., et al., *Alternatives to current flow cytometry data analysis for clinical and research studies.* Methods, 2018. **134-135**: p. 113-129.
297. Korin, B., et al., *High-dimensional, single-cell characterization of the brain's immune compartment.* Nat Neurosci, 2017. **20**(9): p. 1300-1309.
298. Yao, Y., et al., *Multiparameter Single Cell Profiling of Airway Inflammatory Cells.* Cytometry B Clin Cytom, 2017. **92**(1): p. 12-20.
299. Leelatian, N., et al., *Single cell analysis of human tissues and solid tumors with mass cytometry.* Cytometry B Clin Cytom, 2017. **92**(1): p. 68-78.
300. Kay, A.W., D.M. Strauss-Albee, and C.A. Blish, *Application of Mass Cytometry (CyTOF) for Functional and Phenotypic Analysis of Natural Killer Cells.* Methods Mol Biol, 2016. **1441**: p. 13-26.
301. Lin, D. and H.T. Maecker, *Mass Cytometry Assays for Antigen-Specific T Cells Using CyTOF.* Methods Mol Biol, 2018. **1678**: p. 37-47.
302. See, P., et al., *Mapping the human DC lineage through the integration of high-dimensional techniques.* Science, 2017. **356**(6342).
303. Lay, J.C., D.B. Peden, and N.E. Alexis, *Flow cytometry of sputum: assessing inflammation and immune response elements in the bronchial airways.* Inhal Toxicol, 2011. **23**(7): p. 392-406.
304. Lafferty, K.J. and A.J. Cunningham, *A new analysis of allogeneic interactions.* Aust J Exp Biol Med Sci, 1975. **53**(1): p. 27-42.
305. Guo, Y. and A.Y. Wang, *Novel immune check-point regulators in tolerance maintenance.* Frontiers in Immunology, 2015. **6**.
306. Chen, L., *Co-inhibitory molecules of the B7-CD28 family in the control of T-cell immunity.* Nat Rev Immunol, 2004. **4**(5): p. 336-347.
307. Symington, F.W., W. Brady, and P.S. Linsley, *Expression and function of B7 on human epidermal Langerhans cells.* J Immunol, 1993. **150**(4): p. 1286-95.
308. Balzano, C., et al., *CTLA-4 and CD28: similar proteins, neighbouring genes.* Int J Cancer Suppl, 1992. **7**: p. 28-32.
309. June, C.H., et al., *Role of the CD28 receptor in T-cell activation.* Immunol Today, 1990. **11**(6): p. 211-6.
310. Linsley, P.S., et al., *Immunosuppression in vivo by a soluble form of the CTLA-4 T cell activation molecule.* Science, 1992. **257**(5071): p. 792-5.
311. Inaba, K., et al., *The tissue distribution of the B7-2 costimulator in mice: abundant expression on dendritic cells in situ and during maturation in vitro.* J Exp Med, 1994. **180**(5): p. 1849-60.
312. Lenschow, D.J., et al., *Differential up-regulation of the B7-1 and B7-2 costimulatory molecules after Ig receptor engagement by antigen.* J Immunol, 1994. **153**(5): p. 1990-7.
313. Hutloff, A., et al., *ICOS is an inducible T-cell co-stimulator structurally and functionally related to CD28.* Nature, 1999. **397**(6716): p. 263-6.
314. Ito, T., et al., *Plasmacytoid dendritic cells prime IL-10-producing T regulatory cells by inducible costimulator ligand.* J Exp Med, 2007. **204**(1): p. 105-15.
315. Latchman, Y., et al., *PD-L2 is a second ligand for PD-1 and inhibits T cell activation.* Nat Immunol, 2001. **2**(3): p. 261-8.
316. Yang, H., et al., *Correlation Between PD-L2 Expression and Clinical Outcome in Solid Cancer Patients: A Meta-Analysis.* Frontiers in Oncology, 2019. **9**(47).

317. Picarda, E., K.C. Ohaegbulam, and X. Zang, *Molecular Pathways: Targeting B7-H3 (CD276) for Human Cancer Immunotherapy.* Clin Cancer Res, 2016. **22**(14): p. 3425-31.
318. Chapoval, A.I., et al., *B7-H3: a costimulatory molecule for T cell activation and IFN-gamma production.* Nat Immunol, 2001. **2**(3): p. 269-74.
319. Ling, V., et al., *Duplication of primate and rodent B7-H3 immunoglobulin V- and C-like domains: divergent history of functional redundancy and exon loss.* Genomics, 2003. **82**(3): p. 365-77.
320. Villadolid, J. and A. Amin, *Immune checkpoint inhibitors in clinical practice: update on management of immune-related toxicities.* Translational Lung Cancer Research, 2015. **4**(5): p. 560-575.
321. Robert, C., et al., *Ipilimumab plus dacarbazine for previously untreated metastatic melanoma.* N Engl J Med, 2011. **364**(26): p. 2517-26.
322. Srivastava, N. and D. McDermott, *Update on benefit of immunotherapy and targeted therapy in melanoma: the changing landscape.* Cancer Manag Res, 2014. **6**: p. 279-89.
323. Sharon, E., et al., *Immune checkpoint inhibitors in clinical trials.* Chin J Cancer, 2014. **33**(9): p. 434-44.
324. Hargadon, K.M., C.E. Johnson, and C.J. Williams, *Immune checkpoint blockade therapy for cancer: An overview of FDA-approved immune checkpoint inhibitors.* Int Immunopharmacol, 2018. **62**: p. 29-39.
325. Toyokawa, G., et al., *High Frequency of Programmed Death-ligand 1 Expression in Emphysematous Bullae-associated Lung Adenocarcinomas.* Clin Lung Cancer, 2017. **18**(5): p. 504-511 e1.
326. Kanai, O., et al., *Efficacy and safety of nivolumab in non-small cell lung cancer with preexisting interstitial lung disease.* Thorac Cancer, 2018. **9**(7): p. 847-855.
327. Biton, J., et al., *Impaired Tumor-Infiltrating T Cells in Patients with Chronic Obstructive Pulmonary Disease Impact Lung Cancer Response to PD-1 Blockade.* Am J Respir Crit Care Med, 2018. **198**(7): p. 928-940.
328. Mark, N.M., et al., *Chronic Obstructive Pulmonary Disease Alters Immune Cell Composition and Immune Checkpoint Inhibitor Efficacy in Non-Small Cell Lung Cancer.* Am J Respir Crit Care Med, 2018. **197**(3): p. 325-336.
329. Delaunay, M., et al., *Immune-checkpoint inhibitors associated with interstitial lung disease in cancer patients.* Eur Respir J, 2017. **50**(2).
330. Ahmad, S.M., et al., *PD-L1-specific T cells.* Cancer Immunol Immunother, 2016. **65**(7): p. 797-804.
331. Riva, A. and S. Chokshi, *Immune checkpoint receptors: homeostatic regulators of immunity.* Hepatol Int, 2018. **12**(3): p. 223-236.
332. Ritprajak, P. and M. Azuma, *Intrinsic and extrinsic control of expression of the immunoregulatory molecule PD-L1 in epithelial cells and squamous cell carcinoma.* Oral Oncol, 2015. **51**(3): p. 221-8.
333. Youngnak-Piboonratanakit, P., et al., *The expression of B7-H1 on keratinocytes in chronic inflammatory mucocutaneous disease and its regulatory role.* Immunol Lett, 2004. **94**(3): p. 215-22.
334. Rodig, N., et al., *Endothelial expression of PD-L1 and PD-L2 down-regulates CD8+ T cell activation and cytolysis.* Eur J Immunol, 2003. **33**(11): p. 3117-26.
335. Van de Laar, E., et al., *Cell surface marker profiling of human tracheal basal cells reveals distinct subpopulations, identifies MST1/MSP as a mitogenic signal, and identifies new biomarkers for lung squamous cell carcinomas.* Respiratory Research, 2014. **15**(1): p. 160.
336. Hofmeyer, K.A., A. Ray, and X. Zang, *The contrasting role of B7-H3.* Proceedings of the National Academy of Sciences, 2008. **105**(30): p. 10277.
337. Sakai, N. and A.M. Tager, *Fibrosis of two: Epithelial cell-fibroblast interactions in pulmonary fibrosis.* Biochim Biophys Acta, 2013. **1832**(7): p. 911-21.

338. Zhang, G., et al., *Soluble CD276 (B7-H3) is released from monocytes, dendritic cells and activated T cells and is detectable in normal human serum.* Immunology, 2008. **123**(4): p. 538-46.
339. BLF. *The Battle for Breath*. 2016 [cited 2019 12/08/19]; Available from: https://statistics.blf.org.uk.
340. WHO. *The top 10 causes of death*. Fact Sheets 2018 [cited 2019 12/08/19]; Available from: https://www.who.int/news-room/fact-sheets/detail/the-top-10-causes-of-death.
341. Gee, M.H. and K.H. Albertine, *Neutrophil-endothelial cell interactions in the lung.* Annu Rev Physiol, 1993. **55**: p. 227-48.
342. Lohmann-Matthes, M.L., C. Steinmuller, and G. Franke-Ullmann, *Pulmonary macrophages.* Eur Respir J, 1994. **7**(9): p. 1678-89.
343. Jiang, B., et al., *The co-stimulatory molecule B7-H3 promotes the epithelial-mesenchymal transition in colorectal cancer.* Oncotarget, 2016. **7**(22): p. 31755-71.
344. Dancer, R.C., A.M. Wood, and D.R. Thickett, *Metalloproteinases in idiopathic pulmonary fibrosis.* Eur Respir J, 2011. **38**(6): p. 1461-7.
345. Yoon, B.R., et al., *Functional phenotype of synovial monocytes modulating inflammatory T-cell responses in rheumatoid arthritis (RA).* PLoS One, 2014. **9**(10): p. e109775.
346. DiDomenico, J., et al., *The immune checkpoint protein PD-L1 induces and maintains regulatory T cells in glioblastoma.* Oncoimmunology, 2018. **7**(7): p. e1448329.
347. Peng, X., et al., *CD4+CD25+FoxP3+ Regulatory Tregs inhibit fibrocyte recruitment and fibrosis via suppression of FGF-9 production in the TGF-beta1 exposed murine lung.* Front Pharmacol, 2014. **5**: p. 80.
348. Jiang, N., M. Li, and X. Zeng, *Correlation of Th17 cells and CD4(+)CD25(+) regulatory T cells with clinical parameters in patients with systemic sclerosis.* Chin Med J (Engl), 2014. **127**(20): p. 3557-61.
349. Hector, A., et al., *Regulatory T-cell impairment in cystic fibrosis patients with chronic pseudomonas infection.* Am J Respir Crit Care Med, 2015. **191**(8): p. 914-23.
350. Iannitti, R.G., et al., *Th17/Treg imbalance in murine cystic fibrosis is linked to indoleamine 2,3-dioxygenase deficiency but corrected by kynurenines.* Am J Respir Crit Care Med, 2013. **187**(6): p. 609-20.
351. Tan, H.L., et al., *The Th17 pathway in cystic fibrosis lung disease.* Am J Respir Crit Care Med, 2011. **184**(2): p. 252-8.
352. Lammertyn, E.J., et al., *End-stage cystic fibrosis lung disease is characterised by a diverse inflammatory pattern: an immunohistochemical analysis.* Respir Res, 2017. **18**(1): p. 10.
353. Jernudd-Wilhelmsson, Y., Y. Hörnblad, and G. Hedenstierna, *Ventilation-perfusion relationships in interstitial lung disease.* Eur J Respir Dis, 1986. **68**(1): p. 39-49.
354. Lagerstrand, L., L. Hjelte, and H. Jorulf, *Pulmonary gas exchange in cystic fibrosis: basal status and the effect of i.v. antibiotics and inhaled amiloride.* Eur Respir J, 1999. **14**(3): p. 686-92.
355. Wagner, P.D., et al., *Ventilation-perfusion inequality in chronic obstructive pulmonary disease.* The Journal of clinical investigation, 1977. **59**(2): p. 203-216.
356. Guenthart, B.A., et al., *Regeneration of severely damaged lungs using an interventional cross-circulation platform.* Nat Commun, 2019. **10**(1): p. 1985.
357. Loontiens, S., et al., *Purification of high-quality RNA from a small number of fluorescence activated cell sorted zebrafish cells for RNA sequencing purposes.* BMC Genomics, 2019. **20**(1): p. 228.
358. Shanker, S., et al., *Evaluation of commercially available RNA amplification kits for RNA sequencing using very low input amounts of total RNA.* J Biomol Tech, 2015. **26**(1): p. 4-18.
359. Wijeyekoon, R.S., et al., *Monocyte Function in Parkinson's Disease and the Impact of Autologous Serum on Phagocytosis.* Front Neurol, 2018. **9**: p. 870.

Appendix

Appendix 1. Radiopaedia Citation Details

Appendix Table 1.1 The details of the images in Figure 1.4,(The regional heterogeneity observed in chronic lung disease on domputed tomography (CT), chapter one) sourced from radiopaedia.org

Image	Radiopaedia Reference
Ai	Case courtesy of Dr David Cuete, Radiopaedia.org, rID: 24495
Aii	Case courtesy of Dr Jeremy Jones, Radiopaedia.org, rID: 13441
Aiii	Case courtesy of Dr Augusto César Vieira Teixeira, Radiopaedia.org, rID: 23229
Bi	Case courtesy of Dr David Cuete, Radiopaedia.org, rID: 33436
Bii	Case courtesy of Rogério Augusto Lima Guarneri, Radiopaedia.org, rID: 31651
Biii	Case courtesy of Dr Mohammad Taghi Niknejad, Radiopaedia.org, rID: 21347
Ci	Case courtesy of Dr Bruno Di Muzio, Radiopaedia.org, rID: 58437
Cii	Case courtesy of Radswiki, Radiopaedia.org, rID: 11344
Ciii	Case courtesy of Dr David Cuete, Radiopaedia.org, rID: 29080

Appendix 2 . General Reagents and Consumables

Appendix Table 2.1 The supplier and catalogue number details of the main regents and consumables used throughout the course of the thesis.

Methodology	Reagent	Supplier	Catalogue Number
Flow Cytometry	*Pharm Lyse (10x)*	*Becton Dickinson*	*555899*
	True-Nuclear™ Transcription Factor Buffer Set	*Biolegend*	*424401*
	123count eBeads	*ThermoFisher*	*01-1234-42*
	Dnase	*Sigma-Aldrich*	*D5025-15KU*
	Liberase™ TL	*Sigma-Aldrich*	*05401020001*
	HBSS w/o CA & Mg (1x) *HBSS (1X)*	*Life Technologies*	14170088 24020091
	pluriStrainer® 500µm	*Cambridge Bioscience*	43-50500-50
	Falcon 70µm cell strainer	*Scientific Laboratory Supplies Ltd*	352350
	PBS	*ThermoFisher*	14040133
	Zombie UV™ Fixable Viability Kit	*Biolegend*	423108
	DMSO	*Sigma*	472301-100ML
Luminex/ICM	*Luminex human 12-plex plates*	*Merck*	HCYTOMAG-60K-12
	BCA Protein Assay Kit	*Pierce, Thermo Scientific*	23227
	RIPA Buffer	*Sigma-Aldrich*	R0278-50ML
	Quantibody® Human Immune Checkpoint Molecule Array 1	*RayBiotech*	QAH-ICM-1-4
	cOmplete Protease Inhibitor Cocktail	*Sigma-Aldrich*	11697498001
IHC of ICM	*Anti-PD-L1 (clone 28-8)*	*Abcam*	Ab205921
	OptiView DAB IHC detection kit	*Roche*	760-700
	Anti-B7-H3	*Abcam*	Ab219648
	ultraView Universal DAB	*Roche*	760-500
CyTOF	*FBS HI*	*Fisher Scientific*	10500064
	RMPI-1640	*Thermo Scientific*	R0883
	CD45 MicroBeads	*Miltenyi Biotech*	130-045-801
	LS+ Positive Selection Columns	*Miltenyi Biotech*	130-042-401
	Maxpar® Cell Staining Buffer	*Fluidigm*	201068
	Human TruStain FcX (FC Receptor Blocking Solution	*Biolegend*	422301
	Maxpar® Water	*Fluidigm*	201069
	EQ Four Element Calibration Beads	*Fluidigm*	201078

Appendix 3. Flow Cytometry Antibody Panel

Appendix Table 3.1 The clone, supplier and catalogue number details of the main flow cytometry antibodies used throughout the course of the thesis.

	Antibodies		***Supplier***	***Catalogue Number***
Fluorochrome	**Marker**	**Clone**		
FITC	CD66b	G10F5	*Biolegend*	(BL) 305104
PerCP-efl710	CD8	SK1	*eBioscience*	(eBS) 46-0087-42
Pacific Blue	CD4	SK3	*Biolegend*	344620
BV510	CD45	HI30	*Biolegend*	344620
BV650	CD56	HCD56	*Biolegend*	318344
BV711	CD3	SK7	*Biolegend*	344838
BV785	CD16	3G8	*Biolegend*	302046
Alexa 700	HLA-DR	LN3	*Biolegend*	327014
APC-Cy7	CD14	M5E2	*Biolegend*	301820
PE-Cy5	CD19	HIB19	*Biolegend*	302210
PE-Cy7	CD64	10.1	*Biolegend*	305022
APC	Siglec-8	7C9	*Biolegend*	347106
BV605	CD117	104D2	*Biolegend*	313218
PE	FOXP3	206D	*Biolegend*	320108

Appendix 4. Methodology Protocols

Appendix Table 4.1 The details for methodology protocols used throughout this thesis and any details of modifications to the original source.

Protocol	***Methodology Section***	***Accessed from***	***Modifications***
BioLegend Zombie UV cell viability staining	2.5.2	https://www.biolegend.com/en-us/products/zombie-uv-fixable-viability-kit-9336	Standard cell staining protocol with washes rather than no-wash sequential staining option
BioLegend Intracellular staining protocol	2.5.2	https://www.biolegend.com/protocols/true-nuclear-transcription-factor-staining-protocol-for-5ml-tubes/4267/	As directed, but samples ran within 48h rather than immediately
Lysis of tissue	2.6	https://www.gbiosciences.com/image/pdfs/protocol/786-489_protocol.pdf	Decreased volume of RIPA buffer by half to increase final concentration of protein
BCA protein assay	2.6	https://www.thermofisher.com/document-connect/document-connect.html?url=https%3A%2F%2Fassets.thermofisher.com%2FTFS-Assets%2FLSG%2Fmanuals%2FMAN0011430_Pierce_BCA_Protein_Asy_UG.pdf&title=VXNlciBHdWlkZTogUGllcmNlIEJDQSBQcm90ZWluIEFzc2F5IEtpdA	Microplate protocol rather than test tube option
Luminex assay	2.6	https://www.merckmillipore.com/GB/en/product/MILLIPLEX-MAP-Human-Cytokine-Chemokine-Magnetic-Bead-Panel-Immunology-Multiplex-Assay,MM_NF-HCYTOMAG-60K#anchor_PR	As directed, with samples at a concentration of 1 mg/ml total protein
RayBiotech Immune checkpoint assay	2.8.1	https://doc.raybiotech.com/pdf/Manual/QAH-ICM-1.pdf	As directed, with samples at a concentration of 0.6 mg/ml total protein
Fluidigm Maxpar cell surface staining (CyTOF)	2.9.3	https://www.fluidigm.com/binaries/content/documents/fluidigm/search/resourceTypes/protocol/hippo%3Aresultset/maxpar-cell-surface-staining-400276-pr/fluidigm%3Afile	As directed but with optimised suggestions from the MCCIR biobank. Rhodium 103 was also used in place of Cisplatin for cell viability as this was compatible with the metals used for CD45 conjugation.

Appendix 5. CD4+ to CD8+ T cell ratio in Chronic Obstructive Pulmonary Disease

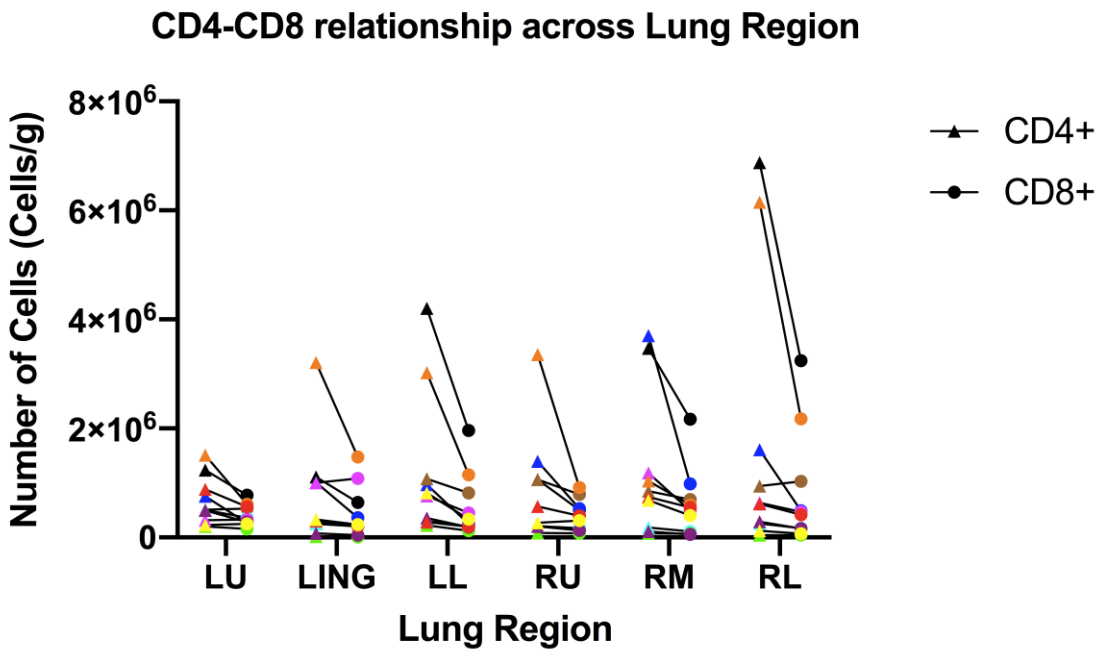

Appendix Figure 5.1. Characterisation of the CD4+ to CD8+ T cell ratio across the chronic obstructive pulmonary disease lung. Each patient in the cohort is characterised by a distinct colour, demonstrating the total CD4+ (triangle) and CD8+ (circle) cell numbers across different regions of their lung (n=10 for all regions except RU, n=9). The lines represent the relationship between the two cell types within the same patient. LTx 61, LTx-80 and LTx-92 (orange, black and blue respectively) were found to have an elevated CD4+ to CD8+ ratio, in areas of increased total T cell number.

Appendix 6. Chapter Three Regional Statistical Summary

Appendix Table 6.1. Statistical analysis summary for leukocyte numerical data from chapter three. Statistical summary of all differences in leukocyte subset numbers between regions for all diseases determined by a generalized estimating equation with Bonferroni post-test correction.

GEE Statistical Analysis (Leukocyte number)			
Disease Cohort	**Leukocyte Subset**	**Overall p value**	**Pairwise post hoc values**
COPD	CD45+	0.054	NA
	CD64+ Macrophages	0.024	LU v LL (0.009) Ling v LL (0.006)
	CD3+ T cells	0.148	NA
	CD19+ B cells	0.028	LU v LL (0.032) Ling v RM (0.004) RM v RL (0.036)
	CD56+ NK cells	<0.001	LU v LL (0.005) Ling v RL (<0.001) RU v RL (0.046)
	CD66b+ Granulocytes	0.203	NA
	CD14+ Monocytes	0.377	NA
CF	CD45+	<0.001	Ling v RM (<0.001)
	CD64+ Macrophages	<0.001	No significant post hoc results
	CD3+ T cells	<0.001	LU v LL (0.016) Ling v LL (<0.001) LL v RM (0.002) LL v RL (0.012)
	CD19+ B cells	0.240	NA
	CD56+ NK cells	<0.001	Ling v LL (0.025) Ling v RM (0.039)
	CD66b+ Granulocytes	<0.001	Ling v RM (<0.001) RM v RL (0.032)
	CD14+ Monocytes	<0.001	Ling v RM (0.022) RU v RL (0.001)
ILD	CD45+	Left; 0.024 Right; 0.008	LU v LL (0.006) RU v RL (0.004)
	CD64+ Macrophages	Left; 0.142 Right; 0.394	NA
	CD3+ T cells	Left; <0.001 Right; <0.001	LU V Ling (<0.001) LU v LL (<0.001) RU v RL (<0.001) RM v RL (0.003)
	CD19+ B cells	Left; 0.750 Right; 0.073	NA
	CD56+ NK cells	Left; <0.001 Right; <0.001	LU V Ling (<0.001) LU v LL (<0.001) RU v RL (<0.001)
	CD66b+ Granulocytes	Left; <0.001 Right; 0.010	LU v LL (<0.001) RU v RL (0.007) RM v RL (0.032)
	CD14+ Monocytes	Left; 0.625 Right; 0.187	NA

Abbreviations: COPD= chronic obstructive pulmonary disease, CF= cystic fibrosis, ILD= interstitial lung disease, LU=left upper, Ling= lingular, LL=left lower, RU= right upper, RM= right middle, RL= right lower, NA= not applicable

Appendix Table 6.2. Statistical analysis summary for percentage of total leukocyte pool data from chapter three. Statistical summary of all differences in leukocyte subset percentage of the total leukocyte pool between regions for all diseases, determined by a generalized estimating equation with Bonferroni post-test correction.

GEE Statistical Analysis (Percentage)			
Disease Cohort	**Leukocyte Subset**	**Overall p value**	**Pairwise post hoc values**
COPD	CD64+ Macrophages	0.015	LU v LL (0.004) Ling v LL (0.034) LL v RM (0.010) LL v RL (0.003)
	CD3+ T cells	0.479	NA
	CD19+ B cells	<0.001	LU v Ling (0.012) LU v RL (0.003) Ling v RU (0.030) Ling v RM (0.005) RU v RL (0.019) RM v RL (<0.001)
	CD56+ NK cells	0.023	No significant post hoc results
	CD66b+ Granulocytes	0.005	Ling v LL (<0.001) Ling v RU (0.005) LL v RL (0.015) RU v RL (0.041)
	CD14+ Monocytes	<0.001	RU v RL (0.022) RM v RL (0.018)
CF	CD64+ Macrophages	0.367	NA
	CD3+ T cells	<0.001	Ling v LL (0.038) LL v RL (0.046)
	CD19+ B cells	0.079	NA
	CD56+ NK cells	<0.001	LL v RM (<0.001) RM v RL (0.018)
	CD66b+ Granulocytes	0.233	NA
	CD14+ Monocytes	<0.001	LU v RM (0.021) LL v RU (0.022) LL v RM (0.012) RU v RM (<0.001) RU v RL (0.001)
ILD	CD64+ Macrophages	Left; 0.034 Right; 0.135	No significant post hoc results
	CD3+ T cells	Left; 0.011 Right; 0.007	LU V Ling (0.008) LU v LL (0.044) Ling v LL (0.004) RU v RL (0.008)
	CD19+ B cells	Left; 0.063 Right; 0.424	NA
	CD56+ NK cells	Left; <0.001 Right; <0.001	LU V Ling (<0.001) LU v LL (<0.001) RU v RL (<0.001)
	CD66b+ Granulocytes	Left; 0.352 Right; 0.695	NA
	CD14+ Monocytes	Left; 0.003 Right; 0.015	LU v Ling (0.001) LU v LL (0.003) RU v RL (0.014)

Abbreviations: COPD= chronic obstructive pulmonary disease, CF= cystic fibrosis, ILD= interstitial lung disease, LU=left upper, Ling= lingular, LL=left lower, RU= right upper, RM= right middle, RL= right lower, NA= not applicable

Appendix 7. Chapter Three Regional Heterogeneity Luminex Data

The concentration of 13 cytokines and chemokines were assessed across different regions of the COPD and ILD lung (n=6, n= left; n=8, right; n=5). The concentrations of interferon gamma (IFNγ) was undetectable for all samples and could not be graphed, whilst granulocyte macrophage colony stimulating factor (GM-CSF), IL-10, IL-12p70, IL-1β, and IL-2 were below the limit of detection (3.2pg/ml) for most samples. IL-12p40, IL-1α, IL-4 and TNFα had detectable levels in more than half the samples. The majority of this data was not reported in the main text, but is included in Appendix Figures 2 and 3.

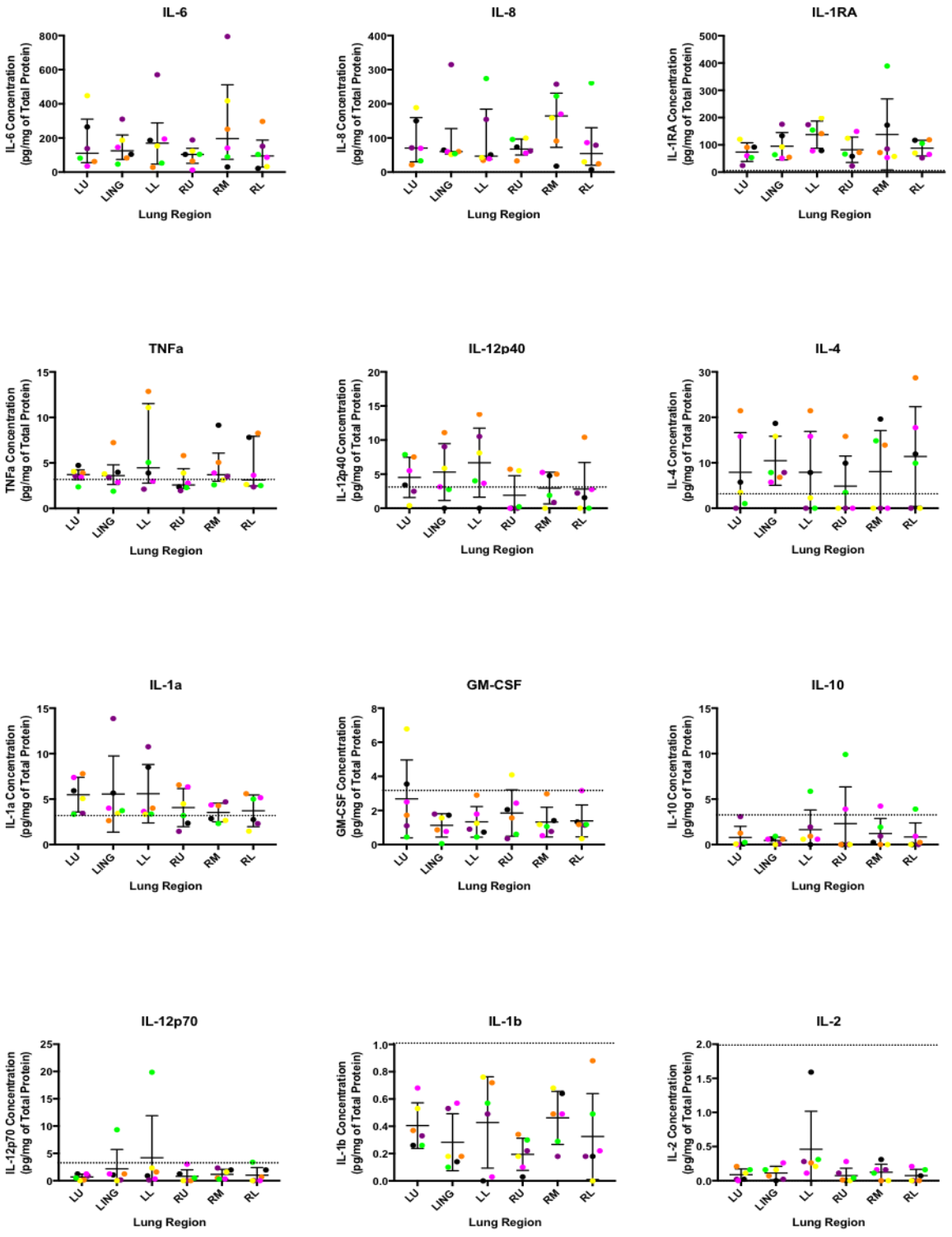

Appendix Figure 7.1 The regional concentration of cytokines and chemokines across the chronic obstructive pulmonary disease lung. The concentration of each cytokine or chemokine was measured per milligram of total protein in lung tissue lysate from six regions of the lung (n=6). Each patient in the cohort is characterised by a distinct colour, representing the cytokine concentrations in each region per patient. All scatter plot bar and lines represent mean ±SD, with the exception of IL-6 and IL-8 scatter plots which represent median + IQR. Statistical analysis was not performed due to the large number of samples below the limit of detection (dotted line).

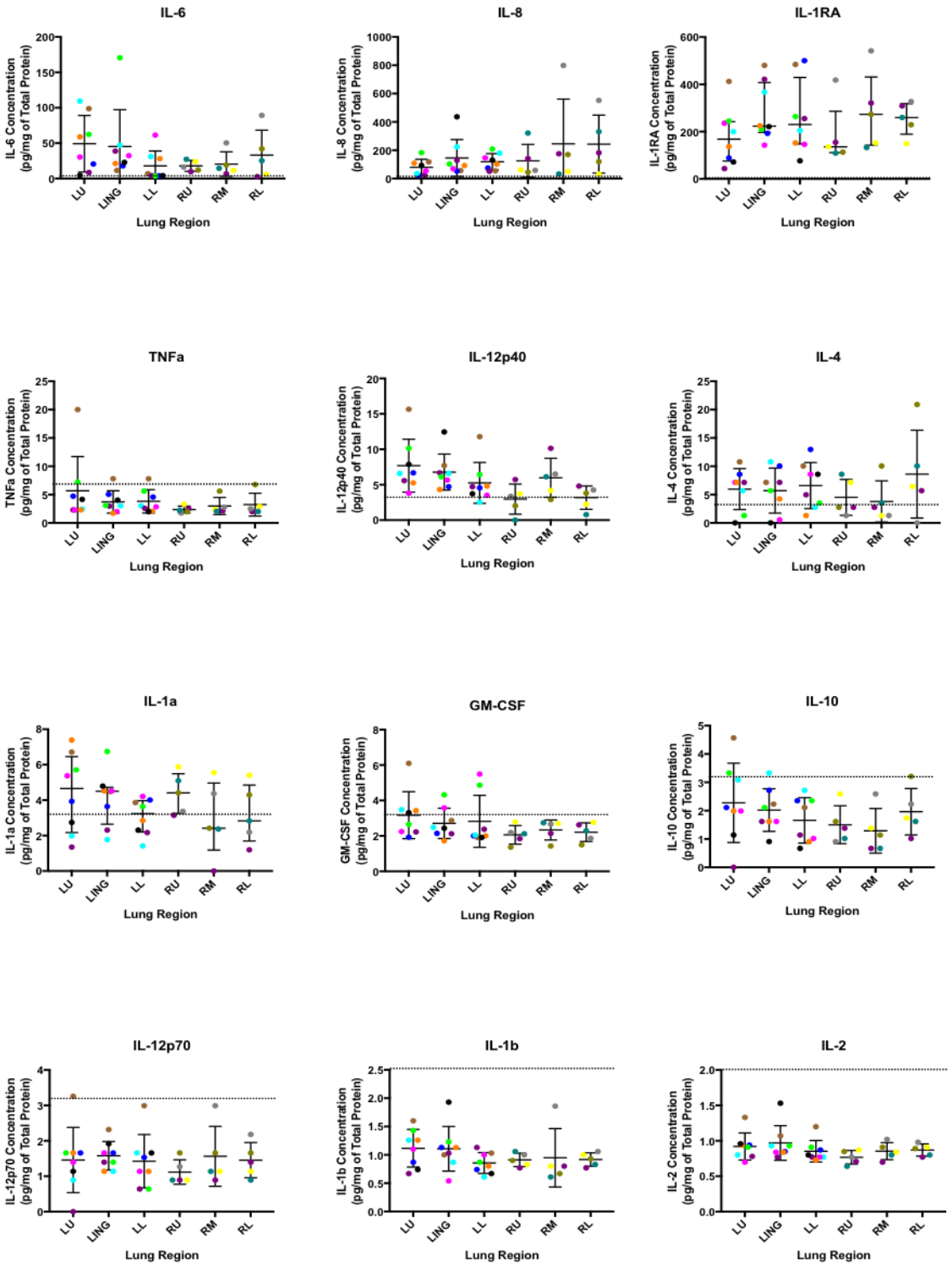

Appendix Figure 7.2. The regional concentration of cytokines and chemokines across the interstitial lung disease lung. The concentration of each cytokine or chemokine was measured per milligram of total protein in lung tissue lysate from different regions of the lung (left; n=8*, right; n=5*). Each patient in the cohort is characterised by a distinct colour, representing the cytokine concentrations in each region per patient. All scatter plot bar and lines represent mean ±SD, with the exception of the IL-1RA scatter plots which represent median + IQR. Statistical analysis was not performed due to the large number of samples below the limit of detection (dotted line). *LTx-51 received a double lung transplant and therefore has data points for both lungs (in purple).

Appendix 8. Chapter Three Additional Clinical Correlation Data

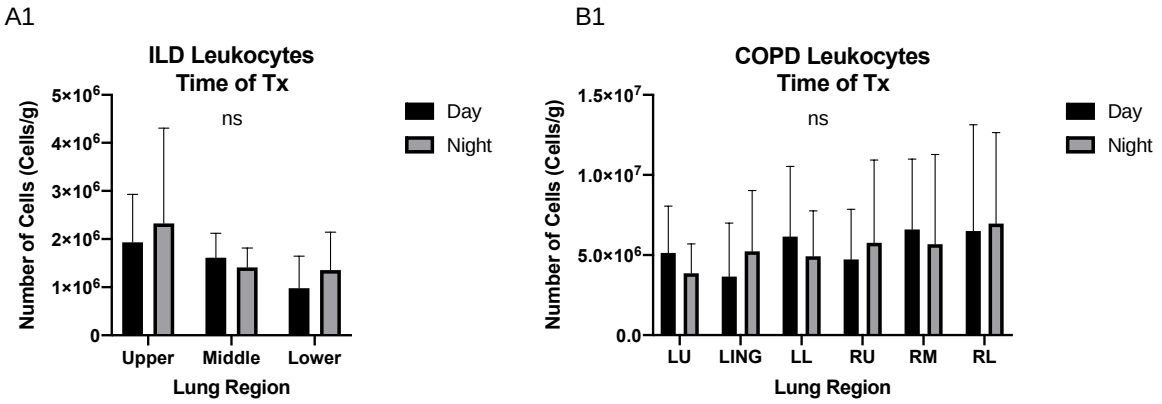

Appendix Figure 8.1 Correlating the total number of leukocytes in (A) interstitial lung disease (ILD) and (B) chronic obstructive pulmonary disease (COPD) with transplant time. The total number of leukocytes per gram of tissue in each region was assessed based on transplant time in (A) ILD (day; n=6, night; n=8*) and (B) COPD (day; n=4, night; n=5). All bars represent mean +SD, statistical differences between parameters were determined by a two-way ANOVA of grouped data, significance p > 0.05 reported as ns. *Patient LTx-51 underwent a double lung transplant, and has leukocyte data from both lungs.

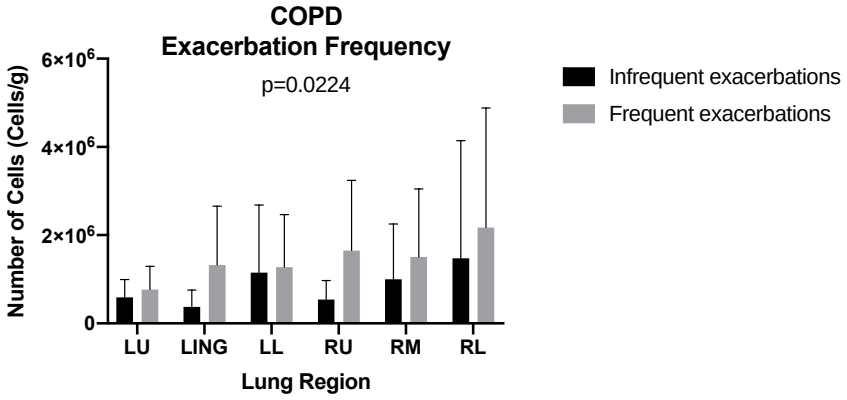

Appendix Figure 8.2 Correlating the CD4+ T lymphocytes to exacerbations in chronic obstructive pulmonary disease (COPD). The number of CD4+ T lymphocytes per gram of tissue in each region was assessed based on the frequency of exacerbations in the year preceding transplant (infrequent; n=6, frequent; n=4). All bars represent mean +SD, statistical differences between parameters were determined by a two-way ANOVA of grouped data, significant p value reported.

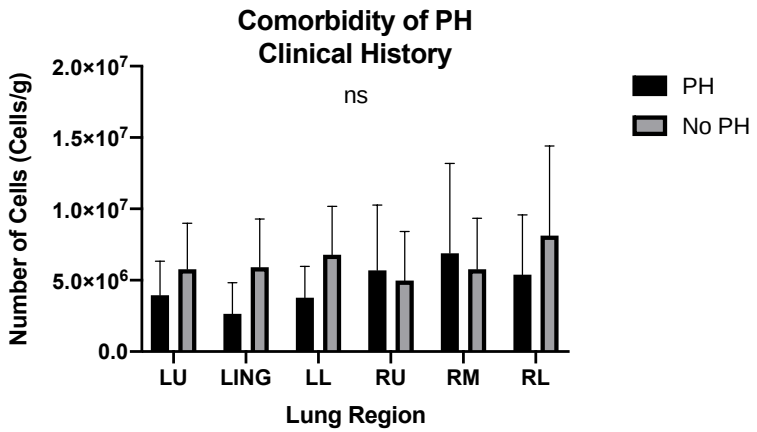

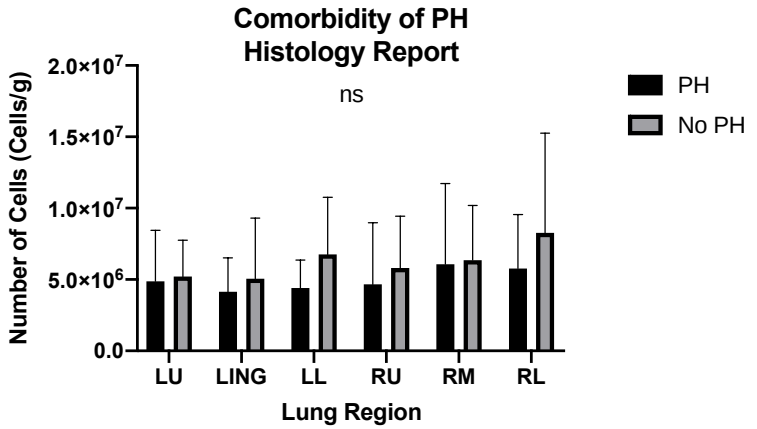

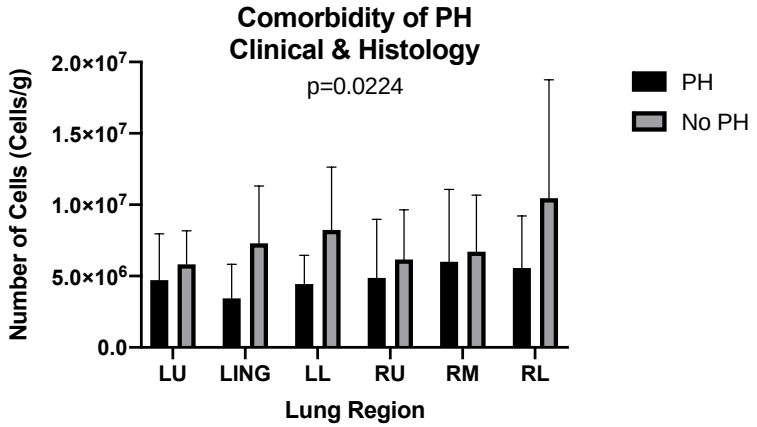

Appendix Figure 8.3 Correlating the total number of leukocytes to evidence of pulmonary hypertension (PH) in chronic obstructive pulmonary disease (COPD). The total number of leukocytes per gram of tissue in each region was assessed based on evidence of PH in the clinical history notes (PH; n=4, No PH; n=6), histology reports (PH; n=5, No PH; n=5) or in both (PH; n=7, No PH; n=3). All bars represent mean +SD, statistical differences between parameters were determined by a two-way ANOVA of grouped data, significant p value reported, significance p > 0.05 reported as ns.

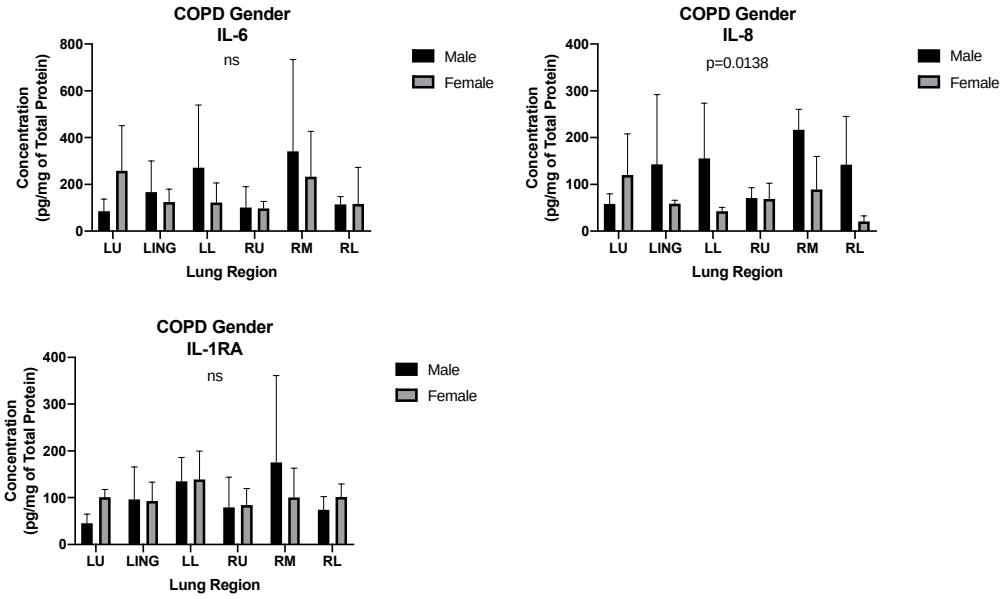

Appendix Figure 8.4 Correlating the concentration of cytokines to gender in chronic obstructive pulmonary disease (COPD). The concentration of interleukin (IL)-6, IL-8 and IL-1RA per milligram of total protein in each region was assessed based on gender (n=3 males, n=3 females) within the COPD cohort. All bars represent mean +SD, statistical differences between parameters were determined by a two-way ANOVA of grouped data, significant p value reported, significance $p > 0.05$ reported as ns.

Appendix 9. Interstitial Lung Disease Medication Information

Appendix Table 9.1 The list of medications patients were noted to be taking prior to trasnplantion, obtained from the transplant medical records held by Manchester University NHS Foundation Trust.

Drug	LTx Patients
Prednisolone	55, 51 (off at Tx), 41, 13, 53, 59
Mycophenolate	55
Septrin	55
Warfarin	55
Azithromycin	44
Cetirizine	44
Gabapentin	44, 53
Omeprazole	44
Pirfenidone	44, 13, 52, 43
Nebivolol	44
Amitriptyline	44
Atorvastatin	44, 41
Senna	44
Diltiazem	44
GTN spray	44
Aspirin	41, 53, 43
Ramipril	41
Ezetimibe	41
Nintedanib	42, 59
Oramorph	13, 43
Lansoprazole	13
Simvastatin	13
Alendronic acid	13
n-acetylcysteine	13
Azathioprine	53, 59 (switched to Nintedanib)
Insulin	53
Metformin	53
Citalopram	53
Amlodipine	53
Statin	43
Symbicort	43

Appendix 10. Chapter Six Immune Checkpoint Regional Statistical Summary

Appendix Table 10.1. Statistical analysis summary for regional immune checkpoint data from chapter six. Statistical summary of all differences in immune checkpoint expressions between regions for all diseases determined by a generalized estimating equation with Bonferroni post-test correction.

Immune Checkpoint Analysis			
Disease Cohort	**Immune checkpoint molecule**	**Overall p value**	**Pairwise post hoc values**
COPD	B7-1	<0.001	LU v LL (0.007) LU v RU (0.010) LU v RM (0.007) Ling v LL (<0.001) Ling v RU (<0.001) Ling v RM (0.004)
	B7-2	<0.001	LU v LL (0.008) Ling v LL (0.008) LL v RU (0.003) RU v RM (0.047) RU v RL (0.025)
	B7-H1	<0.001	LU v RL (0.024)
	B7-H2	<0.001	No significant post hoc results
	B7-H3	0.018	No significant post hoc results
	CD28	<0.001	LU v LL (0.019) Ling v LL (0.011)
	CTLA-4	<0.001	Ling v LL (0.015)
	ICOS	<0.001	No significant post hoc results
	PD-1	<0.001	LU v LL (<0.001) LU v RU (0.006) Ling v LL (0.048)
	PD-L2	0.005	LU v Ling (<0.001) LU v RM (0.039) LU v RL (0.033)
CF	B7-1	<0.001	LU v LL (<0.001) LU v RL (<0.001)
	B7-2	<0.001	No significant post hoc results
	B7-H1	<0.001	Ling v RM (<0.001) Ling v RL (<0.001)
	B7-H2	0.732	
	B7-H3	<0.001	LU v LL (0.042) Ling v LL (<0.001) Ling v RU (<0.001) Ling v RM (0.037)
	CD28	0.003	LU v RU (0.015) Ling v LL (0.001) Ling v RM (0.016) RM v RL (0.024)

Immune Checkpoint Analysis			
Disease Cohort	**Immune checkpoint molecule**	**Overall p value**	**Pairwise post hoc values**
CF continued	CTLA-4	<0.001	LU v LL (0.046)
	ICOS	<0.001	LU v Ling (<0.001) LU v LL (<0.001) LU v RU (<0.001) LU v RM (<0.001) LU v RL (0.004) Ling v RM (0.002) Ling v RL (0.028) LL v RL (0.039) RU v RM (0.033) RM v RL (0.003)
	PD-1	<0.001	LU v RU (0.002) LU v RL (0.007) Ling v RL (0.021) LL v RL (<0.001)
	PD-L2	<0.001	Ling v RU (<0.001) RU v RM (0.017) RU v RL (0.001)
ILD	B7-1	Left; 0.011 Right; 0.007	LU v Ling (0.037) Ling v LL (0.014) RU v RM (0.035)
	B7-2	Left; 0.186 Right; 0.445	NA
	B7-H1	Left; 0.304 Right; 0.306	NA
	B7-H2	Left; 0.109 Right; 0.493	NA
	B7-H3	Left; 0.032 Right; 0.691	Ling v LL (0.016)
	CD28	Left; 0.202 Right; <0.001	RU v RM (0.039)
	CTLA-4	Left; 0.118 Right; 0.189	NA
	ICOS	Left; 0.353 Right; 0.286	NA
	PD-1	Left; 0.737 Right; 0.001	RM v RL (0.019)
	PD-L2	Left; 0.871 Right; 0.508	NA